

AN ABSTRACT OF THE DISSERTATION OF

Selene Fregosi for the degree of Doctor of Philosophy in Wildlife Science presented on May 1, 2020.

Title: Applications of Slow-moving Autonomous Platforms for Passive Acoustic Monitoring and Density Estimation of Marine Mammals.

Abstract approved:

Holger Klinck

David K. Mellinger

Selina Heppell

Advances in mobile autonomous vehicles for oceanographic sensing provide new opportunities for passive acoustic monitoring of marine mammals. Acoustically equipped mobile autonomous platforms, including gliders, deep-water profiling floats, and drifting surface buoys can survey for a variety of marine mammal species over intermediate spatiotemporal scales. Additionally, such mobile platforms may provide an effective tool for population density estimation of marine mammals. This dissertation advances our understanding of how gliders, deep-water floats, and surface drifters can be used for passive acoustic monitoring and density estimation of two cetacean species, fin whales (*Balaenoptera physalus*), and Cuvier's beaked whales (*Ziphius cavirostris*).

One glider and two drifting deep-water floats were simultaneously deployed in the vicinity of a deep-water cabled hydrophone array offshore of San Clemente Island, California, USA. The glider was able to follow a pre-defined track while float movement was somewhat unpredictable. Fin whale 20 Hz pulses were recorded by all recorders throughout the two-week deployment and presence at hourly and daily scales were comparable across all recorders. Performance of an automated template detector did not differ by recorder type. However, the glider data contained up to 78% fewer fin whale detections per hour compared to the floats or stationary hydrophones because of increased low-frequency flow noise present during glider descents. Flow noise was

related to glider speed through water and dive state. Glider speeds through water of 25 cm/s or less are suggested to minimize flow noise.

The cabled hydrophone array was also used to estimate fin whale localizations and tracks concurrently with the glider survey. These tracks were used in a trial-based approach to estimate a detection function for six-minute snapshots containing fin whale 20 Hz pulses. Detection probability was strongly dependent on 40 Hz noise levels (flow noise) recorded on the glider. At the median noise level of 97 kHz dB re 1 $\mu\text{Pa}^2/\text{Hz}$, maximum detection range was nearly 40 km and the estimated effective survey was 870 km^2 . Density of fin whales was estimated as 2.4 whales per 1000 km^2 (coefficient of variation, CV 0.55) using a group size estimate from the tracked whales and an externally derived vocal rate from tagged fin whales. The framework presented here could be applied to other baleen whale species to advance the use of autonomous gliders for density estimation of cetacean species.

A second two-week glider and float deployment was conducted concurrently with the deployment of a commonly used deep-water stationary recorder, the High-frequency Acoustic Recording Package (HARP) and an array of drifting near-surface recorders in the Catalina Basin, California, USA. Acoustic recordings were analyzed for the presence of multiple marine mammal species, including beaked whales, delphinids, and minke whales and were compared across the glider, float, and HARPs. Detections of beaked whale echolocation clicks were variable across recorders, likely due to differences in the recording limits of each system, the spatial distribution of the recorders, and the short detection radius of such a high-frequency, directional signal type. Delphinid whistles and clicks were prevalent across all recorders, and at levels that may have masked beaked whale vocalizations. Minke whale (*Balaenoptera acutorostrata*) boing sounds were detected almost identically across all recorder types, as was expected given the relatively long detection range of the boing call type.

Spatially explicit capture-recapture was used to estimate density of Cuvier's beaked whales from the near-surface drifting array of acoustic recorders. A snapshot approach was used with presence or absence of echolocation clicks within a 1-minute snapshot acting as the sampling unit. Using external estimates of group size and echolocation probability in a 1-minute snapshot, the density of Cuvier's beaked whales, from the two best models was estimated at 5.48 animals per 1000 km² (CV 0.46). This estimate was similar to estimates calculated using trial-based and distance sampling approaches applied to the same data set. Simulation experiments were conducted to investigate potential bias in estimated density caused by the configuration of the drifting array. Bias from the array configuration was found to be negligible, increased array spacing (approximately doubling and tripling between-sensor spacing) decreased bias, and the drifting aspect of the recorders also decreased bias, compared to simulations with stationary sensors.

This work provides evidence that animal presence and absence at broad spatial scales such as hours and days are comparable across gliders, deep-water floats, and stationary recorders. The spatial advantage of mobile instruments is most pronounced for species with short acoustic detection ranges, such as beaked whales. Marine mammal density can be estimated from gliders and mobile drifters using either a trial-based or SECR approach examples presented here provide an exciting advance in marine mammal population monitoring.

©Copyright by Selene Fregosi
May 1, 2020
All Rights Reserved

Applications of Slow-moving Autonomous Platforms for Passive Acoustic
Monitoring and Density Estimation of Marine Mammals

by
Selene Fregosi

A DISSERTATION

submitted to

Oregon State University

in partial fulfillment of
the requirements for the
degree of

Doctor of Philosophy

Presented May 1, 2020
Commencement June 2020

Doctor of Philosophy dissertation of Selene Fregosi presented on May 1, 2020

APPROVED:

Co-Major Professor, representing Wildlife Science

Co-Major Professor, representing Wildlife Science

Co-Major Professor, representing Wildlife Science

Head of the Department of Fisheries and Wildlife

Dean of the Graduate School

I understand that my dissertation will become part of the permanent collection of Oregon State University libraries. My signature below authorizes release of my dissertation to any reader upon request.

Selene Fregosi, Author

ACKNOWLEDGEMENTS

I have written and re-written this section of my dissertation in my head too many times to count. Typically, I'd be lying in bed, trying to sleep, and I would attempt to craft the perfect acknowledgements section. But, each morning when it came time to actually get the words on paper, they were never right. I finally realized that whatever I write here will always feel inadequate. How do I put into words how essential the guidance, support, and love of my colleagues, friends, and family were to my actually getting my PhD? I couldn't have done this scientifically without the help of so many great scientists, mentors, and role models. I couldn't have done this mentally without the team of fellow grad students, friends, and family holding me up along the way. My mom sent me a bracelet the week of my defense. It says: "She thought she could, so she did" with the date of my defense. I love it; it makes me feel proud and reminds me that this was not an easy journey. But many times I didn't think I could. With this acknowledgements section I want to say, "*You all* thought I could, so I did."

I am so thankful to the faculty and staff of the Hatfield Marine Science Center (HMSC), the OSU Department of Fisheries and Wildlife, and NOAA's Pacific Marine Environmental Laboratory. I am so lucky to have worked with such a supportive, fun, and welcoming community. My dissertation research would not have been possible without extensive financial support. Foremost, the National Defense Science and Engineering Graduate Fellowship enabled me to pursue my PhD. Grants from the Office of Naval Research and the Navy's Living Marine Resources Program funded the field efforts presented here. Completion of this dissertation was possible through GRAships with the Gulf of Mexico Research Institute's LADC-GEMM project, a BOEM-funded glider project in the Gulf of Mexico, and a NAVFAC contract. The specific grant numbers that funded each project can be found in the acknowledgements section of each data chapter. Additionally, I was supported through TAships and scholarships from the FW department, including the Briggs Scholarship, Robert Anthony Graduate Scholarship, and Thomas G. Scott Grant Scholarship. My research was supported with the HMSC Mamie Markham Research Award and the Lylian Brucefield Reynolds Scholarship. I was able to travel with help from the Hatfield

Student Organization Travel Award, Mastin and Munson Travel Awards, and a travel award from the OSU Grad School.

I am so grateful to the unending support and guidance of my committee. Holger Klinck, thank you for sticking with me through a PhD and introducing me to gliders and how awesome they can be. Thanks for encouraging me to “sprechen Matlab.” And thank you for letting me stay in Oregon when you went to Cornell, and then welcoming me with a desk space at Cornell when I moved east. It’s all good! Dave Mellinger, getting to have you not only on my committee but as a true co-advisor and mentor has been amazing. Thank you for supporting me with glider piloting work, always asking how I’m doing as a person not just as a scientist, and for your patience explaining technical acoustics problems. Danielle Harris – I have enjoyed working with you and learning from you immensely. You are a wonderful role model and thanks for always having time to take my calls even across different time zones. Ari Friedlaender, I am so lucky to have had you on my committee. You have had an impact on my graduate career from the days I applied to programs You always provided a listening ear when I had questions or concerns about science or life. It is a wonderful thing to have you in my corner. Selina Heppell – thank you for “adopting” me in my final two years. Being a part of the Heppell lab was a blast and I couldn’t have asked for a more helpful guide for navigating the department and grad school system. Finally, Doug Maguire, I finished before you retired! Thanks for being my GCR again; you always brought the laughs and smiles.

My dissertation was hugely collaborative, and I was fortunate to work with a wonderful group of co-authors. While their specific contributions to each chapter are highlighted below, I wanted to say some additional thanks. Haru Matsumoto let me take his LMR grant to the next level and conduct the detailed comparison work. Haru – thanks for your patience and taking the time to teach me about acoustic calibration and some basic engineering. You were always seemed to say “good job!” when I most needed it. Steve Martin, Brian Matsuyama, and David Moretti were my collaborators from the U.S. Navy and provided access and tools for working with the Navy range data. Thank you all for always being available to chat and the encouraging and helpful

discussions of the project and the importance of the work. Simone Baumann-Pickering welcomed me to her lab for a whole week to learn the ins and outs of beaked whale detection and provided the HARPs for our Catalina Comparison. Thank you, Simone, for your willingness to host me, and thanks to Jenny Trickey for letting me share your office for the week and for your beautifully written protocols. Finally, Jay Barlow, thank you for basically being an honorary committee member. Our every-other-week AFFOGATO meetings were some of the most productive hours of my PhD. Thank you for your willingness to listen to discussions of work you weren't even a co-author on, your patience in explaining difficult topics to me, and your thorough and thoughtful review of manuscripts.

Sharon Nieukirk was not officially on my committee, but she was an integral part of my grad school and PhD journey. Sharon, I can't really put into words how much your friendship and mentorship means to me (trying not to get emotional as I write this!) I truly would not have survived without you. Alex Turpin – thank you for being such a fun co-worker, in the field and the lab. None of this would have been possible without your work getting our gliders, Will, Otis, and Otis, Jr. to record sound. Anatoli Erofeev and Steve Pierce were my glider pilot mentors and “spirit guides.” Anatoli, I will never forget when SG608 was lost during recovery in 2015. When I called you in a panic you knew just what to say to put me at ease. Most of what I have learned about glider piloting I learned from Anatoli and Steve through hands on experience under their guidance; thank you both for your endless patience with me and for being calm and cool role models.

I can't possibly thank all my FWGSA, HSO, friends and lab mates sufficiently. The communities in Corvallis and Newport are so special and not that I took it for granted, but I sure miss you all!! Samara thanks for all the carpooling and being the best office mate. Remember when we were finally driving over the new road and we didn't even realize it? I would have not survived this, mentally or physically, without my Corvallis High School Wellness crew. The small band of FW PhD students that were part of “Group” provided the therapy, advice, and general sounding board during

so many struggles. Thank you all for reminding me to have self-care and be kind to myself.

I want to thank my Santa Cruz family/cheering squad. Brandon Southall gave me my first paying job in marine mammal science and has let me keep being a part of the SEA team all these years – thank you! Alison Stimpert – thank you for being such a great friend, amazing inspiration, and all-around hilarious person. Jillian Sills and Caroline Casey, I think of you two as my grad cohort from afar. Even though we are far apart you guys are always in my heart (aww). I can't wait to be roomies at the next conference. Colleen Reichmuth, this dissertation is dedicated to you because I am literally only here because of you. You knew I could do this grad school thing from the beginning, and you have guided and supported me every single step of the way. You are the most amazing scientist and most caring person and you inspire me more than you could ever know. I'm not crying!

And finally, so many thanks to my family. Mom and Dad (Vicki and Mike Fregosi), your love and support has never wavered (including financial support – I'm still on that family cell phone plan!) and your confidence that I could do this kept me going. All the cards these last few months, and the flights to come home, and even now the Zoom calls have gotten me through this last year. Thank you to the moon and back. Matt and Anthony – you are the very best brothers I could ask for. Thanks for listening to me drone on about boring stuff, flying me home for engagement dinners, and giving me shopping tips. Christina Lawson – I don't know how you know when to call me just when I need it most, but you do. You mean the world to me. Thanks for visiting me whenever I was in LA for field work, or joining me at conferences, and also for buying me all the Harry Potter swag I never knew I needed. Mike Burns, I don't know how or why you love me, but thank you. You are there, no matter how stressed or sad I feel, making sure I eat and making me laugh. Thanks for supporting me when I was struggling, and for celebrating each victory with me along the way. I am so lucky to have a partner that gets this academic life and I couldn't navigate it without you. Last but certainly not least – Piper and Murph, my daughters, thanks for all the kisses, all the snugs, and for generally thinking I am the most important thing in the world.

CONTRIBUTION OF AUTHORS

Chapter 2: Comparison of fin whale 20 Hz call detections by deep-water mobile autonomous and stationary recorders

Selene Fregosi conducted the field work, conducted the acoustic and statistical analyses, and wrote the manuscript. Danielle V. Harris provided input on data analysis and interpretation. Haruyoshi Matsumoto, David K. Mellinger, and Holger Klinck obtained funding for the project and provided analysis and interpretation support. Haruyoshi. Matsutmoto also assisted with field work. Christina Negretti assisted with detector performance analysis. Stephen W. Martin, Brian Matsuyama, and David J. Moretti provided access, analysis, and interpretation support for the Navy data. Peter J. Dugan ran the fin whale detector on all datasets. All authors reviewed and edited the manuscript. This manuscript was published in the *Journal of the Acoustical Society of America*, Volume 147, Issue 2, February 2020.

Chapter 3: Detection probability and density estimation of fin whales by a Seaglider

Selene Fregosi conducted the field work, conducted the acoustic and statistical analyses, and wrote the manuscript. Danielle V. Harris, and Jay Barlow provided input on data analysis and interpretation. Haruyoshi Matsumoto, David K. Mellinger, and Holger Klinck obtained funding for the project and provided analysis and interpretation support. Haruyoshi Matsutmoto also assisted with field work. Stephen W. Martin and Brian Matsuyama provided localizations of fin whales and tracking software for the Navy data.

Chapter 4: Detections of whale vocalizations by simultaneously deployed bottom-moored and deep-water mobile autonomous hydrophones

Selene Fregosi conducted field work, conducted the acoustic and statistical analyses, and wrote the manuscript. Haruyoshi Matsumoto and Simone Baumann-Pickering provided instrumentation. Simone Baumann-Pickering provided beaked whale detector analysis training and her team analyzed the HARP data. Danielle V. Harris, David K.

Mellinger, Jay Barlow, and Holger Klinck assisted with field work and provided help with analysis and interpretation. All authors obtained funding for this work and edited and reviewed the final manuscript.

Chapter 5: Detection probability of Cuvier's beaked whales by a mobile acoustic array using a spatially explicit capture-recapture approach

Selene Fregosi conducted the spatially explicit capture-recapture simulation and case study analysis, participated in the field work, and wrote the manuscript. Jay Barlow, Len Thomas, and Danielle Harris obtained funding for this work and provided analysis and interpretation support. Jay Barlow and Danielle Harris conducted the field work. Emily Griffiths conducted the acoustic analysis for beaked whale clicks. The results of the case study are included in a separate manuscript in preparation by Jay Barlow, Selene Fregosi, Len Thomas, Danielle Harris, and Emily T. Griffiths titled "Acoustic detection range and population density of Cuvier's beaked whales estimated for near-surface hydrophones" to be submitted to the Journal of the Acoustical Society of America.

TABLE OF CONTENTS

CHAPTER 1: GENERAL INTRODUCTION	1
Marine mammal conservation and management	1
Passive acoustic monitoring of marine mammals.....	2
Passive acoustic recording technologies.....	3
Stationary recorders	4
Vessel-based recorders.....	5
Mobile autonomous platforms	6
Seaglider operation	8
APEX float/QUEphone operation.....	9
DASBR operation	9
Density estimation of animals from acoustics	10
Plot sampling	11
Distance sampling.....	12
Spatially explicit capture-recapture	13
Density estimation from slow-moving platforms	14
Objectives	15
Tables.....	17
 CHAPTER 2: COMPARISON OF FIN WHALE 20 HZ CALL DETECTIONS BY DEEP-WATER MOBILE AUTONOMOUS AND STATIONARY RECORDERS	18
Abstract.....	19
Introduction.....	20
Methods	27
Acoustic systems.....	27
Field deployment	28
Acoustic analyses.....	30
Results.....	36
Call detection	36
Noise levels	38
Discussion.....	40

TABLE OF CONTENTS (Continued)

Conclusion	47
Acknowledgements.....	49
Tables.....	50
Figures	55
CHAPTER 3: DETECTION PROBABILITY AND DENSITY ESTIMATION OF FIN WHALES BY A SEAGLIDER	64
Abstract.....	65
Introduction.....	66
Methods	74
Acoustic data collection and analysis	74
Fin whale tracking.....	75
Detection function estimation	76
Density estimation	80
Results.....	82
Trial-based detection function	82
Estimated density	83
Discussion.....	83
Detection function estimates.....	83
Estimation of density	88
Acknowledgements.....	90
Tables.....	91
Figures	92
CHAPTER 4: DETECTIONS OF WHALE VOCALIZATIONS BY SIMULTANEOUSLY DEPLOYED BOTTOM-MOORED AND DEEP-WATER MOBILE AUTONOMOUS HYDROPHONES	99
Abstract.....	100
Introduction.....	101
Materials and Methods.....	104
Recording platforms and PAM systems.....	104

TABLE OF CONTENTS (Continued)

Field Experiment.....	105
Acoustic analyses.....	106
Results.....	109
Recording durations	109
Beaked whales	110
Delphinid clicks and whistles	112
Minke whale boings	112
Discussion.....	113
Conclusions.....	120
Funding.....	121
Acknowledgments	121
Tables.....	122
Figures	125
CHAPTER 5: DETECTION PROBABILITY OF CUVIER’S BEAKED WHALES BY A MOVING ACOUSTIC ARRAY USING A SPATIALLY EXPLICIT CAPTURE-RECAPTURE APPROACH	133
Abstract.....	134
Introduction.....	135
Methods	141
Field effort	141
Acoustic analysis	142
Encounter rates on the glider and float	143
Estimating effective area surveyed using SECR	143
Density estimator	146
Simulations with varied sensor spacing.....	147
Simulations with larger sample size	149
Results.....	149
Encounter rates of Cuvier’s beaked whales	150
Effective survey area and density estimate.....	151
Simulations of varied sensor spacing.....	152

TABLE OF CONTENTS (Continued)

Simulation of larger sample size.....	152
Discussion.....	153
Case study results.....	153
Simulations	156
Applications to gliders and deep-water floats.....	156
Acknowledgements.....	159
Tables.....	160
Figures	171
 CHAPTER 6: GENERAL CONCLUSIONS AND FUTURE DIRECTIONS	 182
Contribution to the field.....	182
Future directions	185
 DISSERTATION REFERENCES.....	 187
 APPENDIX A: CHAPTER 2 SUPPLEMENTARY MATERIALS	 204
 APPENDIX B: CHAPTER 3 SUPPLEMENTARY MATERIALS.....	 219
 APPENDIX C: CHAPTER 4 SUPPLEMENTARY MATERIALS.....	 224
Supplementary Figures and Tables.....	225
Minke whale boing detector – Ishmael preference file.....	229

LIST OF FIGURES

<u>Figure</u>	<u>Page</u>
Figure 2.1. Map of platform paths, the outline of the Southern California Offshore Range (SCORE) enclosing the locations of the bottom-moored hydrophones, and seafloor bathymetry in the deployment area.....	55
Figure 2.2. Dive profiles of the Seaglider (SG158) and QUEphones (Q001 and Q002)	56
Figure 2.3. Precision and recall metrics for the fin whale 20-Hz pulse detector.....	57
Figure 2.4. Detections per hour for each mobile platform (open triangles and solid black line) and the corresponding closest bottom-moored hydrophone (orange circles, solid orange line) during that hour.....	58
Figure 2.5. Example Long Term Spectral Average (LTSA) plot (10 sec, 1 Hz) showing 24 hours of acoustic data recorded by SG158, Q001, Q002 from 12/26/2015 16:00 to 12/27/2015 16:00 UTC	59
Figure 2.6. Spectral Probability Density (SPD) plots for SG158, Q001, and Q002, up to 5 kHz, using methods outlined in Merchant <i>et al.</i> (2013) on the 10 kHz sample rate LTSA of the entire deployment calculated with a 1 Hz, 10 sec Hann window for each mobile platform.....	60
Figure 2.7. Power spectrum density levels at 12 Hz, 40 Hz and 3000 Hz for all three mobile platforms for a 24-hour period from 12/26/2015 16:00 to 12/27/2015 16:00 UTC (same 24-hour period shown in Figure 2.5).....	61
Figure 2.8. Prediction plots for final regression models at each frequency	62
Figure 2.9. Theoretical maximum detection range over the duration of a single glider dive, Dive 28, on 12/26/2015 at 20:33 UTC.....	63
Figure 3.1. Map of Seaglider, SG158, survey path (black line) and the general location of the SCORE hydrophone array (white dashed box)	93
Figure 3.2. Flowchart outlining the steps from fin whale vocalizations to detection trials	94
Figure 3.3. Final localized whale tracks	95
Figure 3.4. Spectrum levels at 40 Hz on the glider in 1-minute intervals over time (top) and histogram distribution (bottom) for the first three days of the survey	96

LIST OF FIGURES (continued)

<u>Figure</u>	<u>Page</u>
Figure 3.5. Snapshots that were detected (black circles) or not detected (outlined black triangles) by the glider as a function of distance from the track segment to the glider and the median 40 Hz spectrum level on the glider during that snapshot for the subset of snapshots (n = 170) used in the detection function analysis.....	97
Figure 3.6. Detection probability estimated from snapshots with 40 Hz spectrum levels between 90 and 100 dB re 1 $\mu\text{Pa}^2/\text{Hz}$	98
Figure 4.1. Map of deployment area and recording platform locations. HARPs H01 and H02 are shown as colored squares (yellow and purple)	125
Figure 4.2. Occurrence of Cuvier’s beaked whale clicks by recorder platform	126
Figure 4.3. Mobile platform locations when beaked whales (Panels A-C) and minke whales (Panel D) were detected	127
Figure 4.4. Dive profile of Seaglider (top panel) and QUEphone (bottom panel) showing platform depth over time	129
Figure 4.5. Distribution of mobile platform (Seaglider – top, red and QUEphone – bottom, blue) depths when Cuvier’s beaked whale clicks were detected.....	130
Figure 4.6. Daily presence of delphinid vocalizations (whistles and clicks) by recording platform.....	131
Figure 4.7. Occurrence of minke whale boings by recorder platform. Top panel: Percentage of recorded minutes with boings	132
Figure 5.1. Map of platform survey tracks and known whale locations.....	171
Figure 5.2. Relative sensor locations and pairwise distances between the four DASBRs for the by-snapshot (n = 275) sessions (six distances calculated per snapshot)	172
Figure 5.3. Relative sensor locations and pairwise distances between the four DASBRs for each of the 25 by dive sessions (six distances calculated per session)	173
Figure 5.4. Diagram of simulation workflow. For each simulation run, trap locations are defined for 25 sessions.....	174
Figure 5.5. Relative sensor locations and pairwise distances between the four DASBRs for the simulations looking at increased sensor spacings	175

LIST OF FIGURES (continued)

<u>Figure</u>	<u>Page</u>
Figure 5.6. Detection probabilities as calculated using SECR with by-snapshot sessions	176
Figure 5.7. Histograms and empirical cumulative distribution functions of the case study simulation results for density (top) and effective survey area (bottom) for 100 simulations where the case study detection function parameters and true case study sensor locations were used as simulated inputs	177
Figure 5.8. Histograms and empirical cumulative distribution functions of the 500 m-expanded sensor spacing simulation results for density (top) and effective survey area (bottom) for 100 simulations	178
Figure 5.9. Histograms and empirical cumulative distribution functions of the 1000 m expanded sensor spacing simulation results for density (top) and effective survey area (bottom) for 100 simulations	179
Figure 5.10. Histograms and empirical cumulative distribution functions of the stationary sensor spacing simulation results for density (top) and effective survey area (bottom) for 100 simulations	180
Figure 5.11. Histograms and empirical cumulative distribution functions of the increased sample size simulation results for density (top) and effective survey area (bottom) for 100 simulations	181

LIST OF TABLES

<u>Table</u>	<u>Page</u>
Table 1.1. Comparison of advantages and disadvantages of different passive acoustic monitoring methods used for marine mammal science	17
Table 2.1. Deployment and recording durations for each recorder	50
Table 2.2. Start and end times of overlapping recording periods in which all mobile platforms were deployed and M3R was active but excluding periods when M3R data was not properly recorded.....	51
Table 2.3. Detector performance evaluation metrics by recorder type.....	52
Table 2.4. Median (50 th), 5 th , and 95 th percentile 12, 40 and 3000 Hz power spectrum density levels (dB re 1 $\mu\text{Pa}^2/\text{Hz}$; 10 sec Hann window, 0% overlap) for all mobile platforms	53
Table 2.5. Regression model outputs of the final preferred model at each frequency of interest.....	54
Table 3.1. Number and proportion of snapshots recorded by the glider with fin whale 20 Hz pulses present, for each glider dive and averaged across all glider dives	91
Table 3.2. Density of snapshots with fin whale calls present and density of fin whales for the 90-hour glider survey	92
Table 4.1. Deployment and recovery times for each recording platform, with total hours of data recorded, and distance travelled for the glider and QUEphone	122
Table 4.2. Summary of total durations of acoustic data recorded by each platform and minutes, hours, days, and/or encounters for four types of marine mammal vocalization: Cuvier’s beaked whale echolocation clicks, beaked whale echolocation click type BW43 clicks, small delphinid whistles and clicks, and minke whale boings.....	123
Table 4.3. Beaked whale encounters by the Seaglider (SG), QUEphone (QUE) and HARPs (H01 and H02)	124
Table 5.1. Deployment and recovery times for the Seaglider (SG607), QUEPhone (Q003), and DASBRs (B1-B4).....	160
Table 5.2. Deployment and recovery times for DASBRs.....	161
Table 5.3. Formulas for the four tested models	163

LIST OF TABLES (continued)

<u>Figure</u>	<u>Page</u>
Table 5.4. Distances from the Seaglider and QUEphone to the 23 beaked whale locations	164
Table 5.5. (on next page) Capture history for the four DASBRs used in the case study, when each dive was grouped as a session.....	165
Table 5.6. Model results for the by-dive sessions model fit	167
Table 5.7. Model results for the by-minute sessions model fit.....	168
Table 5.8. Density estimator inputs and density of Cuvier's beaked whales estimated for the three top detection function models	169
Table 5.9. Simulation results for the compound half normal simulations	170

LIST OF APPENDIX FIGURES

<u>Figure</u>	<u>Page</u>
Figure A1. LTSA (80 sec, 10 Hz) of 10 kHz downsampled data for the deployment duration for SG158, Q001, and Q002 with each instruments dive profile overlaid (right y-axis).....	205
Figure A2. Distribution of signal-to-noise ratios (SNR) for true detections (TP: true positives), false alarms (FP: false positives), and missed calls (FN: false negatives). Median and interquartile range (IQR; 25-75%) are listed in the legend.....	206
Figure A3. Top: Boxplots for Kruskal-Wallis test for differences in precision across the instrument types with all glider dive states together (left; sg158) and separated by ascent and descent (right) compared to the float (q001) and fixed-recorders (M3R)	207
Figure A4. Top: Boxplots for Kruskal-Wallis test for differences in recall across instrument types, with all glider dive states together (left; sg158) and separated by ascent and descent (right), compared to the float (q001) and fixed-recorders (M3R)	208
Figure A5. Boxplot of median detections per hour for each M3R hydrophone, colored by instrument depth.....	209
Figure A6. Exploratory plots of raw data (all minutes)	210
Figure A7. Exploratory plots of 30-minute binned median data	211
Figure A8. Exploratory plots of 30-minute binned median data, with outliers removed	212
Figure A9. Residual and normality plots used for checking model assumptions for the median 12 Hz power spectrum density levels.....	213
Figure A10. Normalized residual and normality plots for median 12 Hz power spectrum density levels after applying variance and correlation structures in a generalized least squares regression of the full model	214
Figure A11. Residual and normality plots used for checking model assumptions for the median 40 Hz power spectrum density levels.....	215
Figure A12. Normalized residual and normality plots for median 40 Hz power spectrum density levels after applying variance and correlation structures in a generalized least squares regression of the full model	216

LIST OF APPENDIX FIGURES (continued)

<u>Figure</u>	<u>Page</u>
Figure A13. Residual and normality plots used for checking model assumptions for the median 3 kHz power spectrum density levels.....	217
Figure A14. Normalized residual and normality plots for median 3 kHz power spectrum density levels after applying variance and correlation structures in a generalized least squares regression of the full model	218
Figure B1. Example equalized spectrogram of a single snapshot on the focal SCORE hydrophone (top) and the glider (middle) showing a gap in calls used to confirm the tracked whale was recorded on the glider.....	220
Figure B2. Example equalized spectrogram of a single snapshot on the focal SCORE hydrophone (top) and the glider (middle) showing multiple whales present on both recorders, but the pattern still allowed confirmation of the tracked whale being recorded by the glider	221
Figure B3. Distribution of scored snapshots (n = 589) by 40 Hz noise level on the glider	222
Figure B4. Snapshots that were detected (black circles) or not detected (outlined black triangles) by the glider as a function of distance from the track segment to the glider and the median 40 Hz spectrum level on the glider during that snapshot	223
Figure C1. Sound speed profile collected by Seaglider SG607	225
Figure C2. Distances between a single recording platform, shown in the title of each plot, and the three other deep-water recorders for all Cuvier's beaked whale encounters on the named recording platform.....	226
Figure C3. Distances between a single recording platform, indicated in the title of each plot, and the three other deep-water recorders for all minke whale boing encounters	227

LIST OF APPENDIX TABLES

<u>Table</u>	<u>Page</u>
Table C1. Localized Cuvier's beaked whales (from Barlow <i>et al.</i> 2018) with distances to deep-water recorders at that minute.....	228

For Coll

Applications of slow-moving autonomous platforms for passive acoustic monitoring and density estimation of marine mammals

CHAPTER 1: GENERAL INTRODUCTION

Marine mammal conservation and management

Marine mammals are an important component of the marine ecosystem, but historical overexploitation has left many marine mammal populations vulnerable. While historical exploitation of marine mammal species is no longer the primary threat to their existence, many populations are still recovering from previous overharvest and populations are at risk from new threats such as climate change, pollution (chemical and noise), and increased human use of the ocean (*e.g.*, ship strike, drilling, noise, overfishing; Read, 2010). In the U.S., marine mammals are protected by the Marine Mammal Protection Act (MMPA; 1972) and the Endangered Species Act (ESA; 1973), and are managed by two primary agencies, including the U.S. National Marine Fisheries Service (NMFS; cetaceans, phocid seals, and otariids) and the U.S. Fisheries and Wildlife Service (USFW; sea otters, walrus, polar bears, and manatees; Read, 2010). These agencies require valid population estimates to assess the current status of a given species and its risk level, to make management plans on appropriate take levels, and to assess the success of new management practices (Hammond, 2010; Wade, 1998). Knowledge of when and where marine mammals occur is fundamental in marine mammal science, and therefore there is a need to develop more efficient and effective ways of monitoring marine mammal populations. The broad motivation for this dissertation is to advance methodologies for the conservation and management of marine mammals by creating a framework to use slow-moving mobile autonomous platforms and passive acoustics to estimate marine mammal population densities over broad spatiotemporal scales.

Passive acoustic monitoring of marine mammals

The ability of scientists to study marine mammals, in particular cetaceans, with traditional visual techniques is limited by the aquatic habitat and wide ranges of these species. Observations of foraging, social interactions, mating, and other behaviors are difficult, as most of these activities occur below the sea surface. Some species, such as beaked whales, exhibit cryptic behavior, foraging at extreme depths and surfacing for only short times with inconspicuous blows (Tyack *et al.*, 2006), and so are even more difficult to survey visually (Barlow *et al.*, 2013). Even when animals can be observed at the surface, visual observations are limited to daylight hours and calm, workable weather conditions. Further, remote offshore habitats are often inaccessible due to logistic and financial constraints.

Alternatively, marine mammals can be studied by passively listening to the sounds they produce. Sound is an important sensory system for many marine mammals and a variety of underwater sounds are produced by marine mammals. While light is transmitted poorly underwater, sound travels well (over four times as fast as in air, and over longer distances) and so is likely a more effective sensory modality than vision. Marine mammals rely on sound for many life functions including social communication, mate selection, and foraging. For example, male fin whales (*Balaenoptera physalus*) produce loud, long durations of “song” that can be heard over tens to hundreds of kilometers away and is thought to play a role in breeding (Croll *et al.*, 2002; Širović *et al.*, 2007, 2013; Watkins *et al.*, 1987). Bottlenose dolphins (*Tursiops truncatus*) are known to produce signature whistles that are unique to individuals and are used in social interactions and for individual identification (Janik and Sayigh, 2013). Echolocation, or the process of using short-duration, click sounds (typically >10 kHz) to find and capture prey and navigate the environment, is used by all toothed whales, or odontocetes (Au, 1993). We can utilize these animal-produced sounds, and their efficient underwater transmission, to study marine mammals through passive acoustic monitoring.

Passive acoustic monitoring (PAM) is an effective tool for studying marine mammals and can be used in studies of both basic ecology and for more applied conservation and management purposes over a variety of spatial and temporal scales. PAM

is an efficient method compared to visual observations because acoustic observations can be made in daytime or nighttime hours, under harsh weather conditions, over time scales of months to years, and in remote locations otherwise not reachable by ship (Mellinger *et al.*, 2007). The breadth of PAM applications to marine mammals include studies of behavior (*e.g.*, Barlow *et al.*, 2018; Stimpert *et al.*, 2015), identification of critical habitat (*e.g.*, Yack *et al.*, 2013), tracking of seasonal migrations (*e.g.*, Guazzo *et al.*, 2017), understanding the effects of and responses to increased human-generated or background ocean noise (*e.g.*, Helble *et al.*, 2020; Tyack *et al.*, 2011), and facilitating migration and management of populations sensitive to human impacts (Van Parijs *et al.*, 2009). Finally, PAM provides a cost-effective and efficient method to collect necessary data for estimation of marine mammal abundance and density (*e.g.*, Barlow and Taylor, 2005; Hildebrand *et al.*, 2015; Kyhn *et al.*, 2012; Lewis *et al.*, 2007; Marques *et al.*, 2009; Norris *et al.*, 2017), which is the focus of much of this dissertation.

Passive acoustic recording technologies

Many different methods exist for PAM of marine mammals (see Mellinger *et al.*, 2007). They can be broken down into a few broad categories: stationary autonomous recorders (*e.g.*, Lammers *et al.*, 2008; Wiggins *et al.*, 2012), cabled arrays (*e.g.*, Jarvis *et al.*, 2014; Oswald *et al.*, 2011), vessel-borne recorders (*e.g.*, Barlow and Taylor, 2005; Miller and Tyack, 1998), animal-mounted tags (*e.g.*, Burgess *et al.*, 1998; Johnson and Tyack, 2003), and mobile autonomous systems (*e.g.*, Moore *et al.*, 2007; Verfuss *et al.*, 2019; Wiggins *et al.*, 2010). Depending on the system and study goals, instruments can be deployed for hours to years and can record continuously or on a duty cycle. Archival instruments must be recovered for data analysis, while real-time systems can send data back via satellite, radio, or wired communication in real time or near-real time. Each of these systems have a variety of advantages and disadvantages, which are discussed for stationary and mobile recorders in the following two subsections and for mobile autonomous systems in the following section. Animal-mounted tags are not discussed further as they are not included in this dissertation and are comparatively not as “passive” since they require direct tagging of a focal individual.

Stationary recorders

Stationary recording platforms are perhaps the most widely used PAM system for marine mammal surveys and have many distinct advantages. Recorders are fixed in space typically through a mooring on the sea floor. These systems can collect long-term datasets over months to years and provide great temporal resolution with recordings possible through all hours of the day and any weather conditions (Mellinger *et al.*, 2007). Stationary recorders are generally very quiet systems, designed to reduce self-noise (Sousa-Lima *et al.*, 2013) and are not known to affect the behavior of the study animals (Mellinger *et al.*, 2007). Autonomous stationary platforms are typically the least expensive PAM tool (Lammers *et al.*, 2008; Mellinger *et al.*, 2007; Sousa-Lima *et al.*, 2013). Most are archival and must be recovered to retrieve collected data, but if the platform includes a surface component, near-real time data collection is possible (Baumgartner *et al.*, 2018; Spaulding *et al.*, 2009). Cabled stationary recorders can also provide data in near-real time, and potentially over decades, which allows for both immediate and long-term monitoring (Klinck *et al.*, 2016b; Miksis-Olds *et al.*, 2019; Moretti *et al.*, 2016; Oswald *et al.*, 2016; Van Parijs *et al.*, 2009). However, installations of cabled systems are rare. Both single recorders and arrays cabled to shore are expensive and so are typically installed and managed by governments or large organizations and locations are restricted to areas that are important to those organizations (Barnes *et al.*, 2007; Mellinger *et al.*, 2007; Sousa-Lima *et al.*, 2013). An array of stationary recorders, either cabled or autonomous, can be used to track and identify individual vocalizing animals by using the time difference of arrival (TDOA) of the same signal received across multiple recorders to triangulate the source location of the vocalization (Hatch *et al.*, 2012; Helble *et al.*, 2016). Further, marine mammal abundance and density can be estimated from a variety of fixed recorder configurations (Marques *et al.*, 2013).

The primary limitation to fixed recorders, particularly a single instrument, is that they provide limited spatial coverage. The monitoring area of a PAM platform depends on the local sound propagation environment, ambient sound conditions, and the amplitude and frequency characteristics of the target sound (Helble *et al.*, 2013b; Mellinger *et al.*, 2007; Širović *et al.*, 2007; Ward *et al.*, 2011; Zimmer *et al.*, 2008). Underwater sound

transmission dictates that low-frequency marine mammal signals (< 1 kHz) may be detected tens to hundreds of kilometers away from the sound source (Širović *et al.*, 2007; Stafford *et al.*, 2007). Conversely, higher-frequency signals (>25 kHz) are likely only detectable within a few kilometers (Zimmer *et al.*, 2008), or even just tens of meters as frequencies increase (>100 kHz; Kyhn *et al.*, 2012). Calls can also be masked by natural (*e.g.*, wind, rain) and human-generated (*e.g.*, ships, sonar) noise, which further reduces the detection range (Helble *et al.*, 2013a; Stafford *et al.*, 2007; Ward *et al.*, 2011). As mentioned above, fixed recorders can be deployed as an array of multiple recorders, which provides greater spatial coverage; however, deploying multiple recorders increases survey costs and required data processing, which can be challenging when datasets are many terabytes in size (Lammers *et al.*, 2008; Van Parijs *et al.*, 2009; Roch *et al.*, 2016; Sousa-Lima *et al.*, 2013). While some bearing and range information can be estimated from single stationary recorders using propagation modelling approaches, these methods are not as widely applicable as localizing from arrays of hydrophones (*e.g.*, Küsel *et al.*, 2011; Thode, 2000; Tiemann *et al.*, 2006).

Vessel-based recorders

Another commonly used PAM platform is a hydrophone array towed behind a vessel, which has several advantages over fixed recorders. A moving vessel provides better spatial coverage than fixed recorders (Mellinger *et al.*, 2007). Additionally, acoustic and visual observations can be made concurrently and data are provided in real time, which allows identification of species-specific sounds and linking of behavior to acoustic recordings (Miller and Tyack, 1998; Rankin *et al.*, 2007; Rankin and Barlow, 2005). Towed arrays are also capable of tracking and identifying vocalizing individuals (Quick and Janik, 2012; Thode, 2004) and can be used to estimate animal density using a distance sampling framework (Barlow and Taylor, 2005; Buckland *et al.*, 2001; Lewis *et al.*, 2007, 2018; Norris *et al.*, 2017).

Vessel-based PAM surveys are limited in their temporal coverage and have additional disadvantages of added noise and potential impacts on survey animals. The greatest limitation for vessel-towed arrays is temporal coverage. Vessel operations are

costly, so surveys typically last only a few weeks in duration (Mellinger and Barlow, 2003; Mellinger *et al.*, 2007). Further, times when surveys can be safely conducted are limited by weather; some areas are only accessible during certain seasons (Mellinger and Barlow, 2003; Mellinger *et al.*, 2007; Norris *et al.*, 2012a). Additionally, vessels and arrays being towed behind vessels are prone to low-frequency (<200 Hz) motor and flow noise, which can mask baleen whales that vocalize in the same frequency band (Barlow *et al.*, 2008; Mellinger and Barlow, 2003; Thode, 2004). Finally, a vessel-based survey introduces vessel presence and noise during the survey which may alter the vocal behavior (*e.g.*, changes in calling rate, frequency, and amplitude) of the animals of interest (Guerra *et al.*, 2014; Holt *et al.*, 2009; Lesage *et al.*, 1999).

Mobile autonomous platforms

Since their development in the last two decades, a variety of mobile autonomous platforms have been used in oceanographic research around the world. The term “mobile autonomous platforms” encompasses a variety of autonomous underwater and surface vehicles and floats, most of which were originally developed for oceanographic sampling. These platforms were developed to provide a cost-effective alternative to expensive vessel-based research cruises, and aimed to sample the far reaches of the world’s oceans (Roemmich *et al.*, 2009). In this Introduction I will not focus on the full breadth of platforms available, but rather how three specific autonomous mobile systems have been adapted for passive acoustic monitoring and their broad advantages and disadvantages compared to stationary and vessel-based technologies described above. Verfuss *et al.* (2019) provide an extensive review of all types of unmanned vehicles, including surface, underwater, and aerial systems, currently used for marine mammal research.

This dissertation focuses on three types of mobile autonomous platform: gliders, deep-water profiling floats, and surface drifting buoys. In particular, this research covers the Seaglider (Huntington-Ingalls Industries, Lynnwood, WA, USA), a modified Autonomous Profiling Explorer (APEX) float (Teledyne Webb Research, North Falmouth, MA, USA) called a QUEphone (Matsumoto *et al.*, 2006), and the Drifting Acoustic Spar Buoy and Recorder (DASBR; Griffiths and Barlow, 2015). Both the Seaglider and APEX

float were developed to provide a cost-effective alternative to traditional ship-based oceanographic research. Rudnick (2016) provides an excellent review of glider technologies and oceanographic applications and Roemmich *et al.* (2009) provide a global program of deep-water profiling float deployments and oceanographic surveys. The DASBR was designed specifically for marine mammal acoustic research, so while not used for wider oceanographic sampling, it does provide a promising alternative to vessel-based marine mammal acoustic surveys. Hereafter, the term “glider” is used interchangeably with Seaglider, “float” is used to refer to the QUEphone (unless otherwise specified in each chapter), and “surface drifter” is used interchangeably with DASBR.

The primary motivation for using mobile autonomous platforms for passive acoustic monitoring of marine mammals is to enable data collection over intermediate temporal and spatial scales, compared to fixed or vessel-based surveys, at a moderate cost. The low-power operation of these platforms allows them to be deployed for weeks to months, so not as long as some traditional fixed recorders, but longer than vessel surveys (Verfuss *et al.*, 2019). In the case of gliders, the added ability to follow a specified survey path allows them to traverse bathymetric and oceanographic features (*e.g.*, Burnham *et al.*, 2019) and management boundaries (*e.g.*, Silva *et al.*, 2019), providing the spatial coverage traditionally available only with vessel surveys or costly, extensive stationary arrays. The systems are autonomous and can be deployed from relatively small vessels so they can transit to (in the case of gliders) and survey in remote, or otherwise inaccessible, areas in all seasons (Baumgartner *et al.*, 2014; Burnham *et al.*, 2019; Nieu Kirk *et al.*, 2016). While deep-water and surface floats cannot be steered, they do move with currents and so there is potential to cover large spatial areas, depending on local ocean currents (Griffiths *et al.*, 2019; Matsumoto *et al.*, 2015). Floats are considerably less expensive than gliders so multiple instruments can be deployed in over large spatial scales, and catastrophic loss of an instrument is less concerning, although still not ideal (Griffiths *et al.*, 2019; Keating *et al.*, 2018). Because of these advantages, gliders and floats provide a useful tool for surveying novel regions, and if density could be estimated from glider-collected data, our understanding of marine mammal populations could be greatly extended.

Like any passive acoustic system, gliders and floats have disadvantages as well. Gliders, while relatively quiet systems, are prone to glider-generated noise, either from internal moving parts or low-frequency flow noise generated as a glider moves through the water (Fregosi *et al.*, 2020; Matsumoto *et al.*, 2015). Drifting buoys or floats are less prone to platform-generated noise because they have fewer or no mechanical parts and do not move against water currents; however, this limits horizontal movement. Any horizontal movement is driven by local water currents, so sampling may be biased to areas of particular current activities. Finally, the vertical and horizontal movement of these systems makes potential density estimation complex and prone to violation of several traditional density estimation assumptions. Initial work assessing survey design principles has been done (Harris *et al.*, in revision) and these considerations are discussed further in the density estimation section of this introduction.

Seaglider operation

The Seaglider is a buoyancy-driven system that operates with very low power consumption and relatively low vehicle-generated noise levels because there is no propeller (Eriksen *et al.*, 2001). Vehicle movement is achieved through changes in the glider's volume. Oil is moved between a reservoir inside the sealed pressure hull and an expandable bladder outside the pressure hull. To dive, the glider passively bleeds oil into the internal reservoir, which reduces the glider's buoyancy, causing it to descend vertically in the water column. When the desired depth is reached, the glider actively pumps oil from the reservoir to the bladder, which expands and increases the glider's volume, making the glider less dense than the surrounding sea water and causing it to rise. Horizontal motion is generated from stationary wings that create lift as the glider moves vertically. The glider steers by small changes in its center of gravity. The internal batteries can be moved forward and aft to change glider pitch (also changed with changes in oil distribution) and can be rotated to change glider roll. When the Seaglider is at the surface, communication is possible via Iridium satellite from an antenna on the glider's tail to a shore-based basestation, which a pilot then accesses remotely from anywhere there is a reliable internet connection. The Seaglider uploads its GPS location and selected data and operation files and can receive

updated pilot commands. The Seaglider can dive to 1000 m; a single dive cycle (descent and ascent) to 1000 m typically takes 4-6 hours. Horizontal speeds are approximately 25 cm/s, or 0.5 knots, on average, travelling about 20 km/day over ground.

The Seaglider was originally developed by the University of Washington's Applied Physics Laboratory (Eriksen *et al.*, 2001) and is one of the most widely used glider types. The Seaglider is now manufactured commercially by Huntington-Ingalls Industries and can be purchased with a passive acoustic monitoring system. Prior to the commercially available acoustic system, the engineering team at Oregon State University and NOAA's Pacific Marine Environmental Laboratory's Cooperative Institute of Marine Resources Studies in Newport, OR, US, installed the Wideband Intelligent Signal Processor and Recorder (WISPR; Embedded Ocean Systems, Inc., Seattle, WA, USA) into three Seagliders in OSU's fleet.

APEX float/QUEphone operation

The APEX float is a low-power, buoyancy-driven system like the Seaglider, but it cannot be steered horizontally; controllable movement is limited to depth changes, with horizontal movement driven by local ocean currents (Davis *et al.*, 2001). Like the glider, oil is moved between an internal reservoir within a pressure housing and an external bladder. Communication is via satellite when the float is at the surface, where GPS location and data files are uploaded to the basestation and target drift depths and surfacing cycle commands can be sent by the pilot. APEX floats can descend to 1500 m and drift speeds are dependent on the currents (typically up to a few km per day). The Quasi-Eulerian hydrophone, or QUEphone, is a modified APEX float with the WISPR acoustic system installed (Matsumoto *et al.*, 2006, 2013).

DASBR operation

The DASBR was developed at NOAA's Southwest Fisheries Science Center specifically for monitoring marine mammals using passive acoustics (Griffiths and Barlow, 2015). The aim was to provide a low-cost, easy-to-deploy, and quiet system that could be used to survey in deep offshore waters. The DASBR has undergone multiple iterations in

the last few years, but the basic design was first described by Griffiths and Barlow (2015). Each DASBR consists of a surface float with a GPS logger cabled to a recording system and a two-element vertical hydrophone array suspended at ~100 m depth; the hydrophones are separated by about 10 m. A weight at the base of the DASBR keeps the hydrophones in a vertical orientation (Barlow and Griffiths, 2017). The vertical array allows for estimation of bearing angles to echolocating beaked whales, and if clicks are detected on multiple DASBRs, animals can be localized and tracked (Barlow *et al.*, 2018; Barlow and Griffiths, 2017). Currently DASBRs can be deployed for days to weeks (Griffiths *et al.*, 2019; Keating *et al.*, 2018); if they are to remain in one area, they are typically recovered and re-deployed periodically.

Density estimation of animals from acoustics

To successfully manage and conserve wildlife populations, it is necessary to monitor populations over time and space. Estimating population density or abundance provides a metric for identifying population trends and assessing the effectiveness of implemented management strategies. Absolute population abundance and population density are linked by the equation

$$N = D * A \quad (1.1)$$

where N is the abundance of animals, D is the density of animals per unit area, and A is the area surveyed. The field of animal density estimation is broad, and methods are continually being developed and improved. Often, density is estimated from visual sightings of the animals of interest. Alternatively, density can be estimated from some indirect indicator of an animal's presence, such as visual observations of whale blows or recorded acoustic vocalizations, rather than direct sightings of animals (Buckland, 2006; Buckland *et al.*, 2015; Marques *et al.*, 2013). Different types of acoustic events can be monitored and counted including counting individual calls or echolocation clicks, individual animals, or groups of animals. Further, acoustic events that occur instantaneously such as a single call or echolocation click are known as “cues” and methods that use these acoustic events are known as “cue counting.” Alternatively, the presence of acoustic signals within a set time period can be counted; these time periods are known as “snapshots.” Estimating density

from acoustic data is particularly effective for marine mammals because many species spend the majority of their lives underwater and are difficult to survey visually, but vocalize reliably (Barlow *et al.*, 2013; Marques *et al.*, 2013).

There are several methods for estimating density from acoustic data (see Marques *et al.* 2013 for a thorough review), including plot sampling, distance sampling, and spatially explicit capture-recapture (SECR). These three methods are highlighted here as they have been implemented with marine mammals and have potential applications with autonomous vehicles such as gliders. The choice of method depends on the survey configuration and the amount of information available about the locations of detected acoustic events. Marques *et al.* (2013) provides a flowchart for selecting the best method for each survey design. For consistency with existing literature, I am following the notation used in the equations presented in Marques *et al.* (2013).

Plot sampling

Mathematically, the simplest method is plot sampling. The total number of detected acoustic events, n , is divided by the survey area, a , and one or more estimated multipliers, \hat{r} , (such as a vocalization rate, the proportion of the population that vocalizes, or group size) that convert density of acoustic events to density of animals to estimate density of animals, \hat{D} (a circumflex indicates that a variable is an estimate rather than an exact value).

$$\hat{D} = \frac{n}{a\hat{r}} \quad (1.2)$$

Cue counting or snapshot analyses will also require effort (other than the area surveyed) to be included in the denominator (time for cue counting and total number of snapshot periods for snapshot analyses).

In the case of plot sampling, it is assumed that all acoustic events within the survey area are detected (Marques *et al.*, 2013). Density estimates of two cetacean species, sperm whale and Blainville's beaked whale (*Mesoplodon densirostris*), have been calculated this way using an extensive cabled hydrophone array operated by the U.S. Navy (Moretti *et al.*, 2010; Ward *et al.*, 2012). Ward *et al.* (2012) demonstrated a snapshot approach using the number of clicking sperm whales within a 10-minute snapshot as the acoustic event of

interest, while Moretti *et al.* (2010) counted cues, with each diving group of Blainville's beaked whales (identified from echolocation clicks initiated at the start of each dive) counted as an acoustic event. However, counting all acoustic events is rarely feasible in practice; these types of arrays only exist in a few places in the world and access is restricted.

Distance sampling

Distance sampling overcomes the need to count all acoustic events with certainty by accounting for the proportion of acoustic events that are missed (Buckland *et al.*, 2001). Distance sampling surveys can be conducted as line-transect or point-transect surveys. In the case of line-transect surveys, a set of track lines is randomly distributed through the larger survey area and a vessel traverses the transect, counting animals or cues along the way. Conversely, point-transect surveys consist of a set of randomly distributed survey points, where an observer, or a recorder, surveys for a particular period of time (Buckland *et al.*, 2001). In either case, only a portion of a larger survey area is actually surveyed, but this exact portion is not known. If distances to detected acoustic events can be measured (from an array of hydrophones capable of localizing cues, both stationary and towed, or in a few cases from single recorders, *e.g.*, Harris *et al.*, 2013; Tiemann *et al.*, 2006; Wiggins *et al.*, 2004), then detection probability can be modeled as a function of distance from the recorder, known as the detection function, $g(y)$ (Buckland *et al.*, 2001). From this, an average probability of detection, \hat{p} , can be estimated and placed in the denominator of the density estimator

$$\hat{D} = \frac{n}{\hat{p}a\hat{r}} \quad (1.3)$$

The $\hat{p}a$ term can be combined to form a single variable, \hat{a}_e , the effective survey area. The average probability of detection, \hat{p} , reduces the survey area, a , to the effective survey area, \hat{a}_e , where the same number of animals are present (both detected and undetected) as those detected within the larger survey area, a (Buckland *et al.*, 2001).

Distance sampling has been used to estimate density of a variety of marine mammals through both visual and acoustic line-transect surveys from a vessel (Barlow and Taylor, 2005; Gerrodette *et al.*, 2011; Norris *et al.*, 2017) and point-transect surveys from

fixed acoustic recorders (Marques *et al.*, 2011; McDonald and Fox, 1999). However, distance sampling has its own set of assumptions that may or may not hold in all marine mammal acoustic surveys. Distance sampling assumes that animals are not moving, that distances to detections are measured accurately, and that detection probability at the survey trackline or point is either certain (equal to 1) or is known (Buckland *et al.*, 2001). The number, frequency, and temporal coverage of appropriate surveys remains limited due to the high cost of vessel-based surveys or deployment of appropriate stationary arrays, and the difficulty of estimating detection probability from single recorders because single sensors typically do not provide information on the bearing and range to the sound source.

Spatially explicit capture-recapture

Alternatively, spatially explicit capture-recapture (SECR; also called spatial capture-recapture, SCR) with acoustic data does not require distances to detected cues to be measured. Instead it requires multiple recorders, with known locations, to record the same acoustic event simultaneously (Borchers, 2012; Efford *et al.*, 2009b; Stevenson *et al.*, 2015). The spacing of the recorders and pattern of which recorders did and did not detect the same acoustic event are used to model an average detection probability and effective survey area using a maximum likelihood approach (Borchers and Efford, 2008; Efford *et al.*, 2009b). Density is then estimated as above for distance sampling, but using \hat{a}_e in the denominator rather than \hat{p} and a

$$\hat{D} = \frac{n}{\hat{a}_e \hat{r}} \quad (1.4)$$

While the requirements for SECR are relatively basic (known recorder locations and that acoustic events can be detected on multiple recorders simultaneously; Borchers, 2012), applying the method to marine mammals is still in its infancy and can be difficult to implement practically in the marine environment. As an example, SECR has been applied to minke whales (*Balaenoptera acutorostrata*), using a permanent Navy array to estimate density over both a short and long time scale (Marques *et al.*, 2012; Martin *et al.*, 2013).

Density estimation from slow-moving platforms

Autonomous underwater vehicles, such as gliders, deep-water profiling floats, and surface drifters, have proven to be effective survey platforms for passive acoustic monitoring (PAM) of marine mammals and there is an interest in using these mobile autonomous platforms to estimate marine mammal density (Gkikopoulou, 2018; Harris *et al.*, 2017; Küsel *et al.*, 2017; Marques *et al.*, 2013). Applying passive acoustic density estimation methods to such slow-moving platforms is not straightforward, and this dissertation aims to address some of the considerations.

A primary concern that applies to gliders, deep-water profiling floats, and surface drifters is the slow movement of these platforms. Unbiased density estimation using distance sampling requires that animals are detected at their initial location (*i.e.*, there is not animal movement; Buckland *et al.*, 2001). If animals can move more quickly than the survey platform, they could be counted more than once as they moved around in the survey area, which would lead to an overestimation of density (Buckland *et al.*, 2001; Glennie *et al.*, 2015). Further, any animal movement, either towards or away from the recorder, could bias the measured distances, leading to either over- or under-estimations of density (Buckland *et al.*, 2001). If the survey platform is moving faster than the typical animal movement, such as a vessel transect, this assumption holds. Conversely, if the survey is of a point-transect design, the survey platform is stationary (slower than animal movement) and a “snapshot” or “cue counting” approach is used where observations are made within some time period duration over which animal movement is negligible (Buckland, 2006). Use of snapshots is a reasonable approach to account for potential animal movement in relation to a slow-moving platform (Harris *et al.*, in revision). The glider or float track can be divided into temporal snapshots and each snapshot is then treated as a point-transect sample, rather than treating the path as a continuous survey transect (Harris *et al.*, in revision).

Gliders, which are the most complex of the three systems addressed in this dissertation, in terms of operation and movement, have a few additional issues. Gliders are in constant motion, both horizontally and vertically. This constant movement likely affects the detection probability due to changes in the sound propagation environment and because

of glider-generated flow noise. Sound speed underwater varies with water depth, temperature, and salinity; underwater sound propagation is affected by differences in sound speed (Urick, 1983). Detection probability as a function of range to the detected acoustic event may differ as the glider changes depth and is subject to different sound propagation regimes. Sound propagation may also change as the glider moves horizontally over different bathymetric and oceanographic features, and therefore the detection probability may vary over a survey duration. Additionally, the glider moves up and down in the water column, which turns the traditionally two-dimensional (2D) detection probability as a function of range into a three-dimensional (3D) problem (Buckland *et al.*, 2015). Detection functions are estimated from horizontal range, which is the distance between the acoustic event and the recorder as they lie in a 2D plane (in the marine case, either the seafloor or sea surface). This may become a problem as the glider could be at 900 m depth, directly beneath a whale vocalizing near the surface, and in this case the horizontal range would be 0 m but the acoustic event would truly be 900 m away from the recorder. It may be possible to account for these depth differences if the differences are constant or uniformly distributed (Buckland *et al.*, 2015), but this has not been fully explored for gliders. Variables such as ambient or flow noise levels, glider depth, and location within the survey can likely be addressed by including them as covariates in the detection function, but this highlights the complicated nature of detection probability from a moving platform, and the motivation for this dissertation.

Objectives

The goal of this dissertation is to improve our understanding of how gliders and deep-water profiling floats can be used as passive acoustic platforms for marine mammal monitoring. I focus on two primary gaps in knowledge: how do the detection capabilities of mobile autonomous platforms compare to more traditional bottom-moored systems (Chapters 2 and 4) and how to estimate marine mammal population density from mobile autonomous platforms (Chapters 3 and 5). I address the comparison and density estimation questions for two model species: fin whales and Cuvier's beaked whales. These species were selected because they represent two distinct types of marine mammal vocalizations

that are emitted in vastly different ways and propagate through the water differently, so are likely detected differently. Chapters 2 and 3 focus on fin whale 20 Hz calls – a loud, omnidirectional, low-frequency (<100 Hz) baleen whale call type that can be heard over tens to hundreds of kilometers – and Chapters 4 and 5 focus on Cuvier's beaked whale echolocation clicks – a high-frequency (>25 kHz), highly directional sound that can be heard over only a few kilometers.

Tables

Table 1.1. Comparison of advantages and disadvantages of different passive acoustic monitoring methods used for marine mammal science. Cabled systems cost the most of these systems by far, but the costs are shared among many user communities and the cost for marine mammal acoustic work is relatively low.

Type	Duration	Temporal coverage	Spatial coverage	Visual observations	Cost
Stationary autonomous	years	***	*	No	\$
Mobile autonomous	months	**	**	No	\$\$
Vessel-based	weeks/months	**	**	Yes	\$\$\$
Animal-borne	days	*	*	Yes	\$\$
Cabled	years	***	* to ***	sometimes	\$\$\$/\$

CHAPTER 2: COMPARISON OF FIN WHALE 20 HZ CALL DETECTIONS BY
DEEP-WATER MOBILE AUTONOMOUS AND STATIONARY RECORDERS

Selene Fregosi, Danielle V. Harris, Haruyoshi Matsumoto, David K. Mellinger, Christina
Negretti, David J. Moretti, Stephen W. Martin, Brian Matsuyama, Peter J. Dugan, Holger
Klinck

Published in the Journal of the Acoustical Society of America

Volume 147, Issue 2

Abstract

Acoustically equipped deep-water mobile autonomous platforms can be used to survey for marine mammals over intermediate spatiotemporal scales. Direct comparisons to fixed recorders are necessary to evaluate these tools as passive acoustic monitoring platforms. One glider and two drifting deep-water floats were simultaneously deployed within a deep-water cabled hydrophone array to quantitatively assess their survey capabilities. The glider was able to follow a pre-defined track while float movement was somewhat unpredictable. Fin whale (*Balaenoptera physalus*) 20 Hz pulses were recorded by all hydrophones throughout the two-week deployment. Calls were identified using a template detector, which performed similarly across recorder types. The glider data contained up to 78% fewer detections per hour due to increased low-frequency flow noise present during glider descents. The glider performed comparably to the floats and fixed recorders at coarser temporal scales; hourly and daily presence of detections did not vary by recorder type. Flow noise was related to glider speed through water and dive state. Glider speeds through water of 25 cm/s or less are suggested to minimize flow noise and the importance of glider ballasting, detector characterization, and normalization by effort when interpreting glider-collected data and applying it to marine mammal density estimation are discussed.

Introduction

Passive acoustic monitoring (PAM) is an efficient and cost-effective tool for studying vocal marine mammal species (Mellinger *et al.*, 2007). PAM has been extensively used to study marine mammal behavior (Barlow *et al.*, 2018; Stimpert *et al.*, 2015), identify critical habitats (Yack *et al.*, 2013), understand seasonal migrations (Guazzo *et al.*, 2017), estimate animal density and abundance (Hildebrand *et al.*, 2015; Norris *et al.*, 2017), and facilitate mitigation and management of populations sensitive to human impacts (Van Parijs *et al.*, 2009). Various PAM methods exist, including fixed autonomous and cabled systems (Ioup *et al.*, 2016; Jarvis *et al.*, 2014; Wiggins and Hildebrand, 2007), ship-towed hydrophone arrays (von Benda-Beckmann *et al.*, 2010; Miller and Tyack, 1998; Rankin *et al.*, 2008), and more recently, a range of mobile autonomous platforms (Verfuss *et al.*, 2019). These include subsurface floats and gliders (Baumgartner *et al.*, 2018; Klinck *et al.*, 2012; Matsumoto *et al.*, 2013), surface drifters (Barlow *et al.*, 2018; Lillis *et al.*, 2018), and autonomous surface vehicles (Bittencourt *et al.*, 2018; Klinck *et al.*, 2016a).

Fixed, or bottom-moored, recorders are perhaps the most widely used instrument for marine mammal research. Both autonomous and cabled fixed recorders enable users to collect long-term datasets (months to years in duration), can be deployed in remote areas, record at night and in poor weather conditions, and are not known to affect the behavior of the animal of interest (Mellinger *et al.*, 2007). They are generally very quiet systems, designed to reduce self-noise (Sousa-Lima *et al.*, 2013). They are typically the least expensive PAM method, and use is widespread (Lammers *et al.*, 2008; Mellinger *et al.*, 2007; Sousa-Lima *et al.*, 2013). Cabled systems can provide data in near-real-time and over decades, allowing for both immediate and long-term monitoring (Van Parijs *et al.*, 2009).

However, cabled systems are expensive and so are more typically deployed by governments or large organizations and are restricted to those organizations' areas of interest (Barnes *et al.*, 2007; Mellinger *et al.*, 2007; Sousa-Lima *et al.*, 2013). Arrays of multiple fixed recorders allow for tracking and identifying individual vocalizing animals (Hatch *et al.*, 2012; Helble *et al.*, 2016). Advances in statistical methodologies have allowed for estimation of animal abundance and density from a variety of fixed recorder configurations (Marques *et al.*, 2009, 2013). Autonomous fixed recorders have provided invaluable information on changes in marine mammal populations (*e.g.*, Davis *et al.*, 2017).

The major limitation to a single fixed recorder is the limited spatial coverage. Spatial coverage of any recorder varies with the local sound propagation and ambient sound conditions and by the amplitude and frequency of the target sound (Helble *et al.*, 2013b; Mellinger *et al.*, 2007; Širović *et al.*, 2007; Ward *et al.*, 2011; Zimmer *et al.*, 2008). Lower frequency (< 1kHz) signals are potentially detectable over tens to hundreds of kilometers (Širović *et al.*, 2007; Stafford *et al.*, 2007) while higher frequency signals may only be detectable a few kilometers away or less (Zimmer *et al.*, 2008). Both natural and human-generated noise (from ships, weather, etc.) may mask calls of interest and further reduce the detection range (Helble *et al.*, 2013a; Stafford *et al.*, 2007; Ward *et al.*, 2011). A large array of instruments can be deployed to cover a greater survey area, including diverse habitats; however, this increases costs and processing the huge quantities of collected data (often many tens of terabytes) can be challenging (Lammers *et al.*, 2008; Van Parijs *et al.*, 2009; Roch *et al.*, 2016; Sousa-Lima *et al.*, 2013).

Ship-towed acoustic recorders are also commonly used for marine mammal surveys. These mobile systems provide better spatial coverage than fixed instruments (Mellinger *et al.*, 2007). They can combine visual and acoustic observations allowing identification of species-specific sounds (Rankin *et al.*, 2007; Rankin and Barlow, 2005), or linking of acoustic and surface behavior (Miller and Tyack, 1998). Towed recorders can provide information on important habitat (Yack *et al.*, 2013) and have the advantage of providing data in real-time (Van Parijs *et al.*, 2009). Like fixed arrays, towed arrays can be used to track vocalizing animals (Thode, 2004), identify calling individuals (Quick and Janik, 2012), and estimate animal abundance or density using a distance sampling framework (Buckland *et al.*, 2001; Norris *et al.*, 2017).

Ship-based instruments also have their disadvantages, primarily limited temporal coverage. Surveys typically last only a few weeks due to the high cost of ship operations over extended time periods (Mellinger and Barlow, 2003; Mellinger *et al.*, 2007). Surveys are limited by weather conditions and seasonal accessibility to an area (Mellinger and Barlow, 2003; Mellinger *et al.*, 2007; Norris *et al.*, 2012a). Ships generate low-frequency noise and ship-towed arrays generate low-frequency flow noise as they move through the water which may mask low-frequency vocalizing baleen whale species (Barlow *et al.*, 2008; Mellinger and Barlow, 2003; Thode, 2004). Lastly, ship presence and associated vessel noise may alter the vocal behavior of the animals of interest (*e.g.*, Guerra *et al.*, 2014; Holt *et al.*, 2009; Lesage *et al.*, 1999), and echosounders have been found to influence the vocal behavior of beaked whales (Cholewiak *et al.*, 2017).

Over the past few decades, two types of deep-water mobile autonomous platforms, gliders and profiling floats, have been developed for oceanographic research (Roemmich

et al., 2009; Rudnick *et al.*, 2004). They provide *in situ* measurements of temperature, salinity, oxygen, currents, and many other metrics (Roemmich *et al.*, 2009; Rudnick *et al.*, 2004). They can provide processed data in near real-time via satellite connection (Roemmich *et al.*, 2009; Rudnick *et al.*, 2004). These low power platforms can cover large, otherwise inaccessible areas and be deployed for weeks to months at a time, providing data across both large spatial and temporal scales at an intermediate cost to cabled or ship-based systems (Roemmich *et al.*, 2009; Rudnick *et al.*, 2004).

Two such instruments are the SeagliderTM (Kongsberg Underwater Technologies, Inc, Lynnwood, Washington, USA) and the QUEphone, an acoustically equipped APEX float (Teledyne Webb Research, North Falmouth, Massachusetts, USA). The Seaglider is remotely piloted using Iridium satellite communications to transit between specified waypoints or along a defined heading. It dives up and down in the water column, to maximum depths of 1000 m, through small changes in buoyancy created by pumping oil in and out of an external bladder. Pump operation can be adjusted to change vertical speed and thrust. Roll and pitch are altered through lateral and rotational movement of internal batteries. Dive cycles typically last 4-6 hours, with brief surface intervals for communication with a shore station. The QUEphone is capable of descending to 1,500 m. Once the platform reaches the programmed depth, it drifts passively with the currents. Like the Seaglider, depth is controlled through small changes in buoyancy created by expansion or contraction of an external bladder. Dive cycles typically last 24 hours, and dive depth and timing can be controlled remotely via Iridium satellite communication.

More recently, gliders and floats have been outfitted with a variety of passive acoustic recorders (Baumgartner and Fratantoni, 2008; Klinck *et al.*, 2012; Küsel *et al.*,

2017; Matsumoto *et al.*, 2006; Moore *et al.*, 2007; Van Uffelen *et al.*, 2017). Several studies have demonstrated the ability of such platforms to record and detect many marine mammal species (Baumgartner *et al.*, 2013; Klinck *et al.*, 2016a; Küsel *et al.*, 2017; Matsumoto *et al.*, 2013), including near-real-time observations (Baumgartner *et al.*, 2013; Davis *et al.*, 2016; Klinck *et al.*, 2012). Surveys have included offshore regions that are otherwise difficult to study (Burnham *et al.*, 2019; Nieukirk *et al.*, 2016).

Mobile autonomous platforms provide intermediate temporal and spatial coverage between fixed and ship-based PAM methods (Verfuss *et al.*, 2019). Thus far, battery and storage constraints have limited deployments to four months or less, depending on the platform, instrumentation, and survey specifications, but there is potential for improvements in capacity (Cauchy *et al.*, 2018; Klinck *et al.*, 2015a; Mellinger *et al.*, 2017). Although a glider moves much slower than a ship ($\sim 1/2$ knot; Rudnick *et al.*, 2004), and a profiling float's movement is current driven and so can be difficult to control or predict (Roemmich *et al.*, 2009), the area surveyed by these mobile autonomous platforms extends beyond what is possible with a fixed recorder.

However, the vertical and horizontal movement of gliders and floats present potential challenges and special considerations for collecting and interpreting data, compared to traditional PAM methods. The ability of any acoustic system to record and detect a sound of interest depends on the recording system hardware and software (Mellinger *et al.*, 2007), the survey environment (Helble *et al.*, 2013b; Küsel *et al.*, 2011), and the analysis process (Leroy *et al.*, 2018; Marques *et al.*, 2013; Širović, 2016). Specifically, hardware and software limits, detector performance, and survey effort must be quantified for each recording system before meaningful interpretation of the collected

data is possible. Unique operational aspects of gliders and floats may affect detector performance and how survey effort is defined.

Generally, detector performance can be influenced by a) transient platform self-noise that triggers a false positive detection and b) sustained platform-generated flow noise and/or increased ambient noise conditions which may lead to excessive missed detections (Helble *et al.*, 2013a; Leroy *et al.*, 2018; Ward *et al.*, 2011). Autonomous mobile platforms may be more prone than other platforms to false positive detections. Glider and float buoyancy adjustments are made via a loud, motorized pump (Matsumoto *et al.*, 2015; Roemmich *et al.*, 2009; Rudnick *et al.*, 2004), and the glider's flight path is controlled by changes in the glider's pitch or roll orientation via motor-driven changes in the center of mass (Matsumoto *et al.*, 2015; Rudnick *et al.*, 2004). Additionally, Seagliders are operated at speeds that correspond to large Reynolds numbers (very approximately, the velocity times length divided by fluid kinetic viscosity) of 350,000 to 600,000 (Rudnick, 2004). Motion or flow within any fluid becomes turbulent when the Reynolds number is sufficiently large, and turbulent flow introduces low-frequency noise as low-frequency pressure waves. This flow noise has been documented previously on acoustically equipped Seagliders (Matsumoto *et al.*, 2015; dos Santos *et al.*, 2016).

Defining survey effort for a mobile platform is more complicated than a fixed recorder or towed array. Total survey effort for a mobile platform can be considered in terms of the area covered and the time spent monitoring (Marques *et al.*, 2013). For a glider or float, survey effort in the time domain is dependent not only on the sampling regime and duty cycle, but also operational differences such as surfacing periods and depth or dive state dependent operation of the recorder. In the space domain, survey effort depends on

the platform's velocity and its maximum detection radius. Within a maximum detection radius, target signals will be detected with some probability, which is often a function of range – *i.e.*, calling animals further away will tend to be more difficult to detect (Marques *et al.*, 2013). Quantifying differences in the detection probability becomes increasingly complex for a vertically and horizontally moving platform as detection range may be altered by the sound propagation environment (Helble *et al.*, 2013b) as it changes with platform depth or location, or platform-induced flow noise (Matsumoto *et al.*, 2015).

These variables all have the potential to influence a recording system's performance, and thus the interpretation of data collected by that system. But to date, no thorough comparison of detection capabilities between fixed or ship-towed recorders and deep-water autonomous mobile recorders has been performed. Such comparisons are necessary across a range of marine mammal sound types to gain a better understanding of the advantages and limitations of these mobile platforms as PAM systems, enable comparison with historical data sets, and ultimately estimate animal abundance and density (Marques *et al.*, 2013; Thomas and Marques, 2012; Verfuss *et al.*, 2019).

Here we present a comparative study of system performance detecting a low-frequency marine mammal call for two types of deep-water autonomous mobile platforms and a fixed seafloor hydrophone array. One acoustically equipped glider (Seaglider) and two acoustically-equipped profiling floats (QUEphone) were deployed simultaneously in the vicinity of a well-studied stationary hydrophone array at the Southern California Offshore Range (SCORE; Jarvis *et al.*, 2014). We used an automated detector to quantify the presence of fin whale, *Balaenoptera physalus*, 20-Hz pulses (Watkins *et al.*, 1987) in data collected from the three recorder types. (Another species detected, Cuvier's beaked

whales, *Ziphius cavirostris*, will be the subject of future analyses). We compared detector performance, total calls detected, hourly detection rates, and hourly and daily presence and absence of calls across the recorder types. For the glider, we examined how detection rates changed with platform movement and platform-induced noise levels. Finally, we provide recommendations for future steps to improve and expand applications of mobile autonomous vehicles for marine mammal research.

Methods

Acoustic systems

The Wideband Intelligent Signal Processor and Recorder (WISPR), commercially available from Embedded Ocean Systems, Inc. (Seattle, Washington USA), has been integrated into both the Seaglider and QUEphone. WISPR receives signals via a single omni-directional hydrophone (HTI-92-WB, High Tech Inc., Gulfport, Mississippi, USA; sensitivity: -175 dB re 1V/ μ Pa +/- 3 dB frequency response from 2 Hz to 50 kHz). A frequency-dependent gain curve, which approximately matches the inverse of the typical deep-water ambient sound profile, is applied prior to digitization (see Matsumoto *et al.*, 2015). The analog signal is recorded at a 125 kHz sampling rate with 16-bit resolution and compressed using the Free Lossless Audio Codec (FLAC). The recording system on both the glider and float operates continuously and can be programmed to turn on and off at a specified depth. Depth limits can also be modified remotely via Iridium satellite communication during a deployment.

The Marine Mammal Monitoring on Navy Ranges system (M3R; Jarvis *et al.*, 2014) connects to an extensive cabled, bottom-mounted hydrophone array operated by the

U.S. Navy at SCORE, approximately 150 km northwest of San Diego off the western shore of San Clemente Island in the San Nicolas Basin. The array of 178 hydrophones is typically used for tracking underwater vehicles and also provides input data to the M3R system, which is capable of recording, detecting, and localizing marine mammal vocalizations (Ierley and Helble, 2016; Jarvis *et al.*, 2014; Moretti *et al.*, 2016). The hydrophones are moored near the seafloor at depths from 800-1,800 m and spaced approximately 4 km apart. The bandwidth of the subset of 79 hydrophones used in this study is from ~50 Hz to 50 kHz but are useable down to 20 Hz (Jarvis *et al.*, 2014; Moretti *et al.*, 2016). The M3R system records the SCORE array at a sample rate of 96 kHz and 16-bit resolution in a packet format; data can also be processed and viewed in real-time (Jarvis *et al.*, 2014; Moretti *et al.*, 2016).

Field deployment

One acoustic Seaglider (SG158) and two QUEphones (Q001 and Q002) were deployed on 22 December 2015 just north of SCORE for a performance comparison with the M3R system (Figure 2.1 and Table 2.1). The glider surveyed the area in evenly spaced (~10 km) transects, repeatedly diving to 1000 m depth (Figure 2.2). The QUEphones were deployed 17 km apart with the expectation that they would drift southeast in parallel to cover approximately equal areas of the SCORE range. They were initially programmed to drift at a depth of 1000 m, surfacing every 24 hours (Figures 2.1, 2.2). However, the current systems in the Southern California Bight are complex (*e.g.*, Bray *et al.*, 2002; Dong *et al.*, 2009; Hickey, 2003) and not easy to predict over small temporal and spatial scales. Q002 initially drifted northward and away from the range while Q001 drifted to the east across

the range very slowly (Figure 2.1). To change the drift direction and speed, drift depth was increased to 1,200 m and then decreased to 500 m (Figure 2.2), causing Q002 to reverse course and drift to the south and southeast, and causing Q001 to drift more quickly to the east.

To conserve battery and data storage space, the WISPR system on Q001, Q002, and SG158 was turned off at depths shallower than 200 m. Mid-frequency (500 Hz to 25 kHz) ambient ocean sound levels are typically higher near the surface (Hildebrand, 2009), and Cuvier's beaked whales, a separate target species of this deployment, are known to echolocate primarily below 200 m (Johnson *et al.*, 2004). Therefore, depths above 200 m were deemed non-optimal recording conditions and the system was powered off. On SG158, the hydrophone was mounted inside the hull in the rear third of the glider, near the external buoyancy bladder. For the QUEphones, the hydrophones were mounted externally on the top, near the antenna. All mobile platforms were recovered on 4 January 2016.

Concurrent with the mobile survey, the M3R system recorded acoustic data from 79 bottom-mounted hydrophones. The 8 TB hard drives utilized for acoustic recording on the range wrote data at an insufficient speed, which caused write errors as the data drives approached capacity (after ~96 hours of recording on each). This caused two major data dropouts as the first and then second disks filled, resulting in loss of approximately 100 hours of data per hydrophone (out of 372 total deployment hours; Table 2.1). To maintain uniformity in comparisons of detection abilities across all recorder types, analyses were restricted to the periods when all three mobile systems were deployed and the SCORE array was recording properly (Table 2.2), hereafter referred to as the overlap periods.

Acoustic analyses

Initial data processing included downsampling glider and float WISPR recordings to 1 and 10 kHz sampling rates for easier viewing of the low-frequency noise and fin whale calls and converting the M3R recordings from the packet format to FLAC files using the MATLAB-based toolbox Raven-X (Dugan *et al.*, 2018, 2016).

Call detection

A spectrogram correlation template detector (Mellinger and Clark, 2000) targeting fin whale 20 Hz pulse calls (Watkins *et al.*, 1987) was run across all datasets using the MATLAB-based toolbox Raven-X (Dugan *et al.*, 2018, 2016). The template algorithm tested three synthetic frequency sweep templates: (1) 17 to 24 Hz over ~1 second, (2) 19 to 26 Hz over ~1.25 seconds, and (3) 18 to 23 Hz over ~1.5 seconds. All template spectrograms had a 2 kHz sampling rate, 2048 sample Hann window (3 dB filter bandwidth: 1.404 Hz) with 75% overlap. For each candidate fin call, a single detection event was finalized against the template that had the highest normalized spectrogram correlation score. Call duration and bandwidth were set according to the finalized template. Signal-to-noise ratio (SNR) was calculated in MATLAB using the M29 measurement from Mellinger and Bradbury (2007).

Detector performance across recorder types was evaluated through manual annotation of a subset of recordings from M3R, SG158, and Q001. A five-minute sample period was randomly selected from within every seventh hour initially, and then within every third hour to increase the sample size, resulting in samples taken from within every third to fourth hour (e.g. 0000, 0300, 0700, 1000, 1400, etc.) throughout the overlap period. These hours were selected to avoid coinciding with the timing of platform dive cycles or

potential diel patterns in vocalizations. For each five-minute annotation period, a single M3R hydrophone was randomly selected for manual annotation to ensure the detector was evaluated over a spatially representative sample of M3R hydrophones. If the five-minute period fell when the glider or QUEphone's acoustic system was off (because it was at or near the surface) that hour was skipped. Fin whale 20 Hz calls (30-15 Hz, 1 sec duration downsweeps) were manually annotated by an experienced analyst (CN) in Raven Pro 1.5 (Ithaca, New York, USA) on the 1 kHz sampling rate data using a 2048-sample Hann window (3 dB filter bandwidth: 0.702 Hz) with 95% overlap. The SNR for each manual detection was calculated the same way as the detector-generated detections, in MATLAB using the M29 measurement from Mellinger and Bradbury (2007). Manual detections were considered true detections and compared to detector outputs using custom MATLAB scripts; detections were classified as true positives if they overlapped with the manually marked call by at least 50% in both time and frequency. Visual inspection of a subset of false positives and missed detections confirmed this overlap criterion was appropriate. Precision (proportion of total detections that were correct detections), recall (proportion of true calls that were correctly detected), and false positive rate (the proportion of total detections that were incorrect detections) were calculated as outlined in Mellinger *et al.* (2016). Precision and recall were not normally distributed, so a Kruskal-Wallis test was performed to test the null hypothesis that precision and recall values for each recorder type had equal distributions. A *post hoc* Dunn's multiple comparison test on significant results identified pairwise differences.

For each recorder, detections were binned hourly and normalized by total recording minutes in that hour (hereafter referred to as detections per hour). Median detections per

hour and interquartile ranges (IQR; 25-75%) were calculated for M3R per deployment hour (median across all hydrophones) and per hydrophone (median across all deployment hours). A Kruskal-Wallis test was used to test the null hypothesis that detections per hour across all M3R hydrophones had equal distributions. Then, the closest M3R hydrophone to each mobile platform for each hour was identified by the shortest great-circle distances between each M3R hydrophone and mean latitude and longitude of the mobile platform during that hour. Because detections per hour were non-normally distributed, a Wilcoxon signed rank test was used to test the null hypothesis that detections per hour on each mobile platform had the same distribution as the detections per hour on the closest M3R hydrophone at each hour. Exploratory analyses showed apparent higher flow noise levels during glider descents compared to ascents so glider detections per hour were categorized by dive state and again compared to the closest M3R hydrophone using a Wilcoxon signed rank test. Glider dive states were assigned using the vertical velocity measured by the glider's pressure sensor every minute. Hours with all negative vertical velocities were categorized as descents and hours with all positive vertical velocities were categorized as ascents. Hours with a mix of positive and negative vertical velocities were not included in the statistical analysis. Finally, the number of detections per hour was compared to mean platform depth per hour for the three mobile recorders. To test the null hypothesis of no correlation between the number of detections per hour and platform depth, a Spearman's rank correlation test was selected as it can account for the non-normality and unequal variance. Significance of all statistical tests was assessed at the 5% ($p = 0.05$) level.

Noise levels

To examine inter and intra-recorder differences in sound levels across both frequency and time, Long-Term Spectral Average plots (LTSAs; Wiggins and Hildebrand, 2007), with 10 sec temporal and 1 Hz frequency resolution were calculated from 10 to 5000 Hz for each mobile platform. Spectral Probability Density (SPD) plots were created from the LTSAs following the methods outlined in Merchant *et al.* (2013). SPD is the empirical probability density of the power spectral density at each frequency. It allows examination of how sound level variation is distributed in both frequency and time in a long-term acoustic dataset (Merchant *et al.*, 2013). Median (50th), 5th, and 95th percentile levels were calculated for each mobile platform, and for the glider during ascents and descents separately, at three frequencies of interest: 12 Hz (“low flow noise”), 40 Hz (“high flow noise”) and 3000 Hz (“wind noise”). The 12 and 40 Hz frequency points were selected as indicators for low-frequency flow noise on either side of the frequency band of fin whale 20-Hz pulses. Sound levels below 50 Hz have been used previously to characterize flow noise over animal-borne acoustic recording tags (*e.g.*, von Benda-Beckmann *et al.*, 2016; Goldbogen *et al.*, 2006) and have been found to be correlated with Seaglider speed (dos Santos *et al.*, 2016), and 3000 Hz, above typical flow-noise frequencies, was selected to represent wind-driven ambient ocean noise to examine changes in sound levels over time and with glider state. A frequency of 3000 Hz has proven useful to describe surface wind in a passive acoustic glider application and in acoustic animal-borne tag recordings (von Benda-Beckmann *et al.*, 2016; Cauchy *et al.*, 2018). All noise levels reported hereafter are power spectrum density levels in dB re 1 $\mu\text{Pa}^2/\text{Hz}$.

A regression analysis was used to explore the relationship of glider speed and orientation with low- and mid-frequency noise levels. All three power spectrum density levels were modeled against vehicle dive state as a categorical variable (ascent vs descent defined by positive or negative glider measured vertical velocity, respectively), and an estimate of speed through water and time as continuous variables, in R 3.5.3 (R Core Team, 2019). We assumed noise levels were consistent over one minute and extracted the lowest 12, 40 and 3000 Hz power spectrum density level (10 sec Hann window, 0% overlap) per minute to represent noise level in that minute (to remove transient sounds). Speed through water was estimated as the vertical velocity divided by the sine of vehicle pitch. Glider vertical speed and pitch are directly measured by the glider's sensors but are collinear with one another, so they were combined into a single simplified explanatory variable. While the glider's on-board movement models do calculate total vehicle velocity and horizontal speed through water, those parameters have been shown to have high errors (Van Uffelen *et al.*, 2013, 2016), so were not included. Dives 1 through 6 were excluded from the regression analysis because these were shallow trimming dives (less than 200 m) in which the glider pilot is adjusting many flight parameters to balance the glider for the *in situ* ocean conditions. Finally, noise levels and speed through water were binned every 30 minutes. Time was defined as the start of each 30-minute bin and median values of noise level and speed through water in each bin were used to build the final regression data set ($n = 500$ bins). Binning was performed because the full dataset ($n = 15,377$ minutes) was too computationally expensive to model successfully. Median values were used for noise level and speed through water because minute-scale data were not always normally distributed

within each 30-minute bin. The full model included an interaction term between speed through water and dive state:

$$\begin{aligned} \text{noise} \sim & \text{speedThroughWater} + \text{diveState} + \text{time} \\ & + \text{speedThroughWater}:\text{diveState} \end{aligned}$$

Model fitting was conducted at each frequency band independently. Residual plots were inspected and diagnostic tests were conducted to check the assumptions of constant error variance, error independence, and normality. Cook's distance was used to remove outliers, which corresponded to time periods when the glider's motors were on. These data violated assumptions of independence and equal error variance at all three frequencies. A Generalized Least Squares (GLS) model was selected because it is an extension of linear regression that allows for heteroscedasticity and non-independence by applying weighted variance and correlation structures (Zuur *et al.*, 2009). The optimal variance and correlation structures were chosen for each frequency independently using the full model and comparison of Akaike's Information Criteria (AIC). Inclusion of the interaction terms and all explanatory variables was verified using a step-down procedure and comparing AIC scores. Predictions of power spectrum density levels were calculated at speeds of 13 to 31 cm/s for ascents and 24 to 53 cm/s for descents, in 1 cm/s increments, with time held constant for 12 and 40 Hz. These values were selected because they spanned the minimum and maximum speed values for each dive state, and median time was used as the constant time value. Because speed through water was not included in the final 3000 Hz model, predictions of power spectrum density at 3000 Hz were calculated at times of 0 to 12 days, in 12-hour increments. Significance of all coefficients was assessed at the 5% ($p = 0.05$) level.

Results

M3R recorded 220 hours per hydrophone (Table 2.1), or 17,380 total hours on 79 hydrophones, during the 220 hours of the overlapping periods (Table 2.2). SG158 recorded 178 hours, and Q001 and Q002 recorded 200 and 203 hours of the overlapping periods, respectively (Table 2.1). An LTSA of the entire deployment period for all mobile recorders can be found in Figure A1.¹ The glider covered a total distance of 261 km, at an average rate of 19 km/day, while the QUEphones drifted 47 km (Q001) and 53 km (Q002) both at a rate of less than 4 km/day (Table 2.1).

Call detection

A total of 49, 58, and 64 five-minute periods were annotated for the SG158, Q001, and M3R recordings, respectively (Table 2.3). Overall detector performance was similar for all recorders, with median precision over 86% and median recall over 50% (Table 2.3 and Figure 2.3; $\chi^2(2) = 5.46$, $p = 0.07$, and $\chi^2(2) = 2.13$, $p = 0.34$). Variability within each recorder, across five-minute sample periods, was high, with IQRs from 15 to 22%. When glider ascents and descents were treated as separate groups, precision during descents was near perfect (median 100%; almost zero false alarms) and was statistically different than the other recorders and glider ascents ($\chi^2(3) = 22.64$, $p < 0.001$). Conversely, recall was elevated during glider ascents (fewer misses), compared to glider descents, Q001, and M3R, but this difference was not statistically significant. Median recall was not the same across all recorder types and glider dive states ($\chi^2(3) = 9.02$, $p = 0.03$), however, the *post hoc* Dunn's multiple comparison test, which adjusts for the number of comparisons, showed no significant difference in any of the pairwise comparisons. Detection SNR

distributions and results from the detector evaluation statistical tests can be found in Figures A2-4.¹

Fin whale detections were present on all days on all M3R hydrophones. Total detections per M3R hydrophone ranged from 29,093 to 46,707 (median 42,176). Median hourly detections across the deployment duration ranged from 4.0 (IQR 1.0 – 12.75) to 322.0 (IQR 310.5 – 333.0) detections per hour. Only 24 total hours, or 0.1% of total possible hours of all hydrophones, had no fin whale detections. Median detections by hydrophone, across all deployment hours, ranged from 149 (IQR 106.5 – 211.0) to 217.5 (IQR 174.0 – 264.0) detections per hour. A Kruskal-Wallis test showed that variation in median detections was significant across hydrophones ($\chi^2(78) = 555.47$, $p < 0.001$), with more southerly, shallower hydrophones having fewer detections (Figure A5¹).

Q001 had 39,214 and Q002 had 41,265 total detections, with detections present on all days. Q001 and Q002 had median hourly detection rates of 204.0 (IQR 152.0 – 246.0) and 218 (IQR 154.0 – 255.0) detections per hour, respectively (Figure 2.4). Q002 had only one hour in which no detections were reported (0.5%). Detections per hour on Q001 were not significantly different from the detections per hour on the closest M3R hydrophone ($Z = -0.8$, $p = 0.4$; Figure 2.4). Similarly, hourly detection counts for Q002 were not significantly different from detections per hour at the closest M3R hydrophone ($Z = -0.7$, $p = 0.5$; Figure 2.4), or from Q001 ($Z = -1.7$, $p = 0.08$). Detections per hour did not correlate with platform depth for either Q001 ($\rho = -0.113$, $p = 0.1037$) or Q002 ($\rho = 0.027$, $p = 0.692$).

SG158 had a total of 20,522 detections, with detections present on all days. The median number of detections per hour was 96.3 (IQR 48.0 – 171.5; Figure 2.4). After

normalizing for recording time, six hours (2.7%) had no fin whale detections. The median number of detections per hour by the glider was less than half the median number of detections per hour by Q001 and Q002 and the closest M3R hydrophone (Q001: $Z = -11.1$, $p < 0.0001$; Q002: $Z = -11.5$, $p < 0.0001$; M3R: $Z = -11.8$, $p < 0.0001$; Figure 2.4). When glider ascents and descents were examined separately, the median number of detections per hour during glider descents was 78% less than M3R ($Z = -7.37$, $p < 0.0001$) but during ascents was only 18% less than M3R ($Z = -6.49$, $p < 0.0001$; Figure 2.4). Hourly detections did not correlate with glider depth ($\rho = 0.095$, $p = 0.187$). Hourly detection counts for each recorder are available in Supplemental Table 2.1.¹

Noise levels

Overall noise levels measured by all instruments were variable, and relatively high throughout the deployment (Table 2.4; Figures 2.5, 2.6), likely due to periods of high wind, wave, and rain activity as is typical in the winter months offshore of the Channel Islands. LTSA and spectral probability density plots were marked by high received levels around 20 Hz, a signature of the near-constant fin whale calling activity (Figures 2.5, 2.6). Elevated noise levels below 60 Hz can be observed for SG158 in the LTSA (Figure 2.5), particularly during descents. Sound levels across all frequencies were more variable for SG158 than Q001 or Q002 (Figure 2.6). Median power spectrum density levels for all instruments were 5 to 12 dB higher at 12 Hz than 40 Hz and 17-27 dB higher at 40 Hz than 3000 Hz (Table 2.4 and Figure 2.7). Median power spectrum density levels on the glider were 15, 10, and 4 dB louder than the QUEphones at 12, 40, and 3000 Hz, respectively (Table 2.4 and Figure 2.7).

Glider ascents were generally quieter than glider descents. Ascents tended to be slower, with a steeper glider pitch angle. Mean glider speed was 9.3 (SD: 1.4) cm/s during ascents and 12.4 (SD 2.4) cm/s during descents. Glider pitch was bimodal for both ascents and descents. Ascents showed a main peak at 24° and a smaller peak at 34° (median 24.2°). Descents showed a main peak at 18° and a smaller peak at 29° (median 17.9°). The steeper pitch angles that created these secondary peaks coincided with time periods when the glider was within a few km of the target waypoint where it is programmed to perform a steeper dive to not overshoot that waypoint.

Regression analysis results varied for each frequency of interest, including the optimal model and correlation structure. Exploratory and residual plots can be found in Figures A6 to A14.¹ The independence assumption was no longer violated after applying an autocorrelation-moving average (ARMA) correlation structure of order $p = 1$ and $q = 0$ to all frequencies. Non-constant variance was accounted for at 12 and 40 Hz using an identity variance structure which allowed variance to differ by dive state. The preferred variance structure at 3000 Hz was a combined variance structure including an identity structure of dive state and a constant-plus-power structure which allowed variance to also differ by time.

The preferred model at 12 Hz included explanatory variables for speed through water, dive state, and the interaction between speed through water and dive state, but did not include time. All explanatory variables had a significant effect on 12 Hz noise levels (Table 2.5). During ascents 12 Hz noise levels increased 1.3 dB with every 1 cm/s increase in speed through water. During descents, 12 Hz noise levels increased only 0.65 dB per 1 cm/s increase in speed through water (Table 2.5) but descents were generally faster, and

louder, than ascents (Figure 2.8). The full model was preferred at 40 Hz, with strong correlations with speed through water, dive state, and the interaction term. Time was a significant explanatory variable ($p = 0.0021$) but the effect was minimal (-0.0002, Table 2.5). At 40 Hz, a 1 cm/s increase in speed increased noise levels by 0.34 dB during ascents and by 0.60 dB during descents (Table 2.5, Figure 2.8). Like at 12 Hz, descents were generally louder at 40 Hz as well (Figure 2.8). Only dive state and time were preferred in the best model of 3000 Hz noise levels, and time did not have a significant effect (Table 2.5, Figure 2.8). Descents were, on average, only slightly (1.5 dB) louder than ascents (Table 2.5).

Discussion

Through analysis of recordings collected by simultaneously deployed passive acoustic recorders, we have provided validation that acoustically equipped deep-water mobile autonomous platforms such as Seagliders and QUEphones can successfully monitor low frequency marine mammal vocalizations. This study provides the first documentation of potential differences in survey capabilities of gliders and profiling floats compared to stationary bottom-mounted recorders. Overall detector performance did not vary by recorder type but was highly variable depending on noise conditions. Fine scale temporal differences in the number of fin whale call detections by each system were related to operational differences including depth-dependent duty cycling and glider speed. Elevated glider speeds introduced flow noise in the frequency band of fin whale calls which, at times, completely masked fin whale calls. However, hourly and daily presence of fin whale call detections, as is typically reported in baleen whale monitoring surveys, were the same

across all recorder types. Further, flow noise was not apparent in spectra at higher frequencies and was indeed not significant at 3000 Hz. Interestingly, number of detections per hour did not vary with mobile platform depth. This study supports future use of acoustically-equipped gliders to provide intermediate spatiotemporal coverage in surveys of low-frequency vocalizing marine mammals and proposes sampling and flight considerations for future deployments.

The glider surveyed over 250 km in two weeks. It followed the designated survey plan very well, traversing the target survey area (the SCORE range) near its predicted speed of 20 km/day. The effects of local currents on SG158's ability to follow its programmed track were minimal compared to other Seaglider deployments (Harris *et al.*, 2017). This supports that control of a Seaglider is sufficient to set up and conduct a design-based survey with defined transects (Buckland *et al.*, 2001; Harris *et al.*, 2017; Verfuss *et al.*, 2019) and *et al.*, 2001; Verfuss *et al.*, 2019). Conversely, drift speed and direction of the QUEphones were depth-dependent and difficult to predict. For example, while Q001 and Q002 were deployed only 17 km apart both drift speed and direction of each varied over the deployment duration. Although both floats eventually drifted onto SCORE, they spent considerably less time recording in the target survey area compared to the glider. Relying on a drifting platform to follow a planned survey track may be risky unless the currents of the area are well-documented and understood. While it may be possible to follow survey design principles (*e.g.*, Buckland *et al.*, 2001) to deploy an array of drifting recorders to cover a representative portion of a larger study area (*e.g.*, Griffiths and Barlow, 2016), the survey design cannot always be ensured.

Total hours recorded by the glider and both QUEphones did not equal the total time they were at sea, nor the total hours recorded by the M3R system. The glider and QUEphone had fewer total recorded hours than the M3R system because the PAM system was shut off at depths shallower than 200 m to preserve battery and storage space (Figure 2.2 and Figure A1 – black bars¹). This duty cycle was specific to this deployment, the dive cycle durations for the glider and QUEphones, and the WISPR recording system. The difference in recording time across recorders was easily quantified by normalizing call counts by recording duration. PAM system operation can be adjusted to operate almost continuously (excluding surface intervals) or at any duty cycle desired, and in future work call counts should be normalized accordingly. Additionally, call counts may need to be further adjusted for the times in which the glider or QUEphone buoyancy pump operates (less than 10 minutes or ~3% of total recording time per dive), which masks any possible detections during that time (Matsumoto *et al.*, 2015).

Deployment-scale detector performance was not negatively affected by glider or float platform self-noise (motor or flow noise), but this finding is specific to the low-frequency, relatively long duration and regular calling bouts of this study's target species. The near-zero false alarm rate observed during glider descents, when flow noise was greatest, was conceivably because any faint or reflected calls were masked from detection by the detector and the manual observer. Precision will still need to be assessed on a species, call-type, and detector/deployment basis since transient broadband platform noise may cause false detections of transient broadband marine mammal sounds, like echolocation clicks.

Hour-to-hour variability in detector performance observed on both mobile and stationary recorders was likely due to the highly variable, weather-related, 10-5000 Hz soundscape (ambient sound levels) observed during the deployment, and because of the near-constant fin whale calling that sometimes resulted in a “chorus band” around 20 Hz. This hour-to-hour variability likely explains why differences in precision were significant only between glider ascents and descents, but not between the glider (all dive states), floats, and M3R. Variability in recording conditions can alter detector performance and discussions of the assessment and reliability of detector performance over long-term datasets spanning multiple seasons, different soundscapes, and particularly between and within analysts is ongoing (Leroy *et al.*, 2018; Širović, 2016). Because the glider is likely subject to non-constant recording conditions, it is important that that detector performance is thoroughly characterized when detectors are used to analyze mobile platform-collected data.

Increased low frequency flow noise during the glider’s descending phase essentially decreased the maximum detection range of the glider relative to its detection range in only ambient noise. For example, we could model a simple theoretical scenario and calculate the range, r , over which a 15-23 Hz fin whale call could be detected, in 20 m depth bins from 200 to 1000 m, using the sonar equation:

$$RL_d = SL - 15 \log_{10}(r) - t$$

where RL_d is the received level in the 15-23 Hz band at depth bin d , SL is source level estimated as 189 dB re 1 μ Pa at 1 m (Weirathmueller *et al.*, 2013), and t is the detection threshold, here 11 dB SNR over the 95th percentile noise level. This equation assumes a 1000 m deep, flat-bottomed environment with propagation loss due only to spreading at an

intermediate rate between spherical and cylindrical (Urick, 1983), with negligible absorption. Maximum detection radius decreased up to 97% during descents compared to ascents, within the same depth bin (Figure 2.9). Conversely, we found no correlation between platform depth and number of calls detected per hour for either the QUEphones or the glider. This was somewhat surprising given the relatively shallow calling depth of fin whales (Stimpert *et al.*, 2015) and given that such depth-dependence has been observed in monitoring beaked whales (Gkikopoulou, 2018). It is possible there were depth-dependent effects above 200 m where the mobile platforms did not record. This theoretical change in detection range, and the number of detections per hour, was not because of propagation differences of low frequency sounds at depths below 200 m or the shape of the sound speed profile, but instead solely because of the increased flow noise on the glider. Platform depth likely did not affect detection of fin whale calls below 200 m due to their low frequency and omnidirectional nature.

The difference in area and time surveyed by the glider due to flow noise was not anticipated and the resulting pattern appears specific to this deployment, rather than to all surveys or Seagliders. While dos Santos *et al.* (2016) reported similarly high levels of low-frequency flow noise, they did not compare differences across dive state. Increased flow noise during descents in our study was opposite that observed by Matsumoto *et al.* (2015) where a similarly equipped Seaglider showed increased flow noise during ascents. Therefore, we do not recommend altering the recording schedule to coincide only with glider ascents. Rather, attempts to mitigate flow noise should be made at the glider piloting stage by increasing dive durations and reducing thrust to decrease the glider's vertical speed during both dive states.

This difference in this study and Matsumoto *et al.* (2015) was likely due to differences in glider buoyancy and centers of mass compared to the local water density profile, not differences in piloting parameters. The same pilots flew both deployments using standard speeds and settings typical for oceanographic research. This highlights the critical importance of proper glider ballasting along with efficient, slow flight. If the glider is not properly ballasted for the water conditions in the survey area, the pilot may not have the ability to finely control the glider's descent or ascent rate throughout the mission. If it is not properly ballasted, the glider may need to perform more rolling or pitching maneuvers, creating excessive self-noise. Further, while the pilot can fly the glider at slow ascent and descent rates, it does so at the cost of forward progress. In areas with strong ocean currents, or complex pycnoclines, achieving the target speed and/or maintaining the survey plan may not be possible. Proper preparation and glider testing, as well as knowledge of the oceanographic conditions for the survey area, are essential steps in a successful and efficient glider deployment.

Because overall glider speed is difficult to accurately measure in practice (Van Uffelen *et al.*, 2013, 2016), defining the glider speed at which low-frequency flow noise becomes “too much” is not trivial. For this study we used a speed-through-water calculation to examine the effects of pitch and vertical velocity together. However, speed through water is not a programmable setting for the Seaglider. Instead, pitch and vertical velocity must be set individually (and even those are set through a suite of other parameters and then calculated and selected by the glider system). Speed through water varies by both vertical velocity (adjusted by changes in buoyancy) and pitch (adjusted by shifting the glider's center of mass). If pitch is held constant, increasing vertical velocity increases the

speed through water. Conversely, if vertical velocity is held constant, increasing the pitch decreases speed through water. High vertical velocities with high pitches would result in the same speed through water as a low vertical velocity and low pitch angle. Based on our regression analysis and visual inspection of the data, keeping speed through water below 25 cm/s should minimize flow noise (Figure 2.8). In looking towards future Seaglider surveys, we conservatively suggest 10 cm/s vertical velocity and pitch angles of around 30 degrees as the preferred flight parameters to limit flow noise that may reduce a recorder's detection range for marine mammal calls of interest below 60 Hz (Figure 2.5). Vertical velocities of 10 cm/s match the recommended value for maximum efficiency of Seaglider flight (School of Oceanography and Applied Physics Laboratory, 2011). If vertical velocities of 10 cm/s are not possible due to ballasting or local oceanographic conditions, then pitch should be increased to try to counter act the increased vertical velocity, although this will decrease the total distance over ground traveled per dive.

Neither QUEphone exhibited any flow noise, which was expected since the QUEphones drifted with the water and currents, rather than through or against it. While flow noise could be possible during QUEphone ascents and descents, it appears unlikely since typical ascent and descent speeds are less than 10 cm/s (ascending or descending 1000 m over 3-4 hours). Testing of greater ascent and descent speeds would be needed to investigate this further. The QUEphone hydrophone placement differed from SG158, with the hydrophone mounted on the top of the float while the glider's hydrophone was on the tapered aft portion. While hydrophone placement could influence flow noise generation, we do not expect that is the reason flow noise was not observed on the QUEphones but was on the glider. The glider's aft hull hydrophone placement surely placed it in a region

prone to the turbulence of vortex shedding, but as the regression analysis showed, speed is an important component to flow noise generation. Future comparisons of different glider hydrophone placement may provide improvements to the flow noise observed here.

Our findings show that in future work estimating density of low-frequency animals from moving platforms, it will be critical to assess how call detectability changes with recorder depth and dive state, ideally on a per-survey basis. Call detectability could be influenced not only by platform-generated flow noise, but also because a vertical profiling glider or float is moving up and down through local oceanographic conditions and stratification that affect sound propagation. If minimum glider speeds cannot be maintained due to local oceanographic conditions such as changes in water density and currents, survey effort could be adjusted to focus only on periods when low frequency noise levels are within an appropriate threshold, or detection probability could be modeled with glider dive state as a covariate. Further, the effect of glider flow noise will need to be reassessed for higher-frequency vocalizing marine mammals such as odontocetes, as the elevated noise level on dive descents was negligible above a few hundred hertz and glider speed had no effect on noise levels at 3000 Hz.

Conclusion

Underwater gliders and deep-water profiling floats provide a novel method for passive acoustic monitoring of low frequency marine mammal species. Survey capabilities of these platforms are different than stationary, bottom moored recorders. Overall assessment of animal presence and absence, at the hourly and daily scales, did not vary between a stationary, bottom-moored system and a mobile platform. The difference in rates

of detection of individual calls observed on the glider was tightly coupled with increased flow noise levels caused by increased glider vertical speed. We quantified these differences and identified how these differences need to be addressed or can be mitigated in future work on estimating animal density and abundance from slow-moving acoustic platforms such as gliders and floats.

We propose that gliders and floats are efficient platforms for recording and detecting low frequency marine mammal vocalizations such as 20 Hz fin whale calls. Because detection capabilities are comparable to other methods, they could be used in conjunction with different recorder types (*e.g.*, moored recorders, surface drifters, or towed arrays) to comprehensively survey an area of interest. The glider allowed us to survey a large area with a single hydrophone and the dual deployment of two QUEphones provided moderate spatial coverage of the area of interest. Despite differences in total detections on the glider, overall detectability of fin whale calls was high, and hourly and daily presence were consistent with the stationary recorders. However, much work is still needed to apply differences in calls detected and survey effort to estimate density and abundance and to conduct similar comparisons across a range of marine mammal vocalization types.

Acknowledgements

The authors thank Alex Turpin for his work on implementing the acoustic system on the glider and floats and for his help in the field, Ronald Morrissey and the crew of the *RSC4* for assistance with the field work, and Anatoli Erofeev for glider piloting services and expertise. We thank Mark Baumgartner, two additional anonymous reviewers, and Ari Friedlaender and Selina Heppell (SF's PhD Committee) for their thoughtful review and feedback on the manuscript. Funding for this work was provided by the Living Marine Resources Program Grant Number N39430-14-C-1435 and Office of Naval Research Grant Number N00014-15-1-2142. SF was supported by the National Science and Engineering Graduate Fellowship. This is PMEL Contribution No. 4932.

¹See supplementary material at <https://doi.org/10.1121/10.0000617> or this dissertation Appendix A (figures only) for additional data tables and figures. Data includes normalized hourly detection counts of fin whale 20 Hz pulses for all mobile and stationary recorders. Additional figures include LTSAs of the full deployment for all three mobile instruments, the SNR distribution of detections and Kruskal-Wallis test outputs for the detector assessment, variation in M3R detections per hour across all M3R hydrophones, and exploratory and residual plots for the regression analysis.

Tables

Table 2.1. Deployment and recording durations for each recorder. Deployment and recovery times for M3R are the times hydrophone recording started and stopped. Overlapping recording hours refers to the time periods where all recorders were deployed and the M3R system was recording. See Table 2.2 for start and stop times of the overlap periods. Hours reported for M3R are per hydrophone (with 79 hydrophones); all M3R hydrophones recorded the same duration.

Recorder	Deployed (UTC)	Recovered (UTC)	Duration (hours)	Total hours recorded	Overlapping recorded hours	Distance traveled (km)	Speed (km/day)
SG158	12/22/15 2:42	1/4/2016 16:33	325.8	258.4	179.3	261.0	19.2
Q001	12/22/15 4:51	1/4/2016 20:46	327.9	300.9	200.2	47.1	3.5
Q002	12/22/15 3:16	1/4/2016 16:49	325.5	301.8	203.7	53.0	3.9
M3R (per hydrophone)	12/21/15 5:22	1/5/2016 17:24	372.0	268.4	220.0	n/a	n/a

Table 2.2. Start and end times of overlapping recording periods in which all mobile platforms were deployed and M3R was active but excluding periods when M3R data was not properly recorded. All detection and noise comparisons were done only during these periods.

	Start	Stop	Duration (hours)
Period 1	12/22/2015 4:51	12/26/2015 3:42	94.9
Period 2	12/27/2015 22:45	12/31/2015 23:59	97.2
Period 3	1/3/2016 12:41	1/4/2016 16:33	27.9
		Total	220.0

Table 2.3. Detector performance evaluation metrics by recorder type. Precision and recall are reported as median and interquartile ranges of metrics calculated for each individual 5-minute sampling period. Correct Detections and Missed Detections are the total pooled counts across all sample periods. Total false alarms for all sample periods were normalized by total minutes sampled to get False Alarms per Hour. Seaglider (SG158) sample periods were further separated by dive state (ascent and descent).

Recorder	Sample periods	Precision (IQR)	Recall (IQR)	Correct detections	Missed detections	False alarms per hour
SG158	49	95.3% (20.6)	57.2% (22.6)	415	336	27.2
<i>ascent</i>	31	86.3% (40.0)	63.1% (22.7)	351	241	42.2
<i>descent</i>	18	100% (0.0)	50% (35.0)	64	95	1.3
Q001	58	87.1% (20.2)	52.4% (16.4)	813	751	29.2
M3R	64	92.5% (15.4)	50.7% (20.0)	737	754	24.4

Table 2.4. Median (50th), 5th, and 95th percentile 12, 40 and 3000 Hz power spectrum density levels (dB re 1 $\mu\text{Pa}^2/\text{Hz}$; 10 sec Hann window, 0% overlap) for all mobile platforms. Glider (SG158) percentiles are further separated into ascent and descent dive states.

Recorder	12 Hz				40 Hz				3000 Hz			
	95%	50%	5%	$\Delta 5-95\%$	95%	50%	5%	$\Delta 5-95\%$	95%	50%	5%	$\Delta 5-95\%$
SG158	116.4	102.1	85.0	31.4	78.1	90.0	109.1	31.0	44.5	66.4	77.6	33.1
<i>ascent</i>	106.6	97.7	83.4	23.2	76.5	87.0	108.2	31.7	44.3	66.1	76.4	32.1
<i>descent</i>	117.4	106.5	98.4	18.9	84.1	94.1	108.3	24.2	44.6	67.0	77.7	33.1
Q001	99.3	87.5	79.0	20.3	69.7	80.1	91.5	21.8	49.8	62.1	71.1	21.3
Q002	95.9	84.7	76.3	19.6	69.2	79.7	90.9	21.7	42.3	62.4	70.6	28.3

Table 2.5. Regression model outputs of the final preferred model at each frequency of interest. Speed through water (stw) was calculated as vertical velocity divided by the sine of the pitch angle and is the median value for each 30-minute bin. Dive state (ds) is a categorical variable including descent (negative vertical velocity) and ascent (positive vertical velocity). Time is the start time of each 30-minute bin, in minutes from the start of the first dive. The two-way interaction between speed through water and dive state is given as stw:ds.

Variable	Coefficient	Standard Error	t-value	p-value
12 Hz				
intercept	65.2357	1.1453	56.9582	<0.0001
speed through water	1.2975	0.0497	26.1131	<0.0001
dive state (descent)	14.5623	1.5009	9.7021	<0.0001
stw:ds	-0.6434	0.0547	-11.7566	<0.0001
40 Hz				
intercept	77.6547	1.5129	51.3286	<0.0001
speed through water	0.3392	0.0581	5.8438	<0.0001
dive state (descent)	-7.5296	1.7210	-4.3750	<0.0001
time	-0.0002	0.0001	-3.0990	0.0021
stw:ds	0.2624	0.0623	4.2121	<0.0001
3000 Hz				
intercept	67.8096	2.1321	31.8046	0.0000
dive state (descent)	1.5043	0.1966	7.6531	0.0000
time	-0.00056391	0.0003183	-1.771	0.0772

Figures

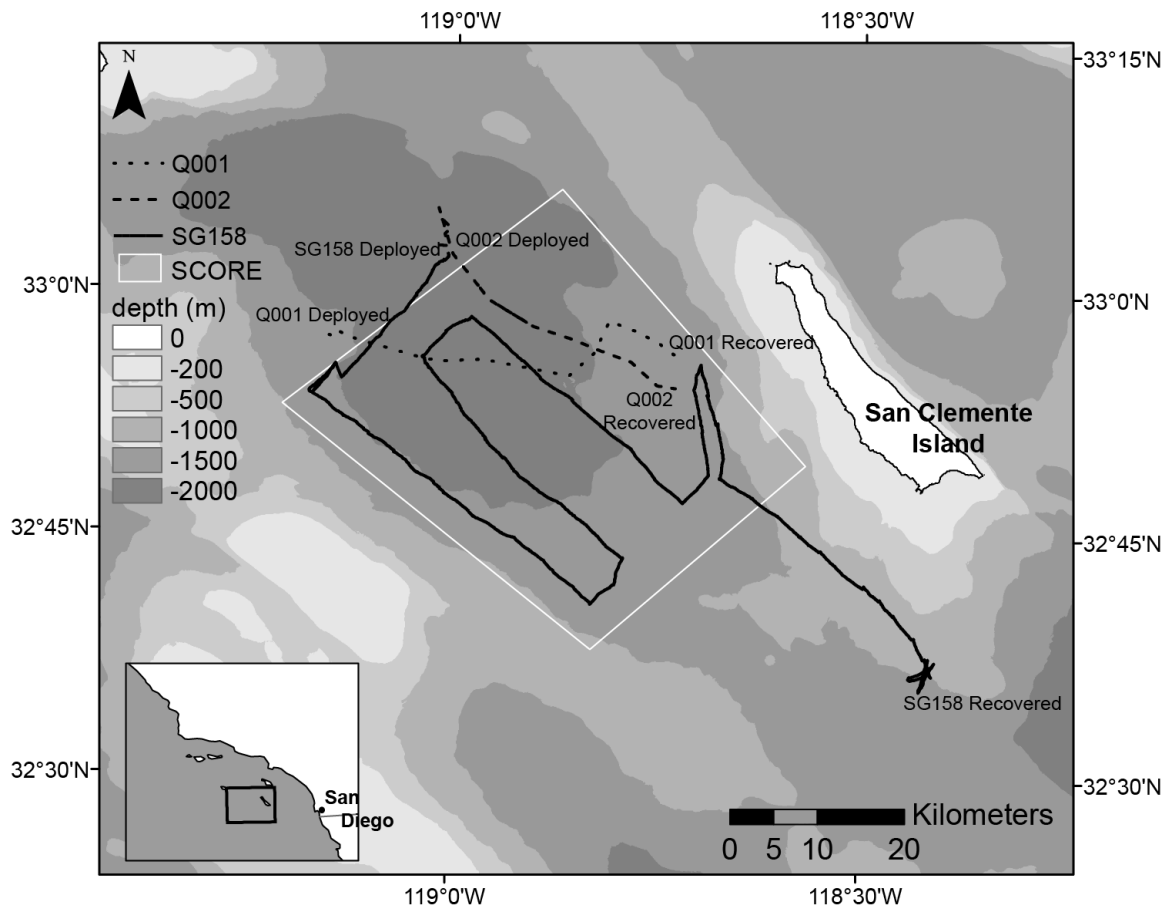


Figure 2.1. Map of platform paths, the outline of the Southern California Offshore Range (SCORE) enclosing the locations of the bottom-moored hydrophones, and seafloor bathymetry in the deployment area. The Seaglider, SG158 (solid line), was deployed on the NE side of the range, and then transited across the range according to pre-planned waypoints. Q001 (dotted line) and Q002 (dashed line) were deployed along the north edge of the range, about 17 km apart, and drifted to the SE. The SCORE hydrophones are generally evenly spaced across the range (within the white solid box), with each hydrophone approximately 4 km apart.

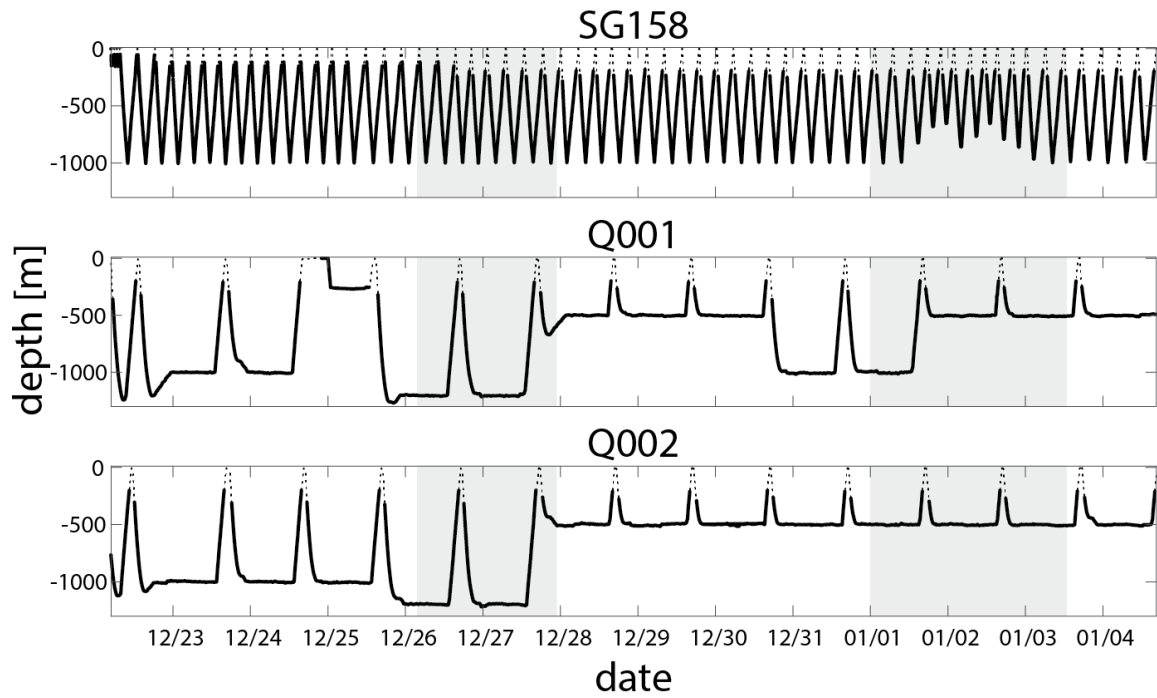


Figure 2.2. Dive profiles of the Seaglider (SG158) and QUEphones (Q001 and Q002). Black solid lines indicate PAM system is on, dotted lines indicate PAM system off. Gray shaded areas indicate times when the M3R recorder was not operational and were excluded from call detection analyses.

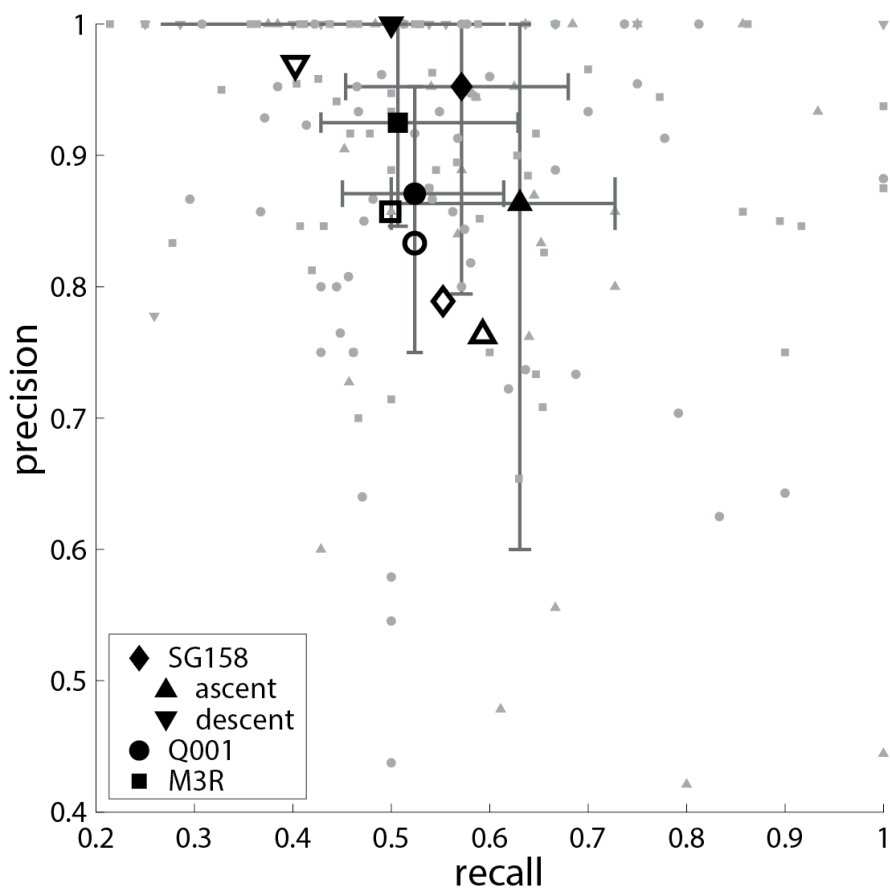


Figure 2.3. Precision and recall metrics for the fin whale 20-Hz pulse detector. Small gray shapes are precision and recall rates for each individual 5-minute sample period. Solid black shapes with error bars are median and interquartile range of all individually marked 5-minute periods for each recorder. Open black shapes indicate overall precision and recall values calculated from pooled counts of correct detections, misses, and false alarms. SG158 is further broken down by dive state with 5-minute periods during ascents as upward pointing triangles and descent periods represented by downward facing triangle.

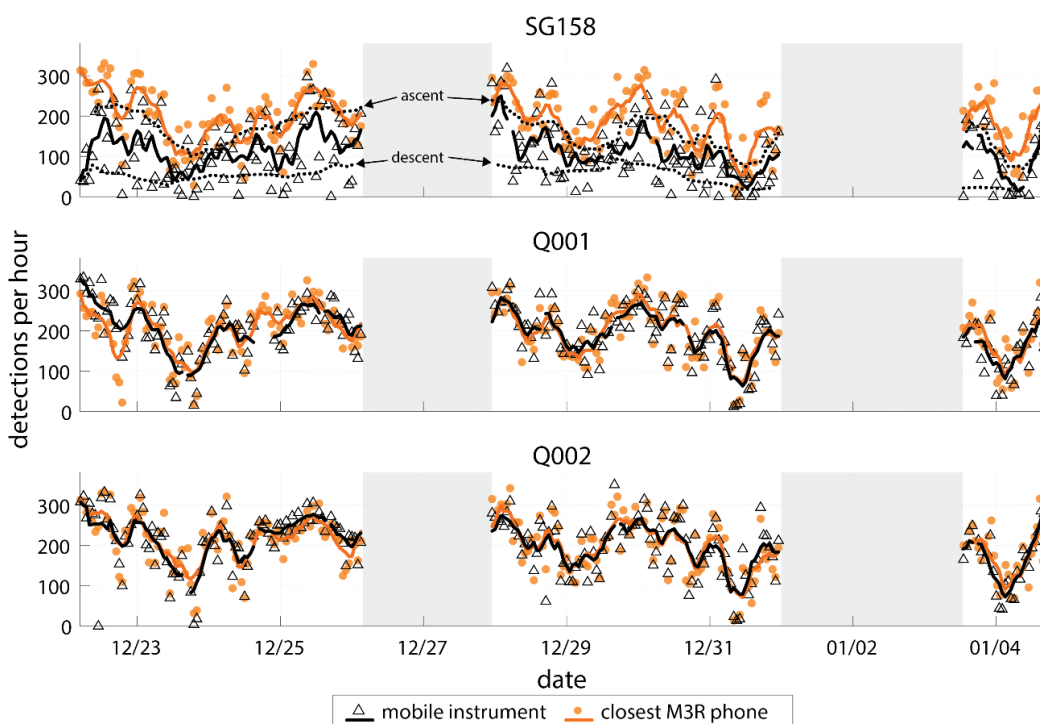


Figure 2.4. Detections per hour for each mobile platform (open triangles and solid black line) and the corresponding closest bottom-moored hydrophone (orange circles, solid orange line) during that hour. Lines represent smoothed counts over 6 hours. Smoothed counts for SG158 during ascents and descents only are shown as the dotted black line and indicated with arrows in the top panel.

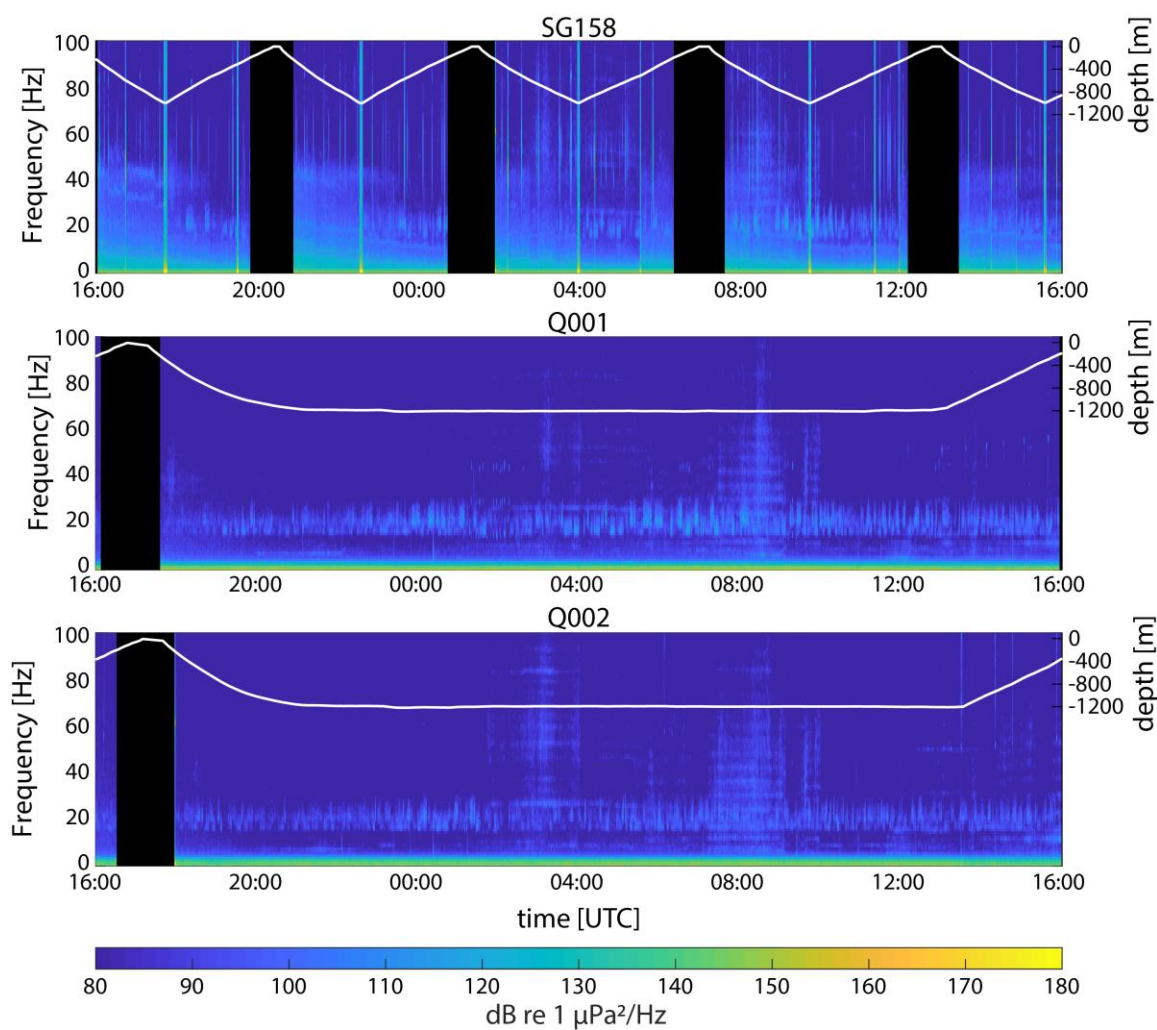


Figure 2.5. Example Long Term Spectral Average (LTSA) plot (10 sec, 1 Hz) showing 24 hours of acoustic data recorded by SG158, Q001, Q002 from 12/26/2015 16:00 to 12/27/2015 16:00 UTC. The white solid line and right-hand y-axis indicate platform depth at the time of the acoustic recording. Black bands indicate breaks in recording when the platform was at the surface. Fin whale 20-Hz pulses are visible in the LTSA as lighter blue portions around 20 Hz. Light blue-green vertical stripes in the glider spectrogram are broadband noise caused by the glider's buoyancy pump inflating at the bottom of each dive.

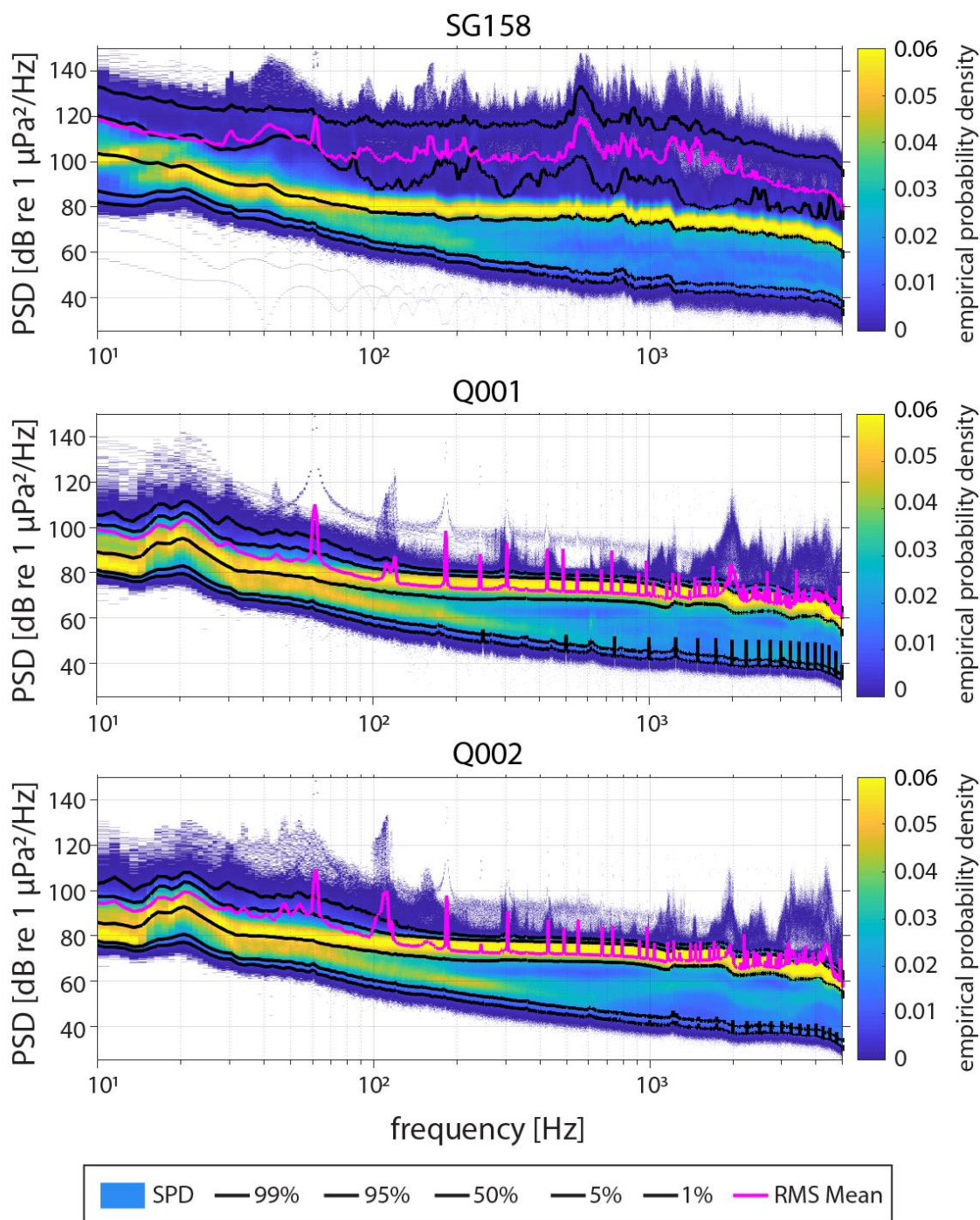


Figure 2.6. Spectral Probability Density (SPD) plots for SG158, Q001, and Q002, up to 5 kHz, using methods outlined in Merchant *et al.* (2013) on the 10 kHz sample rate LTSA of the entire deployment calculated with a 1 Hz, 10 sec Hann window for each mobile platform. Y-axis units are power spectrum density (PSD) level. Width of SPD shows variability in noise levels across the deployment duration.

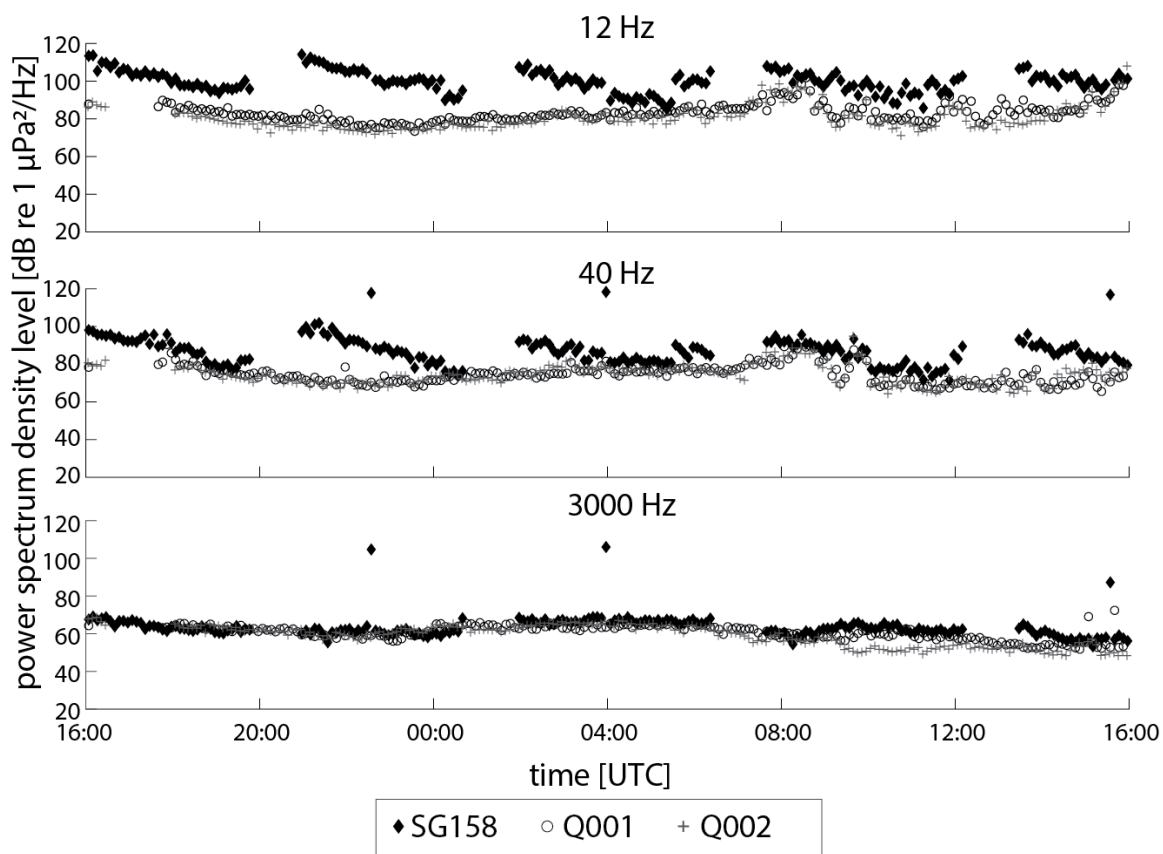


Figure 2.7. Power spectrum density levels at 12 Hz, 40 Hz and 3000 Hz for all three mobile platforms for a 24-hour period from 12/26/2015 16:00 to 12/27/2015 16:00 UTC (same 24-hour period shown in Figure 2.5). Each point represents the lowest power spectrum density level calculated over a 10 second Hann window, each sixth minute of the 24-hour period where the PAM system was active. Every sixth minute was selected to reduce the clutter of the plot. During relatively quiet periods (e.g. 16:00-03:00) the glider (solid diamonds) minimum power spectrum density levels at 12 Hz and 40 Hz are shown to decrease over a given dive, decreasing to levels similar to the QUEphones (open circles and plus signs), while levels at 3000 Hz match those of the QUEphones, regardless of dive state. Intermittent extreme high values at the ends and middle of dives indicate times when the glider or QUEphone pump was on. Gaps in points align with time periods where the PAM system was off.

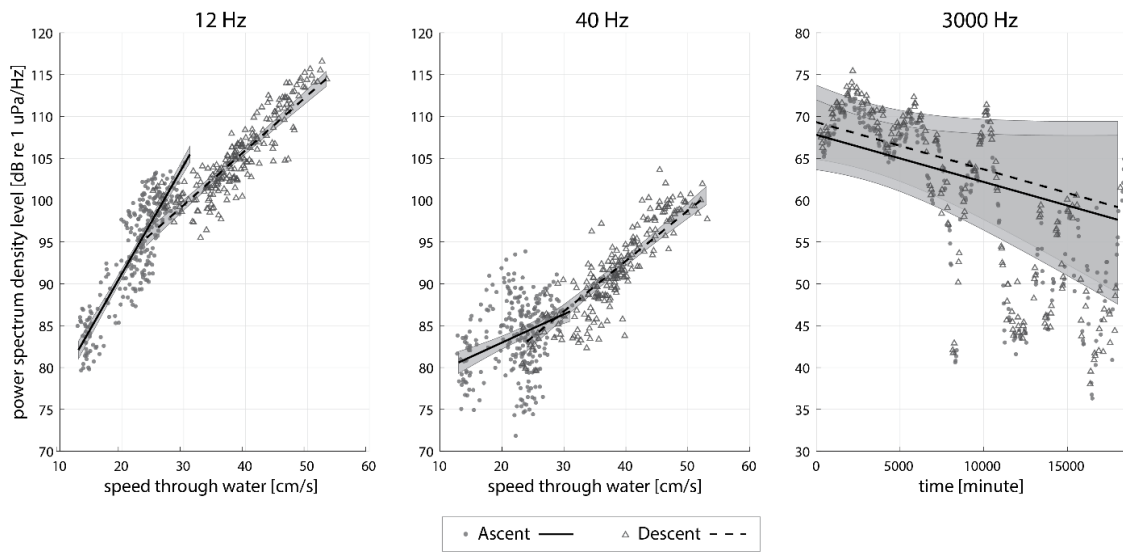


Figure 2.8. Prediction plots for final regression models at each frequency. For 12 Hz (left plot) and 40 Hz (center plot), power spectrum density levels are plotted against glider speed through water for ascents (filled circles) and descents (open triangles). Lines are predicted flow noise levels with changes in speed through water in 1 cm/s intervals at each dive state (ascent – solid line, descent – dotted line), with 95% confidence intervals shaded around each line. For 3000 Hz, because speed through water was not included in the final model, power spectrum density levels are plotted against time in minutes from start of deployment.

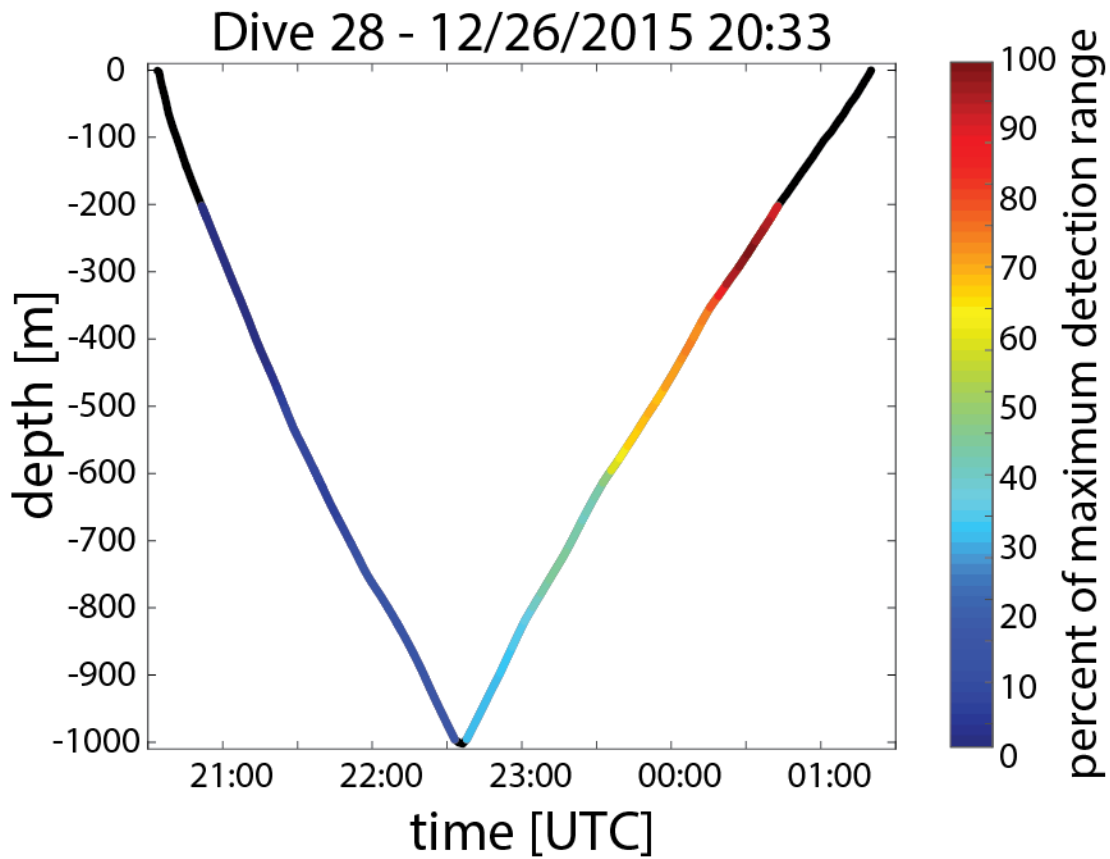


Figure 2.9. Theoretical maximum detection range over the duration of a single glider dive, Dive 28, on 12/26/2015 at 20:33 UTC. Estimated maximum detection range was calculated every 20 meters of glider depth based on a call source level of 189 dB re1 μ Pa @ 1 m (Weirathmueller *et al.*, 2013), transmission loss at an intermediate rate between spherical and cylindrical spreading ($15 \cdot \log_{10}(r)$; Urick, 1983), a detection threshold of 11 dB SNR, and the noise level as the 95th percentile level in that 20 meter bin. Detection ranges were then normalized as a percent of the maximum detection range within the dive.

CHAPTER 3: DETECTION PROBABILITY AND DENSITY ESTIMATION OF FIN
WHALES BY A SEAGLIDER

Selene Fregosi, Danielle V. Harris, Haruyoshi Matsumoto, David K. Mellinger, Stephen
W. Martin, Brian Matsuyama, Jay Barlow, and Holger Klinck

Abstract

Gliders may provide an effective tool for passive acoustic density estimation of marine mammals. To estimate density from acoustic data collected by a single-hydrophone glider platform, an estimate of detection probability, and subsequently an effective survey area, are required. An array of hydrophones cabled to a shore-based processing and recording facility was used to estimate fin whale localizations and tracks concurrently with a glider survey. Fin whale tracks were used as detection trials and a detection function for snapshots containing fin whale 20 Hz pulses recorded by the glider was modeled using a generalized additive model. Detection probability was strongly dependent on 40 Hz noise levels recorded on the glider. At the median noise level of 97 dB re 1 $\mu\text{Pa}^2/\text{Hz}$, detection probability was near one at zero horizontal distance, and maximum detection ranges were near 40 km. The estimated effective survey area at this noise level was 870 km^2 . Using estimates of vocal rates and group size from tagged and tracked fin whales, respectively, the density of fin whales was estimated as 2.4 whales per 1000 km^2 (coefficient of variation 0.55). The framework presented here could be applied to other baleen whale species to advance the use of autonomous gliders for density estimation of cetacean species.

Introduction

To successfully manage and conserve marine mammal populations, it is necessary to monitor population levels and trends over time and space, and estimated population density is a useful metric for identifying potential population changes. Often, marine mammal population densities are estimated from visual sighting data. Alternatively, density can be estimated from some indicator of an animal's presence, called a cue, such as visual observations of whale blows, or recorded acoustic vocalizations, rather than direct sightings of animals (Buckland, 2006; Marques *et al.*, 2013). Estimating density from acoustic data is particularly effective for marine mammals because many species spend the majority of their lives underwater and are difficult to survey visually but vocalize reliably (Barlow *et al.*, 2013; Marques *et al.*, 2013).

Autonomous underwater vehicles, such as gliders, have proven to be effective survey platforms for passive acoustic monitoring (PAM) of marine mammals. Gliders have been used to acoustically detect and survey a variety of marine mammal species (*e.g.*, Baumgartner *et al.*, 2013; Klinck *et al.*, 2016; Küsel *et al.*, 2017; Silva *et al.*, 2019) and there is an interest in using these systems to estimate marine mammal densities (Gkikopoulou, 2018; Harris *et al.*, 2017; Küsel *et al.*, 2017; Marques *et al.*, 2013).

Gliders provide a few advantages over traditional stationary or vessel-based methods (see Verfuss *et al.*, 2019 for a review of autonomous systems). The primary advantage of gliders is that they provide increased spatial coverage compared to a stationary sensor, and increased temporal coverage compared to a vessel-based survey. Gliders can be flown in areas that are typically hard to access due to offshore location or poor weather (Baumgartner *et al.*, 2014; Klinck *et al.*, 2015a), they can traverse bathymetric and oceanographic features (Burnham *et al.*, 2019; Nieukirk *et al.*, 2016; Silva *et al.*, 2019), and some systems can provide near-real-time detection information (Baumgartner *et al.*, 2013, 2018; Klinck *et al.*, 2012). Additionally, gliders collect oceanographic data (*e.g.*, temperature and salinity) concurrently with acoustic data collection, which can be used to calculate *in situ* sound speed profiles and examine animal occurrence in relation to environmental variables (*e.g.*, Silva *et al.*, 2019). Because of these advantages, gliders provide a useful tool for surveying hard-to-reach areas. If density could

be estimated from glider-collected data, our understanding of marine mammal populations could be improved. However, applying passive acoustic density estimation methods to glider data is not straightforward because of the glider's slow movement and typical single-hydrophone instrumentation.

Several methods have been implemented to estimate the density of marine mammals from acoustic data, including plot sampling, distance sampling, and spatially explicit capture-recapture (see Marques *et al.* 2013 for a thorough review). Different types of acoustic events can be monitored and counted, including counting individual calls or echolocation clicks, individual animals, or groups of animals. Further, acoustic events that occur instantaneously such as a single call or echolocation click or the start of a foraging dive are known as “cues” and methods that use these acoustic events are known as “cue counting” (*e.g.*, Marques *et al.*, 2011, Moretti *et al.*, 2010). Alternatively, the presence of acoustic signals within a set time period can be counted; these time periods are known as “snapshots” (*e.g.*, Hildebrand *et al.*, 2015, Kyhn *et al.*, 2012; Ward *et al.*, 2012). The choice of an acoustic event of interest and density estimation method depends on the type of acoustic data collected and the collection platform, acoustic behavior of the target species, and the amount of information available about the source locations of acoustic events.

The simplest method, mathematically, is plot sampling. The total number of detected acoustic events, n , is divided by the survey area, a , and one or more multipliers, \hat{r} (the circumflex indicates an estimated value), such as a vocalization rate, the proportion of the population that vocalizes, or group size, that converts acoustic events to animals to get density of animals, \hat{D} , using

$$\hat{D} = \frac{n}{a\hat{r}} \quad (3.1)$$

Cue counting or snapshot analyses will also require effort (other than the area surveyed) to be included in the denominator (time for cue counting and total number of snapshot periods for snapshot analyses).

In the case of plot sampling, it is assumed that all acoustic events within the survey area are detected (Marques *et al.*, 2013). Densities of two cetacean species have been estimated this way using an extensive cabled hydrophone array operated by the U.S. Navy (Moretti *et al.*, 2010; Ward *et al.*, 2012). However, counting all acoustic events is rarely

feasible in practice because the exact survey area is not known, and these types of arrays only exist in a few places in the world and their access is restricted.

Distance sampling overcomes the need to count all acoustic events with certainty by accounting for the proportion of acoustic events that are missed (Buckland *et al.*, 2001). Generally, the likelihood an acoustic event is detected decreases as its source location gets further from the receiver, just as in visual surveys animals are more difficult to see further from the observer. Acoustic distance sampling can take the form of line-transect distance sampling using a vessel towing a hydrophone array, or fixed point-transect distance sampling, in which a stationary recorder is the survey point (Buckland *et al.*, 2001). If distances to detected acoustic events can be measured (from stationary or towed hydrophone arrays capable of localizing acoustic events), or in a few cases from single recorders, (*e.g.*, Harris *et al.*, 2013; Tiemann *et al.*, 2006; Wiggins *et al.*, 2004), then detection probability can be modeled as a function, called the detection function $g(y)$, of the horizontal distance, y , from the recorder (Buckland *et al.*, 2001). For marine mammal species that can be vocalizing at depth, or for acoustic recorders that can be located in the water column or on the sea floor, horizontal distance is the distance between the recorder and the acoustic event projected onto a horizontal plane. If the depth of the animal and the recorder is known, then horizontal range can be calculated from the slant range. The detection function then provides the information necessary to estimate an average probability of detection, accounting for the missed acoustic events, which allows density to be estimated as

$$\hat{D} = \frac{n}{\hat{p}a\hat{r}} \quad (3.2)$$

where n is the number of acoustic events detected, \hat{p} is the average probability of detection, a is the survey area, and \hat{r} represents the multipliers necessary to convert acoustic events to number of animals. The $\hat{p}a$ term can also be combined to create a single variable, \hat{a}_e , the effective survey area. The average probability of detection, \hat{p} , reduces the survey area, a , to the effective survey area, \hat{a}_e , where the same number of animals is present (both detected and undetected) as those detected within the survey area, a (Buckland *et al.*, 2001).

Distance sampling has four key assumptions that may or may not hold in a given marine mammal acoustic survey: that animals are detected at their initial location (*i.e.*, there is no animal movement), that distances to detections are measured accurately, that detection probability at zero horizontal distance from the survey trackline or point (symbolized as $g(0)$) is either certain (equal to 1) or known, and that the animals are distributed independently of the survey lines or points (Buckland *et al.*, 2001). Using robust survey design and modifications to conventional distance sampling allow for these assumptions to be relaxed or overcome in some cases (*e.g.*, mark-recapture distance sampling can be used to estimate $g(0)$; Laake and Borchers, 2004). Distance sampling has been used to estimate density of a variety of marine mammals through both visual and acoustic line-transect surveys from a vessel (Barlow and Taylor, 2005; Gerrodette *et al.*, 2011; Norris *et al.*, 2017) and point-transect surveys from fixed acoustic recorders (Marques *et al.*, 2011; McDonald and Fox, 1999). Yet the number, frequency, and temporal coverage of appropriate surveys remains limited due to the high cost of vessel-based surveys or deployment of appropriate stationary arrays, and the difficulty of estimating detection probability from single recorders.

Alternatively, spatially explicit capture-recapture (SECR; also called spatial capture-recapture, SCR) with acoustic data does not require distances to detected acoustic events to be measured. Instead it requires multiple recorders, with known locations, to record the same acoustic event simultaneously (Borchers, 2012; Efford *et al.*, 2009b; Stevenson *et al.*, 2015). The spacing of the recorders and pattern of which recorders did and did not detect the same event are used to model an average detection probability as a function of the source location of the acoustic event (which is not known) and the effective survey area can be derived from the detection function (Borchers and Efford, 2008). Density is estimated as above with distance sampling, but using \hat{a}_e in the denominator rather than \hat{p} and a

$$\hat{D} = \frac{n}{\hat{a}_e \hat{r}} \quad (3.3)$$

While the requirements for SECR are relatively basic (known recorder locations and that acoustic events can be detected on multiple recorders simultaneously; Borchers, 2012),

applying the method to marine mammals is still in its infancy. As an example, SECR has been applied to minke whales (*Balaenoptera acutorostrata*), using a permanent Navy array to estimate density over both a short and long time scale (Marques *et al.*, 2012; Martin *et al.*, 2013).

Of these three density estimation approaches, distance sampling is promising for application to autonomous underwater gliders. In the case of plot sampling, it is necessary to define the survey area where detection within the area is certain and detections outside the area can be excluded. It is difficult to envisage a situation where that could be properly defined for a mobile, deep-water glider. Hypothetically an SECR approach is possible but would require multiple coordinated gliders. To our knowledge, such a survey for marine mammals has not been done and would be both financially and logistically complex. SECR is an important area for future development, but estimation of glider underwater position can be error-prone and the potential bias of that error would need to be investigated (Van Uffelen *et al.*, 2013, 2016a). While a distance sampling approach, with some glider-specific adaptations, is promising, the horizontal and vertical movement of the glider presents unique considerations (Fregosi *et al.*, 2020; Gkikopoulou, 2018; Harris *et al.*, 2017; Küsel *et al.*, 2017; Marques *et al.*, 2013). The three primary considerations are that slow glider movement may violate the first distance sampling assumption that animals are detected at their initial location, the detection probability cannot currently be estimated from the glider data alone, and the three-dimensional (3D) glider movement may mean the detection probability changes over the course of a dive cycle and a survey.

Typical horizontal glider speeds (25 cm/s, Rudnick *et al.*, 2004) are slower than typical marine mammal movement (1-2 m/s, Sato *et al.*, 2007). Because the glider moves more slowly than the animals of interest, the distance sampling assumption that animals are detected at their initial location, in other words that there is no animal movement, does not hold. If animals can move more quickly than the survey platform, they could be counted more than once as they moved around in the survey area, which would lead to an overestimation of density (Buckland *et al.*, 2001; Glennie *et al.*, 2015). Further, any animal movement, either towards or away from the recorder, could bias the measured distances, leading to either over or under estimations of density. This assumption can be overcome

by using a snapshot or cue-counting approach, where the glider track is divided into temporal snapshots and each snapshot is then treated as a point-transect sample, rather than treating the glider's path as a continuous survey transect (Harris *et al.*, in revision). The appropriate snapshot duration is a duration over which animal movement is negligible, but detection is still possible. Even so, a snapshot-based point-transect distance sampling approach still requires an accurate estimate of the detection probability or the effective survey area (Buckland *et al.*, 2001; Marques *et al.*, 2013).

Accurately measuring the distances to a detected acoustic event, in order to build the detection function necessary for distance sampling, is difficult using data from a single glider alone as gliders are typically single-hydrophone systems (Cato, 1998). Single hydrophone systems do not provide information on the bearing and range to the sound source; at least three sensors are traditionally needed to estimate location of a sound source. This inability to directly measure distances to detected events violates the distance sampling assumption that ranges to detected acoustic events can be estimated without error (Buckland *et al.*, 2001). Küsel *et al.* (2017) instrumented a glider with two hydrophones, one on each wing, and was able to estimate bearing angles and generate animal tracks for sperm whales (*Physeter macrocephalus*). The authors demonstrated that multi-hydrophone systems may allow for direct distance measurements in the future; however, the hydrophone spacing (only 1 m along the wingspan of a Seaglider) and method used would not work well for low-frequency (<100 Hz) baleen whale vocalizations which have call wavelengths longer than 15 m (Küsel *et al.*, 2017).

If range to detected acoustic events cannot be measured directly, as is the case with most glider systems, the necessary detection probability can be estimated using auxiliary data (Marques *et al.*, 2013). Range estimates and detection probability can be modeled using the sonar equation and propagation modeling. However, these modeled estimates rely on accurate inputs for call frequency and amplitude characteristics (*i.e.*, source levels and directionality), animal vocal behavior, ambient noise levels and local transmission loss and detection probability estimates may be sensitive to variability in these model inputs (Frasier *et al.*, 2016; Helble *et al.*, 2013b; Küsel *et al.*, 2011; Marques *et al.*, 2013; Zimmer *et al.*, 2008). Alternatively, animal locations can be measured from additional instruments

and set of detection “trials” can be assembled. For each trial, whether the known location animal was detected or not can be used to build a detection function. For example, Kyhn *et al.*, (2012) conducted a visual survey at the same time and place as an acoustic survey. Shore-based observations provided known animal locations in relation to the acoustic recorders so a detection function could be estimated for the acoustic recorder alone (Kyhn *et al.*, 2012). Marques *et al.* (2009) estimated a detection function for bottom-moored hydrophones using a similar trial-based approach. Animal-borne tags (*e.g.*, DTAGs; Johnson and Tyack, 2003) provided animal location and vocal activity information which was then used to quantify ranges at which the bottom-moored hydrophone did or did not detect echolocation clicks (Marques *et al.*, 2009). A similar approach to Kyhn *et al.* (2012) and Marques *et al.* (2009), using known animal locations estimated from additional instruments as trials, is the approach pursued in this work to estimate a detection function for a single-hydrophone glider.

Lastly, the horizontal and vertical glider movement may affect the detection probability due to changes in the sound propagation environment and because of glider-generated flow noise. The glider moves up and down in the water column, which turns the traditionally two-dimensional (2D) detection probability as a function of range into a 3D problem (Buckland *et al.*, 2015). For example, detection functions are estimated from horizontal range between the acoustic event and the recorder. This horizontal range is the distance between the two objects as they lie in the same 2D plane. But in the case of a glider, the glider could be at 900 m depth, directly beneath a vocalizing whale near the surface (*i.e.*, fin whales vocalize at 10-15 m depth; Stimpert *et al.* 2015). In this case, horizontal range would be 0, but the acoustic event at 900 m range may not be detected with certainty. If these depth differences are constant or uniformly distributed, they may be accounted for (Buckland *et al.*, 2015), but this has not been fully explored for gliders. Additionally, sound speed underwater varies with water depth, temperature, and salinity; underwater sound propagation is affected by differences in the sound speed profile (Urlick, 1983). Detection probability as a function of range to the detected event may be different when the glider is in deep water compared to when it is near the surface as it changes depth and is subject to different propagation paths. Sound propagation may also change as the

glider moves horizontally over different bathymetric and oceanographic features, and therefore the detection probability may vary over a survey duration. Additionally, there is evidence that the glider-generated low-frequency flow noise can vary during a given survey, which would change the detection probability as well (Fregosi *et al.*, 2020). However, variables such as ambient or flow noise levels, glider depth, and location within the survey can be addressed by including them as covariates in the detection function, but this highlights the complicated nature of detection probability from a moving platform.

We conducted an experiment to determine the feasibility of estimating fin whale (*Balaenoptera physalus*) density using an acoustic glider. The primary objectives were to (1) assess the ability to estimate the detection probability of acoustic signals produced by fin whales from an autonomous underwater glider using whale localizations generated using data from a stationary array cabled to shore, and (2) develop a framework for estimating both the density of acoustic events and density of fin whales from glider-collected acoustic data. We use a trial-based approach, leveraging an extensive array capable of tracking baleen whales to provide known animal locations and using song presence or absence within a six-minute snapshot as the acoustic event. Glider noise levels in the same frequency band as fin whale calls were included as a covariate in the detection function. Fin whales were selected as the focal species for several reasons. Calls were plentiful in the recorded data, and they provide an example of a low-frequency baleen whale call that can be detected over tens of kilometers. Fin whale calling behavior (*e.g.*, source level, call rate, calling depth) is relatively well documented (Croll *et al.*, 2002; Moore *et al.*, 1998; Stimpert *et al.*, 2015; Watkins, 1981), which is necessary for estimating animal density from call density. Finally, fin whales are of conservation concern because they are present in Southern California year-round (*e.g.*, Barlow and Forney, 2007; Campbell *et al.*, 2015; Širovic *et al.*, 2015), feeding and breeding in an area with high levels of anthropogenic activity including commercial shipping, military exercises, and recreational fishing and boating activity, and are still considered endangered as a result of depletion by historical whaling.

Methods

Acoustic data collection and analysis

For two weeks in December 2015 and January 2016, a Seaglider (SG158; Huntington-Ingalls Industries, Lynnwood, WA, USA) equipped with a single hydrophone surveyed in the vicinity of the Southern California Offshore Range (SCORE) where an array of bottom-mounted hydrophones cabled to shore is operated by the U.S. Navy (Figure 3.1). The Seaglider was deployed on 22 December 2015 on the north side of the range and surveyed the area in evenly spaced (~10 km) transects, continuously diving between the sea surface and 1000 m depth. It was recovered southeast of SCORE on 4 January 2016 (Figure 3.1). The Seaglider recorded passive acoustic data with the Wideband Intelligent Signal Processor and Recorder (WISPR; Embedded Ocean Systems, Inc, Seattle, WA, USA). Recordings were made continuously when the glider was below 200 m depth via a single omni-directional hydrophone (HTI-92-WB, High Tech Inc., Gulfport, Mississippi, USA; sensitivity: -175 dB re 1V/ μ Pa +/- 3 dB frequency response from 2 Hz to 50 kHz). The hydrophone was mounted inside the hull of the rear third of the glider, near the external buoyancy bladder. The system recorded at a 125 kHz sampling rate with 16-bit resolution (+/-5 V clipping level) and was compressed using the Free Lossless Audio Codec (FLAC). Prior to digitization, a frequency-dependent gain curve approximately matching the inverse of a typical deep-water ambient sound profile was applied (see Matsumoto *et al.*, 2015) to maximize dynamic range across the recorded frequency spectrum. After the recovery of the glider, data were downsampled to 1 kHz to facilitate the analysis of low-frequency fin whale calls.

Glider noise levels at 40 Hz were calculated for every minute of recording, as described in Fregosi *et al.* (2020). A frequency of 40 Hz was chosen because it is adjacent to but exclusive of the frequency range of fin whale calls. It adequately captured changes in flow noise without including fin whale calls. To remove transient sounds like glider motor noise, the lowest 40 Hz power spectrum density level (calculated with a 10 s Hann window and 0% overlap) per minute was extracted to represent noise level in each minute. All noise levels reported hereafter are power spectrum density levels in dB re 1 μ Pa²/Hz.

While the glider was deployed, acoustic data from an array of bottom-moored hydrophones at SCORE were archived using the Marine Mammal Monitoring on Navy Ranges (M3R) system (Jarvis *et al.*, 2014). The hydrophones are located off the western shore of San Clemente Island in the Southern California Bight. They are moored at 800-1800 m of water in a grid with approximately 4 km spacing between hydrophones (Figure 3.1). The subset of 79 hydrophones used in this study record data at a 96 kHz sampling rate and 16-bit resolution. A 50 Hz high pass filter is applied to recordings, providing a frequency response range of ~50 Hz to 48 kHz, but acoustic data are usable down to 20 Hz (Jarvis *et al.*, 2014; Moretti *et al.*, 2016). The M3R system is capable of recording, detecting, and localizing marine mammal vocalizations, and data can be processed and viewed in real-time (Jarvis *et al.*, 2014; Martin and Matsuyama, 2015; Moretti *et al.*, 2016). Data were initially recorded in a proprietary packet format, and later converted to FLAC using the MATLAB-based Raven-X toolbox (Dugan *et al.*, 2018, 2016). These files were also downsampled to 1 kHz for fin whale analysis. The 8 TB hard drives utilized for acoustic recording on the SCORE array wrote data at an insufficient speed, which caused write errors as the data drives approached capacity (after ~96 hours of recording on each). This caused two major data dropouts as the first and then second disks filled, resulting in loss of approximately 100 hours of data per hydrophone (out of 372 total deployment hours). A subset of 94 hours of recordings (from 22 Dec 2015 05:00 UTC to 26 Dec 2015 03:00 UTC; the first continuous recording period before data write issues began) was used in the following detection function and density estimation analysis.

Fin whale tracking

Fin whale calls were localized in 2D (latitude and longitude without depth information) using time-difference-of-arrival methods similar to those described by Martin *et al.* (2015) for minke whales and Helble *et al.* (2015) for humpback whales (*Megaptera novaeangliae*) at the Pacific Missile Range Facility (Figure 3.2). The method has been demonstrated to work for fin whales at SCORE. Localizations were then grouped into “tracks” using a custom MATLAB (Mathworks, Natick, MA, USA) routine (Martin and Matsuyama 2015; Figure 3.2). Subsequent localizations were not connected or interpolated

in any way, so the term “track” in this case means a set of localizations grouped according to the settings outlined below. This program allowed localizations to be filtered by the localization least squares estimate and the number of hydrophones that contributed to the localization. We allowed a maximum least squares value of 0.055 sec and required detections from at least 6 hydrophones per localization. Localizations were grouped into tracks by setting a maximum distance (0.01° degrees latitude and longitude, or approximately 1.1 km north to south and 0.9 km east to west at 32°N) and time (900 seconds) between consecutive localizations and setting a minimum number of localizations to constitute a track (8 localizations). These settings were selected using trial and error and the final settings balanced using only high-quality localizations and biologically realistic travel speeds while still providing enough tracks for analysis.

Detection function estimation

A detection function was modeled using a trial-based approach, with each trial consisting of a six-minute snapshot where a fin whale track was generated by the SCORE hydrophone array, and the glider was recording. To assess the feasibility of a trial-based approach to estimate detection probability, just the first 90 hours of glider data were analyzed using the following detection probability estimation process. Snapshot durations of six minutes were chosen to minimize potential whale movement while maximizing the ability to match call sequences across instruments. Based on mean fin whale travel speeds of 4 km/hr observed when fin whales were producing regular call sequences (Soule and Wilcock, 2013), we would not expect whales to travel more than 400 m per snapshot. This distance is relatively small compared to known detection ranges for fin whale calls of tens of kilometers (Širović *et al.*, 2007; Stafford *et al.*, 2007). Conversely, six minutes was sufficient to capture natural variation in the generally stereotypic fin whale 20-Hz pulses, such as short breaks in call sequences or deviation from the doublet pattern typically observed in these data, which was needed to match tracks to glider recordings. Inter-pulse-intervals typically ranged between 15 and 25 seconds, so each snapshot contained upwards of 20 calls.

Multiple whales and tracks were sometimes recorded at the same time, so we could not assume that calls recorded on the glider at the same time a track occurred were the same calls that generated the track. Therefore, spectrograms of the glider and SCORE array recordings for each snapshot were cross-correlated and visually inspected. Each trial was manually given a binary score as a detection (1) or non-detection (0) on the glider. An overview of the analysis steps from fin whale localization to detection trial scoring is provided in Figure 3.2.

For each track, a “focal hydrophone” was selected as the SCORE hydrophone that generated the most localizations for that track. If more than one hydrophone had the maximum number of localizations, the hydrophone closest to the track was selected as the focal hydrophone. For each track, spectrograms (2048 sample Hamming window, 90% overlap, frequency resolution 0.4883 Hz, time resolution 0.205 seconds) were generated for both the focal SCORE hydrophone data and the glider data from 1 kHz downsampled data. Spectrograms were band-pass filtered to 10 to 30 Hz. Each spectrogram was equalized to remove continuous noise sources by subtracting the median levels of the previous 4 seconds, at each frequency. The SCORE hydrophone and glider spectrograms were viewed side-by-side for all tracks. The glider spectrogram was divided into six-minute snapshots; the number of snapshots per track was dependent on the track length, averaging 3 windows per track but having as many as 58 windows for the longest track.

Each glider spectrogram window was cross-correlated to the focal SCORE hydrophone spectrogram for the corresponding time period, padded with an additional 66 seconds of data at the start and end of the SCORE spectrogram, using normalized 2D cross-correlation in MATLAB. The 2D cross-correlation function allowed for cross correlation of spectrograms (images) rather than waveforms; visual inspection of spectrograms to confirm matches was more informative than visual inspection of waveforms by the human analyst. The 60-second padding was added to allow for differences in travel time of calls to each recorder, for calls traveling up to ~100 km (assumed sound speed 1500 m/s). The cross-correlation score and timing offset for the cross-correlation peak were recorded for each snapshot, and spectrograms for the focal hydrophone and glider were plotted using the cross-correlation offset to align them in time. If no calls were visible on the glider

spectrogram, the trial was marked as a “non-detection”. If the pattern of calls on the glider and focal hydrophone matched, the trial was marked as a “detection”. If visual inspection of spectrogram plots, cross-correlation scores, and cross-correlation offset timing were unclear because of the presence of multiple whales or excessive glider noise, a trial was marked as “not sure” and was removed from further analysis. See Figures B1 and B2 for example displays used for scoring. Because the start and end of each glider snapshot were generated based on track start and end times, it was possible to have multiple snapshots for the same period in time, if multiple tracks were generated at that time. To remove any potential ambiguity from these times with multiple whale tracks (because often matching of sequences across the stationary and glider-generated spectrograms was too difficult when multiple whales were present), any snapshots that overlapped in time with any other snapshot was not included in the detection function estimation.

For each trial, horizontal distance from the mean of the track localizations within that six-minute snapshot to the mean dead-reckoned glider location (from the glide-slope model) during the snapshot was estimated as the great-circle distance between two sets of latitude and longitude coordinates. Animal and glider depth were not accounted for in the horizontal distance estimation; distances were measured as if the track and glider at the same depth. If no localizations were available within a given snapshot (the gap between subsequent track localizations could be as large as 900 seconds as set in the filtering process), no distance could be calculated, and that trial was removed. From previous work we knew that 40 Hz spectrum levels in the glider data were highly variable and changed with glider changes in speed as low-frequency flow noise was generated (Fregosi *et al.*, 2020), therefore 40 Hz levels were included in the detection function model and extracted for each snapshot. The median 40 Hz noise level for each six-minute snapshot was calculated from the one-minute levels calculated above. Lastly, each snapshot had a track number, which served as a proxy for time.

The detection probability for each snapshot as a function of range and 40 Hz spectrum level was estimated using a generalized additive model (GAM; Wood, 2017). A GAM approach was chosen because it is more flexible than a generalized linear model and does not require a detection function shape to be specified. It is more flexible because it

allows the probability of detection at zero distance to be estimated and does not require that the detection probability decreases monotonically with range. The response variable was the binary detection and non-detection score and was modeled as a Bernoulli trial with a logit link function. The explanatory variables were univariate thin plate regression splines for horizontal distance and median 40 Hz spectrum level. A random effect for track number was included in the model because multiple snapshots from the same track could not be considered independent samples. The model was fit using the *gamm4* package (Wood and Scheipl, 2017) in program R (version 3.6.2; R Core Team, 2019). A detection function was first estimated for all snapshots. Exploratory analysis showed that at the quietest noise levels (<85 dB), detection was likely not near zero at the maximum horizontal distances measured (55 km). The average detection probability is estimated by integrating the detection function from zero to some maximum distance (beyond which you would not expect to detect acoustic events). It is necessary to know with certainty that a detected acoustic event was detected within the specified maximum distance. If the detection function does not reach zero by this maximum distance, then it is not known with certainty that all detected events occurred within the maximum distance; some may have occurred beyond the specified maximum range. In that case, integrating the detection function over that range would likely underestimate detection probability and so overestimate density. Therefore, a detection function was again calculated for just snapshots with 40 Hz spectrum levels between 90 and 100 dB re 1 $\mu\text{Pa}^2/\text{Hz}$ (inclusion was based on rounding dB levels to the nearest integer value). A single median detection function was calculated based on the median noise level for snapshots with noise levels from 90 to 100 dB.

Effective survey area (ESA), \hat{a}_e , was calculated from the estimated median detection function following point-transect distance sampling methods (Buckland *et al.*, 2001) and the equation

$$\hat{a}_e = 2\pi \int_{r=0}^w yg(y)dy \quad (3.4)$$

where $g(y)$ is the detection function, the probability of detection at horizontal range y , and w is the truncation distance defined as the range at which probability of detection is essentially zero. A value of 60 km was used for w based on previous estimates of fin whale

detection range (Širović *et al.*, 2007; Stafford *et al.*, 2007). Effective detection radius (EDR) was calculated using

$$EDR = \sqrt{(\hat{a}_e/\pi)} \quad (3.5)$$

Because variance estimates for non-independent data can be underestimated, variance for ESA and EDR calculations was estimated empirically using a jackknife procedure with glider dive number as the resampling unit (Efron, 1982). The coefficient of variation (CV) is presented as the measure of precision and was calculated as the standard error divided by the mean.

Density estimation

The density of acoustic events and of individual animals was estimated using a point-transect approach (Buckland *et al.*, 2001), where the glider track was divided into snapshots, each representing a sampling point. An acoustic event as recorded on the glider was defined as a six-minute snapshot with 40 Hz spectrum levels between 90 and 100 dB containing fin whale song as a sequence of 20 Hz pulses. Acoustic events were scored manually by visual inspection of spectrograms of each possible six-minute snapshot (2048 sample Hamming window, 90% overlap, frequency resolution 0.4883 Hz, time resolution 0.205 seconds, equalization applied by subtracting median noise in 1 Hz bands averaged over 4 previous seconds). The density of acoustic events, \hat{D}_s , was estimated as

$$\hat{D}_s = \frac{n}{k\hat{a}_e} \quad (3.6)$$

where n is the number of acoustic events detected, k is the total number of six-minute snapshots with 40 Hz spectrum levels between 90 and 100 dB re 1 $\mu\text{Pa}^2/\text{Hz}$ recorded by the glider, and \hat{a}_e is the ESA estimated with Equation (3.4). Variance for the proportion of snapshots with calls (n/k) was estimated empirically using a jackknife approach with glider dive ($n = 18$) as the resampling unit (Efron, 1982). No estimate of false-positive rate was needed (as is typically included in acoustic density estimation because all detections were marked manually).

The density of individual fin whales, \hat{D} , was then estimated by accounting for the probability of a fin whale singing in a six-minute snapshot and the average group size for fin whales using

$$\hat{D} = \frac{n\hat{s}}{k\hat{a}_e\hat{P}_v} \quad (3.7)$$

where \hat{P}_v is the estimated probability of a fin whale vocalizing within a six-minute snapshot, and \hat{s} is the estimated average group size. The probability of a fin whale vocalizing within a six-minute snapshot, \hat{P}_v , was estimated from calling behavior data from ten tagged fin whales in Southern California presented in Stimpert *et al.* (2015). Each tag record was divided into six-minute snapshots, and the proportion of snapshots containing calls produced by the tagged animal was calculated. The proportion of snapshots with calls was calculated for each tagged animal as the mean of the proportions for all possible snapshot start times (0 to 5 minutes into the tag record), and then the mean across all tags was used in the density estimate. Variance in the probability of a snapshot containing vocalizations was calculated using a jackknife approach with tag number as the resampling unit. Sex information was not available for all tagged whales so a sex ratio of 50:50 males to females was assumed, and thus the probability of a whale vocalizing within a six-minute snapshot was the estimated probability for all fin whales, regardless of sex. The probability of a fin whale calling in a six-minute snapshot (\hat{P}_v) was calculated from tag data where calls could be attributed to the calling animal from accelerometer data (Goldbogen *et al.*, 2014; Stimpert *et al.*, 2015) thus, that probability is for a single fin whale. Further, Stimpert *et al.* (2015) did not find any relationship between group size and calling behavior. However, when quantifying the proportion of snapshots containing fin whale calls (n/k), there was evidence that some snapshots may have contained calls from multiple individuals (as evidenced by call sequences with different received levels and timing patterns). If it was assumed each snapshot only contained a single whale calling (similar to assuming a group size of 1), the density estimate may be biased low. To account for this, a proxy for group size (\hat{s}) was estimated from the tracking data by counting the number of individual tracks visible in each snapshot (k) and taking the mean number of tracks across all snapshots that contained tracks. Variance in the density estimate was calculated from the

combined CV values of the proportion of snapshots with calls, the effective survey area, and the probability of vocalizing in a six-minute snapshot using an approximation of the delta method (Marques *et al.*, 2013; Seber, 1982). Confidence intervals (CI; 95%) were estimated by assuming a log-normal distribution of estimated density, following Buckland *et al.* 2015, pg. 107.

Results

Trial-based detection function

A total of 77 tracks occurred during the 90 hours of glider recordings analyzed and were located throughout the study area (Figure 3.3). These tracks generated 859 six-minute snapshots that were manually scored (415 detections, 174 non-detections, 270 excluded for non-definitive assessment; Figures B3, B4). Spectrum levels at 40 Hz varied over glider dive cycles in a predictable pattern (Figure 3.4). Levels were generally between 80 and 105 dB. Levels above 110 dB represent times when the glider buoyancy pump operated at the bottom of each dive cycle (Figure 3.4).

After limiting snapshots to just those that were between 90 and 100 dB and removing any snapshots that overlapped in time (62 snapshots), the final subset of snapshots used to model the detection function included 170 snapshots from 40 tracks and consisted of 82 detections and 88 non-detections (Figure 3.5). Differences in detectability at increased horizontal distances and higher noise levels occurred as expected from acoustic transmission loss and masking, with fewer detections at greater horizontal distances and higher noise levels (Figure 3.5). At the quieter noise levels (~90 dB), the detection function showed a shoulder with detection probability 1.0 (certain) up to about 30 km, and then a monotonic drop as horizontal distance increased (Figure 3.6). Detection probability at horizontal distance zero was 1.0 (certain) between 90 and 96 dB. The median noise level for all snapshots with 40 Hz levels between 90 and 100 dB was 97 dB, and at that noise level, the maximum detection range was almost 40 km (Figure 3.6). Effective survey area, \hat{a}_e , for the median detection probability at noise levels of 97 dB was estimated to be 870 km² (jackknife CV 0.231); EDR was 16.6 km (jackknife CV 0.116).

Estimated density

The 90-hour survey spanned 18 glider dives (Dives 7 through 24), and 343 snapshots recorded by the glider had 40 Hz spectrum levels between 90 and 100 dB (mean 19.05 snapshots per dive; standard deviation 5.43; Table 3.1). The proportion of snapshots with fin whale 20 Hz pulses, n/k , was 0.466 (jackknife CV 0.121), and the density of call-present snapshots was 0.533 call present snapshots per 1000 km² (jackknife CV 0.231; 95% CI 0.341 – 0.833; Table 3.2). The average number of whales tracked within a single snapshot (with at least one whale present; \hat{s}) was 1.17 whales (CV 0.025). Only three snapshots contained the three whales, the maximum number of tracked whales observed in a single snapshot. The probability of a fin whale vocalizing in a six-minute snapshot, \hat{P}_v , as calculated from tagging data presented in Stimpert *et al.* (2015), was 0.259 (jackknife CV 0.480). Estimated fin whale density for the 90-hour survey was 2.409 whales per 1000 km² (jackknife CV 0.547; 95% CI 0.884 – 6.567; Table 3.2).

Discussion

We demonstrate that a detection function can be estimated using a trial-based method with whale tracks localized by a stationary cabled array as the trials and that density can be estimated using an approach based on point-transect distance-sampling. Results indicate that glider flow noise, in the same frequency band as the fin whale calls of interest, was an important covariate in the detection function, and therefore noise levels are a critical consideration in estimating fin whale density.

Detection function estimates

The estimated effective detection radius of 16.6 km seems reasonable for periods when 40 Hz spectrum levels were between 90 and 100 dB. While it is considerably shorter than maximum ranges found in the Southern Ocean (up to 56 km; Širović *et al.*, 2007), noise levels in that study were significantly quieter (on average 80 dB re 1 $\mu\text{Pa}^2/\text{Hz}$ at 220 Hz). Unfortunately, that study does not report an EDR or distribution of detection ranges but only a maximum range (Širović *et al.*, 2007). But the maximum ranges at the lowest

noise levels in this study are close to the maximum range from Širović *et al.* (2007). Propagation modeling was used to estimate detection areas for fin and blue (*B. musculus*) whales from stationary deep-water hydrophones deployed in Southern California, but the estimated areas are irregular shapes and so couldn't be directly compared with EDR and ESA from this study (Širovic *et al.*, 2015). Conversely, the effective survey area is quite similar to that found for fin whales in the western Pacific Ocean near Wake Island, as detected from ocean bottom seismometers (973 km²; Harris *et al.*, 2018). Harris *et al.* (2018) included calls recorded in all ambient noise (10 to 30 Hz) conditions up to 124 dB so it is possible the noise conditions in that study were more similar to this work.

The noise levels on the glider were higher than those used in a propagation modeling approach to detection range estimation (Stafford *et al.*, 2007). However, the detection probability for the glider in this work is higher than estimated by Stafford *et al.* (2007), which suggested a steep drop-off in detection probability with near-zero probability at only 10 km when ambient noise levels at 25 Hz were 91 dB. This could be because of different units of detection (single calls vs. calls within a snapshot) mediated by the season of the glider survey. The glider work took place in the winter when fin whales were calling in long song-bouts, which meant that there was a greater probability that multiple calls were detected and so song was more detectable than short intermittent series of pulses that are more common in the summer (Thompson and Friedl, 1982; Watkins *et al.*, 2000)

The primary limitation of this work was that the collected data did not include snapshots with horizontal ranges between the glider and tracked whales that were greater than 55 km, which limited the maximum range of inference. This was due in part to the limitations of the hydrophone array to localize whales very far from the array because of the array's size. For a target species such as a fin whale, it would have been preferable to have maximum distances up to 100 km (Stafford *et al.*, 2007). In quiet conditions, we might expect fin whales to be heard that far (Stafford *et al.*, 2007) and so would ideally estimate the detection function out to that range. Perhaps future efforts could direct the glider to survey off the SCORE range with the idea that whales at large distances to the glider on the range could be localized and increased distances could be included in the trial. However, the bathymetry at SCORE may limit such an approach. San Clemente Island

borders the range to the east and west of the hydrophone array is relatively shallow water. Flying the glider north of the hydrophone array may provide the best opportunity to improve the available distances. The variability in noise levels in the frequencies of and near fin whale 20-Hz pulses on the glider provided a sort of natural experiment in which the changes in noise levels could be used to estimate a reasonable detection probability with the available data. The low-frequency flow noise varied predictably due to the glider's ballasting and flight parameters. Descents were significantly faster, and flow noise was higher than during ascents (Fregosi *et al.*, 2020). Analyzing snapshots that had 40 Hz spectrum levels between 90 and 100 dB ensured we had data that could estimate the tail of the detection function, where detection probability is near zero. If the tail of an estimated detection function does not reach zero, then inference of maximum detection range is not possible and estimates of average detection probability may be biased low. When counting snapshots with acoustic events present, it is necessary to know that any snapshot detected was made within a certain maximum detection radius, the truncation distance. If the detection function does not reach zero at some distance it is not given that any detected snapshot was within that maximum distance; snapshots may be detected that originated beyond the maximum distance which would bias density high.

Additional biases in this detection function could be due to the localization, tracking, and filtering processes used to generate the detection trials, but we suggest these are minimal and do not detract from the demonstration of estimating a detection function for a glider. The localization and tracking process implemented here is regularly used for studies of baleen whale behavior on Navy ranges (Helble *et al.*, 2015; Martin *et al.*, 2015). Foremost, it is important to state the glider detection function is for trackable whales. We assume that there is no difference in detectability for trackable and non-trackable whales in our estimate of total fin whale density, but we do not have empirical evidence of this in this study. An individual calling in regular sequences is likely more trackable than an individual making intermittent calls because of specified tracking and filtering parameters used (minimum number of hydrophones, minimum number of localizations required to constitute a track). We tried to address this by also using sequences of calls (within a six-minute snapshot) as the detected acoustic event. However, being able to restrict detections

by this criterion was only possible because of the abundance of call sequences available during this winter survey. A comparison with fin whale trackability in summer months may provide insight into the appropriateness of this assumption and how it may best be accounted for. The number of available tracks and whales available in this relatively short experiment allows the filtering to be relatively restrictive, including only high-quality localizations (least squares score < 0.055 sec) and those with more than the minimum number of necessary hydrophones (6 versus 4). Further, track locations were not interpolated; if there was a gap in track localizations over a particular snapshot, that snapshot was excluded. This meant no assumptions of animal location between localizations was needed, although by our estimates this would likely not have been an issue (based on average travel distances of a few hundred meters in six minutes compared to detection ranges over ten kilometers). Investigation into how tracks with more relaxed filtering or using interpolated locations could be explored to better understand these potential biases.

Application of the detection function presented here to longer-duration glider surveys, or surveys where survey-specific detection function estimation is not possible, may be acceptable if the same noise level restriction is applied to the snapshot detection process of the external survey. Noise at 40 Hz was a key parameter in the detection function and accounting for noise levels may allow this detection function to be carefully applied to additional surveys. More work on variability in detection functions across regions and seasons is needed to understand the potential variability in detection functions for gliders. Low frequency, glider-generated flow noise is a dominant component of glider recordings regardless of survey location or season (Fregosi *et al.*, 2020; Matsumoto *et al.*, 2015; dos Santos *et al.*, 2016) and measuring this noise is relatively straightforward. Therefore, noise may be advantageous in this case because the effect of ambient noise on detectability (Helble *et al.*, 2013b; Ward *et al.*, 2011) is likely negligible compared to glider-generated flow noise. While theoretically restricting snapshots by the 40 Hz noise level could introduce bias, we feel it is appropriate to assume the total number of whales does not change with flow noise levels on the glider, because the noise on the glider is tied directly to glider speed rather than environmental conditions (*e.g.*, weather, sound propagation,

presence of ships). At the same time, the location and time of the survey, in regard to animal behavior, would need to be considered before applying the detection function widely (Marques *et al.*, 2013); this detection function is specific to Southern California during the fall and winter when fin whales are singing.

The manual matching and detection process used in this work was intensive and, while important for this initial demonstration, may be difficult to implement for a longer duration study. A fully automated cross-correlation process to match tracked fin whales to fin whales detected on the glider was not possible, primarily because there was such an abundance of fin whale calls, with many instances of multiple animals detectable and some very distant calls and multipath path detections. Limiting the data to the relatively higher noise levels reduced ambiguity by decreasing the number of snapshots that contained faint, and distance calls. The snapshots with the quietest noise levels may represent the conditions in which true sequence matches were the most difficult to determine. This was evident by the lack of available data points with low noise levels and long horizontal ranges (Figure B4). It is not the case that these conditions did not occur; rather, when those conditions were met, a definitive detection/non-detection could not be made and typically those points were marked as unsure and excluded. But, if this detection probability, and the six-minute song-present snapshot, was again used as the sampling unit for a longer-term deployment, a more streamlined and unambiguous process for a detection versus a non-detection would be needed. Possibly a minimum or maximum number of calls present in each snapshot could be used, or a minimum SNR level for all calls.

Including glider depth as a covariate in the detection function was not entirely possible in this study because of the strong effect of glider-generated flow noise on the modeled detection function. We explored including glider depth in the detection function model, but glider depth and 40 Hz noise level were weakly correlated (increasing noise level at shallower depths) so they could not both be included in the GAM. However, this observed correlation was driven by the snapshots with mean glider depths above 200 m; these snapshots had only relatively high noise levels (> 96 dB). If only snapshots with glider depths of 400 m or greater were examined, there was no correlation between glider depth and 40 Hz noise level and including depth in as a covariate in the GAM did not

improve the model. Although sound propagation can vary with depth, previous work showed that the number of detections of individual fin whale 20 Hz pulses did not vary with glider depth (Fregosi *et al.*, 2020). It is possible the high variability of 40 Hz noise levels dominates the detection function results and limited our ability to investigate the possible minor role of depth. Depth as a covariate in detection functions warrants more research, and may be able to be investigated in an experiment without the strong influence of 40 Hz flow noise.

Estimation of density

The density of fin whales estimated by a glider (2.4 whales per 1000 km²) was similar to the overall density of fin whales in Southern California from 2004 to 2013 estimated from visual line-transect survey (2.73 whales per 1000 km²) by Campbell *et al.* (2015). The coefficient of variance of the glider-generated estimate (CV 0.55) was more than double that of Campbell *et al.* (2015; CV 0.19), likely because of the high variance of the call rate multiplier as calculated from only a small sample of tagged fin whales. However, for just the winter season, the glider estimate was almost 4 times larger than that from the visual surveys (0.65 whales per 1000 km²), where peak densities occurred in summer and fall (Campbell *et al.*, 2015). Variance on the visual estimate for winter was higher than the overall estimate and was closer to the variance of the glider-generated estimate (0.42; Campbell *et al.*, 2015). While it is useful to generally compare the glider-generated density estimate to that from historical visual line-transect surveys, the glider survey covered a much smaller area than the efforts by Campbell *et al.* For this reason, we do not suggest using this glider-based estimate to make conclusions about changes in population trends, as was possible in Campbell *et al.* (2015).

Inputs for multipliers used in density estimation should ideally be collected from the survey region and time period where the survey takes place. Density estimation assumes these parameters are accurate for the time and place of the main survey. The tagged animal estimate of call rate applied here is for fin whales in Southern California (Stimpert *et al.*, 2015). While the tagging work occurred in the fall (September and October) and the glider survey occurred in December and January, the primary call type

on the tagged animals was 20 Hz pulses in regular sequences, suggesting that the call rate from fall tagging work is applicable to the 20 Hz sequences detected on the glider. In estimating total fin whale density, we assumed the sex ratio of the tagged animals is representative of the sex ratio of all fin whales in the area. This assumption may not hold if tagging efforts were biased. For example, if permitting did not allow tagging of females with calves, it is possible fewer females were tagged, which would mean the probability of a whale vocalizing would be biased high and the density estimate would be biased low. By comparing the CV of the density of snapshots with fin whale calls (0.23) and the CV of fin whale density (0.55), it is clear that adjustment for call rate had the greatest effect on the variance of the density estimate. Because of the small size of the tag dataset and the large confidence intervals on the density estimate (0.9 – 6.6 animals/1000 km²), the density estimate provided here is presented as an example of how animal density could be estimated if appropriate multipliers are available but should not be widely extrapolated to the larger Southern California Bight region or used to infer changes in population size.

With this experiment, estimates of density from the glider-collected data could possibly be compared to a plot sampling estimate of animals tracked on the range (count all animals and assume none are missed within the range, similar to the methods of Moretti *et al.*, (2010) and Ward *et al.*, (2012)) which is a unique opportunity to directly compare two density estimates for the same time and place using two different methods. We suggest such comparisons as the focus of future work.

The ability to use acoustically-equipped autonomous deep-water gliders to estimate cetacean population density has the potential to greatly expand our capabilities for long-term and broad spatial monitoring of marine mammals. This work provides an empirical detection function for fin whales and a proof-of-concept density estimate of fin whales for a small example 90-hour survey. The approach used – leveraging the ability of a cabled array to track individual animals and setting up detection trials with those tracks – could be applied to other baleen whale species such as humpback and blue whales that are also trackable through stationary arrays.

Acknowledgements

The authors thank Alex Turpin (Oregon State University) for his work on implementing the acoustic system on the glider and floats and for his help in the field, Ronald Morrissey (Naval Undersea Warfare Center) and the crew of the *RSC4* for assistance with the field work, and Anatoli Erofeev (Oregon State University) for glider piloting services and expertise. Special thanks to Tyler Helble, and Len Thomas for discussions of fin whale tracking and density estimation. Funding for this work was provided by the Living Marine Resources Program Grant Number N39430-14-C-1435 and Office of Naval Research Grant Number N00014-15-1-2142. SF was supported by the National Science and Engineering Graduate Fellowship. This is PMEL Contribution No. 5101.

Tables

Table 3.1. Number and proportion of snapshots recorded by the glider with fin whale 20 Hz pulses present, for each glider dive and averaged across all glider dives. Standard deviation is given in parentheses for the number of snapshots and number of snapshots with calls and the jackknife CV is given in parentheses for the mean proportion of snapshots with calls. Snapshots analyzed are only those where median 40 Hz spectrum levels in the six-minute snapshot were between 90 and 100 dB re 1 $\mu\text{Pa}^2/\text{Hz}$.

Dive number	Number of snapshots (k)	Number of snapshots with calls (n)	Proportion of snapshots with calls (n/k)
7	27	19	0.704
8	26	19	0.731
9	14	0	0.000
10	15	2	0.133
11	19	8	0.421
12	27	18	0.667
13	34	17	0.500
14	16	7	0.438
15	18	7	0.389
16	14	5	0.357
17	17	7	0.412
18	16	12	0.750
19	18	6	0.333
20	16	2	0.125
21	15	9	0.600
22	16	13	0.813
23	17	12	0.706
24	18	5	0.278
Mean	19.05 (5.43)	9.33 (5.82)	0.464 (0.121)

Table 3.2. Density of snapshots with fin whale calls present and density of fin whales for the 90-hour glider survey. Coefficient of variation (CV) was calculated for each random variable using a jackknife approach and CV for the final density was estimated using the delta method.

Proportion of snapshots with calls, n/k		Effective survey area, \hat{a}_e (km ²)		Density of call-present snapshots, \hat{D}_s (per 1000 km ²)		Estimated average "group size" per snapshot, \hat{s}		Probability of vocalizing in six-minute snapshot, \hat{P}_v		Density, \hat{D} (per 1000 km ²)	
mean	CV	mean	CV	mean	CV	mean	CV	mean	CV	mean	CV
0.464	0.12	870.1	0.23	0.533	0.26	1.17	0.025	0.259	0.48	2.41	0.55

Figures

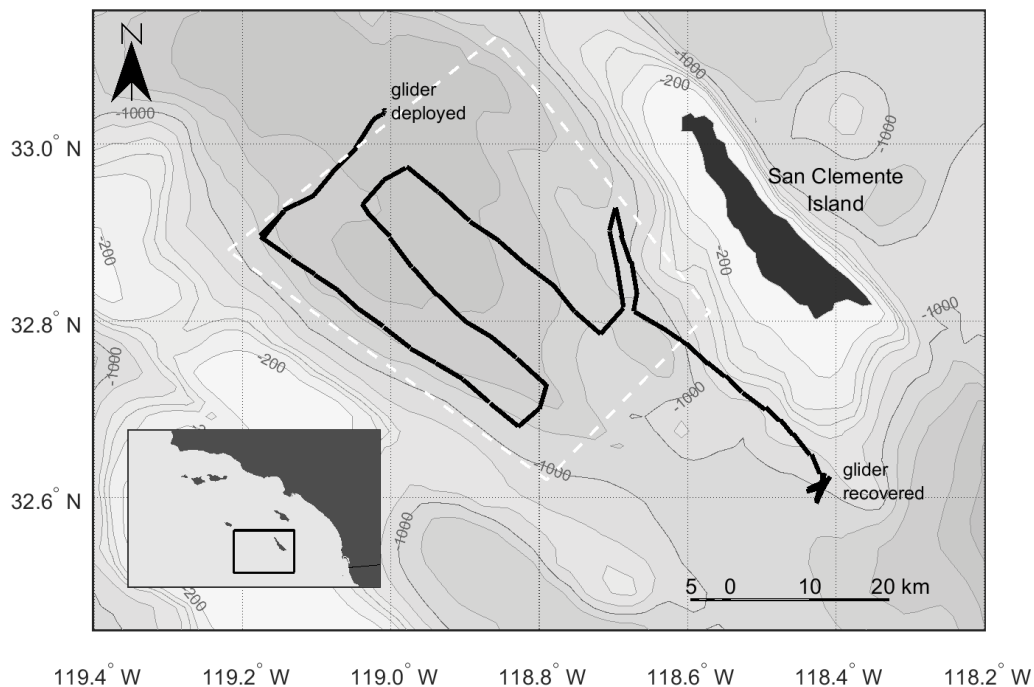


Figure 3.1. Map of Seaglider, SG158, survey path (black line) and the general location of the SCORE hydrophone array (white dashed box). The glider was deployed to the north west of the SCORE array and recovered south of the eastern end of San Clemente Island. Bathymetry is shown in 200 m contours from -200 m (white) to -2000 m (darkest gray). Bathymetry data is from NOAA's National Centers for Environmental Information (Amante and Eakins, 2009).

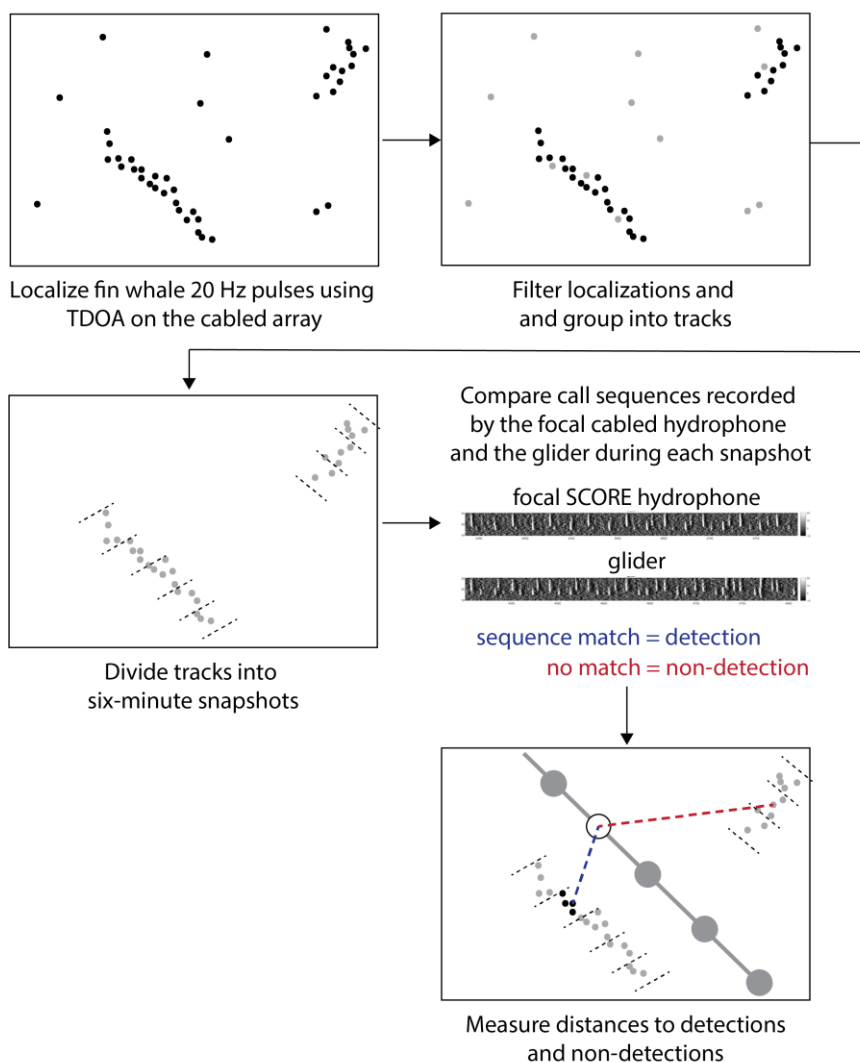


Figure 3.2. Flowchart outlining the steps from fin whale localizations to detection trials. Fin whale 20 Hz pulses are first localized using time difference of arrival (TDOA) methods applied to the cabled array recordings. Localizations are filtered by accuracy and grouped into tracks. Tracks are then divided into six-minute snapshots. The spectrogram of the snapshot period recorded on the focal hydrophone (hydrophone with most localizations contributed to the track) was then cross correlated with the spectrogram of the same time period recorded on the glider. If the sequence of calls matched, the trial was scored as a detection, and if no calls were present on the glider recording or the sequence did not match, it was scored as a non-detection.

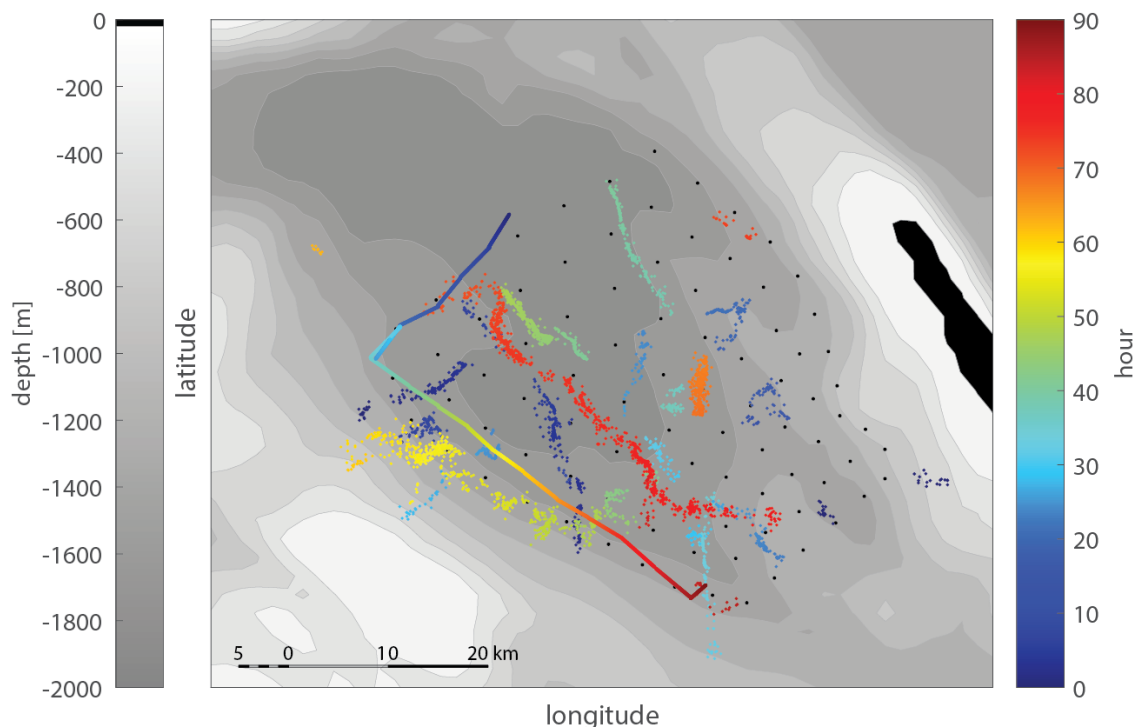


Figure 3.3. Final whale localizations and the glider track. Localizations that make up whale tracks are shown as colored points; color represents time in hours from the start of the glider deployment. The glider track is shown as the colored line with the same time coloration as the localizations and is generated from straight-line interpolation between surface GPS positions. Black squares show approximate location of the SCORE hydrophone array. Localizations that contributed to final tracks were generated from at least 6 hydrophones and had a least squares value of less than 0.055 sec. A minimum of 8 localizations were necessary to generate a track, and subsequent locations had to be within 0.01° latitude and 0.01° longitude and 900 seconds or less between locations. Bathymetry is shown in 200 m contours from -200 m (white) to -2000 m (darkest gray). San Clemente Island is in black to the right side of the map. Bathymetry data is from NOAA's National Centers for Environmental Information (Amante and Eakins, 2009).

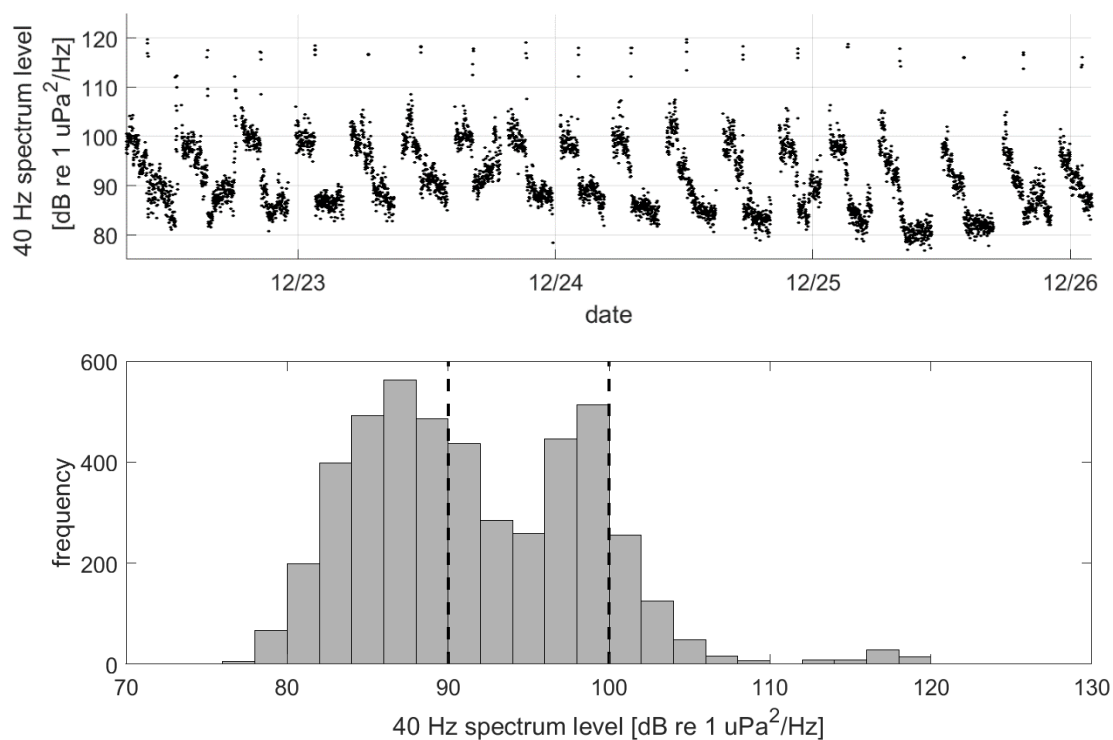


Figure 3.4. Spectrum levels at 40 Hz on the glider in 1-minute intervals over time (top) and histogram distribution (bottom) for the first three days of the survey. Spectrum levels were calculated using a 10 sec Hann window. Lowest levels per minute are displayed to exclude transient sounds such as glider pitch and roll maneuvers. The decrease in 40 Hz levels from the start to end of a dive cycle is due to faster glider speed, with higher noise, during descents and slower glider speed, with lower noise, during ascents. Glider pumping activity, which lasts several minutes at the bottom of each dive cycle, is the likely source of the levels above 110 dB re 1 $\mu\text{Pa}^2/\text{Hz}$.

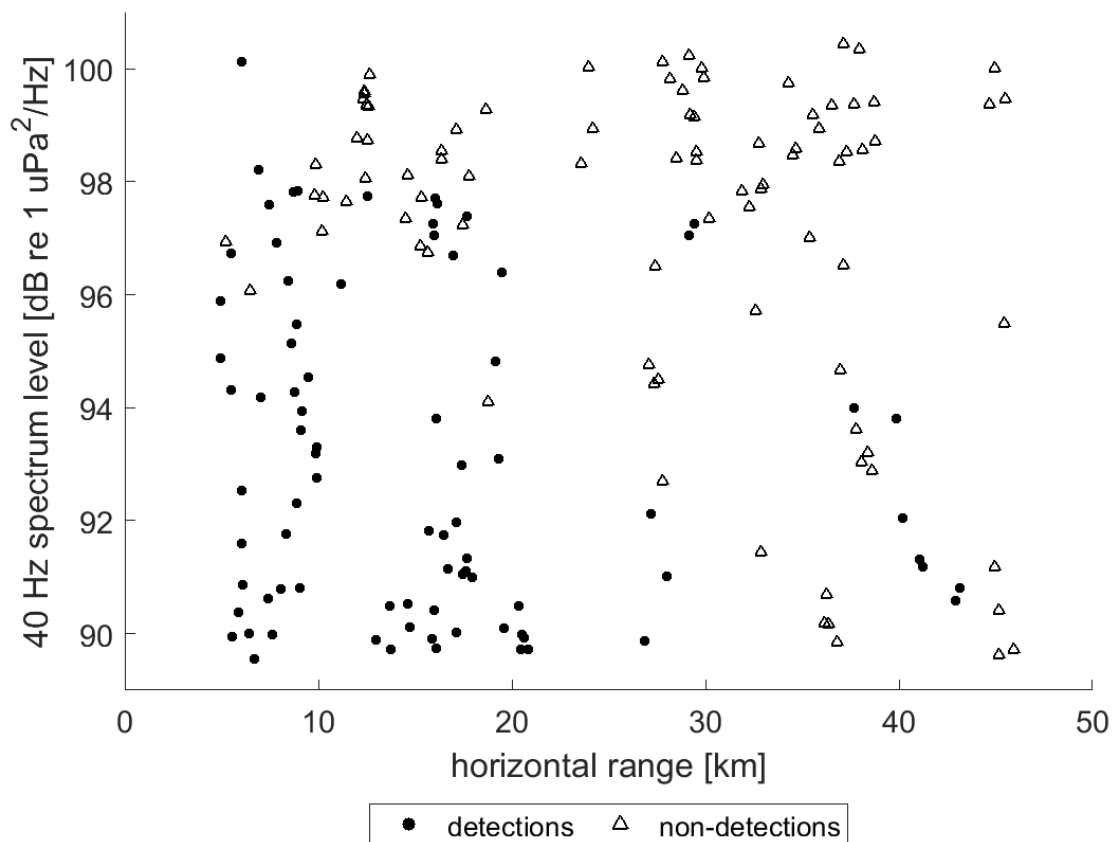


Figure 3.5. Snapshots that were detected (black circles) or not detected (outlined black triangles) by the glider as a function of distance from the track segment to the glider and the median 40 Hz spectrum level on the glider during that snapshot for the subset of snapshots ($n = 170$) used in the detection function analysis.

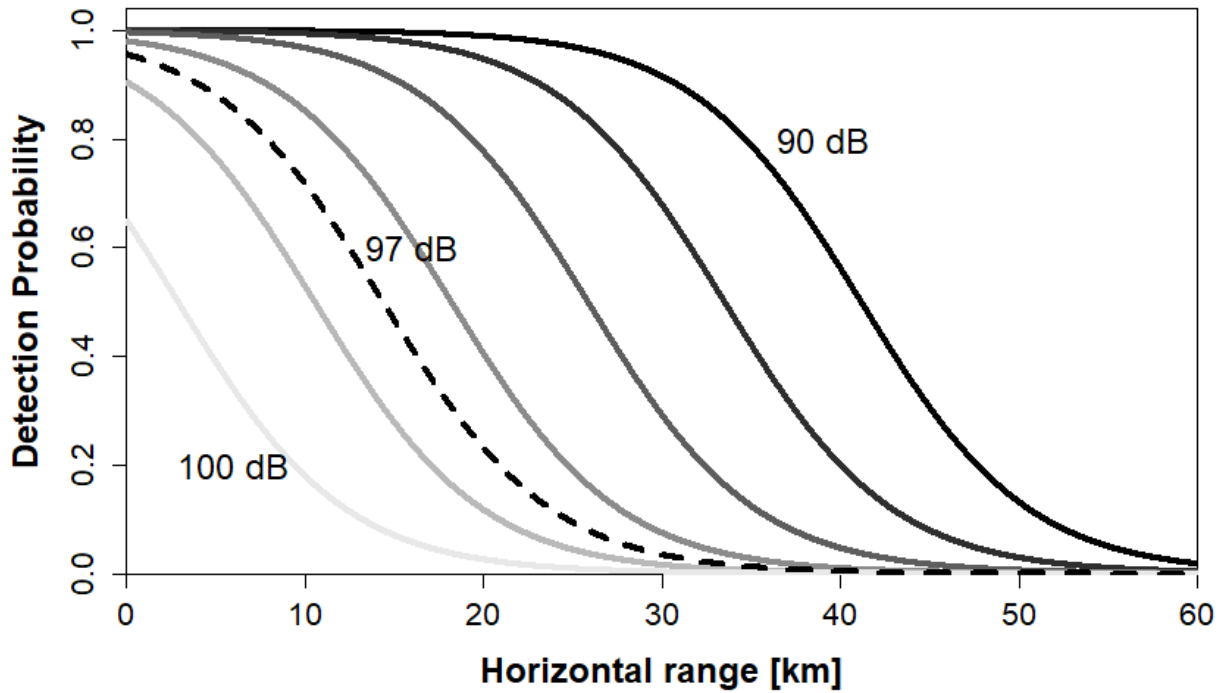


Figure 3.6. Detection probability estimated from snapshots with 40 Hz spectrum levels between 90 and 100 dB re $1 \mu\text{Pa}^2/\text{Hz}$. Detection probabilities are shown for a range of 40 Hz spectrum levels, from 90 dB (black) to 100 dB re $1 \mu\text{Pa}^2/\text{Hz}$ (lightest gray) in 2 dB increments. Detection probability at the median noise level for all snapshots included (97 dB) is shown as the dotted line.

CHAPTER 4: DETECTIONS OF WHALE VOCALIZATIONS BY
SIMULTANEOUSLY DEPLOYED BOTTOM-MOORED AND DEEP-WATER
MOBILE AUTONOMOUS HYDROPHONES

Selene Fregosi, Danielle V. Harris, Haruyoshi Matsumoto, David K. Mellinger, Jay
Barlow, Simone Baumann-Pickering, and Holger Klinck

Abstract

Advances in mobile autonomous platforms for oceanographic sensing have provided new opportunities for passive acoustic monitoring of cetaceans. Such platforms, including gliders and deep-water profiling floats, can survey a variety of cetacean species. However, there are few direct comparisons of these mobile autonomous systems to more traditional methods, such as stationary bottom-moored recorders. Cross-platform comparisons are necessary to enable interpretation of results across historical and contemporary surveys that use different recorder types. Understanding tradeoffs across recording platforms can inform best practices for cetacean passive acoustic monitoring in the future. This study directly compares the passive acoustic monitoring capabilities of a glider (Seaglider) and a deep-water profiling float (QUEphone) to a stationary seafloor system (High-frequency Acoustic Recording Package, or HARP) deployed simultaneously over a two-week period in the Catalina Basin, USA. Two HARPs were deployed 3.9 km apart while a glider and deep-water drifter surveyed within 20 km of the HARPs. Acoustic recordings were analyzed for the presence of multiple cetacean species, including beaked whales, delphinids, and minke whales. Variation in detection rates at one-minute (beaked whales only), hourly, and daily scales were examined. The number of minutes, hours, and days with beaked whale echolocation clicks were variable across recorders, likely due to differences in the recording limits of each system, the spatial distribution of the recorders, and the short detection radius of such a high-frequency, directional signal type. Delphinid whistles and clicks were prevalent across all recorders, and at levels that may have masked beaked whale vocalizations. The number and timing of hours and days with minke whale boing sounds were nearly identical across all recorder types, as was expected given the relatively long propagation distance of boings. This work advances our understanding of how autonomous mobile platforms can be used for acoustic surveys for cetaceans. This comparison provides evidence that gliders and deep-water drifters record cetaceans at similar detection rates to traditional stationary recorders at a single point. Additionally, these mobile platforms provide improved spatial coverage which may be critical for species that produce calls that propagate only over short distances such as beaked whales.

Introduction

Passive acoustic monitoring (PAM) is a cost-effective, non-invasive tool for surveying marine mammal populations, particularly cryptic species such as deep-diving beaked whales (Yack *et al.*, 2013; Zimmer *et al.*, 2008) and minke whales (*Balaenoptera acutorostrata*; Martin *et al.*, 2013; Risch *et al.*, 2013) for which visual sighting methods are less effective (Barlow and Gisiner, 2006; Rankin and Barlow, 2005). Commonly used PAM methodologies include fixed (autonomous or cabled) platforms, either single sensors or arrays of sensors, and arrays of hydrophones towed behind a vessel (Baumann-Pickering *et al.*, 2014; von Benda-Beckmann *et al.*, 2010; Henderson *et al.*, 2016; Martin *et al.*, 2013; Mellinger *et al.*, 2007; Norris *et al.*, 2017; Širović *et al.*, 2015; Yack *et al.*, 2013). Different recording platforms have tradeoffs in survey coverage over space and time (Van Parijs *et al.*, 2009).

Fixed autonomous recorders are valuable tools for monitoring marine mammals, but they have a variety of limitations. They are typically deployed for long time periods (months to years), but spatial coverage is limited to a specific detection radius around the hydrophone (Mellinger *et al.*, 2007). This detection radius is dependent on various factors including acoustic source level and frequency of the target signal, the location, directivity, and behavior of the vocalizing animal, local sound propagation conditions, depth of the acoustic receiver, and ambient noise levels (Gkikopoulou, 2018; Helble *et al.*, 2013b; Kuperman and Roux, 2007; Mellinger *et al.*, 2007; Urick, 1983; Ward *et al.*, 2011; Zimmer *et al.*, 2008). Mean detection radii can range from many tens of kilometers for a low-frequency baleen whale call (*e.g.*, Širović *et al.*, 2007; Stafford *et al.*, 2007) to only a few tens of meters for a highly directional porpoise echolocation click (Kyhn *et al.*, 2012). Deployment locations may be limited by accessibility to the monitoring area and seafloor depth. For example, deploying a fixed autonomous recorder in offshore, deep waters can be logistically difficult. Multiple fixed recorders can be deployed in an array to cover a larger spatial area than a single instrument, and some instruments are cabled to land to provide real-time data streams (Jarvis *et al.*, 2014; Klinck *et al.*, 2016b). However, increasing the number of recorders increases costs and produces terabytes of data that can be difficult to analyze efficiently (Van Parijs *et al.*, 2009; Roch *et al.*, 2016).

Towed arrays solve some of the spatial limitations of fixed hydrophones but have additional logistical constraints. They provide improved spatial coverage; a ship can survey across a variety of habitat types in a short time period (Mellinger *et al.*, 2007). Additionally, visual observers on ship-borne surveys can visually confirm recorded species and identify non-vocalizing animals (Rankin *et al.*, 2007; Rankin and Barlow, 2005) and link acoustic and surface behaviors (Miller and Tyack, 1998). Towed arrays, like fixed arrays, can be used to identify and track vocalizing individual animals (Quick and Janik, 2012; Thode, 2004) and allow for estimation of density or abundance through a distance sampling framework (Barlow and Taylor, 2005; Buckland *et al.*, 2001; Norris *et al.*, 2017). However, towed-array surveys are typically limited to only a few weeks in duration (Mellinger and Barlow, 2003). They are also limited to seasons with workable weather, are not ideal for monitoring low-frequency vocalizing baleen whales because calls are masked by ship and flow noise, and vessel presence can alter vocal behavior of the study animals (Barlow *et al.*, 2008; Guerra *et al.*, 2014; Lesage *et al.*, 1999; Norris *et al.*, 2012b; Thode, 2004).

Mobile autonomous systems have the potential to address the spatiotemporal tradeoff of long-duration, but low spatial coverage possible with fixed recorders and greater spatial coverage, but short durations typical of vessel-based surveys. Untethered platforms can cover large areas in space over longer time periods than a typical vessel-based survey. There are several additional types of mobile autonomous systems we will not discuss here (*e.g.*, autonomous sailboats, Klinck *et al.*, 2014; Wave Gliders, Wiggins *et al.*, 2010; near-surface drifting recorders, Griffiths and Barlow, 2015; see Verfuss *et al.*, 2019 for a thorough review). This study focused on two deep-water mobile autonomous systems: deep-water profiling floats and underwater gliders. Deep-water profiling floats are buoyancy-driven sensor platforms that drift at a pre-programmed depth for weeks to months (Matsumoto *et al.*, 2006; Roemmich *et al.*, 2009). Horizontal movement of deep-water profiling floats follows that of the deep-water currents. Underwater gliders are similar to deep-water profiling floats in their operation and communication, but have the added advantage of being able to traverse currents (Rudnick *et al.*, 2004). However, this horizontal movement comes at the cost of increased low-frequency (<100 Hz) noise from

water flow and noise from platform operation which could mask cetacean sounds of interest (Fregosi *et al.*, 2020).

Acoustically-equipped mobile autonomous platforms, such as underwater gliders and profiling floats, can effectively record a variety of marine mammal species (Baumgartner *et al.*, 2013; Küsel *et al.*, 2017; Matsumoto *et al.*, 2013; Nieu Kirk *et al.*, 2016) including beaked whales (Klinck *et al.*, 2012), delphinids (Silva *et al.*, 2019), and minke whales (Klinck *et al.*, 2015b). Deployments of the two autonomous mobile platform types presented in this study have been conducted at US Navy Ranges as proof-of-concept tests demonstrating that these systems can record marine mammals (Matsumoto *et al.*, 2013; Mellinger and Klinck, 2012). Detection rates of the low-frequency fin whale (*B. physalus*) 20-Hz pulse have been quantitatively compared to a cabled bottom-mounted hydrophone array (Fregosi *et al.*, 2020). However, no quantitative comparison has been made of detection capabilities for these platforms relative to other well-characterized bottom-moored systems, such as the High-frequency Acoustic Recording Package (HARP; Wiggins and Hildebrand, 2007). This comparison is helpful as mobile autonomous recorders become more widely used for marine mammal monitoring. In order to ensure that any differences in results collected by different systems are in fact indicative of real differences in animal distribution, abundance, and/or behavior, it is important we understand the differences introduced by each PAM recorder and platform.

We present results from an experiment in which a glider (Seaglider) and a deep-water profiling float (QUEphone) outfitted with autonomous hydrophone recorders were deployed simultaneously in the vicinity of two fixed recorders (HARPs). The recorders were deployed in the Catalina Basin within the Southern California Bight, where many marine mammal species are known to occur (Barlow, 2016). We compare detection rates for three types of marine mammal vocalizations – beaked whale echolocation clicks, small delphinid whistles and clicks, and minke whale boings – at several temporal scales (by call, encounter, hour, and day). We compare and contrast each vehicle’s capabilities and discuss likely drivers of observed differences. Finally, we provide recommendations for future applications of mobile autonomous vehicles for monitoring a variety of marine mammal species.

Materials and Methods

Recording platforms and PAM systems

The Seaglider™ (Huntington Ingalls Industries, Lynnwood, WA, USA; Eriksen *et al.*, 2001) is a buoyancy-driven, deep-diving autonomous vehicle capable of descending and ascending between the surface and 1000 m depth. Buoyancy is controlled by pumping oil into and out of an external bladder, changing the glider's volume and hence density, and the resultant vertical motion is converted to horizontal motion by the glider's wings. Longitudinal and rotational movement of the internal batteries moves the glider's center of gravity and provide changes in vehicle roll and pitch, allowing the vehicle to be steered towards a waypoint. The glider is remotely controlled by a shore-based pilot via Iridium™ satellite communications, transiting between specified waypoints. Typical speeds are 0.25 m/s (0.5 knots) horizontally and 0.10-0.15 m/s (0.2-0.3 knots) vertically. Dive cycle durations are dive-depth dependent and typically last 4-6 hours, with brief (5-10 min) surface intervals for communication with the shore-based pilot. Additionally, the Seaglider is outfitted with an unpumped conductivity-temperature-depth (CTD) sensor (Sea-Bird Electronics, Inc., Bellevue, WA, USA) that provides *in situ* measurements of salinity and temperature, and therefore sound speed profiles can be accurately estimated.

The QUEphone is a modified APEX™ float (Teledyne Webb Research, North Falmouth, MA, USA; Matsumoto *et al.*, 2006). The QUEphone's depth is controlled by changes in buoyancy in a manner similar to the Seaglider. It is capable of descending to 1500 m. Once at the programmed depth, it drifts passively with the currents rather than navigating between specified waypoints like the Seaglider. Dive depth and timing of surface intervals are controlled remotely via satellite.

Both the Seaglider and QUEphone were outfitted with an acoustic recording system, the Wideband Intelligent Signal Processor and Recorder (WISPR; EOS, Inc., Seattle, WA, USA). WISPR can record continuously at a 125 kHz sampling rate with 16-bit resolution (Matsumoto *et al.*, 2015). The recording system on both the glider and float can be programmed to turn on and off at a set depth and can be reconfigured remotely via satellite. Both the Seaglider and QUEphone were equipped with HTI-92-WB hydrophones with flat sensitivity (± 3 dB) from 2 Hz to 50 kHz (High Tech Inc., Gulfport, Mississippi,

USA). The WISPR system applies a pre-whitening filter configured for typical deep ocean ambient noise to optimize the dynamic range of the system; the spectral effects of this filter were reversed (removed) before the analysis described below. The WISPR system has a relatively low system noise floor. Above 20 kHz the noise floor is approximately 28 dB re 1 $\mu\text{Pa}^2/\text{Hz}$ and approaches ambient sound levels at sea state zero.

The HARP is a stationary autonomous recorder that has been used in many marine mammal passive acoustic monitoring studies (e.g. Hildebrand *et al.*, 2015; Širovic *et al.*, 2015; Wiggins and Hildebrand, 2016). It can record continuously or at a pre-programmed duty cycle at up to 320 kHz and 16-bit resolution for extended periods, and in this configuration had a relatively flat system sensitivity across all frequencies. The noise floor of the HARP above 20 kHz was higher than that of low wind and low sea state ambient sound levels (Wiggins *et al.*, 2018). From 30-60 kHz, the noise floor of the HARP was about 10 dB higher (38 dB re 1 $\mu\text{Pa}^2/\text{Hz}$) than that of the WISPR system.

Field Experiment

Two HARPs (H01 and H02), one Seaglider (SG607), and one QUEphone (Q003) were deployed and operated from 19 July to 2 August 2016, in Catalina Basin, a steep-walled ocean basin between Santa Catalina and San Clemente Islands, California, with a basin floor depth of approximately 1000-1300 m. The HARPs were deployed on 19 July near the center of the basin at a depth of approximately 1,250 m with 4 km of separation (Figure 4.1). They were aligned to follow the dominant surface current observed *in situ* (from deployed surface floats) on the day of deployment. The two HARPs began recording 20 July 2016 at 1100 UTC (H02) and 1200 UTC (H01) and recorded continuously at 200 kHz sample rate with 16-bit resolution. They were recovered at approximately 1600 UTC on 2 August 2016.

The Seaglider was also deployed 19 July 2016 and transited back and forth over the HARPs. The track lines extended 4 km (approximate distance covered in one dive cycle) to the northwest and 4 km to the southeast of H01 and H02 to also follow the dominant surface current (Figure 4.1). The glider was recovered on 1 August 2016 after being piloted away from the HARPs toward the shore of Catalina Island. The QUEphone was deployed

20 July 2016 approximately 4 km southeast of H02 and allowed to drift at 500 m depth for 48 hours before being recovered. This drift depth was selected to keep the QUEphone relatively deep but reduce the risk it would hit the seafloor if it drifted toward the steep walls of the basin. It was repeatedly recovered and redeployed over the next 13 days for a total of five drifts (Table 5.1). The QUEphone drifted generally northwest in line with the glider's transits and HARP deployment locations, but current variation changed the drift pattern slightly from day to day (Figure 4.1). All deployments occurred within a 5 km² area, with adjustments made each day based on the previous day's observed drift patterns. Acoustic data were collected by the glider and QUEphone continuously at 125 kHz sample rate when the platforms were at depths greater than 25 m (to exclude near-surface periods with unusable recordings due to loud surface noise); frequencies in the recordings could be used up to approximately 60 kHz.

Acoustic analyses

Beaked whales

A two-step detection and validation method, modified from (Baumann-Pickering *et al.*, 2013), was used to identify acoustic detections of beaked whales and other odontocetes on all platforms. The general method involved stages of click detection and classification, grouping of clicks into an event, and grouping of events into an encounter. Click detection included running a two-step click detector (Soldevilla *et al.*, 2008) in the Matlab™-based (v2013b, Mathworks, Natick, MA, USA) software package 'Triton' (v1.63, Scripps Whale Acoustics Lab, Scripps Institution of Oceanography, La Jolla, CA, USA), measuring spectral and temporal features of each click using custom Matlab code (Baumann-Pickering *et al.*, 2013), and then grouping clicks that met particular criteria into events. Detected clicks were classified as possible beaked whale clicks if peak frequency was above 32 kHz, center frequency above 25 kHz, duration at least 0.355 ms, and slope at least 23 kHz/ms (Baumann-Pickering *et al.*, 2013). To be included in further analysis, a minimum of 7 detected clicks in each sound file was required (a 75-s segment for HARP recordings and a 120-s segment for WISPR recordings). If more than 13% of all initially detected echolocation signals remained after applying these criteria, the segment was

classified to have beaked whale clicks. Experienced analysts, under the supervision of co-author SB-P, visually assessed each event's clicks to classify the event as either a beaked whale (to the species level, using Baumann-Pickering *et al.*, (2013) when possible) or "other". Beaked whale species that are known to occur in this region and are identifiable by echolocation clicks include Baird's (*Berardius bairdii*), Blainville's (*Mesoplodon densirostris*), Cuvier's (*Ziphius cavirostris*), and Stejneger's (*M. stejnegeri*) beaked whales (Baumann-Pickering *et al.*, 2014, 2018; Dawson *et al.*, 1998; Johnson *et al.*, 2006; Keating *et al.*, 2016; Madsen *et al.*, 2005; Stimpert *et al.*, 2014; Zimmer *et al.*, 2005). Additionally, three unknown beaked whale click types, BW37V, BW40 and BW43 have been recorded in Southern California and may be attributed to Hubbs' (*M. carlhubbsi*, BW37V and BW40) and Perrin's (*M. perrini*, BW43) beaked whales (Baumann-Pickering *et al.*, 2014; Griffiths *et al.*, 2019). Inter-click-interval and mean click spectra were used as the primary discriminating features for species identification of each event.

Click presence or absence per 1-minute bin was quantified; a minute containing a beaked whale click is here called a *click-positive minute*. The total number of 1-minute bins containing clicks was normalized by the total number of 1-minute bins recorded by each hydrophone. Click-positive minutes that were within 30 minutes of each other were merged into a single encounter. Mean encounter length was calculated for each platform type. If encounters overlapped in time by at least one minute, they were identified as a simultaneously detected encounter across platform types. To ensure no encounters of beaked whales were missed, if an encounter occurred on one platform but was not detected on the others, recordings on the other platforms during the encounter time were visually inspected for beaked whales clicks. Additionally, percent of recorded hours and number of days containing click-positive minutes were quantified for each platform.

Spatial distribution of each platform at the time of each click-positive minute and encounter was used to help inform our interpretation of differences in detection rates of click-positive minutes and number and timing of encounters across platform type. First, an estimated "listening space," using a 3.5 km radius circle (area: 38.5 km²), was created around each platform location for every minute of the experiment. This buffer size was selected as an estimate of the maximum detection range of beaked whales by a HARP as

modeled in Hildebrand *et al.* (2015). While we may expect the maximum listening radius for the Seaglider and QUEphone to be further than the HARPs because of the lower noise floor above 20 kHz, we used 3.5 km for all recorders as a conservative estimate. This estimated listening space is not an empirical measure of maximum detection range and is simply an estimate used to illustrate the potential spatial drivers of detection rate differences. Locations for mobile platforms were calculated from straight-line interpolations between surfacing GPS positions. Percentages of recording minutes in which each mobile recorder's 3.5 km listening space overlapped with the listening space around both HARPs by at least 33% were quantified. A threshold of 33% overlap was selected to match the spatial overlap percentage of the two HARPs' listening space with one another. Then, the number of click-positive minutes (for each species identified) that occurred within this buffer overlap time period were summed and the percentage of overlapped recording time with clicks was calculated. Additionally, the horizontal distance from each recorder to the other three deep-water recorders was measured for each beaked whale encounter. Encounter location for the mobile platforms was defined as the median latitude and longitude of the platform within the encounter start and end time. Histograms were generated for distances to other recorders both when encounters were and were not simultaneously detected on other recorders.

To investigate whether beaked whale detections varied with mobile platform depth, the depth at the start of each recording minute was extracted and grouped into 10-meter bins. Bins of 10 meters depth were selected because the glider typically does not descend or ascend greater than 10 meters in one minute. Then the proportion of the recording minutes in each depth bin that contained Cuvier's beaked whale clicks was calculated.

Delphinids

Recordings of whistles and/or echolocation clicks produced by small, shallow-diving delphinids (in this area, *Delphinus capensis*, *D. delphis*, and *Tursiops truncatus*) were identified manually through visual inspection of Long Term Spectral Average plots (LTSAs; Wiggins and Hildebrand, 2007) created and viewed in the Triton Software Package (v1.93). LTSAs were calculated on the full-bandwidth recordings using a 5 s time

average and 100 Hz frequency average. Start and end times of clicking or whistling bouts were marked and occurrence was quantified as hourly and daily presence or absence of clicks and/or whistles. Percentage of total hours and days with delphinid clicks or whistles was calculated. Because delphinid clicks and whistles were so prevalent, and encounter durations could span tens of hours, no encounter-based analysis was conducted.

Minke whales

A simple whistle and moan (tonal sound) detector (Martin *et al.*, 2013, Mellinger *et al.*, 2011) in Ishmael 3.0 beta (compiled June 14, 2018; <http://bioacoustics.us/ishmael.html>) was used to identify minke whale boings in recordings from the glider, QUEphone, and both HARPs. Detector settings are available in Appendix C. Call quality was generally poor, so a low detection threshold was selected to maximize recall. Because this resulted in a high number of false positives, all detections were manually checked to remove false positives. To further ensure no boings were missed, for any occasions when boings were detected on one recorder but not the others, that time period was manually inspected on all recorders for possible missed boings in Raven Pro 1.6 (Cornell Lab of Ornithology, Ithaca, NY, USA). Hourly and daily presence or absence of minke whale boings was then quantified for each recorder, and percentage of total recording hours containing boings was calculated.

Consecutive hours of boings were grouped into encounters, with an encounter defined here as boings with a gap of less than an hour before subsequent boings. Mean location of each mobile platform was extracted for each encounter, and distances between recorders were calculated. Distances between recorders when encounters were and were not simultaneously detected on other recorders were compared with histograms.

Results

Recording durations

Recording durations varied across recording systems due to differences in platform operation and deployment durations. Because they recorded continuously, both HARPS recorded during 309 one-hour bins over 14 days, a total of 308.1 hours for H01 and 308.4

hours for H02 (Table 4.1). The glider recorded for 290.4 hours over 14 days (across 314 one-hour bins, including partial hours). The reduction in total hours recorded compared to the HARPs was because the recording system was turned off at depths shallower than 25 m. The glider traveled over 200 km. The QUEphone recorded for a total of 219.5 hours over 12 days (across 229 one-hour bins, including partial hours). The QUEphone experienced buoyancy and programmatic issues and was not deployed on all days, resulting in the reduced recording hours (see deployment schedule in Table 4.1). Each of the five QUEphone drifts spanned 42 to 45 hours, and in total the QUEphone drifted 63.3 km.

Beaked whales

The QUEphone had the most beaked whale click detections at all analysis scales, with 125 minutes containing Cuvier's beaked whale clicks (095% of the total recording minutes; Table 4.2). Beaked whale clicks were detected on the QUEphone during 13 of 229 total hours of recording (5.68%), and on 6 of 12 (50%) recording days (Table 4.2). The glider had less than half as many Cuvier's beaked whale click-positive minutes (66 minutes, 0.38% of recorded minutes) as the QUEphone recorded during 8 of 314 recording hours (2.55%), on 5 of 14 (36%) recording days (Table 4.2; Figure 4.2). H01 recorded both Cuvier's beaked whale clicks (51 minutes, 0.28%) and click type BW43 clicks (7 minutes, 0.038%) spanning 8 of 309 recording hours (2.59%), on 5 of 14 (36%) recording days (Table 4.2; Figure 4.2). H02 recorded 60 minutes containing Cuvier's beaked whale clicks (0.32% of recorded minutes), during 5 of 309 hours (1.62%) over 4 of 14 (29%) recording days (Table 4.2; Figure 4.2). H01 and Q003 recorded the longest duration encounters (less than 30 minutes silence between consecutive click-positive minutes) of 46 and 47 minutes, respectively. H02 encounters were the longest on average (mean 19.8 minutes, SD 13.1 minutes) while SG607's encounters were the shortest (mean 11.6 minutes, SD 8.7; Table 4.2).

The glider recorded beaked whale clicks throughout its traveled path (Figure 4.3A). QUEphone beaked whale detections occurred primarily on drifts 1, 3, and 4, when the QUEphone was drifting primarily to the north of the HARPs and glider path (Figure 4.3A). A single encounter of Cuvier's beaked whales was detected on all four deep-water

recorders on 22 July 2016 from 16:32 to 17:17 UTC (09:32 to 10:17 local time; Figure 4.3B and Table 4.3). Distances between recording platforms during the encounter ranged from 1.6 to 5.5 km. The glider had two additional encounters that were also detected by the HARPs: on 20 July 2016 at 19:23 UTC (12:23 local time), when the glider was 1.0 km from H01, and on 29 July 2016 at 06:58 UTC (23:58 local time) when the glider was 2.8 km away from H02 (Figure 4.3C and Table 4.3).

The assumed 3.5 km listening spaces around the HARPs overlapped spatially with one another by 33% of each instrument's total listening area (12.7 of 38.5 km² overlapped). The single encounter of Cuvier's beaked whale clicks detected on both HARPs constituted 43% (H01; 21 min) and 47% (H02; 28 min) of each HARPs total minutes with Cuvier's beaked whale clicks. The glider's estimated 3.5 km listening radius overlapped in space by 33% or more with one or both HARPs for 92% of the glider's total recording time, and 100% of the glider's total click-positive minutes (66 minutes). Three encounters, or 45% (30 minutes) of the click-positive minutes while the glider was assumed to overlap in range with the HARPs, were simultaneously detected on either or both HARPs (Table 4.3, Figure 4.3C). The QUEphone movement could not be controlled once it was drifting, and thus its proximity to the HARPS was harder to control. The QUEphone was assumed to overlap in space by 33% or more with one or both HARPs for only 66% of the QUEphone's total recording time. This overlapping time period contained 56 click-positive minutes recorded on the QUEphone (45% of click-positive minutes). One Cuvier's beaked whale encounter detected by the QUEphone and simultaneously detected by both HARPs spanned just 16% (9 minutes) of the Cuvier's click-positive minutes recorded by the QUEphone within the spatial overlap.

Simultaneous detection of Cuvier's beaked whale encounters by multiple recorders was not guaranteed, even when recording platforms were positioned within a few kilometers of one another and estimated listening spaces overlapped substantially (Figure 4.3C, Table 4.3, Figure C2). Two of the encounters recorded on the glider occurred when the glider was less than 1 km horizontally from a HARP, but that HARP did not have detections at that time. Conversely, two of the encounters on H01 occurred when the horizontal distance between the glider and HARP was 1 km, but only one of those

encounters was simultaneously detected by the glider. Visual checks for encounters across platforms did not result in any additional encounters.

The QUEphone drifted at depths below 450 m for 80% of its recorded minutes; it typically hovered between 480 and 520 m (77% of recorded minutes). Aside from a single encounter (3 minutes duration) when the QUEphone was at 292 m, all minutes with clicks occurred when the QUEphone was drifting at or near its designated maximum depth (Figure 4.4). Because the glider moved up and down through the water column, recorded minutes were evenly distributed from 25 to 1000 m (Figure 4.5). The glider had the greatest proportion of recorded minutes containing clicks at 400-500 m, 750-800 m and 950-1000 m and none at 600-750 m and 800-900 m (Figure 4.5, Table 4.3).

Delphinid clicks and whistles

Delphinid clicks and whistles were very common on the recordings of all platforms; they were recorded on all days by all systems (Table 4.2 and Figure 4.6). Total percentages of recording hours containing delphinid clicks and whistles were similar across platforms, with the recordings from mobile platforms containing slightly more hours with clicks and/or whistles (Table 4.2) than the fixed platforms. The glider and QUEphone recordings contained delphinid vocalizations in 80.6% and 84.7% of hourly bins, respectively, while H01 and H02 contained them in 76.7% and 80.3% of 1-hour bins, respectively (Table 4.2). Qualitatively, whistles were more commonly recorded than echolocation clicks by the HARPs. Bouts of both echolocation clicks and whistles were more common on the mobile platforms.

Minke whale boings

Minke whale boings were detected on all four systems with similar patterns of hourly and daily presence and absence (Figure 4.7). Minke whale boings were relatively scarce, with only 7-9 1-hour bins containing boings per recorder over six total encounters that occurred on five separate days (3-5 encounters per recorder; Table 4.2). Two of the six total boing encounters were present on all recorders and one additional encounter was recorded by all but H02. Q003 was not deployed during one of the six encounters when

boings were detected on all other platforms (Figure 4.7). Additionally, two short encounters were detected by Q003 only, one on 28 July and one on 31 July 2016 (Figures 4.3D, 4.7). The QUEphone was within 10 km of the HARPs and glider at the time of these encounters (Figure 4.3D, Figure C3). After normalizing for total recording hours, Q003 had the greatest percent of recording hours with boings (3.6%) compared to 3.1% on SG607 and 2.3% and 2.6% on H01 and H02 respectively (Table 4.2).

Discussion

Through acoustic analyses of data collected by three types of passive acoustic recording systems deployed simultaneously in the Catalina Basin, we have provided a direct comparison of acoustic monitoring of marine mammals by mobile (Seaglider and QUEphone) and stationary (HARPs) recorders. Mobile platforms may provide an advantage when surveying for cetaceans with limited detection ranges when the survey area is relatively large and the distribution of animals is not known. All recorders detected Cuvier's beaked whales, small delphinid whistles and clicks, and minke whale boings. While daily and hourly presence of delphinids and minke whales did not differ by recorder type, the day-, hour-, and minute-scale presence of beaked whale clicks did differ across all recording platforms. These differences are likely related to the areas each recorder monitored and the depth of the platforms rather than the recorder type, but recorder differences may have also contributed to detection differences.

Differences in spatial coverage are likely the greatest driver of differences in beaked whale click presence across and between the different recorder types. Beaked whale group sizes are relatively small and clicks are emitted in a highly directional beam pattern, so detection distances are estimated at less than 1 km for off-axis clicks and up to 4 km for on-axis clicks (Hildebrand *et al.*, 2015; Zimmer *et al.*, 2008). Beaked whale encounters were typically observed as "scanning sequences" of clicks where a short (< 10 s) sequence of clicks showed a rise and fall in amplitude over the sequence. Most likely, this pattern was observed when a relatively distant beaked whale swept its sonar beam across the recorder. This supports the idea that beam width is a critical factor in detectability and that such a sweep would be unlikely to be picked up by another platform 2-3 km away.

Hildebrand *et al.* (2015) estimated a maximum detection distance by HARPs of 3.5 km for Cuvier's beaked whales, with 100% click detection at 400 m or less. Even though the HARPs in this study likely had near-identical detection probabilities, they were deployed 3.9 km apart. Thus, it was not surprising that differences were observed between the HARPs and they did not always detect the same clicking whales. With an estimated maximum listening radius of 3.5 km, the HARPs' listening space overlapped by only 33%. For the single encounter that was detected by both H01 and H02 (and the glider and QUEphone; Figure 4.3B), we might assume the clicking whale or whales were located somewhere between the two recorders. The difference in number of click-positive minutes on each HARP was relatively small, but they occurred at different times and sometimes had different species compositions. Differences in beaked whale presence patterns have been observed in previous studies employing HARPs deployed near each other. Baumann-Pickering *et al.* (2014) highlight the likelihood that local oceanographic conditions and small-scale habitat preferences by beaked whales could lead to different presence and absence observations in space and time and that interpretation of results may be limited with a low density of recorders.

The glider, with its ability to steer and thus travel towards a set waypoint, was able to stay within the vicinity of the HARPs much better than the QUEphone, and thus the comparison of clicks detected on glider and HARPs is possibly more straightforward. The glider had the greatest number of encounters (three) that matched a simultaneous encounter on at least one other recorder, likely because it spent the most time overlapping in estimated listening space with the HARPs – 84% of its recording time occurred when the glider and HARP listening areas were assumed to overlap in space by at least 50%. Conversely, while the QUEphone had the most overall click-positive minutes and greatest number of beaked whale encounters, it had the most dissimilar spatial coverage, compared to the glider and HARPs. Not too surprisingly, then, it had only a single matched encounter with the other recorders.

There is a growing interest in applying acoustic density estimation methods to data collected with mobile autonomous platforms such as gliders, as they have been applied to stationary recorders (Marques *et al.*, 2013; Verfuss *et al.*, 2019). Any density estimation

applications would require some measure of the detection probability or effective detection radius (Marques *et al.*, 2013). Some initial work to estimate detection probability of beaked whales from gliders has been done through simulation (Gkikopoulou, 2018) and leveraging a stationary cabled array (Harris *et al.*, 2017; Thomas *et al.*, 2019); however, more empirical work is needed. Estimates of detection probability or effective detection radius would be very useful for further platform comparisons and could improve the comparison work here by providing a more accurate “listening space” estimate for the mobile platforms.

Cuvier’s beaked whales are associated with complex, steep-slope habitat in some areas (MacLeod and Zuur, 2005; Waring *et al.*, 2001). It is possible that proximity to the steeper walls of Catalina Basin, more ideal beaked whale habitat, drove differences observed across recorder types. H01, which had a greater number of minutes with clicks and percent of minutes with clicks than H02, was located north of H02, slightly closer to the northwestern edge of the deep Catalina Basin. The QUEphone, which had the greatest number of encounters and percent of recording minutes with clicks, spent considerably more time closer to the northeastern slope and steep edge of Catalina Basin (Figure 4.3A) than the other platforms. The glider more or less remained in the center of the basin, but it surveyed an area that extended slightly beyond the HARPs (by about 4 km in each direction) closer to the basin edges. The single-hydrophone systems used in this study do not provide information on animal location, and recording effort in space and time was variable. Therefore, we cannot make any strong inferences about beaked whale distribution within Catalina Basin. However, we can conclude that the glider and/or QUEphone spent time in areas where beaked whales may be more actively foraging, based on tagging studies of foraging behavior, and that spatial differences, even of just a few kilometers, are likely drivers of the differences in detection rates observed.

Recorder depth in relation to beaked whale foraging depth may also have driven the differences in detections by the mobile platforms compared to the HARPs. Diving and foraging behavior in Cuvier’s beaked whales is perhaps the best-studied among all the beaked whale species. They are known to echolocate only below 200 m, and more typically below 450 m (Johnson *et al.*, 2004; Tyack *et al.*, 2006). Tagging and tracking studies

indicate typical foraging depths of 700-2000 m with variability by region (DeRuiter *et al.*, 2013; Gassmann *et al.*, 2015; Schorr *et al.*, 2014; Tyack *et al.*, 2006). Echolocation depths and the strong directionality of the signals support the idea that beaked whales may best be recorded with deep-water instruments (Zimmer *et al.*, 2008). While the HARPs were deployed at 1250 m depth, the QUEphone drifted at 500 m and the glider moved constantly between the surface and 1000 m, spending considerably less time than the QUEphone at depths below 500 m. We hypothesized that glider detection of beaked whale clicks may vary with glider depth, and that total beaked whale detections may be less than the HARPs or QUEphone simply because the glider spends less time at the ideal depths for beaked whale click detection. However, this was not what we observed. Beaked whale clicks were detected on the glider at many different depths and there was no apparent pattern to the distribution of depths at which clicks were recorded.

A recent tracking study by Barlow *et al.* (2018) showed that near-surface (100 m) hydrophones can successfully detect and track Cuvier's beaked whales. They found the mean foraging depth was 967 m (SD 112m) in the Catalina Basin, where maximum seafloor depths are ~1250 m (Barlow *et al.*, 2018). Another tracking study in Southern California found Cuvier's beaked whales foraged 300-400 m above the seafloor (Gassmann *et al.*, 2015). It is possible that due to the highly directional nature of beaked whale clicks, hydrophones located at the foraging depth, rather than directly on the seafloor, may have a higher probability of recording the clicks. This may, therefore, explain the higher detection rates on the QUEphone and glider compared to the HARPs. Increased detection of beaked whale clicks on a deep (300 m) versus shallow (20 m) recorder has been documented previously (Gkikopoulou, 2018). The total number of beaked whale encounters during the two-week deployment was relatively low so it was difficult to assess any relationship between number of detections and platform depth from this small experiment. Additional effort in a basin with higher known beaked whale densities (ideally to increase the overall number of clicks detected) and where the glider is piloted to dive primarily straight up and down at a single waypoint may allow further investigation of the effect of depth.

Sound propagation conditions in the Catalina Basin may have influenced the depths at which the mobile platforms recorded beaked whales. The sound speed during this

experiment, as collected by the glider for the two-week deployment, was generally uniform below 100 m with a slight sound speed minimum near 600 m (see Figure C1). A distinct sound speed minimum in the sound speed profile can form a deep-sound channel where underwater sound becomes “trapped” as it is refracted towards the sound speed minimum, and can thus travel longer distances (Urick, 1983). While the profile does not show a drastic sound speed minimum or a narrow sound channel, the location of the minimum does further support maximizing detections in the 400 to 600 m depth range.

The limitations of each recording system may have also contributed to the differences in beaked whale detections, at least when ambient noise levels were low. The noise floor above 20 kHz was about 10 dB lower for the WISPR system compared to the HARPs. This makes comparing detection rates noticeably more complicated than it would be comparing identical recording systems, regardless of platform movement. When ocean ambient noise is low (at or near sea state zero), the WISPR system’s lower noise floor (~28 dB) may have allowed detection of faint clicks which the HARP may have missed. However, when sea state conditions were 2 or greater the ambient noise levels would have exceeded the WISPR system noise floor and detection range would have been noise limited rather than recorder limited.

Anecdotally, we have a selection of known beaked whale locations which were localized by Barlow *et al.* (2018) at the same time and in the same area as this experiment (Table C1). Of 23 known whale locations, two matched in time with an encounter on the QUEphone, and two matched with an encounter on H01. In all four of these matches, the QUEphone and H01 were over 5.5 km from the localized whale. This detection range is 2 km beyond what has been modeled as the maximum detection range of Cuvier’s beaked whales from a HARP (Hildebrand *et al.*, 2015). We suspect these may be examples of detections of two groups of vocalizing animals at the same time rather than detection of one group on two platforms, but we cannot definitively say so because the single-hydrophone systems used in this study do not allow range estimation or localization. Most (81-96%) of the known whale locations from Barlow *et al.* (2018) were 4 km or further from the mobile platforms or HARPs. Three whale locations from a single encounter were estimated when the QUEphone was less than 2.5 km away, but no clicks were detected on

the QUEphone. The closest whale location to the glider was a single location where the whales were 3.5 km from the glider; the glider was very near the surface at that time and no clicks were detected on the glider. And finally, three whale locations in a single encounter were 3.5 km or less from H01, a single whale location was less than 2.8 km from H02, and no clicks were detected on either HARP. Matches of localized whales to encounters on the mobile platforms or HARPs were rare (and possibly multiple groups of animals). However, none of the locations occurred within a range where we would have expected a detection to be certain (400 m or less; Hildebrand *et al.* 2015) and so the lack of matches to localized whales is not surprising.

Hours and days with detections of delphinids did not differ across the recording platforms. For such abundant, vocally active, large groups of animals, we did not expect differences in recording capabilities of the three platforms, particularly at hourly and daily scales. However, we did observe a difference in the type of delphinid vocalization recorded by the mobile platforms compared to the HARPs. Most encounters of delphinids by the glider or QUEphone were dominated by echolocation clicks. Often, LTSAs were completely saturated between 10 and 50 kHz with long-duration clicking bouts. Whistles were typically present as well but were not as visually apparent as the clicks. Conversely, on the HARPs, whistles were the primary vocalization type observed in the LTSAs and used to mark encounters. Clicks, when present, were much fainter, and clicking bouts were generally much shorter in duration than what was seen on the glider and QUEphone. This difference could be related to the depth of the mobile platforms and the directional nature of echolocation clicks. The mobile platforms recorded at shallower depths than the HARPs, so likely spent more time closer to where small delphinids would be foraging and where echolocation clicks would be received. Whistles, which are more omnidirectional than clicks, particularly at lower frequencies (Branstetter *et al.*, 2012; Janik, 2000; Lammers and Au, 2003), would be more easily detected at depth. When simply monitoring for presence or absence at a broad temporal scale, this difference in proportions of clicks versus whistles may not be important. However, when looking at finer-scale behavior or potentially when trying to estimate density or abundance, these differences would need more study.

Additionally, the large number of hours where delphinid clicks dominated the glider or QUEphone recordings could influence beaked whale detection results, depending on the analysis method used. A similar effect has been seen in previous beaked whale analyses (Baumann-Pickering *et al.*, 2014). Through simple visual inspection for beaked whales in LTSAs, eight encounters were identified on the QUEphone. After running the two-step detection system, an additional five encounters were identified and verified (and the eight manual encounters verified). Four of the five new encounters overlapped with known delphinid encounters on the QUEphone and were visually masked by the dolphin clicks. On the glider, the detection system found one additional encounter, which was not during a delphinid encounter, and another encounter's duration was extended, a time which did overlap with a delphinid encounter. This highlights the importance of using the same analysis methods across recorder types when performing a direct comparison. Had the identical detector and validation process not been used, the differences in number of encounters and minutes with beaked whale clicks would not have been as pronounced.

Detections of minke boings were generally the same across all platforms, which was expected based on the known detection range of boings and the proximity of all recorders in this experiment. Minke whale boings have peak frequencies between 1 and 2 kHz. They are highly stereotyped, loud, and often occur in long bouts of consecutive boings, and therefore are readily detected on multiple hydrophones (Martin *et al.*, 2013). Previous work by Martin *et al.* (2013) estimating minke whale boing density from a bottom-mounted hydrophone array estimated the probability of detecting a boing 10 km horizontal distance from the hydrophone between 0.8 and 0.9, and a detection probability of 0.5 or better out to approximately 25 km horizontal range. For our study, all recorders were within 20 km of one another, and more typically were with 8 km of each other. The result that most boings were detected on by all recorders in this study aligns with the detection ranges found by Martin *et al.* (2013). Detector performance also did not vary by recorder type, with all recorders having a very high false positive rate of 96-98%. This was somewhat surprising because the glider and QUEphone have more moving parts and generate broadband self-noise when operating internal motors and pumps, so we suspected they would have a higher false positive rate. Instead, sources of mid-frequency, long-

duration noise were common on all recorders. The main sources of false positives were low-frequency sonar, unidentified frequency-contour noise, or platform noise. While an improved detector could likely provide improved performance, for this small dataset the basic tonal detector was reasonable and sufficient.

Conclusions

When selecting the ideal platform for a passive acoustic marine mammal survey, it is critical to know the species of interest, understand the acoustic behavior of that species, and identify the primary research or management question. The fundamental differences between the Seaglider, QUEphone, and HARP – the ability to move and maximum deployment duration – make each best suited to answer different questions. Because a Seaglider can follow programmable tracklines, it can cover a large area, and so may be an ideal platform to identify new hotspots or examine habitat preference, particularly for species that are only detectable over short distances such as beaked whales. The QUEphone can also cover large areas, as it drifts passively. But the glider and QUEphone can only be deployed for several weeks, so a single deployment may not identify temporal changes in presence or behavior. Conversely, a stationary recorder can be deployed for months to years, so can answer questions about seasonal and long-term changes. For low-to mid-frequency (20-2000 Hz) baleen whales that produce loud omni-directional signals that can be heard over many tens of kilometers, a stationary recorder can cover a large area, and is likely the most efficient platform. Ideally, these different tools can be used in concert with one another to answer a range of biological and conservation-relevant questions. Regardless of which platform is used, it is necessary to define the survey area and detection probability to estimate animal density or abundance.

Funding

Funding for this work was provided by the Living Marine Resources Program (N39430-14-C-1435), the Office of Naval Research (N00014-15-1-2142) and NOAA's Southwest Fisheries Science Center. SF was supported by the National Science and Engineering Graduate Fellowship.

Acknowledgments

Special thanks to Anatoli Erofeev and Stephen Pierce (Oregon State University, OSU) for their glider piloting guidance and support and to Alex Turpin (OSU) for his work preparing the glider and QUEphone. We thank Bruce Thayre and Ryan Griswold (Scripps Institution of Oceanography, SIO), who deployed and recovered the HARPs. Vessel support was provided by Trevor Oudin and Juan Carlos Aguilar of Wrigley Marine Science Center and Spencer Salmon and the crew of the M/V *Horizon*. We thank Jennifer Trickey and Ally Rice of SIO for their assistance with acoustic analyses of HARP data and guidance for analysis of the mobile recorder data. This manuscript was improved with feedback from Selina Heppell (OSU) and two anonymous reviewers. This is PMEL Contribution No. 4931.

Tables

Table 4.1. Deployment and recovery times for each recording platform, with total hours of data recorded, and distance travelled for the glider and QUEphone. Deployment times for H01 and H02 are approximate.

Recorder	Deployed (UTC)	Recovered (UTC)	Recording duration (hr)	Distance traveled (km)	
SG607	7/19/16 16:14	8/1/16 17:47	290.4	216.4	
Q003	<i>drift 1</i>	7/21/16 18:50	7/23/16 14:57	41.9	12.6
	<i>drift 2</i>	7/23/16 17:00	7/25/16 14:56	44.6	9.7
	<i>drift 3</i>	7/26/16 15:54	7/28/16 14:48	44.8	14.4
	<i>drift 4</i>	7/28/16 15:55	7/30/16 14:55	45.6	14.1
	<i>drift 5</i>	7/30/16 18:08	8/1/16 14:57	42.6	12.5
	all	7/21/16 18:50	8/1/16 14:57	219.5	63.3
H01	7/19/16 17:00	8/2/16 8:03	308.1	stationary	
H02	7/19/16 17:00	8/2/16 7:25	308.4	stationary	

Table 4.2. Summary of total durations of acoustic data recorded by each platform and minutes, hours, days, and/or encounters for four types of marine mammal vocalization: Cuvier's beaked whale echolocation clicks, beaked whale echolocation click type BW43 clicks, small delphinid whistles and clicks, and minke whale boings. Hours recorded indicates the total hours recorded excluding gaps in recording. Hour bins represent hours that have at least 1-minute of recording within that hour, and the number of hourly bins is used in calculations of percent of hours with clicks, whistles, or boings. Days recorded represents calendar days with at least 1 minute of recording on that day.

	Platform	SG607	Q003	H01	H02
Recording durations	Minutes recorded	17,419	13,167	18,484	18,506
	Hours recorded	290.4	219.5	308.1	308.4
	Hour bins	314	229	309	309
	Days recorded	14	12	14	14
Cuvier's beaked whale	Minutes with clicks	75	137	51	60
	Percent minutes with clicks	0.38%	0.95%	0.28%	0.32%
	Number of encounters	7	11	6	4
	Mean encounter duration (SD) in minutes	11.6 (8.7)	14.8 (14.0)	15.1 (14.9)	19.8 (13.1)
	Hours with clicks	8	13	8	5
	Percent hour bins with clicks	2.55%	5.68%	2.59%	1.62%
	Number of days with clicks	5 of 14	6 of 12	5 of 14	4 of 14
BW43	Minutes with clicks	0	0	7	0
	Percent minutes with clicks	0%	0%	0.04%	0%
	Number of encounters	0	0	1	0
	Hours with clicks	0	0	1	0
	Days with clicks	0	0	1	0
Delphinids	Number of encounters	45	35	48	52
	Hours with vocalizations	253	194	237	248
	Percent hour bins	80.57%	84.72%	76.70%	80.26%
	Number of days	14 of 14	12 of 12	14 of 14	14 of 14
Minke whales	Hours with boings	9	8	7	8
	Percent hour bins with boings	3.10%	3.64%	2.27%	2.59%
	Number of days with boings	5 of 14	4 of 12	4 of 14	3 of 14
	Number of encounters	4	5	4	3

Table 4.3. Beaked whale encounters by the Seaglider (SG), QUEphone (QUE) and HARPs (H01 and H02). Click-positive minutes with less than 30 minutes between them were grouped as encounters. Number of click-positive minutes may not equal encounter duration. Species include Cuvier’s beaked whale (Zc) and click type BW43 (Baumann-Pickering *et al.*, 2013). Distances to other recorders are given in km. Bold rows indicate encounters detected by multiple recorders; superscript symbols indicate matched encounters. Times when the glider or QUEphone were not deployed or recording are indicated by “nd” or “off”, respectively.

	Species	Date	Start Time	End Time	Duration (minutes)	Click minutes	Mean depth (m)	Distance (km)			
								SG	QUE	H01	H02
SG	Zc	07/19	17:53	17:55	3	3	415	-	nd	5.5	1.6
	Zc	07/19	19:49	19:51	3	3	764	-	nd	3.9	0.3
	Zc[†]	07/20	19:23	19:25	3	3	765	-	nd	1.0	3.0
	Zc[§]	07/22	16:46	16:58	13	11	968	-	5.5	5.3	1.6
	Zc	07/27	04:33	04:55	23	16	374	-	6.8	2.7	6.6
	Zc[†]	07/29	06:58	07:18	21	16	202	-	3.2	6.6	2.7
	Zc	07/29	20:02	20:16	15	14	507	-	5.2	0.5	4.1
QUE	Zc	07/21	20:18	20:20	3	3	292	7.4	-	5.8	2.2
	Zc	07/22	04:04	04:06	3	3	412	off	-	3.4	2.1
	Zc[§]	07/22	16:44	16:58	15	9	447	5.5	-	3.1	4.7
	Zc	07/22	18:38	19:04	27	27	497	6.1	-	3.3	5.2
	Zc	07/24	01:08	01:10	3	3	507	3.0	-	6.6	3.2
	Zc	07/28	02:29	02:45	17	8	492	7.8	-	3.6	6.6
	Zc	07/28	04:30	04:40	11	8	495	6.0	-	4.1	7.1
	Zc	07/28	07:10	07:16	7	6	505	4.2	-	4.7	7.8
	Zc	07/28	10:24	11:10	47	28	501	3.7	-	5.6	8.8
	Zc	07/29	00:22	00:24	3	3	503	1.8	-	6.4	2.6
	Zc	07/30	03:03	03:29	27	27	502	6.9	-	6.7	7.3
	H01	Zc[†]	07/20	19:22	19:33	12	12		1.0	nd	-
Zc[§]		07/22	16:32	17:17	46	23		5.3	3.1	-	3.9
Zc		07/22	19:58	20:01	4	4		5.3	3.4	-	3.9
Zc		07/24	12:37	12:47	11	4	1276	7.8	3.9	-	3.9
Zc		07/26	09:27	09:36	10	6		1.0	nd	-	3.9
BW43		07/28	21:26	21:46	21	7		3.5	7.1	-	3.9
Zc		08/02	02:51	02:52	2	2		nd	nd	-	3.9
H02	Zc	07/21	17:16	17:25	10	5		5.7	nd	3.9	-
	Zc[§]	07/22	16:26	16:56	31	28	1258	1.6	4.6	3.9	-
	Zc[†]	07/29	06:48	07:18	31	20		2.8	2.3	3.9	-
	Zc	08/01	20:16	20:22	7	6		nd	nd	3.9	-

Figures

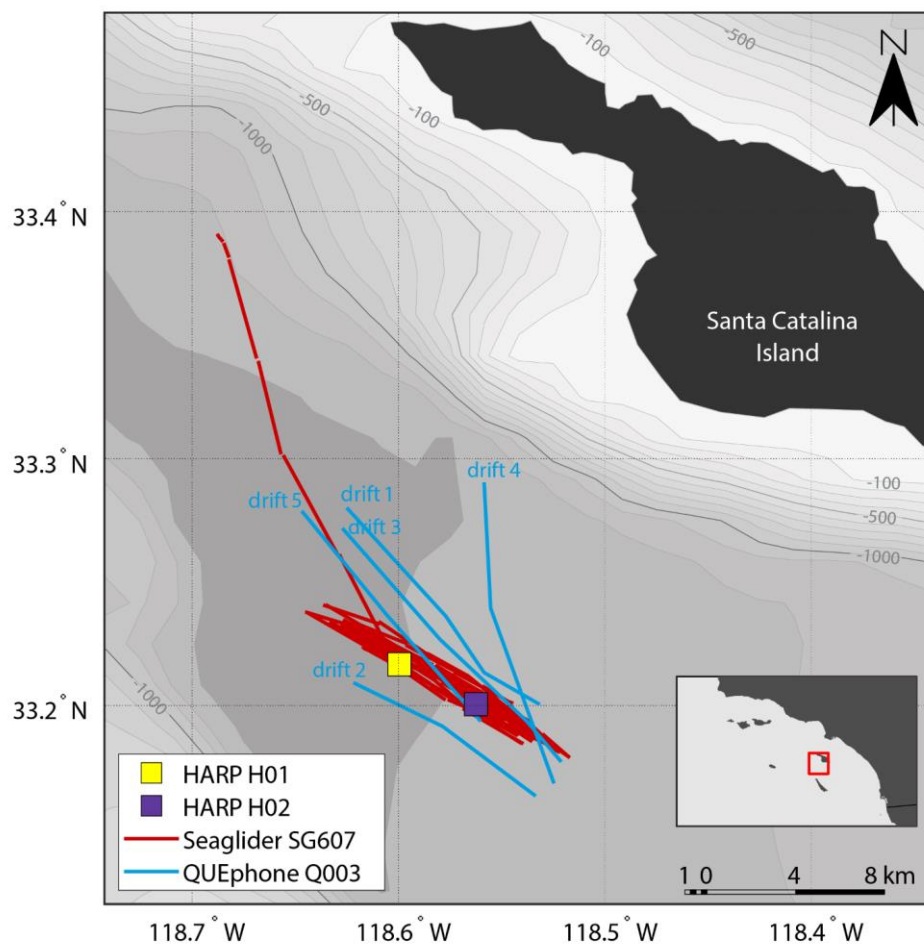


Figure 4.1. Map of deployment area and recording platform locations. HARPs H01 and H02 are shown as colored squares (yellow and purple). Red lines indicate the glider track; the portion departing to the north was when the glider was directed closer to shore for recovery at the end of the experiment. Blue lines indicate QUEphone drift tracks and are labeled in chronological order. Drift direction of the QUEphone was generally from the southeast to the northwest. Mobile platform tracks are straight line interpolations between known GPS surface locations. Bathymetry is shown in 100 m contours from -100 m (lightest gray) to -1300 m (darkest gray). Bathymetry data is from NOAA's National Centers for Environmental Information (Amante and Eakins, 2009). The inset shows the Channel Islands and Southern California Bight Region of Southern California with the study area outlined in red.

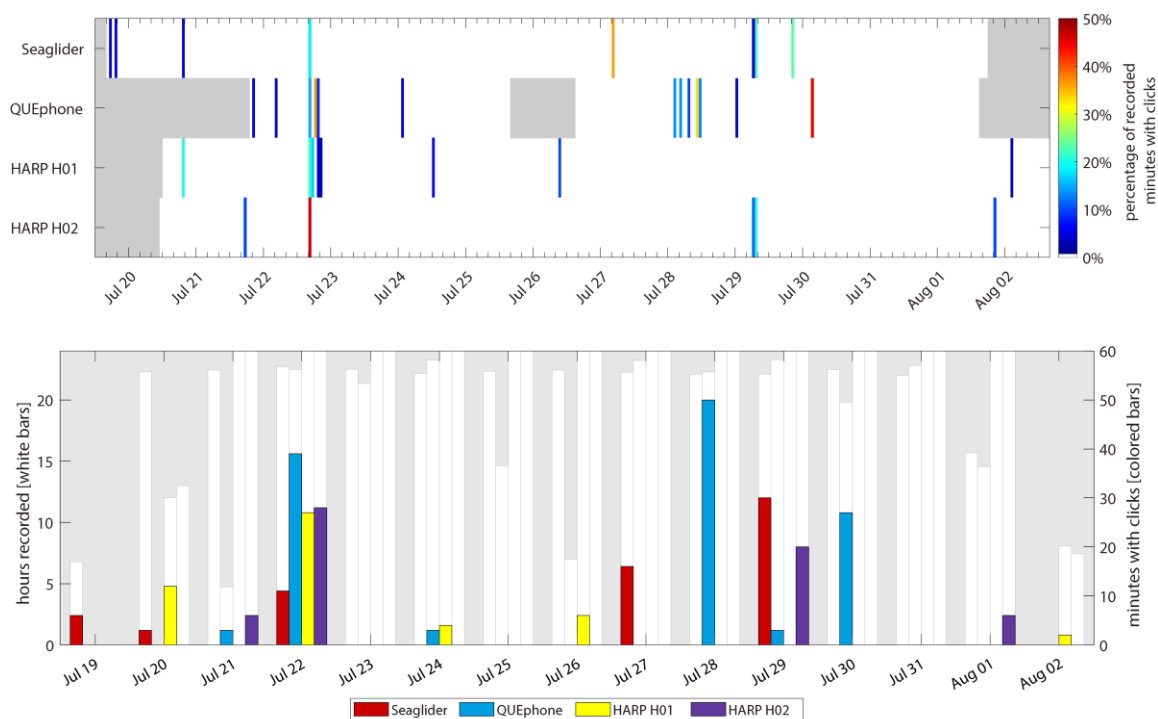


Figure 4.2. Occurrence of Cuvier's beaked whale clicks by recorder platform. Top panel: Percentage of recorded minutes with clicks in each hour. Gray areas indicate times when recorders were not deployed. Color of each 1-hour bar corresponds to percentage of total minutes recorded in that hour with clicks (if 0%, no colored bar is displayed). Bottom panel: Minutes with Cuvier's beaked whale clicks per day. The white bars and left y-axis indicate the total hours recorded per day. No white bar indicates a day where that recorder was either not deployed or not yet recording. The right y-axis and colored bars indicate total minutes per day containing beaked whale clicks.

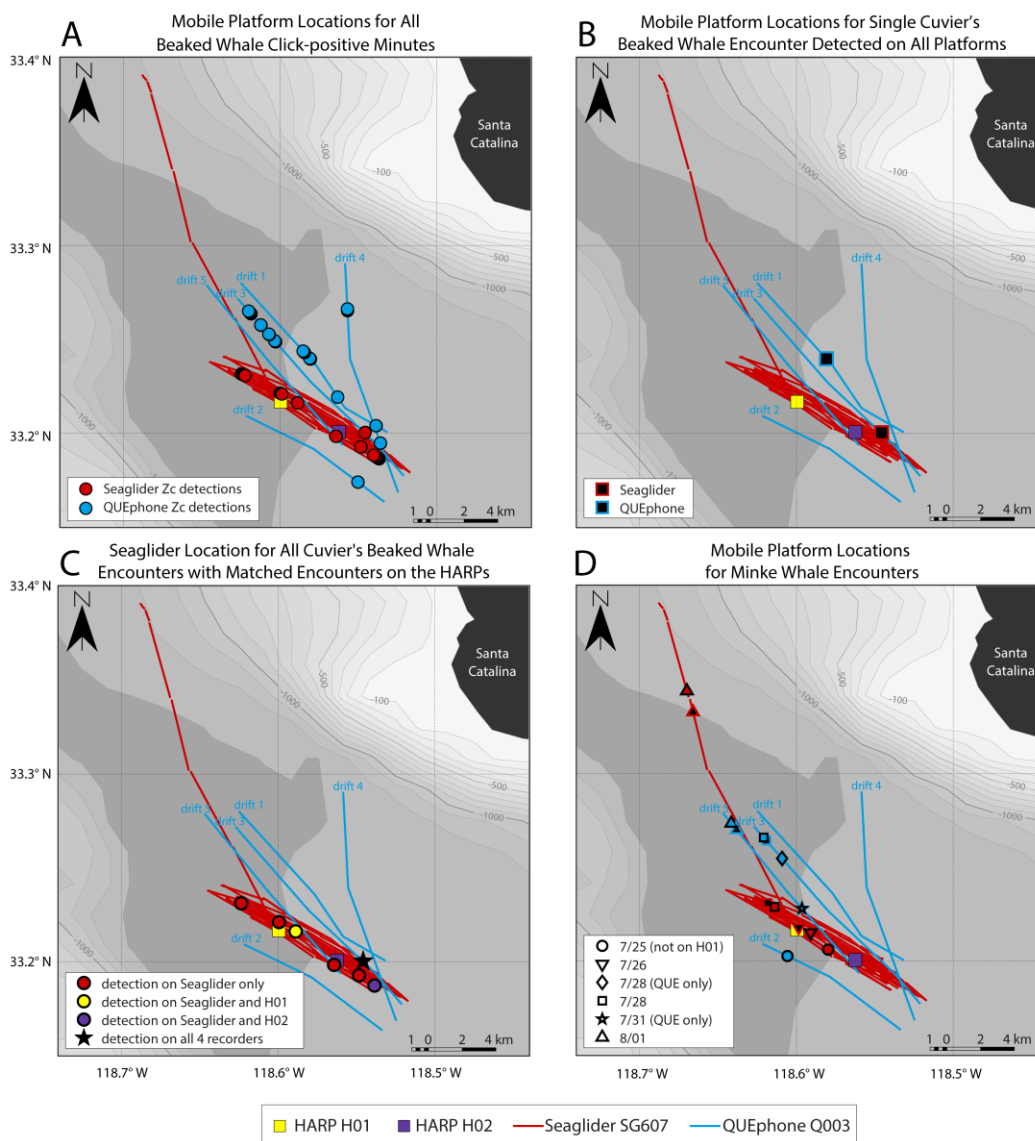


Figure 4.3. Mobile platform locations where beaked whales (Panels A-C) and minke whales (Panel D) were detected. The Seaglider track is shown as red lines; the track departing to the northwest was done to recover the glider closer to shore at the end of the experiment. The QUEphone drift tracks are shown as blue lines and labeled by drift number. Tracks for both platforms are straight-line interpolations of GPS surface positions. HARP locations are shown as squares (H01 – yellow, H02 – purple). Panel A shows the estimated location of each mobile platform for all beaked whale echolocation click-positive minutes. Cuvier's beaked whale (Zc) click-positive minutes are indicated by circles (Seaglider – red, QUEphone – blue). Panel B shows the estimated median location of the Seaglider (red outlined black square) and QUEphone (blue outlined black square) when a single encounter of Cuvier's beaked whales was recorded by all four deep-water recorders on 07/22/2016 16:32 to 17:17 UTC (09:32 to 10:17 local time). All recorders were within 5.5 km of one another at the time of the encounter. Panel C shows the estimated median

Seaglider location when it recorded a Cuvier's beaked whale encounter. Circle color corresponds to which HARP simultaneously recorded the same encounter (encounter detected only on the glider – red, H01 – yellow, H02 – purple). The single encounter recorded by the glider and both HARPs is indicated by a black star (same encounter as in Panel B). Panel D shows the estimated locations of the Seaglider and QUEphone when minke whales boings were detected. Each of six encounters is symbolized by a different shape and encounters were present on all recorders unless otherwise specified in the legend. Platform location at the start (black filled symbol) and end (color fill, black outline symbol) is shown for each encounter. The symbol outline or fill color corresponds to the mobile platform track color (glider – red, QUEphone – blue). If no end symbol (filled black) exists, the encounter was of very short duration with negligible platform movement over the encounter duration, so only a single location is shown.

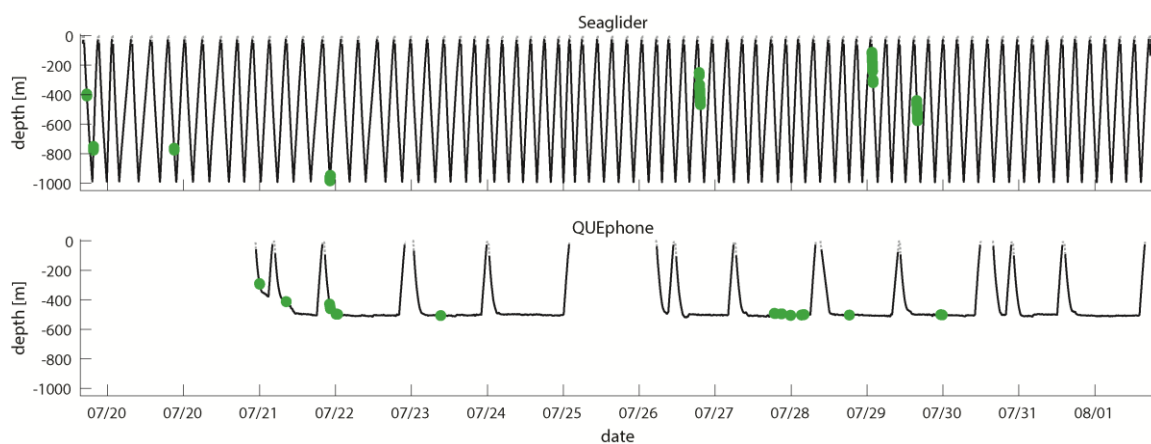


Figure 4.4. Dive profile of Seaglider (top panel) and QUEphone (bottom panel) showing platform depth over time. Minutes with beaked whales clicks present are shown as green circles. Date ticks are at 00:00 UTC of the given day.

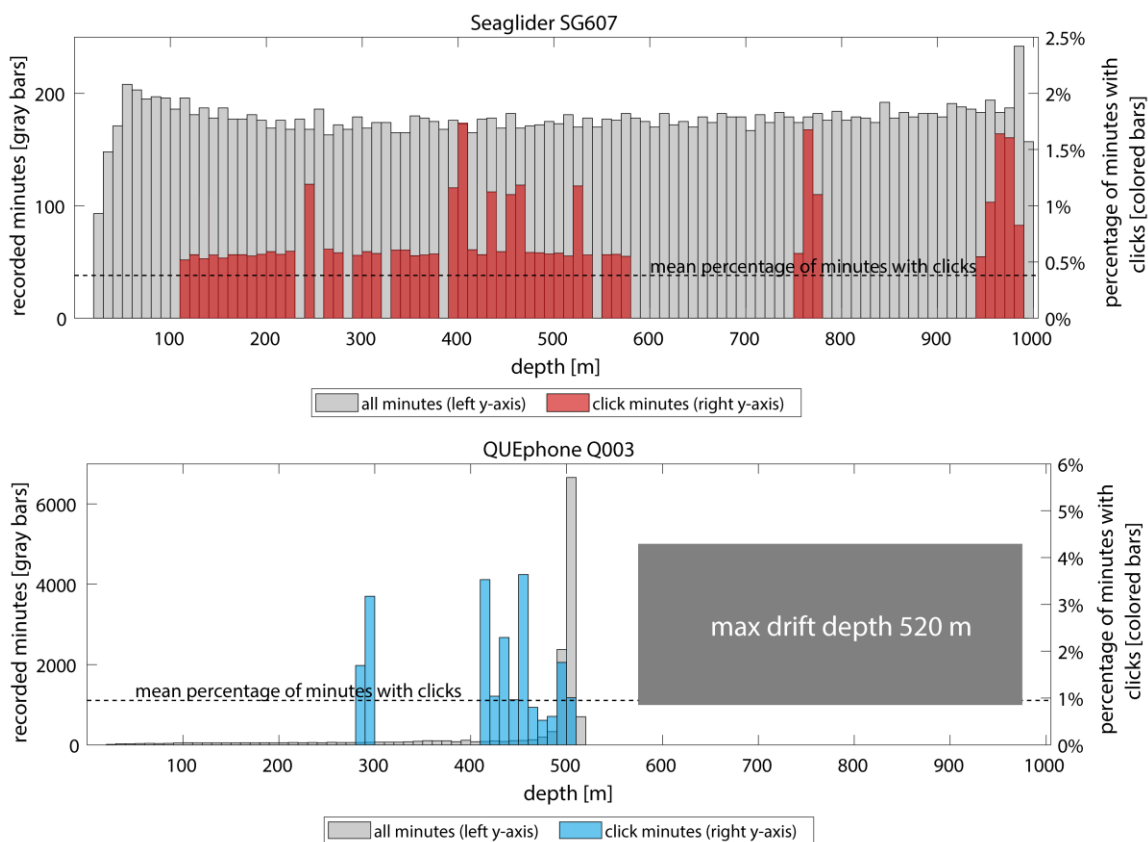


Figure 4.5. Distribution of mobile platform (Seaglider – top, red and QUEphone – bottom, blue) depths when Cuvier’s beaked whale clicks were detected. Gray bars and left y-axes indicate total recorded minutes in each 10 m depth bin. Colored bars and right y-axes indicate percentage of recorded minutes in that depth bin that contained Cuvier’s beaked whale clicks. Mean percentage of minutes with clicks across all depths is indicated by the dotted line. Note at the 490 m depth bin for the QUEphone, blue and gray bars overlap almost wholly. Q003’s maximum depth was 520 m; it typically drifted between 480 and 520 m.

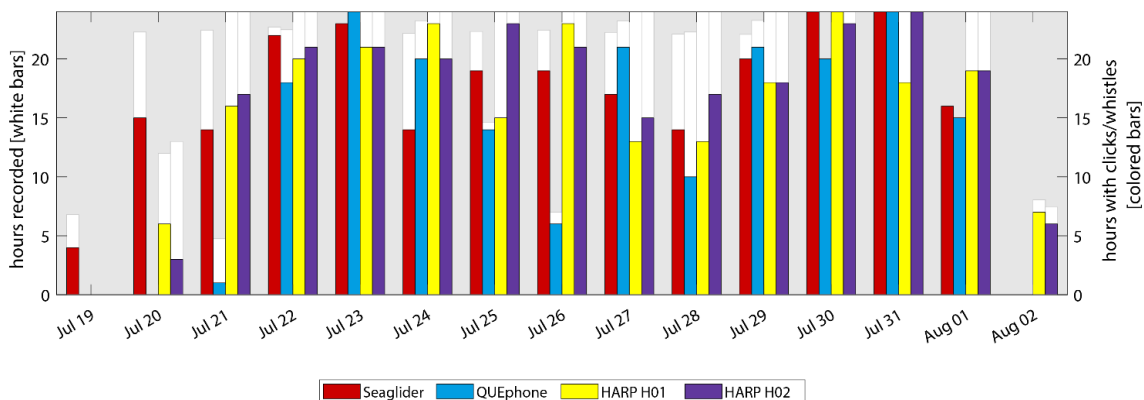


Figure 4.6. Daily presence of delphinid vocalizations (whistles and clicks) by recording platform. White bars and left y-axis indicate the total hours recorded per day by each platform. No white bar indicates a day where that recorder was either not deployed or not yet recording. Colored bars and right y-axis indicate hours per day with delphinid clicks or whistles present.

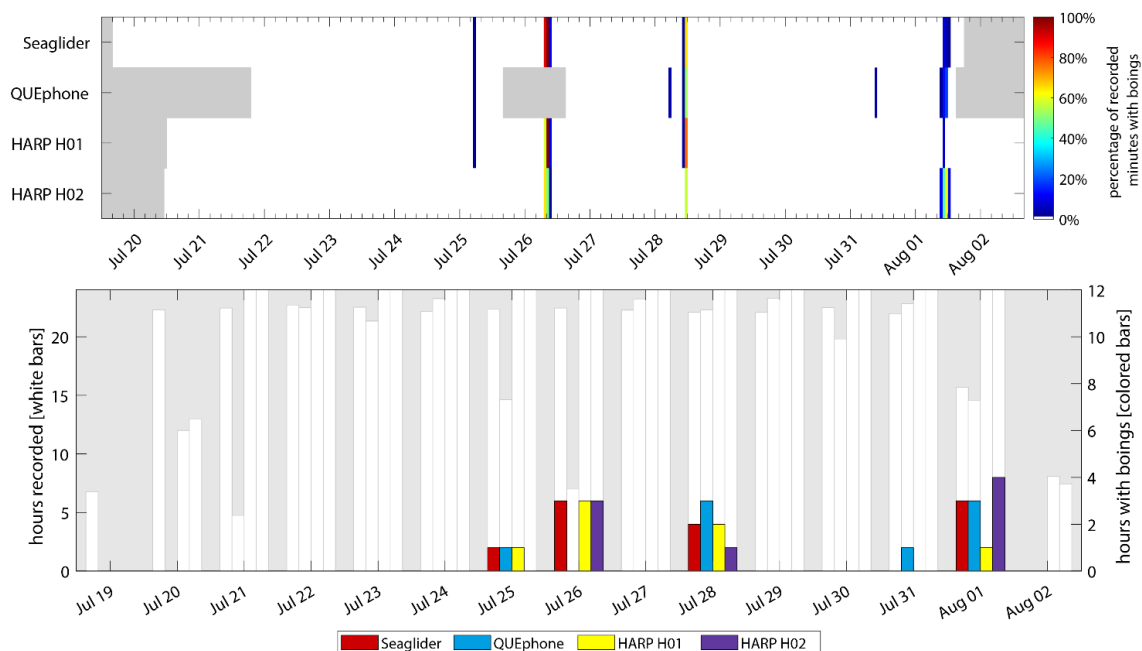


Figure 4.7. Occurrence of minke whale boings by recorder platform. Top panel: Percentage of recorded minutes with boings. Gray areas indicate times when recorders were not deployed. Color of each 1-hour bar corresponds to number of boing detections in that hour, as a percentage of the total minutes recorded in that hour (if 0%, no colored bar is displayed). Bottom panel: Hours with minke whale boings per day. The white bars and left y-axis indicate the total hours recorded per day. No white bar indicates a day where that recorder was either not deployed or not yet recording. The right y-axis and colored bars indicate total hours per day containing minke whale boings. Note scale of right y-axis is only to 12 hours.

CHAPTER 5: DETECTION PROBABILITY OF CUVIER'S BEAKED WHALES BY
A MOVING ACOUSTIC ARRAY USING A SPATIALLY EXPLICIT CAPTURE-
RECAPTURE APPROACH

Selene Fregosi

The results of the case study are included in a manuscript in preparation by Jay Barlow, Selene Fregosi, Len Thomas, Danielle Harris, and Emily T. Griffiths titled "Acoustic detection range and population density of Cuvier's beaked whales estimated for near-surface hydrophones" to be submitted to the Journal of the Acoustical Society of America.

Abstract

Spatially explicit capture-recapture was used to estimate density of Cuvier's beaked whales from a near-surface drifting array of acoustic recorders. A snapshot approach was used with presence or absence of echolocation clicks within a 1-minute snapshot acting as the sampling unit. Each drifting hydrophone recorded an average of 14,832 snapshots, and 1.85% of these snapshots contained Cuvier's beaked whale clicks ($n = 275$ snapshots). Four models to estimate detection probability were tested, and the binary signal strength and compound half normal models were the two best models. Density of Cuvier's beaked whales, from the binary signal strength model and using external estimates of group size and echolocation probability in a 1-minute snapshot, was estimated at 5.48 animals per 1000 km² (coefficient of variation, CV 0.46, 95% confidence interval, CI 2.3 – 12.9 animals per 1000 km²). This density estimate was similar to estimates calculated using trial-based and distance sampling approaches applied to the same data set. Simulation experiments were conducted to investigate potential bias in estimated density caused by the configuration of the drifting array. Bias from the array configuration was found to be negligible. Simulations with increased array spacing (approximately doubling and tripling between-sensor spacing) further decreased this bias. Simulations showed that the drifting aspect of the recorders, which led to a different configuration for every 1-minute snapshot, decreased bias, compared to simulations where sensors were stationary.

Introduction

Accurate estimates of animal population density and/or abundance are critical in species monitoring, conservation, and management. Advances in, and development of, density and abundance estimation methods is a growing field across all taxa, including marine mammals. Methods to estimate marine mammal density and abundance historically utilized shipboard and aerial visual surveys or mark-recapture methods using photo identification of individuals (*e.g.*, Barlow, 1995; Dawson *et al.*, 2008; Urian *et al.*, 2015). Recent advances in statistical methodologies now allow for estimation of density from vocalizing animals using passive acoustic recordings (Marques *et al.*, 2013). Passive acoustics is a useful tool for marine mammal monitoring because marine mammal species rely on sound as their primary sensory modality, are known to vocalize regularly, and vocalizations may be recorded over large distances because sound travels efficiently underwater. Also, acoustic surveys are not limited to daylight hours as visual surveys are and autonomous acoustic surveys can occur in all seasons and weather conditions. Passive acoustic surveys provide a particular advantage for highly cryptic species such as beaked whales, which are difficult to spot or identify visually but vocalize reliably (Barlow *et al.*, 2006, 2013).

Density estimates for marine mammals can be obtained from passive acoustic data using a suite of statistical methods. Density has been estimated from passive acoustic data recorded by a vessel towed array (*e.g.*, Norris *et al.*, 2017), arrays of fixed recorders (*e.g.*, Harris *et al.*, 2018; Marques *et al.*, 2009; Martin *et al.*, 2013), and in some special cases, single fixed recorders (*e.g.*, Harris *et al.*, 2013). Density can be estimated from different types of acoustic detections including individual calls or clicks (cues), presence of calls within a certain time window (snapshots), or a localized individual animal or group. For clarity, any of these types of detections are referred to as an “acoustic event” hereafter. The choice of density estimation method depends on what is feasible with the study system of interest (see Marques *et al.*, 2013 for a useful decision tree).

Two primary approaches for estimating density from acoustic data are distance sampling (Buckland *et al.*, 2001) and spatially explicit capture-recapture (SECR; Borchers, 2012), which can be interpreted as an extension of distance sampling where capture-

recapture data is added but known animal locations are not available (Borchers and Marques, 2017). Both of these methods require an estimate of the effective survey area (ESA) for the denominator of the density estimator (Borchers, 2012; Buckland *et al.*, 2001). The ESA is the area in which the number of animals present (both detected and not detected) equals the number of animals detected in the larger surveyed area (Buckland *et al.*, 2001) and is estimated differently in distance sampling and in SECR.

In distance sampling, an estimate of the average detection probability within the designated survey area is used to estimate the ESA. In a passive acoustic distance sampling fixed point transect survey, detection probability as a function of the animal's distance to the sensor is estimated directly during the survey by measuring the horizontal distance between the sensor and each detected acoustic event. Passive acoustic distance sampling can also be conducted with a towed array line transect survey, and in that case an estimate of distance from the acoustic event to the transect line is required. The distribution of detection distances is used to model a detection function, $g(y)$, which estimates the probability of detecting an acoustic event given its location at horizontal distance, y , from the sensor (Buckland *et al.*, 2001). The ESA is then estimated by multiplying the average probability of detection by the defined survey area; the average probability of detection effectively reduces the defined survey area to the ESA (Buckland *et al.*, 2001). In point transect distance sampling, ESA is calculated for a single sensor and so it can also be helpful to discuss detection probability as the effective detection radius (EDR) which can be thought of as an effective detection range. EDR is related to ESA as the radius of a circle is related to the area of a circle: EDR is the square root of the ESA divided by π .

In typical terrestrial distance sampling, the measured detection ranges used to model the detection function are horizontal ranges with the observation and observer both in a flat, two-dimensional (2D) plane (along the ground). For underwater animals, slant (direct) range, which takes into account animal and sensor depth, can be used in detection function modeling (Marques *et al.*, 2009). If depth information is not available, it can be measured in an assumed 2D plane (projected onto the sea surface), but this may likely lead to measurement error if animals vocalize over a broad range of water depths (Buckland *et al.*, 2015; Marques *et al.*, 2011).

Distance can be empirically measured using an array of hydrophones by measuring the time difference of arrival (TDOA) of a given signal across multiple receivers, as is typical with vessel-based towed array surveys (Norris *et al.*, 2017). Distance sampling assumes the probability of detecting an acoustic event at zero horizontal distance, $g(0)$, is either certain, or has been estimated from other sources. Distance sampling also assumes that animals are distributed randomly in horizontal space, acoustic events are independent, and measurement to each detected acoustic event is without error (Buckland *et al.*, 2001).

In SECR, the spatial configuration of the array of recorders, and the pattern of which recorders did or did not detect each acoustic event (*i.e.*, some recorders “capture” the sound and others do not), provide indirect information on the location of the vocalizing animal. From this, a detection function, can be modeled and an ESA can be estimated (Borchers, 2012). For SECR, the ESA is calculated for the entire array of recorders, so an estimate of EDR from a single recorder is not directly comparable. SECR provides some flexibility over distance sampling in that it does not require distances to the acoustic event to be directly measured. Further, it does not require that detection at zero horizontal distance is certain, and in fact, some models can estimate $g(0)$ when modeling the detection function (Efford *et al.*, 2009b; Marques *et al.*, 2013). SECR assumes that animals are distributed randomly in horizontal space and that acoustic events are independent (Efford *et al.*, 2009b; Marques *et al.*, 2013; Stevenson *et al.*, 2015).

If a detection function cannot be estimated from the acoustic survey itself, either via distance sampling or SECR, auxiliary data may be used to estimate the detection function. A sample of known animal locations, such as from tagged animals (Marques *et al.*, 2009) or by using joint visual and acoustic surveys (Kyhn *et al.*, 2012), can be used to estimate detection probability with a trial-based approach. Each known animal location is considered a detection “trial” with a measured distance from the acoustic sensor. Each measured-distance trial is then scored – 1 if an acoustic event was detected on the sensor at the time of a trial or 0 if no acoustic event was detected – and a detection function can then be modeled using binary regression. Alternatively, acoustic propagation modeling can be used to estimate detection probability as a function of range through simulation (*e.g.*, Frasier *et al.*, 2016; Helble *et al.*, 2013; Küsel *et al.*, 2011). A modeling approach requires

estimates of signal frequency and amplitude characteristics, animal vocal behavior, and ambient noise levels.

Estimating density and abundance of beaked whales is of particular interest for conservation and management because they appear to be highly sensitive to anthropogenic noise. There is strong evidence that beaked whale species respond to Navy sonar by changing diving and foraging behavior, leaving critical habitat, and stranding (D'Amico *et al.*, 2009; DeRuiter *et al.*, 2013; Frantzis, 1998; Miller *et al.*, 2015; Simonis *et al.*, 2020; Tyack *et al.*, 2011). There is great interest in both identifying critical beaked whale habitat for protection and estimating beaked whale densities to monitor population trends and better understand the impacts human activities might have on these animals. While Cuvier's beaked whales are one of the best studied of the beaked whale species (Barlow *et al.*, 2018; DeRuiter *et al.*, 2013; Gassmann *et al.*, 2015; Zimmer *et al.*, 2005), estimates of detection probability and density across much of Cuvier's beaked whale range do not exist (MacLeod *et al.*, 2006).

The first estimate of Cuvier's beaked whale detection probability (Zimmer *et al.*, 2008) used the passive sonar equation to estimate the probability of a near-surface (100 m depth) hydrophone detecting a Cuvier's beaked whale dive. They found near-certain detection at slant ranges up to about 700 m and maximum detection range, of an on-axis click, of about 4 km. More recently, another acoustic modeling estimate was generated for a deep-water hydrophone detecting Cuvier's beaked whales (individual clicks and groups) in the Gulf of Mexico (Hildebrand *et al.*, 2015). Hildebrand *et al.* (2015) estimated groups could be detected with certainty at horizontal ranges of about 600 m, maximum ranges of 3.5 km, and an EDR of about 2.4 km (ESA~ 18 km²). Two additional studies in Southern California have been able to track Cuvier's beaked whales up to 2.5 and 3.5 km from a deep-water, stationary array (Gassmann *et al.*, 2015) and a near-surface drifting array (Barlow *et al.*, 2018), respectively.

Autonomous underwater vehicles, such as gliders and deep-water profiling floats equipped with PAM technologies, are now being used to acoustically monitor cetacean species (Baumgartner *et al.*, 2013; Burnham *et al.*, 2019; Klinck *et al.*, 2012; Matsumoto *et al.*, 2013; Silva *et al.*, 2019). There is a growing interest in the ability to estimate animal

abundance from float- or glider-collected acoustic data, particularly beaked whale species (Gkikopoulou, 2018; Harris *et al.*, 2017). Slow-moving autonomous platforms present unique challenges for density estimation and traditional assumptions (*i.e.*, no animal movement relative to the survey platform, accurate measurement of distances to detected acoustic cues, and certain detection at the survey trackline or point) may not hold (Harris *et al.*, in revision; Marques *et al.*, 2013). In particular, bias is introduced by the slow vehicle movement relative to animal movement (Glennie *et al.*, 2015). A snapshot approach can be used to overcome this bias by choosing a snapshot length over which animal movement is negligible. A snapshot approach is recommended for density estimation of beaked whales, regardless of survey type (Barlow *et al.*, 2013). Conceptually, each snapshot along the glider's flight path can be treated as an individual point transect, and the whole glider survey can be analyzed using a point transect framework to estimate detection probability (Harris *et al.*, in revision), and is recommended for density estimation of beaked whales (Barlow *et al.*, 2013).

Most gliders and deep-water floats currently being used are single-hydrophone systems, so estimating range to the vocalizing animal is not possible from the acoustic data alone. Therefore, the detection probability must be estimated using secondary means. An experiment aimed at quantifying the detection probability of beaked whales from an acoustically equipped Seaglider and deep-water profiling float (QUEphone) was undertaken in summer 2016. The goal was to utilize a concurrently deployed array of near-surface drifting recorders, Drifting Acoustic Spar Buoy Recorder (DASBR; Griffiths and Barlow, 2015), to localize individual beaked whales, and then use the localized whales as detection trials in a trial-based framework to estimate the detection function of both the glider and float. If a detection probability could not be estimated using the trial-based method, due to a low sample size of localized whales or a low number of matches of localized whales to click detections on the glider and/or float, SECR was proposed as an alternative method to estimate detection probability. Unfortunately, low overall encounter rate of Cuvier's beaked whales during this experiment did not allow for empirical estimates of detection probability from a glider and float using either trial-based or SECR approaches.

While sample size was insufficient on the glider and QUEphone, the drifting array recorded enough beaked whale clicks for further analysis. The Drifting Acoustic Spar Buoy Recorder (DASBR; Griffiths and Barlow, 2015) is a relatively new recording platform that shows promise as a survey tool for cryptic beaked whale species (Griffiths *et al.*, 2019; Griffiths and Barlow, 2016). The DASBR is a free-floating near-surface recorder that consists of a two-element vertical array suspended at about 100-m depth with 10-m separation between the hydrophones (Griffiths and Barlow, 2015). By measuring the TDOA of a click between the two hydrophones, or the TDOA between a direct-path click and its surface reflection on a single hydrophone, a detection angle to the vocalizing animal can be measured (Barlow and Griffiths, 2017). If clicks are detected on three or more DASBRs within a 1-minute snapshot, the intersection of the declination angle cones provides an estimate of animal location in three dimensions (Barlow *et al.*, 2018). The angle and location information can then be used to estimate detection probability necessary to estimate densities from DASBR-collected data.

There is a current effort to estimate the probability of detection and animal density for Cuvier's beaked whales using this DASBR dataset (Barlow *et al.*, in prep). This work aims to compare density estimates using three methods to estimate detection probability: distance sampling, trial-based, and SECR approaches (Barlow *et al.*, in prep). Animal density/abundance surveys are typically designed to allow for only one density estimation process; however, this dataset presents a unique opportunity to directly compare three methods. Each method has advantages and disadvantages, so understanding how they may differ when applied to the same dataset is important.

Here we present the results of this experiment as (1) encounter rates of Cuvier's beaked whales on the glider, float, and DASBRs available for both a trial-based and SECR approaches to estimate detection probability, (2) a case study estimating detection probability of Cuvier's beaked whales from the DASBR array, using an SECR method, (3) a simulation study to confirm the validity of using an SECR method with the case study mobile array configuration and explore potential improvements to use in future efforts. The simulation study was conducted because to our knowledge SECR has not been used with a mobile array. It is critical to understand ideal sensor spacing and relative locations when

implementing SECR with acoustic data (Marques *et al.*, 2013), and the potential issues with a mobile array.

Methods

In July and August 2016, a comparison study was conducted in the Catalina Basin off southern California to assess detection capabilities of two types of mobile autonomous deep-water recorders (a Seaglider and a QUEphone float). At the same time, two High-frequency Acoustic Recording Packages (HARPs), a commonly used stationary deep-water recorder, were deployed in the Basin for comparison to the glider and float (see this dissertation, Chapter 4). Additionally, eight Drifting Acoustic Spar Buoy Recorders (DASBRs) were deployed as an array of near-surface drifting hydrophones in order to localize and track detected beaked whales. This chapter primarily focuses on the data collected by the DASBRs and so detailed methods for their deployment, operation, and acoustic analysis is included below. For more information on the glider and QUEphone operation and acoustic analysis, see Chapter 4.

Field effort

Four to eight DASBRs of two different types were deployed daily in the southeast section of the study area starting on 19 July and ending on 1 August 2016 (Table 5.2, Figure 5.1). The DASBRs were deployed in a grid with approximately 900 m spacing and allowed to drift for 19 to 24 hours (Except for Drift 12 which was 46 hours in duration). DASBR location was recorded approximately every 30 minutes from an externally mounted GPS logger (Gen3 and Trace models, SPOT, LLC, Covington, LA, USA). The DASBRs generally drifted to the northwest (Figure 5.1). Drift paths from day to day were fairly consistent; the array shape was generally maintained over each 24-hour drift. Average drift speeds were 0.83 km/hour (SD 1.70). Three of the DASBRs (with SM2+Bat recorders, Wildlife Acoustics, Inc., Maynard, MA, USA) experienced issues with cabling resulting in poor quality data and were excluded from further analyses. Additionally, since the remaining (fourth) SM2+Bat recorder had a different noise floor and system sensitivity than the remaining four, and therefore likely a different detection range, it was also

excluded from further analyses. The working SM2+Bat recorder could have been included using the SECR approach because SECR allows a covariate for recorder type in the detection function models. However, because the overall goal was a comparison of these different density estimation methods, and that recorder was not included in the distance sampling or trial-based approach, for consistency it was also excluded from the SECR analysis. The four DASBRs that recorded usable data and had identical configurations were each outfitted with a SM3M recorder (also from Wildlife Acoustics, Inc.) which recorded nearly continuously at 256 kHz sampling rate. A 1-minute file was recorded at the top of each hour at 96 kHz to measure ocean ambient noise. This was followed by a five-minute sleep period in which the clock was synchronized with a temperature-compensated clock. Then 27 two-minute sound files (.wav format) were recorded at 256 kHz. Each DASBR recorded on two hydrophones arranged in a vertical array at about 105 m and 115 m depth (10 m separation). The hydrophones, including pre-amplifiers, were HTI-96-min (High Tech Inc., Long Beach, MS, USA) with a sensitivity of -165 dB re 1 V/ μ Pa from 50 Hz to 140 kHz. A 2-Hz high pass filter was applied to both recording channels and 12 dB of gain was added. Additional detail on the DASBR buoy configuration and recording systems can be found in Barlow *et al.* (2018).

Acoustic analysis

The DASBR-collected data were analyzed for beaked whale echolocation clicks using the click detector and classifier in PAMGUARD (Beta v1.15.03) software (Gillespie *et al.*, 2009). Beaked whale clicks can be identified and classified by peak frequencies, inter-click intervals, and in some cases, the presence of a frequency upsweep (Keating and Barlow, 2013). Possible beaked whale click detections were manually reviewed by an experienced analyst (E. Griffiths, NOAA's SWFSC) in PAMGUARD Viewer to confirm whether detections were from Cuvier's beaked whales. Confirmation was based on frequency characteristics, particularly a peak frequency between 32-40 kHz (Baumann-Pickering *et al.*, 2013) with secondary peaks at 18-19 kHz and 22-24 kHz, and a frequency upsweep visible in the spectrogram and Wigner-Ville plot (Keating and Barlow, 2013). Additionally, context clues including inter-pulse interval (IPI; typically, 0.33 to 0.50 s;

Baumann-Pickering *et al.*, 2013), direction to the sound source (bearing angles below the hydrophones), and the consistency of that direction over each two-minute file were used to identify Cuvier's beaked whale clicks (Keating and Barlow, 2013).

Encounter rates on the glider and float

For each known beaked whale localization generated by Barlow *et al.* 2018 from the DASBR data ($n = 23$), the distance between the localization and both the glider and the float in that minute were measured. Additionally, distances between the glider and float and each DASBR, and between DASBRs, were measured over the entire experimental period at 1-minute resolution. Distances were calculated using the Pythagorean theorem, ignoring the curvature of the earth, because distances were relatively short (< 20 km).

Estimating effective area surveyed using SECR

Spatially explicit capture-recapture (SECR) analyses were conducted to estimate the effective survey area, \hat{a}_e . In traditional SECR, whether an individual animal (or in this case a group of animals) is captured and recaptured at a particular trap or multiple traps over time (called sampling occasions) is recorded in a capture history. The number and pattern of capture locations is used to estimate the detection function and ESA (see Borchers 2012 for non-technical overview of SECR). Maximum likelihood methods are used to estimate the detection function parameters (Borchers and Efford, 2008). Traps that do not physically restrain animals, but instead record their presence and leave them available to be captured by other traps, are called proximity traps (Borchers, 2012); hydrophones are proximity traps, and are referred to here as sensors. Acoustic signals can be detected (recaptured) on multiple sensors (traps) at the same time. So for SECR with acoustic data, rather than recaptures occurring over multiple sampling occasions, each capture history is instead a single occasion and utilizes the information about whether an individual detection was captured and recaptured in space on multiple sensors (Efford *et al.*, 2009b).

SECR surveys can be divided into sessions (groups of occasions separated by time or space) and density and ESA are estimated for each session. This extends SECR by

allowing comparisons across sessions (Efford *et al.*, 2009b; Royle *et al.*, 2013). Conversely, sessions can be collapsed together to look at mean density for all sessions (*e.g.*, Marques *et al.*, 2012). Sessions can also be useful because they allow for changes in sensor configuration in time, as occurred with the drifting DASBR array (Efford *et al.*, 2009a).

SECR analysis requires an analysis buffer to be specified. This buffer defines the area, or mask of grid points, over which the likelihood is integrated (Borchers and Efford, 2008) and, in the case of acoustic SECR, the buffer should extend from the hydrophone array to a boundary beyond which individuals are likely not to be detected. It is analogous to the maximum detection radius specified in distance sampling. Density estimates should not change with increased buffer size, if the buffer is sufficiently large (Royle *et al.*, 2013).

Detection probability as a function of horizontal range was modeled using the *secr* package (v3.2.1; Efford, 2019) in R (v3.6.2). The movement of the array of instruments through space and time presented a unique problem to SECR analysis. While previous studies have moved arrays around over time, recorder relative positions and the spacing remained constant (Dawson and Efford, 2009). In this study, both the absolute location and the relative configuration of the sensors changed over time. We broke the survey into sessions and assigned different sensor configurations for each session at two scales. First, each click-positive 1-minute snapshot was treated as a separate session ($n = 275$), hereafter referred to as the “by-snapshot sessions”. Sensor locations for each 1-minute sample were estimated from linear interpolation of satellite geolocation positions (at intervals of up to 30 min.) (Barlow *et al.*, 2018). Each sensor location was normalized by the mean location of the all four sensors in each session, to create sensor configurations in relative space, across sessions (Figure 5.2). Second, each detected beaked whale dive as classified in Barlow *et al.* (2018) was grouped into a session ($n = 25$), hereafter referred to as the “by-dive sessions”. DASBR movement over each dive was between 0 and 668 m (mean 259 m, SD 223 m). The mean of each DASBR’s locations per dive served as the sensor locations for each session. Again, relative sensor locations were used; each individual sensors’ location was normalized by the mean location of all for sensors for each by-dive session. (Figure 5.3).

Binary capture histories were created for each session; all 1-minute sessions had a single capture history per session and by-dive sessions included captures for all click-positive 1-minute snapshots for each dive. The by-dive sessions contained multiple click-positive snapshots, which were treated by *secr* as multiple unique “animals,” or detection objects, captured in that session. Four models for detection probability were initially fit: half normal (HN), hazard rate (HR), compound half normal (CHN), and binary signal strength (BSS) (Table 5.3). The HN model is characterized by a monotonic decrease in probability of detection as a function of range and it has been successfully used in many density estimation methods (Hayes and Buckland, 1983); it is often considered the “default” detection function model (Efford, 2019). In SECR, two parameters are estimated by the HN model: the probability of detection at zero horizontal distance, $g(0)$, and σ which defines the shape of the function. The HR model is also used in distance sampling and is similar to the HN model, but includes an additional estimated scale parameter, z (Hayes and Buckland, 1983). The HR model is not recommended for SECR analysis because of the potentially long tail (Efford, 2019; Efford *et al.*, 2009a), but was included in this analysis because it is often used in distance sampling. The CHN model is an extension of the half normal model that includes an additional scale parameter, z that allows greater variability in the slope of the decrease in detection probability with range (Efford and Dawson, 2009). The BSS is a variant of the signal strength model proposed in Efford *et al.* (2009b) specifically for passive acoustic density estimation, however the BSS model does not require signal strength information. The BSS model does not provide an estimate for $g(0)$ but is defined by two parameters, b_0 and b_1 (Efford, 2019).

All detection functions were fit by maximum likelihood using the more robust conditional likelihood option in *secr* (Borchers and Efford, 2008). A buffer distance of 8000 m was used for all models and was selected based on previous estimates of maximum detection distance of Cuvier’s beaked whale clicks (Hildebrand *et al.*, 2015; Zimmer *et al.*, 2008). A buffer of 8000 m was appropriate for all models except the half normal model, which called for an increasingly larger buffer over successive runs of the model regardless of input buffer size. Reported results are for the 8000 m buffer to be comparable to other

models and because it is generally very unlikely clicks can be detected beyond this distance (Hildebrand *et al.*, 2015; Marques *et al.*, 2009; Zimmer *et al.*, 2008).

Models were compared using Akaike Information Criteria (AIC). ESA and density of minutes containing clicks were derived in the R package *secr* (Efford, 2019). Derived density and ESA values are reported for each session individually, so mean estimates of ESA and density were calculated across all sessions. SECR estimates ESA for the entire array, rather than for a single instrument as in point-transect distance sampling and the trial-based approaches. The array configuration may not lead to a circular ESA so an estimate of effective detection radius is not typically estimated. For comparison to other studies, we calculated a “pseudo” effective detection radius (pEDR) for a single instrument of the array using the mean SECR parameter estimates for each model following the point-transect distance sampling methods of (Buckland *et al.*, 2001). Subsequent snapshots with clicks were likely the same whales detected multiple times, which violates the independence assumption of SECR. While estimates of density and ESA are robust to violation of independence across snapshots, estimates of variance are not (Marques *et al.*, 2013). Therefore, variance for ESA, density of click-positive minutes, pEDR, and all detection function parameters was estimated empirically using a jackknife approach (Efron, 1982), with each of the 11 DASBR drifts treated as replicates for resampling.

Density estimator

Density of Cuvier’s beaked whales was estimated from echolocation clicks using groups of animals detected in a 1-minute snapshot as the sampling unit. A snapshot approach was used because individual animals cannot be identified from their clicks (as was done with minke whales in Marques *et al.* (2012) and Martin *et al.* (2013)). The sampling unit was each 1-minute window with or without at least 3 beaked whale clicks present, representing a group of animals. We assumed that only a single group of clicking animals was detected across the array in any given snapshot. Density of individuals, \hat{D} , is estimated as

$$\hat{D} = \frac{n \hat{s}}{k \hat{P}_e \hat{a}_e} \quad (5.1)$$

where n is the number of snapshots (here 1-minute duration) with clicks on at least one recorder and k is the total number of snapshots. These values were both calculated empirically from the data and variance of the proportion of snapshots that contained clicks (n/k) was estimated using a jackknife approach with drift number as the resampling unit. Mean group size, \hat{s} , and the probability that a group of animals is echolocating within a 1-minute snapshot, \hat{P}_e , were estimated from the literature as follows. Mean group size, \hat{s} , is estimated as 1.9 animals (coefficient of variation, CV 0.07) and is calculated from the mean estimate of group size from 63 visual sightings over seven previous visual surveys in the California Current (Barlow, 2016). The instantaneous probability of echolocating, estimated from the proportion of time echolocating, is 0.199 (CV 0.04) and is taken from a tagging study of Cuvier's beaked whales in similar habitat in southern California (Barlow *et al.*, 2020). According to Barlow *et al.*, (2013), to scale the probability of an individual echolocating to the probability of a group echolocating during a 1-minute snapshot, approximately one percentage point should be added to the instantaneous probability, thus \hat{P}_e is 0.209 (CV 0.04). Finally, \hat{a}_e is the effective survey area, which was calculated using SECR and corresponds to the detection probability of an echolocating group as a function of the groups range. Variance for the density estimate of animals was calculated using the delta method approximation to combine CV values for all density estimator inputs (Marques *et al.*, 2013; Seber, 1982).

Simulations with varied sensor spacing

Sensor spacing and configuration may affect the SECR results, particularly precision (Dawson and Efford, 2009). This experiment was unique in that the distances between sensors changed during the survey as the DASBRs drifted. Further, the between-sensor distances were relatively short (mean 1172.5 m, SD 367.5 m; Figure 5.2) compared to the effective detection radius estimated through a trial-based or distance sampling method (2650 to 3068 m; Barlow *et al.*, in prep). To examine the effect of instrument spacing on SECR results, and test if SECR is an appropriate analysis with the case study data, a series of simulations were conducted.

Simulation populations and capture histories were generated using input values of density and density function parameters from the case study results. See Figure 5.4 for an overview of the simulation workflow. Simulations were run using the compound half normal model in order to be consistent with the distance sampling approach used by Barlow *et al.* (in prep) and because it performed and was shaped nearly identically to the top BSS model (Figure 5.6). Simulations were run using by-dive sessions (25 sessions) since results from the by-dive and by-snapshot sessions were nearly identical and run times for the by-dive sessions were much faster than the by-snapshot sessions (275 sessions). Simulated density was 0.36 objects per km² per session (equal to the density of click positive minutes in the case study). Simulated detection probability parameters were $g(0) = 1$, $\sigma = 957$, and $z = 11.26$. A buffer of 8000 m was used.

The first simulation was conducted to validate the appropriateness of the case study analysis, in particular the sensor spacing and movement, by replicating the case study analysis with known population and detection function inputs. The first simulation used the actual sensor locations for each of the 25 sessions, so sensor configuration and spacing did change slightly between sessions, matching what occurred in the field efforts (Figure 5.3). The second simulation looked more specifically at sensor movement and aimed to assess how the results might differ with an array of fixed sensors. The Session 1 sensor configuration was held constant and used for all 25 sessions in the second simulation. The third and fourth simulations used artificially widened sensor spacing to examine the effect of larger array spacing and maintained the sensor movement between sessions. For the third simulation, mean sensor spacing was approximately doubled (to 2260.6 m SD 521.5) by adding 500 m to each positive easting and northing value or subtracted from each negative easting and northing value (Figure 5.5). An additional 500 m was added or subtracted from each northing and easting for the fourth simulation, approximately tripling the mean distances between sensors to 3373.3 m (SD 746.3; Figure 5.5).

Simulated ESA was calculated using *secr* and averaged across the 25 sessions (25 different sensor configurations) to get a mean simulated ESA for each input set of sensors. Each simulation was run 100 times and means and medians across the 100 runs are reported. Bias was estimated as the difference between the input value and the median of

the simulations, as a percentage of the input value. Simulated SECR fits that resulted in a warning or error were not included in the mean and median calculations. Optimization errors occurred if only a local minimum could be reached, or if the model did not converge.

Simulations with larger sample size

The encounter rates of beaked whales in the case study were relatively low. The study occurred in the summer, when there appears to be a dip in Cuvier's beaked whale presence in the region, compared to winter and spring (Baumann-Pickering *et al.*, 2018; Rice *et al.*, 2018). To investigate how the low sample size may have affected the SECR analysis, an additional simulation was run with a larger simulated population density (5 objects per km²), the actual sensor spacings, and the estimated detection probability parameters from the case study results. Increased density was used as a proxy for increased sample size because it resulted in a greater number of simulated click minutes, which may be expected for a longer duration survey or in a time period with greater animal presence. Mean and median of the estimated density, ESA, and the detection probability model parameters are reported. Bias was calculated as in the previous simulations.

Results

The glider recorded a total of 290.4 hours, or 17,419 1-minute snapshots. It traveled over 215 km with an average speed over ground of 0.69 km per hour (Table 5.1). The QUEphone completed a total of five 2-day drifts, recorded for 219.5 hours, and covered a total of 63.3 km (Table 5.1). Drift speeds ranged from 0.21 to 0.31 km per hour for the 5 drifts (mean 0.28 km/hr SD 0.04). Each DASBR recorded over 245 hours of stereo acoustic data and travelled between 199 and 205 km total (Table 5.1). The mean number of 1-minute snapshots recorded by each DASBR was 14,832.5 minutes (SD 90.2 minutes). DASBR drifts lasted between 19 and 24 hours (except for Drift 12 which was 46 hours duration) and covered 12 to 24 km (Table 5.2). Average drift speeds were 0.83 km/ hour (SD 1.70).

Encounter rates of Cuvier's beaked whales

None of the 23 whale locations calculated by Barlow *et al.* (2018) matched beaked whale encounters on the glider (Table 5.4). The glider was typically quite far from the localized whales (mean = 8.0 km, SD = 3.4). Two whale locations were only 3.5 km from the glider (tracked dive number BL-1); however, the glider was very near the surface for the first location and the PAM system was off as the glider was at the surface for the second location, just 8 minutes later. Only two whale locations were simultaneously detected on the QUEphone (Table 5.4). Mean QUEphone distance to localized whales was slightly lower than the glider (mean = 7.1 km SD = 2.9), but was still most often beyond ranges which are reasonable for detecting Cuvier's beaked whales (Hildebrand *et al.*, 2015; Zimmer *et al.*, 2005). In fact, the two matched locations occurred when the QUEphone was 6.7 and 6.3 km away, so it is possible this was two different localized groups. Conversely, the QUEphone was within 3.5 km of 4 whale locations, but they were not detected on the QUEphone.

The Seaglider and QUEphone contained 66 and 125 minutes with Cuvier's beaked whale clicks, respectively (0.38% and 0.95% of total recording time). The DASBRs contained 147, 195, 140, and 162 minutes with clicks (0.98%, 1.32%, 0.95%, and 1.09%) on B1 through B4, respectively (Table 5.1 and Table 5.2). A total of 475 1-minute snapshots contained clicks on at least one recorder. Of these, 275 snapshots contained clicks on at least one DASBR (Table 5.5). The distribution of number of click-positive minutes that matched 1, 2, 3, and 4 DASBRs was 84, 73, 58, and 60 minutes, respectively (Table 5.5). Of the 275 DASBR click-positive minutes, 26 occurred when the glider was at the surface and was not recording and only three matched click-positive minutes on the glider. These three minutes occurred during by-dive Sessions 2 and 22 (Table 5.5). The glider did have minutes with clicks in the three minutes following the DASBR by-dive Session 1. For the three dives when the glider did have clicks at or near the same time as the DASBRs, the glider was on average 1.3, 1.0, and 2.4 km from the center of the DASBR array (Sessions 1, 2, and 22, respectively). Only 2 of the 275 DASBR click positive minutes matched click-positive minutes on the QUEphone, and 55 of them occurred when the QUEphone was not deployed or was not recording because it was at the surface. This

excluded the QUEphone from 7 of the 25 by-dive sessions. The two matched minutes occurred during by-dive sessions 7 and 8 when the QUEphone was an average of 1.2 and 4.9 km from the center of the array, respectively.

Effective survey area and density estimate

Estimates of detection probability model parameters, density, and ESA did not differ between when the SECR analysis was applied to the dive-based (25) sessions or snapshot-based (275) sessions (Tables 5.6, Table 5.7). Model fitting with only 25 sessions was, not surprisingly, considerably faster than for 275 sessions. The standard errors of parameter estimates were smaller for the fits using the by-snapshot sessions (Table 5.7). For both datasets, the binary signal strength model had the lowest AIC score and the compound half normal and hazard rate models had Δ AIC values less than 3. The half normal model appeared highly dependent on the choice of buffer; it performed much worse (Δ AIC = 49) than the other three models and is not given further consideration.

Mean ESA was 30.71 (jackknife CV 0.26), 30.90 (jackknife CV 0.29), and 31.46 km² (jackknife CV 0.29) for the BSS, CHN, and HR models, respectively (Table 5.7). The pseudo effective detection radius was approximately 2380 m for all models (Table 5.7). Both the CHN and HR models estimated the probability of detection at horizontal distance zero ($g(0)$) at or near 1 and variance of this estimate was low compared to variance of other parameter estimates (Table 5.7). Estimates for the shape, $\hat{\sigma}$, and scale, \hat{z} , parameters for the CHN model were 951 (jackknife CV 0.15) and 15 (jackknife CV 2.5) respectively (Table 5.7). The high variance of the scale parameter for the CHN model did not appear to affect the density or ESA results as variance for ESA was similar to variance for ESA estimated from the BSS and HR models (Table 5.7).

Density estimates from all three competitive models were very similar (5.35-5.48 animals/1000 km²) and variance was similar for the three models (jackknife CV 0.46 – 0.48; Table 5.8). The greatest source of variance in the density estimate was the between-drift variability (CV 0.37) in the proportion of click positive minutes (Table 5.8).

Simulations of varied sensor spacing

Simulations showed that the compound half normal model estimated object density, using an input density and input model parameters near the case study values, with negligible bias (Table 5.9). Bias of the estimated ESA was near 1% for the case study sensor spacing and when sensor spacing was increased by a factor of 2. When sensor spacing was increased by a factor of 3 in all directions, bias of estimated ESA was only 0.11% (Table 5.9 and Figure 5.9). Bias in ESA was largest when the sensors were held stationary across sessions (2.72%) but was still quite low. Estimates of the density of click minutes, \widehat{D}_c , were biased by less than 3% for the actual sensor configuration and decreased to 1.26% and 1.20% when sensor spacing was doubled and tripled, respectively (Table 5.9; Figures 5.7, 5.8, 5.9). Bias of \widehat{D}_c for the stationary sensors was 2.32%. Mean estimated standard error of the \widehat{D}_c estimate also decreased with increased sensor spacing and was slightly greater for the stationary sensor configuration. The greatest variability in model parameter estimates across the simulations was the z , or shape, parameter, as was observed in the case study data. Larger z estimates gave the compound half normal model a larger “shoulder” at probability 1 (Figure 5.6). This shoulder represents a range of distances where detection probability remains stable near 1. Bias of median z estimates increased with increased sensor spacing (>100% at the largest sensor spacing) however the instability in the estimated z parameter did not affect the overall results of \widehat{D}_c and ESA. ESA and \widehat{D}_c bias decreased with increased sensor spacing. All spacing simulations estimated $g(0)$ at or near 1, with near 0% bias.

Simulation of larger sample size

The larger simulated population density of 5 objects per km² resulted in capture histories of around 3850 objects for each simulated run, compared to approximately 275 objects under the case study density. The simulation using a larger simulated population density had lower bias for \widehat{D}_c and ESA (1.02% and 0.70% respectively). Bias for the parameter estimates z and σ were also much lower than for the low-density simulations at all sensor spacings (Table 5.9 and Figure 5.10). The bias for the $g(0)$ parameter was near zero in all simulations.

Discussion

We were able to estimate beaked Cuvier's beaked whale density using spatially explicit capture-recapture methods with a drifting array of near-surface hydrophones. To our knowledge, this is the first time SECR has been applied to beaked whales and to a moving acoustic array. Estimates and variance of estimates obtained with the SECR method were similar to those obtained with trial-based and distance sampling approaches. Simulations showed an SECR approach was appropriate for these data, but that improvements could be made in future efforts to reduce bias and increase precision. Initially, we hoped to estimate detection probability from a glider and QUEphone using a trial-based or spatially explicit capture recapture method, but this was not possible because of the paucity of matched encounters between the glider or QUEphone and the DASBR array. A brief discussion of why we did not have enough encounters and future directions can be found in the last section of the discussion.

Case study results

We can compare the SECR estimates to the distance sampling and trial-based estimates calculated from these same data (Barlow *et al.*, in prep). We chose to compare the SECR results from the compound half normal model because that model was also applied and found to be the best model for the trial-based approach. The SECR estimate of 5.44 animals/1000 km² (confidence interval, CI 2.27-13.06) was higher than either of the other two methods (trial-based: 4.54 animals/1000 km² CI 1.74-11.84; distance sampling: 3.93 CI animals/1000 km² CI 1.72-8.96) but 95% confidence intervals of all methods overlapped substantially. The coefficient of variation was very similar for all methods and was quite high (trial-based 0.52, distance sampling 0.44, SECR 0.47). SECR is the most different from the other methods in that it estimates the ESA of all the instruments; all sensors are treated as a single unit of detection, whereas the trial-based and distance sampling methods look at each DASBR individually, and average the estimates calculated by each sensor to get a mean density. To try to compare more directly, pEDR was calculated for the SECR approach. This estimate was smaller than the EDR for either trial-

based or distance sampling (pEDR of 2.4 km for SECR compared to EDRs of 2.8 and 3.0 km for trial-based and distance sampling, respectively). If ESAs are compared, the SECR estimate is the largest (30.9 km²) compared to the trial-based (24.5 km²) and distance-sampling (28.3 km²) values. As stated above, we would expect ESA to be larger for SECR because it is across all four recorders compared to a single recorder. However, the trial-based or distance sampling ESAs cannot simply be multiplied by the number of sensors and compared because much of their survey area overlapped. Another point of difference is in the proportion of minutes containing clicks (n/k) that is used in the density equation is different for the trial-based and distance sampling methods (1.2%; mean proportion per sensor) than for SECR (1.85%; proportion across all sensors).

Effective detection radii by all methods were similar to those that have been simulated using acoustic modelling (2.4 km, Hildebrand *et al.*, 2015 and 3.0 km Zimmer *et al.*, 2008). Maximum detection ranges were also similar (3.5 – 4.0 km). There are many factors that could lead to differences in these simulated estimates and the DASBR estimates, and it is worth noting that neither of these estimates is for the Southern California region. The estimate of Zimmer *et al.* (2008) was for a similar depth (100 m) near-surface hydrophone in the Mediterranean Sea, while that for Hildebrand *et al.* (2015) was for a bottom-mounted recorder in the Gulf of Mexico. Both Zimmer *et al.* (2008) and Hildebrand *et al.* (2015) estimates for group detection probability were not monotonic decreases with increased range. In both cases, detection probability declined to approximately 0.5 to 0.7 at the one- to two-kilometer range before plateauing for approximately one kilometer before decreasing steeply to near zero. None of the DASBR detection function estimates showed this non-monotonic shape and sudden decrease, but that was a limitation of flexibility of the tested detection probability models (half normal and compound half normal).

The case study SECR estimate was higher than two previous estimates for the region, one based on visual surveys and one using acoustic detections. Cuvier's beaked whale density for the entire U.S. west coast was estimated at 3.2 animals/1000 km² (Barlow, 2016). A snapshot-based approach, using acoustic modeling to estimate the detection function, was used to estimate Cuvier's beaked whale density from a stationary

recorder in Southern California and reached an estimate of 1.7 animals/1000 km² (Hildebrand *et al.*, 2016).

A potential source of bias in our application of SECR, and in the trial-based and distance sampling approaches as well, was that the 1-minute snapshots were often consecutive minutes in time. Therefore, each by-snapshot session could not be considered independent, which violates the independence assumption for SECR. Consecutive click minutes were probably clicks from the same animal or group of animals. For SECR we could assume the bias in estimates of density of ESA was negligible, as Stevenson *et al.*, (2015) found that non-independence only introduced minimal bias. However, the main issue with violation of non-independence is that variance may be underestimated. Empirical estimates of variance, such as a parametric bootstrap, are recommended (Kyhn *et al.*, 2012; Marques *et al.*, 2009; Stevenson *et al.*, 2015), and so a jackknife resampling method was used rather than the estimates of CV generated within SECR.

Much of the work on SECR with acoustic data has focused on adding acoustic information to strengthen the model fit and estimate (Efford *et al.*, 2009b; Stevenson *et al.*, 2015). For example, information about time difference of arrival, received signal strength, and bearing can be added to the binary capture histories and reduce the uncertainty of the sound source location, and therefore the variance of the ESA (Efford *et al.*, 2009b; Stevenson, 2016; Stevenson *et al.*, 2015). The high directionality of beaked whale clicks (Zimmer *et al.*, 2005) is likely a huge source of variance in this work, and if signal strength information were available, directionality could be incorporated in the detection function (Stevenson, 2016). However, no additional inputs could be used in the work here. The DASBRs were not sufficiently time-synchronized to accurately calculate differences in time of arrival. Because we used a snapshot approach to overcome slow instrument movement (Harris *et al.*, in revision), individual clicks (and their received levels) were not the objects of interest, so signal strength could not be included in the model. The number of clicks recorded in each minute may have potential to improve the SECR work, but that was beyond the scope of this study. Click number would need to be implemented into the *secr* or *ascr* R packages.

Simulations

The simulation study presented here provides insight into the validity of the density estimate presented in the case study and into how the method may be improved in the future. While simulations showed that the spacing of the four working recorders, and the fact that they moved during the survey, still provided a reasonably accurate estimate of the ESA, it was likely not ideal. The case study sensor spacing showed the highest bias for the density of objects of all simulations, though it was still less than 3%. Interestingly, bias estimates for detection function parameters, density of objects detected, and estimated ESA did not all follow the same pattern as sensor spacing was increased. While estimates of object density and estimated survey area improved with increased array spacing, the bias of two of the detection function parameters (σ and z) increased with increased array spacing. The $g(0)$ parameter followed the same trend as the density and ESA estimates – bias decreased with increased array spacing. Based on the simulation findings, I would recommend increasing the spacing in future deployments, aiming for approximately 2 km spacing between sensors.

Increasing the sample size, potentially by deploying the array for longer than two weeks, would likely provide the greatest improvement to the density estimate precision. The simulations showed that bias for both density and ESA were 1% or less with a 14-fold increase in sample size. This size increase via extending the duration of recording (2-week survey to 28-week survey) would likely not be feasible in the field, and would introduce errors from changing seasonal densities, but sample size could also potentially be increased with deployment of more DASBRs in the array. This would both increase the minutes with detections, and the array spacing, both of which would likely improve the estimates. The optimal number of DASBRs could be explored with additional simulations.

Applications to gliders and deep-water floats

The SECR method applied here shows promise as a way to estimate detection probability for beaked whales from gliders and deep-water floats, if another experiment could be performed. SECR analysis allows different sensors to be pooled and sensor type to be modeled as a covariate in the detection function estimates. For example, the different

DASBR type that was removed in this analysis to be consistent with the trial-based and distance sampling analysis could have still be included in the SECR analysis. Movement of sensors in the DASBR-only analysis was not a problem and the SECR approach generated results similar to those estimated with a trial-based or distance sampling approach. We can envision applying this framework with additional data – more beaked whale encounters on the glider and float at the same time beaked whales were detected on the DASBRs.

Encounters in this field effort were likely low for several reasons. First, beaked whale encounters in general were low, and Cuvier's beaked whale presence on bottom-mounted recorders has been shown to be low during the summer months (Baumann-Pickering *et al.*, 2018; Rice *et al.*, 2018). In this study, we were restricted to working in July-August because of instrument availability; each was being used in other projects at other times of year. If we were to repeat this experiment, we would prioritize deployment at the known peak in beaked whale presence late fall. The location of the experiment was also restricted. Other basins in the Southern California Bight may have higher densities of beaked whales (Baumann-Pickering *et al.*, 2018; Rice *et al.*, 2018, 2019), but access to those basins to recover and redeploy instruments on a daily schedule, as we were able to do working from Santa Catalina Island, may not be feasible. Most of the Channel Islands are part of the Channel Islands National Park and Channel Islands National Marine Sanctuary, and do not have the infrastructure to act as a basecamp for day trips to reposition recorders. Access and usage can be restricted and require permits. The other Channel Islands (San Clemente and San Nicholas) are controlled by the U.S. Navy and access for civilians is severely restricted.

The unusable data collected by three of the DASBRs may have also reduced our possible matches and limited our ability to apply either trial-based or SECR methods to estimating detection probability for the glider or float. As was seen with the DASBR-only analysis, clicks were often not detected on multiple DASBRs. More usable DASBRs would have widened the reach of the array and possibly led to more whale locations for the trial-based approach and more simultaneous detections on multiple platform types required for SECR. Lastly, the low number of matches was in part due to the limited time the glider and

QUEphone spent within a few kilometers of the DASBRs. The glider was set on a course to fly over the two stationary HARPs. This was a goal of another project; glider operations were arranged to collect data to meet both projects' goals. The glider stayed within range of the HARPs very well, and a comparison of the HARPs to the glider and QUEphone was possible (see Chapter 4, this dissertation or Fregosi *et al.*, in revision). But the mismatch of the glider's travel speed to the DASBRs drift speed meant that, on average, the glider and DASBRs were separated by more than the few kilometers of the maximum detection range expected for Cuvier's beaked whales (Hildebrand *et al.*, 2015; Zimmer *et al.*, 2005). In future efforts it would be beneficial to prioritize flying the glider with the DASBRs rather than on a pre-defined back-and-forth track. One way to do this would be to have the glider do steeper dives so it does not travel as far over ground on each dive. The glider could also be "tethered" to a point in the center of the DASBR array and could just do near-vertical dives at this point. The QUEphone's horizontal movement can't be controlled, and its drift did not match the DASBRs' because it was drifting at 500 m while the DASBRs were at the surface. Future efforts could have the QUEphone drift at a shallower depth, but that in part reduces one of the key features of the QUEphone – that it is recording in deeper, quieter water. The QUEphone also had deployment issues at the start and the middle of the experiment that meant it was deployed for less time. It was not deployed during seven of the DASBR recorded dives, and so those are obvious missed opportunities for comparison.

Acknowledgements

Funding for this work was provided by the Living Marine Resources Program (N39430-14-C-1435), the Office of Naval Research (N00014-15-1-2142) and NOAA's Southwest Fisheries Science Center. SF was supported by the National Science and Engineering Graduate Fellowship. Special thanks to Anatoli Erofeev and Stephen Pierce (OSU) for their glider piloting guidance and support and to Alex Turpin (PMEL) for his work preparing the glider and QUEphone. We are grateful to Emily Griffiths of NOAA's Southwest Fisheries Science Center for her work detecting and reviewing the DASBR acoustic data for beaked whales. Vessel support was provided by Trevor Oudin and Juan Carlos Aguilar of Wrigley Marine Science Center and Spencer Salmon and the crew of the M/V Horizon.

Tables

Table 5.1. Deployment and recovery times for the Seaglider (SG607), QUEPhone (Q003), and DASBRs (B1-B4). The QUEPhone is broken down by the five drifts as well as the total recording and distance traveled across the duration of the experiment. DASBR deployment and recovery times, total time recorded, and distance traveled are sums across all 11 drifts. Individual drifts are broken down in Table 5.2.

Recorder	Deployed (UTC)	Recovered (UTC)	Recording duration		Distance (km)	Click minutes	
			(hr)	(min)			
SG607	7/19/2016 16:14	8/1/2016 17:47	290.4	17419	216.4	75	
Q003	<i>drift 1</i>	7/21/2016 18:50	7/23/2016 14:57	41.9	2513	12.6	48
	<i>drift 2</i>	7/23/2016 17:00	7/25/2016 14:56	44.6	2674	9.7	3
	<i>drift 3</i>	7/26/2016 15:54	7/28/2016 14:48	44.8	2685	14.4	56
	<i>drift 4</i>	7/28/2016 15:55	7/30/2016 14:55	45.6	2736	14.1	30
	<i>drift 5</i>	7/30/2016 18:08	8/1/2016 14:57	42.6	2559	12.5	0
	all	7/21/2016 18:50	8/1/2016 14:57	219.5	13167	63.3	137
DASBRs	B1	7/19/2016 13:04	8/1/2016 15:05	249.4	14965	203.4	147
	B2	7/19/2016 13:15	8/1/2016 14:01	246.5	14791	196.4	195
	B3	7/19/2016 14:06	8/1/2016 14:48	246.1	14765	196.7	140
	B4	7/19/2016 14:13	8/1/2016 14:28	246.8	14809	200.4	162

Table 5.2. Deployment and recovery times for DASBRs. Drift 9 occurred on 7/27-7/28 and only the four SM2+Bat DASBRs were deployed while the batteries in the SM3M DASBRs were replaced.

Drift #	DASBR #	Date		Time (UTC)		Duration (minutes)	Distance (km)	Click minutes
		Start	End	Start	End			
1	B1	7/19/2016	7/20/2016	13:04	14:50	1417	15.31	4
	B2			13:15	15:25	1439	15.23	9
	B3			14:06	15:45	1411	14.99	6
	B4			14:13	15:15	1395	15.19	6
2	B1	7/20/2016	7/21/2016	16:59	16:10	1275	15.04	0
	B2			16:42	15:48	1271	15.75	1
	B3			16:30	15:15	1251	15.21	0
	B4			16:51	15:35	1250	15.09	0
3	B1	7/21/2016	7/22/2016	16:55	14:50	1205	19.08	34
	B2			17:05	14:26	1174	17.86	33
	B3			17:15	15:05	1201	19.25	35
	B4			17:09	15:20	1220	19.56	31
4	B1	7/22/2016	7/23/2016	17:15	15:15	1210	19.29	0
	B2			17:25	14:55	1183	17.93	9
	B3			17:06	14:10	1159	17.20	3
	B4			17:00	14:25	1178	17.97	6
5	B1	7/23/2016	7/24/2016	17:25	15:00	1187	21.60	18
	B2			17:45	14:38	1149	20.64	28
	B3			17:59	15:20	1174	20.71	13
	B4			17:50	14:30	1137	22.59	23
6	B1	7/24/2016	7/25/2016	17:25	14:35	1164	20.44	30
	B2			17:35	14:49	1168	19.76	58
	B3			17:15	14:06	1147	19.77	47
	B4			17:41	15:05	1177	20.09	48
7	B1	7/25/2016	7/26/2016	17:05	14:46	1193	17.88	29
	B2			16:57	14:29	1184	17.35	36
	B3			17:11	14:06	1150	17.43	16
	B4			16:50	14:16	1179	17.39	28
8	B1	7/26/2016	7/27/2016	16:04	15:41	1299	19.52	13
	B2			16:11	15:30	1282	18.96	14
	B3			16:24	15:55	1293	19.46	15
	B4			16:18	16:07	1310	19.95	14
10	B1	7/28/2016	7/29/2016	16:04	15:05	1266	18.70	19
	B2			15:59	14:40	1248	16.96	7

Table 5.2 (Continued)

10	B3	7/28/2016	7/29/2016	15:44	14:55	1275	16.80	5
	B4			15:52	14:17	1233	16.51	3
11	B1	7/29/2016	7/30/2016	16:37	14:45	1217	12.70	0
	B2			16:48	14:55	1216	12.50	0
	B3			16:44	14:26	1194	12.27	0
	B4			16:55	15:06	1220	12.65	0
12	B1	7/30/2016	8/1/2016	17:04	15:05	2531	23.88	0
	B2			16:58	14:01	2478	23.47	0
	B3			17:10	14:48	2510	23.66	0
	B4			16:50	14:28	2510	23.41	0

Table 5.3. Formulas for the four models tested: Half-normal (HN), hazard rate (HR), compound half-normal (CHN) and binary signal strength (BSS). Model formulas are presented as specified in the *secr* package (Efford, 2019), where d is range, σ is the shape parameter, z is the scale parameter, and b_0 and b_1 are functions related to the beta parameters representing intercept and slope, respectively, in the signal strength model presented by Efford *et al.* (2009b).

Detection Model	Formula
Half-normal	$g(0) * e^{\left(\frac{-d^2}{2\sigma^2}\right)}$
Hazard rate	$g(0) * \left(1 - e^{-\left(\frac{d}{\sigma}\right)^{-z}}\right)$
Compound half-normal	$g(0) * \left(1 - \left(1 - e^{-\left(\frac{d^2}{2\sigma^2}\right)}\right)^z\right)$
Binary signal strength	$1 - F(-(b_0 + b_1 * d))$

*for the BSS model, F is cumulative distribution function of the standard normal distribution

Table 5.4. Distances from the Seaglider and QUEphone to the 23 beaked whale locations. Whale locations are taken from Barlow *et al.* (2018) Table 1. The Clicks column indicates if clicks were recorded on the glider or QUEphone within 15 minutes of the location. Times when the glider or QUEphone were not recording are indicated by “OFF” or “Not Deployed” in the Clicks column.

Dive	Time [UTC]	Latitude	Longitude	Depth [m]	Seaglider		QUEphone	
					Clicks	Dist [km]	Clicks	Dist [km]
AI-1	7/22/2016 3:57	33.252	-118.62	1191	OFF	6.0	Yes	6.3
AI-2	7/22/2016 4:24	33.253	-118.61	952	-	5.6	Yes	5.7
AJ-5	7/22/2016 6:28	33.247	-118.64	810	-	8.0	-	7.4
AP-1	7/24/2016 6:16	33.27	-118.63	953	-	12.3	-	12.0
AP-1	7/24/2016 6:21	33.265	-118.63	854	-	12.0	-	11.6
AP-1	7/24/2016 6:23	33.264	-118.63	836	-	11.8	-	11.4
AR-1	7/24/2016 20:30	33.156	-118.56	1193	-	6.5	-	5.4
AS-1	7/24/2016 23:43	33.176	-118.57	734	-	6.9	-	3.5
AW-1	7/25/2016 7:54	33.204	-118.63	959	-	5.8	-	2.25
AW-1	7/25/2016 7:55	33.204	-118.63	925	-	5.9	-	2.3
AW-1	7/25/2016 8:10	33.216	-118.63	840	-	6.1	-	2.5
AY-1	7/25/2016 10:57	33.262	-118.67	1085	-	13.4	-	8.3
AY-1	7/25/2016 11:08	33.259	-118.67	1067	-	13.3	-	8.0
AY-1	7/25/2016 11:14	33.259	-118.67	1247	-	12.7	-	7.5
AY-1	7/25/2016 11:20	33.257	-118.68	693	-	13.6	-	8.1
BH-1	7/26/2016 9:19	33.226	-118.67	976	-	7.6	Not deployed	
BH-2	7/26/2016 9:39	33.225	-118.66	954	-	7.1	Not deployed	
BL-1	7/27/2016 8:11	33.255	-118.6	1169	-	3.6	-	5.9
BL-1	7/27/2016 8:19	33.254	-118.61	1244	OFF	3.5	-	6.0
BM-2	7/27/2016 11:11	33.275	-118.64	671	-	7.9	-	8.7
BM-3	7/27/2016 11:15	33.263	-118.63	1136	-	6.4	-	7.3
BS-1	7/29/2016 12:44	33.224	-118.65	1046	-	5.0	-	9.4
BS-1	7/29/2016 13:07	33.226	-118.65	933	-	4.3	-	9.1

Table 5.5. (on next page) Capture history for the four DASBRs used in the case study, when each dive was grouped as a session. Duration is the time between the first and last click-positive minute for that session. The number of click positive minutes is the sum the number of click positive minutes of all four DASBRs. The number of unique click positive minutes is the number of minutes with click detections on at least one DASBR. Capture frequency is how many unique minutes were detected on one to four of the DASBRs at once. For example, in Session 2 there were five unique click positive minutes, three of which were detected on a single DASBR, one of which was detected on two DASBRs, and one that was detected on three DASBRs, for a total of eight minutes with clicks (recaptures) across all DASBRs.

Table 5.5.

Session	Start Time (GMT)	End Time (GMT)	Duration (min)	No. click positive minutes	No. unique click positive minutes (n)	Capture Frequency			
						1	2	3	4
1	7/19/2016 13:52	7/19/2016 13:53	2	6	2	0	0	2	0
2	7/19/2016 15:19	7/19/2016 16:08	50	8	5	3	1	1	0
3	7/19/2016 17:16	7/19/2016 17:22	7	3	2	1	1	0	0
4	7/19/2016 19:41	7/19/2016 19:59	19	4	3	2	1	0	0
5	7/20/2016 1:24	7/20/2016 1:27	4	2	2	2	0	0	0
6	7/20/2016 8:42	7/20/2016 8:54	13	2	2	2	0	0	0
7	7/21/2016 16:20	7/21/2016 16:20	1	1	1	1	0	0	0
8	7/21/2016 23:49	7/22/2016 0:33	45	89	35	9	9	6	11
9	7/22/2016 2:19	7/22/2016 2:47	29	44	22	7	8	7	0
10	7/23/2016 0:23	7/23/2016 0:34	12	14	7	3	1	3	0
11	7/23/2016 3:51	7/23/2016 3:53	3	4	2	0	2	0	0
12	7/24/2016 2:09	7/24/2016 2:41	33	82	29	5	7	5	12
13	7/24/2016 16:28	7/24/2016 16:48	21	28	15	8	4	0	3
14	7/24/2016 19:06	7/24/2016 19:45	40	34	18	8	4	6	0
15	7/25/2016 0:10	7/25/2016 0:11	2	2	2	2	0	0	0
16	7/25/2016 1:14	7/25/2016 1:17	4	5	4	3	1	0	0
17	7/25/2016 2:14	7/25/2016 2:25	12	8	5	3	1	1	0
18	7/25/2016 3:50	7/25/2016 4:10	21	19	9	3	2	4	0
19	7/25/2016 5:10	7/25/2016 5:18	9	12	6	1	4	1	0
20	7/25/2016 6:53	7/25/2016 7:30	38	75	27	5	7	4	11
21	7/26/2016 5:18	7/26/2016 6:00	43	109	39	5	11	10	13
22	7/27/2016 0:35	7/27/2016 0:47	13	4	2	0	2	0	0
23	7/27/2016 4:10	7/27/2016 4:19	10	32	9	0	1	2	6
24	7/27/2016 7:06	7/27/2016 7:15	10	20	7	1	2	1	3
25	7/29/2016 8:41	7/29/2016 9:12	32	37	20	10	4	5	1
ALL				644	275	84	73	58	60

Table 5.6. Model results for the by-dive sessions model fit. A single parameter estimate is given for each model, pooling all sessions. Density of click-positive minutes per session, effective survey area, and pseudo effective detection radius are means across all drifts; coefficient of variation (CV) was estimated using a jackknife procedure.

Model	ΔAIC	Parameter			Density per session (per km ²)		Effective survey area (km ²)		Pseudo effective detection radius (m)	
		estimate	CV		mean	CV	mean	CV	mean	CV
BSS	0.00	b_0	4.8730	0.21	0.3630	0.3710	30.57	0.25	2370.7	0.15
		b_1	-0.002107	0.19						
CHN	1.98	$\hat{g}(0)$	1.00	0.05	0.3610	0.3860	30.76	0.28	2375.1	0.17
		$\hat{\sigma}$	950.07	0.14						
		\hat{z}	15.36	2.67						
HR	2.77	$\hat{g}(0)$	0.9706	0.04	0.3540	0.3880	31.33	0.27	2398.3	0.17
		$\hat{\sigma}$	2217.17	0.22						
		\hat{z}	8.62	0.45						
HN	49.02	$\hat{g}(0)$	1.00	0.00	0.0540	0.2600	204.23	0.07	5904.6	0.06
		$\hat{\sigma}$	4841.83	0.12						

Table 5.7. Model results for the by-minute sessions model fit. A single parameter estimate is given for each model, pooling all sessions. Density of click-positive minutes per session, effective survey area, and pseudo effective detection radius are means across all drifts; coefficient of variation (CV) was estimated using a jackknife procedure.

Model	ΔAIC	Parameter			Density per session (per km ²)		Effective survey area (km ²)		Pseudo effective detection radius (m)	
		estimate	CV	mean	CV	mean	CV	mean	CV	
BSS	0.00	b_0	4.8720	0.21	0.0328	0.27	30.71	0.26	2371.7	0.16
		b_1	-0.002099	0.20						
CHN	1.96	$\hat{g}(0)$	1.00	0.05	0.0327	0.29	30.90	0.29	2376.1	0.17
		$\hat{\sigma}$	951.09	0.15						
		\hat{z}	15.07	2.54						
HR	2.87	$\hat{g}(0)$	0.9715	0.04	0.0321	0.29	31.46	0.29	2398.2	0.17
		$\hat{\sigma}$	2215.18	0.22						
		\hat{z}	8.58	0.45						
HN	49.26	$\hat{g}(0)$	1.00	0.00	0.0049	0.07	204.47	0.07	5904.2	0.06
		$\hat{\sigma}$	4841.20	0.11						

Table 5.8. Density estimator inputs and density of Cuvier's beaked whales estimated for the three top detection function models: binary signal strength (BSS), compound half normal (CHN) and hazard rate (HR). Coefficient of variation (CV) was calculated empirically using a jackknife approach.

Model	Proportion of snapshots with clicks, n/k		Effective survey area, \hat{a}_e (km ²)		Group size, \hat{s}		Probability a group is echolocating, \hat{P}_e		Density, \hat{D} (per 1000 km ²)	
	mean	CV	mean	CV	mean	CV	mean	CV	mean	CV
BSS			30.71	0.26					5.48	0.46
CHN	0.0185	0.37	30.90	0.29	1.9	0.07	0.209	0.04	5.44	0.47
HR			31.46	0.29					5.35	0.48

Table 5.9. Simulation results for the compound half normal simulations. The first three simulations differed by the input sensor configurations and thus the input effective survey area, \hat{a}_e . The last simulation used the actual sensor locations of the case study, but an increased simulated density, \hat{D}_c , of 5 objects per km². Bias is the percent difference between the input simulation value and the median of all simulation runs.

Simulation	Params	Inputs	Mean	SD	Median	IQR	Bias %
Actual sensor configuration *4 warnings	$\hat{g}(0)$	1	0.9871	0.0209	1.00	0.0201	1.56E-05
	$\hat{\sigma}$	957	930.72	121.36	933.80	156.08	2.42
	\hat{z}	11.26	36.50	87.59	13.91	10.91	23.49
	\hat{D}_c	0.36	0.3561	0.0502	0.3494	0.0789	2.96
	\hat{D}_c SE	-	0.1190	0.0139	0.1179	0.0196	-
	\hat{a}	30.39	31.12	4.00	30.72	6.27	1.07
Stationary sensor configuration *2 warnings	$\hat{g}(0)$	1	0.9852	0.0225	1.00	0.0247	1.83E-05
	$\hat{\sigma}$	957	921.66	131.75	931.93	169.78	2.62
	\hat{z}	11.26	33.72	80.61	12.87	15.36	14.34
	\hat{D}_c	0.36	0.3694	0.0602	0.3684	0.0709	2.32
	\hat{D}_c SE	-	0.1228	0.0171	0.1226	0.0201	-
	\hat{a}	30.39	30.21	4.78	29.41	6.21	2.72
Sensors plus 500 m *16 warnings	$\hat{g}(0)$	1	0.9871	0.0217	1.00	0.0225	3.79E-06
	$\hat{\sigma}$	957	877.42	160.96	905.39	138.71	5.39
	\hat{z}	11.26	6.2450E08	5.7235E09	14.87	23.52	32.10
	\hat{D}_c	0.36	0.3638	0.0272	0.3645	0.0366	1.26
	\hat{D}_c SE	-	0.0978	0.0057	0.0983	0.0076	-
	\hat{a}	40.35	40.05	2.46	39.86	3.32	1.21
Sensors plus 1000 m *46 warnings	$\hat{g}(0)$	1	0.9709	0.0509	1.00	0.0523	8.67E-07
	$\hat{\sigma}$	957	851.90	183.53	862.58	254.77	9.87
	\hat{z}	11.26	8.2523E04	5.4383E05	22.79	67.83	102.40
	\hat{D}_c	0.36	0.3642	0.0232	0.3643	0.0347	1.20
	\hat{D}_c SE	-	0.0845	0.0040	0.0838	0.0052	-
	\hat{a}	52.17	51.88	1.80	52.11	2.75	0.1098
Larger Density *8 warnings	$\hat{g}(0)$	1	0.9952	0.007635	1.00	0.007865	5.89E-06
	$\hat{\sigma}$	957	944.75	33.16	945.50	49.07	1.20
	\hat{z}	11.26	12.88	2.76	11.95	2.35	6.12
	\hat{D}_c	5	5.00	0.2296	4.95	0.3161	1.02
	\hat{D}_c SE	-	0.4488	0.0175	0.4447	0.0228	-
	\hat{a}	30.39	30.43	1.25	30.60	1.93	0.6952

Figures

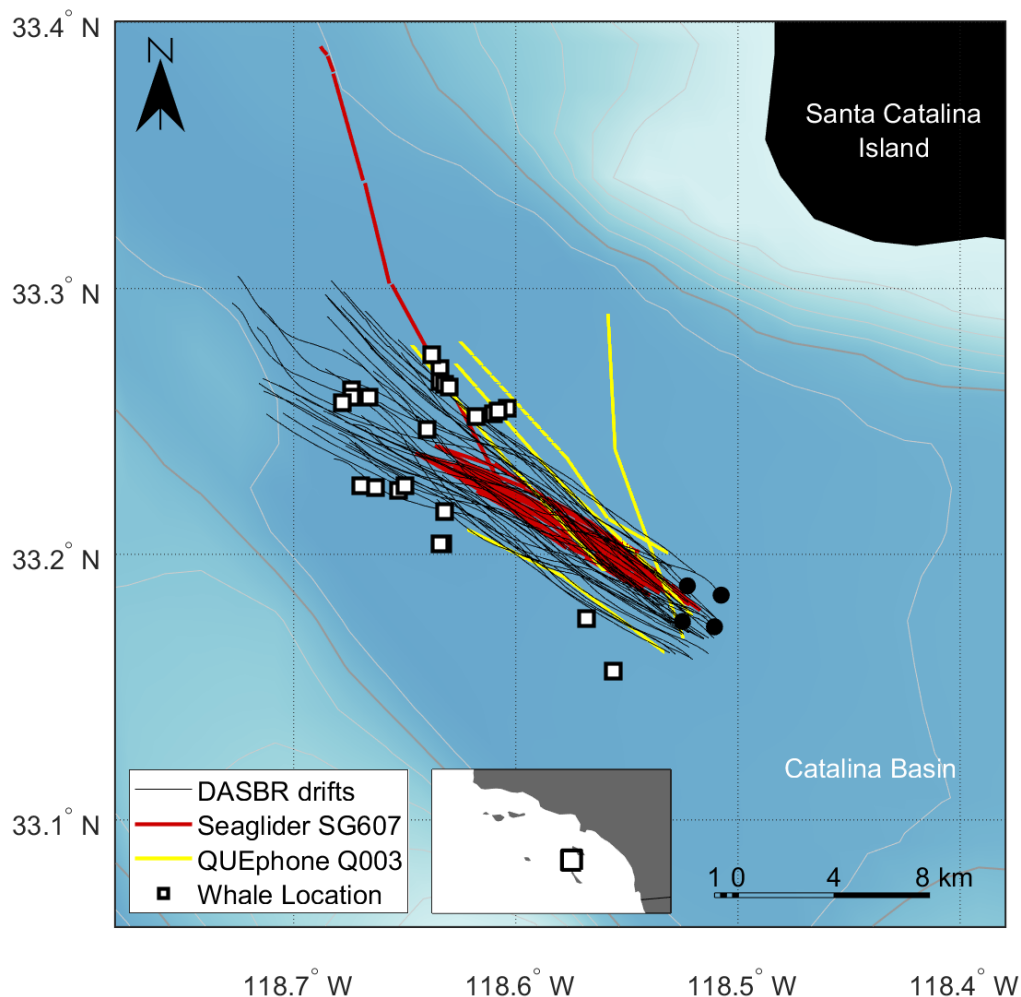


Figure 5.1. Map of platform survey tracks and known whale locations. The Seaglider track is shown in red. It transited back and forth in the center of the basin, then traveled to the north for recovery closer to Catalina Island. The QUEphone drifts are shown in yellow. Each drift started at the southeast part of the basin and drifted to the north – northwest. The DASBR tracks are shown as thin black lines. The starting position of the DASBRs for Drift 12 are shown as black circles to illustrate the typical DASBR starting configuration. Known whale locations, as localized by the DASBRs are indicated by the white squares with black outlines. Contour lines are shown in light gray from 200 to 1200 m, with the 1000 m contour as the thicker line.

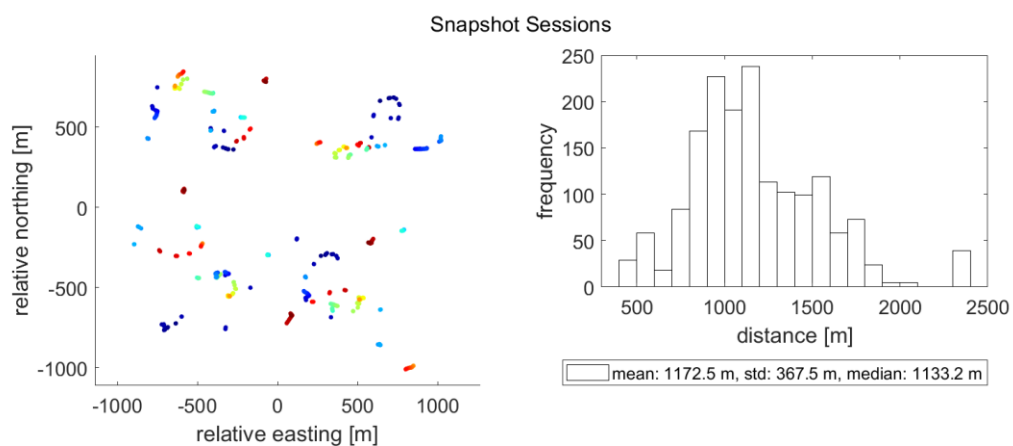


Figure 5.2. Relative sensor locations and pairwise distances between the four DASBRs for the by-snapshot ($n = 275$) sessions (six distances calculated per snapshot). Color of dots corresponds to session number (1 to 275 = blue to red).

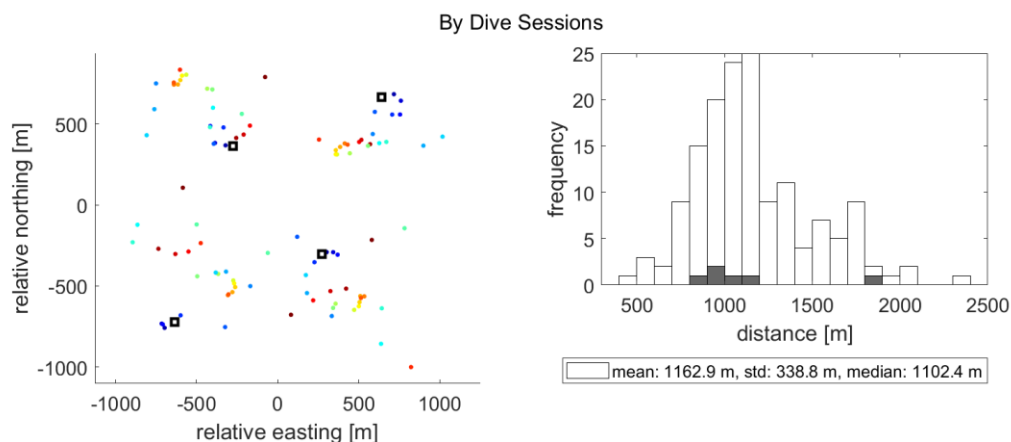


Figure 5.3. Relative sensor locations and pairwise distances between the four DASBRs for each of the 25 by dive sessions (six distances calculated per session). Color of dots corresponds to session number (1 to 25 = blue to red). The first session, which was used as the simulated stationary array is shown in the left plot as black-outlined squares, and the distances are shown in gray in the histogram.

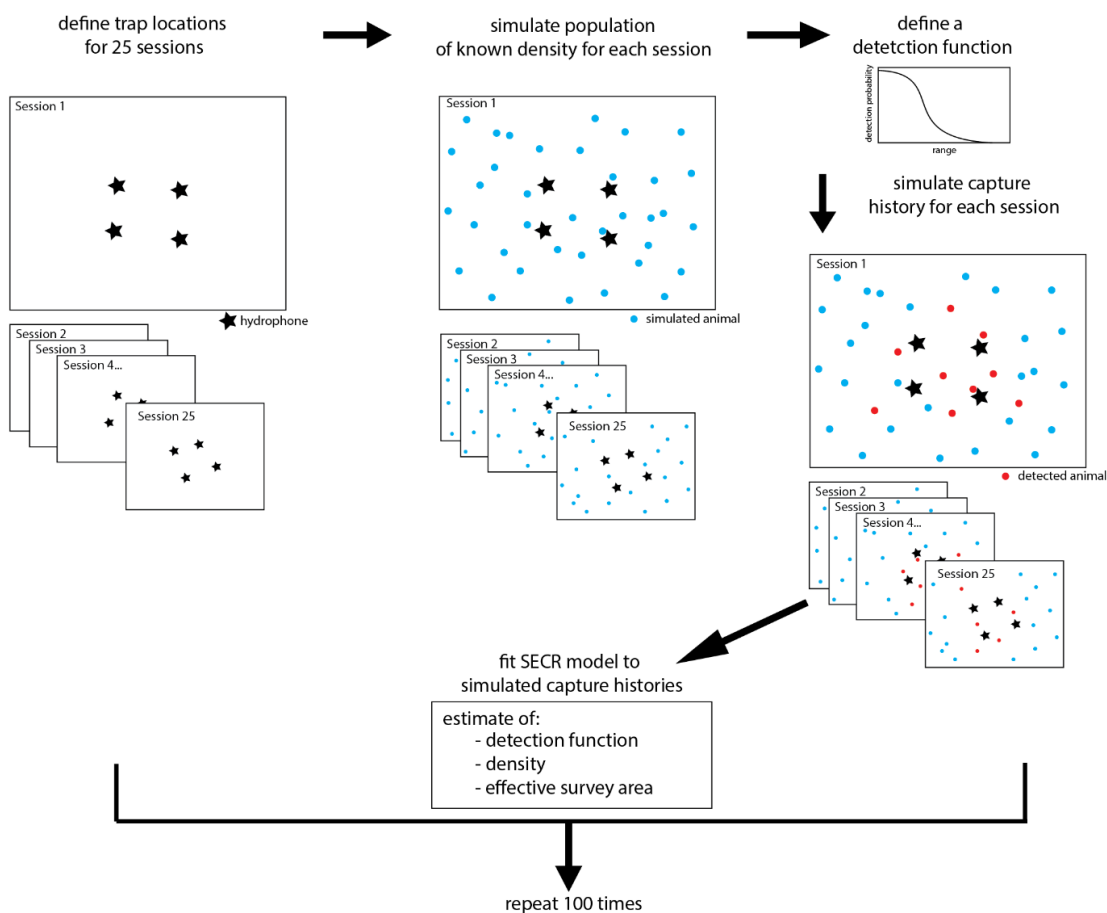


Figure 5.4. Diagram of simulation workflow. For each simulation run, trap locations are defined for 25 sessions. Then a population of detectable “objects,” with an input density, is simulated randomly over the defined survey area; a separate population is simulated for each of the 25 sessions. Next, a detection function is defined by choosing a model, here compound half normal, and specifying a detection probability at zero distance, $g(0)$, and the shape and scale parameters, σ and z . A capture history is simulated for each session from the simulated population and input detection function. Finally, a detection function model with unknown parameter estimates is fit to the simulated capture histories. An estimate of the detection function, density, and effective survey area is generated. This process was repeated 100 times for each set of input parameters.

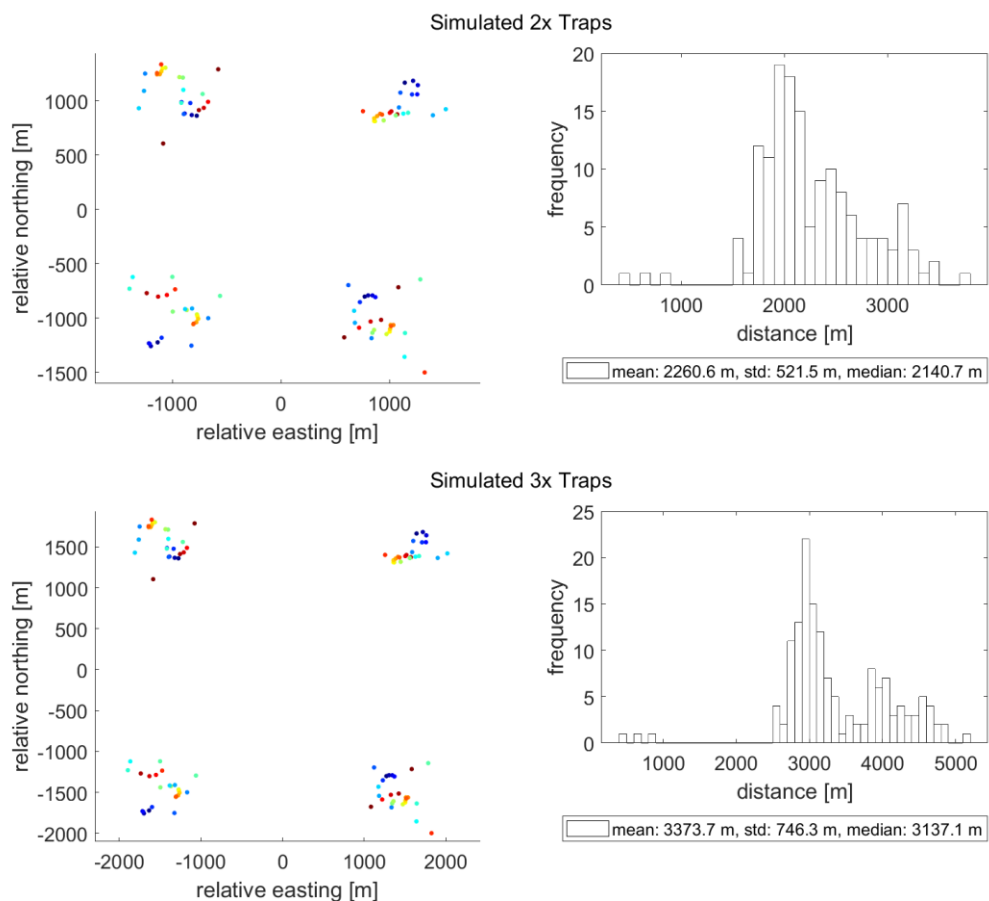


Figure 5.5. Relative sensor locations and pairwise distances between the four DASBRs for the simulations looking at increased sensor spacings. The top plots show the sensor locations and pairwise distances when 500 m was added to the easting and northing values. The bottom plots show the sensor locations and pairwise distances when 1000 m was added. Color of dots corresponds to session number (1 to 25 = blue to red).

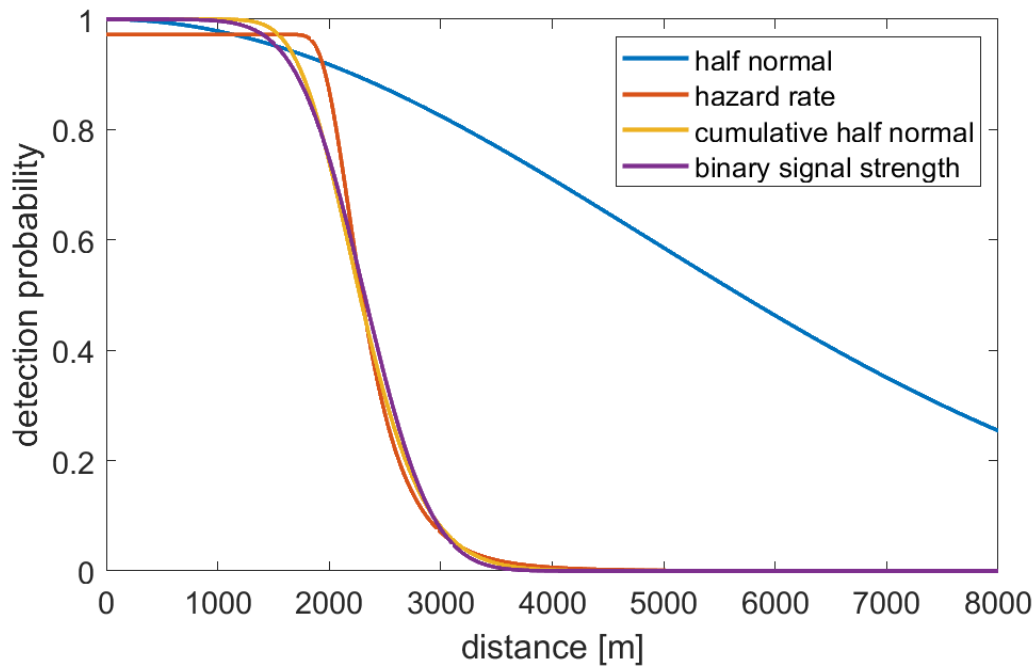


Figure 5.6. Detection probabilities as calculated using SECR with by-snapshot sessions. By-dive session results are not shown because of similarity to by-snapshot results.

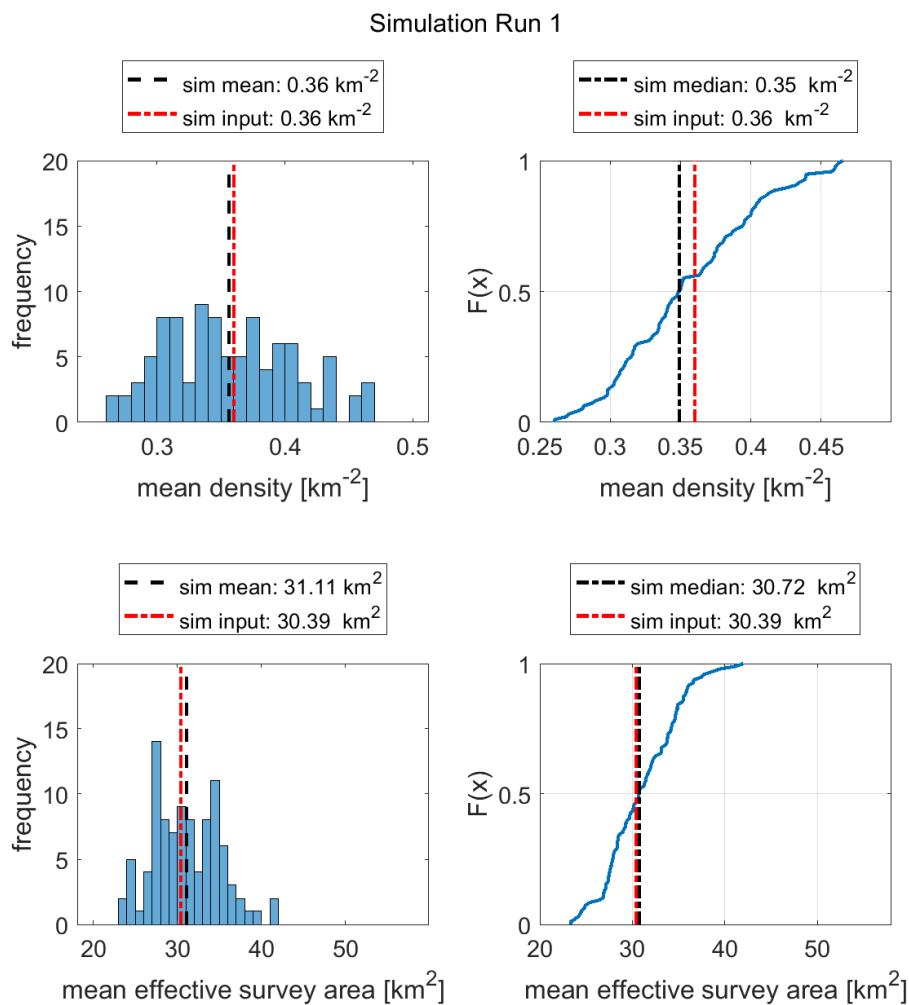


Figure 5.7. Histograms and empirical cumulative distribution functions of the case study simulation results for density (top) and effective survey area (bottom) for 100 simulations where the case study detection function parameters and true case study sensor locations were used as simulated inputs. The histograms (left) show the distribution of simulation estimates. The mean for all 100 simulations is shown as the black dashed line. The empirical cumulative distribution plots (right) show the proportion of simulation estimates (y-axis) that were at or below a given estimate for density or effective survey area. The median is shown as the black dashed line. A steeper slope indicates less variability across simulation estimates. In all plots, the red dot-dash line indicates the simulation input value.

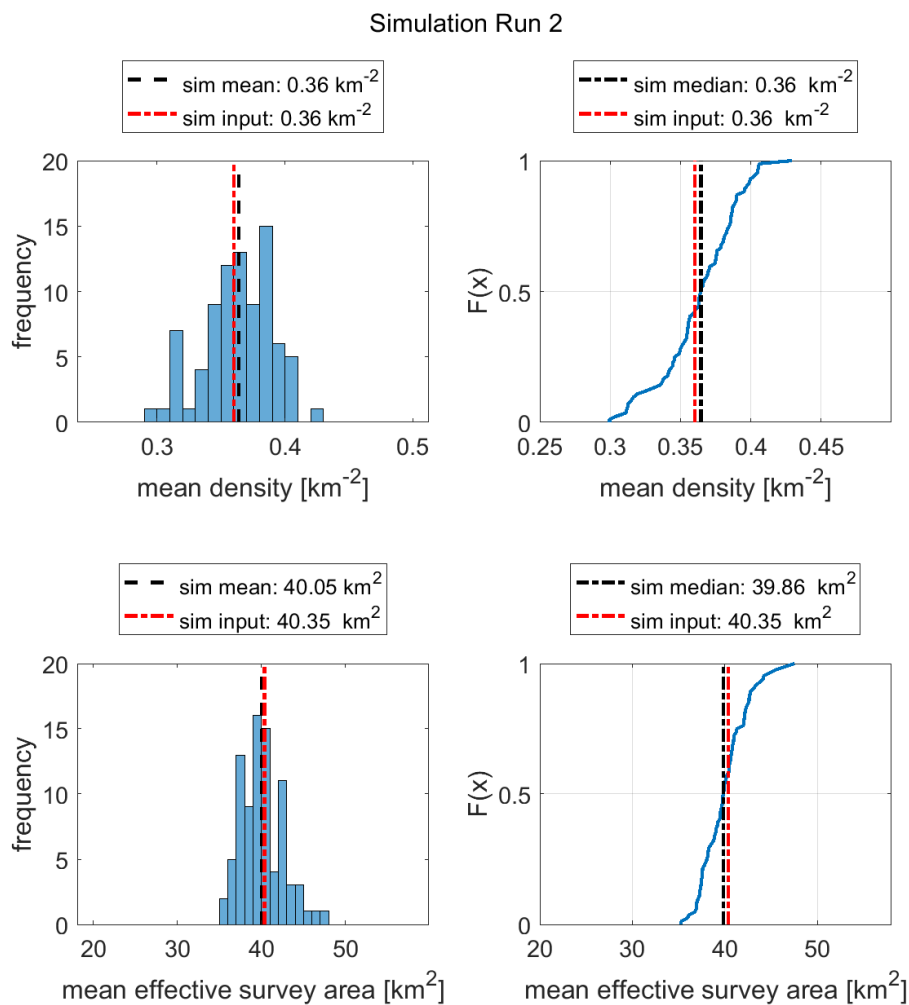


Figure 5.8. Histograms and empirical cumulative distribution functions of the 500 m-expanded sensor spacing simulation results for density (top) and effective survey area (bottom) for 100 simulations. See Figure 5.7 caption for detailed plot descriptions.

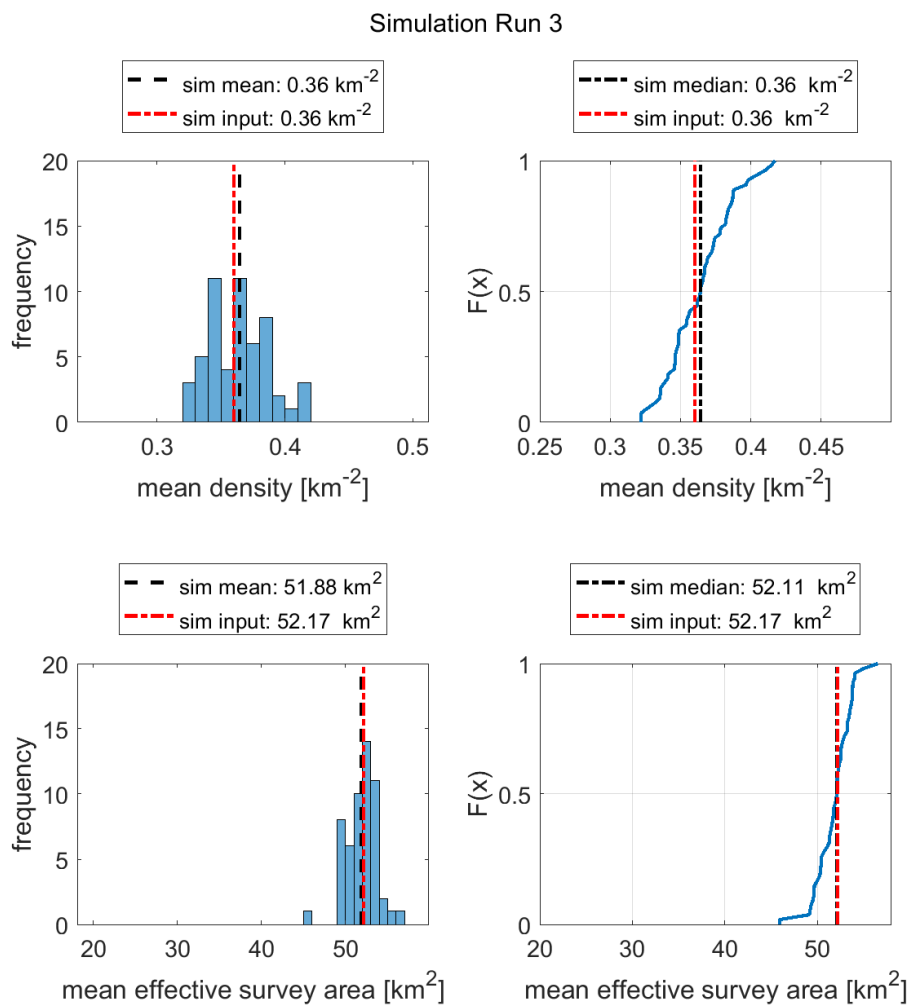


Figure 5.9. Histograms and empirical cumulative distribution functions of the 1000 m expanded sensor spacing simulation results for density (top) and effective survey area (bottom) for 100 simulations. See Figure 5.7 caption for detailed plot descriptions.

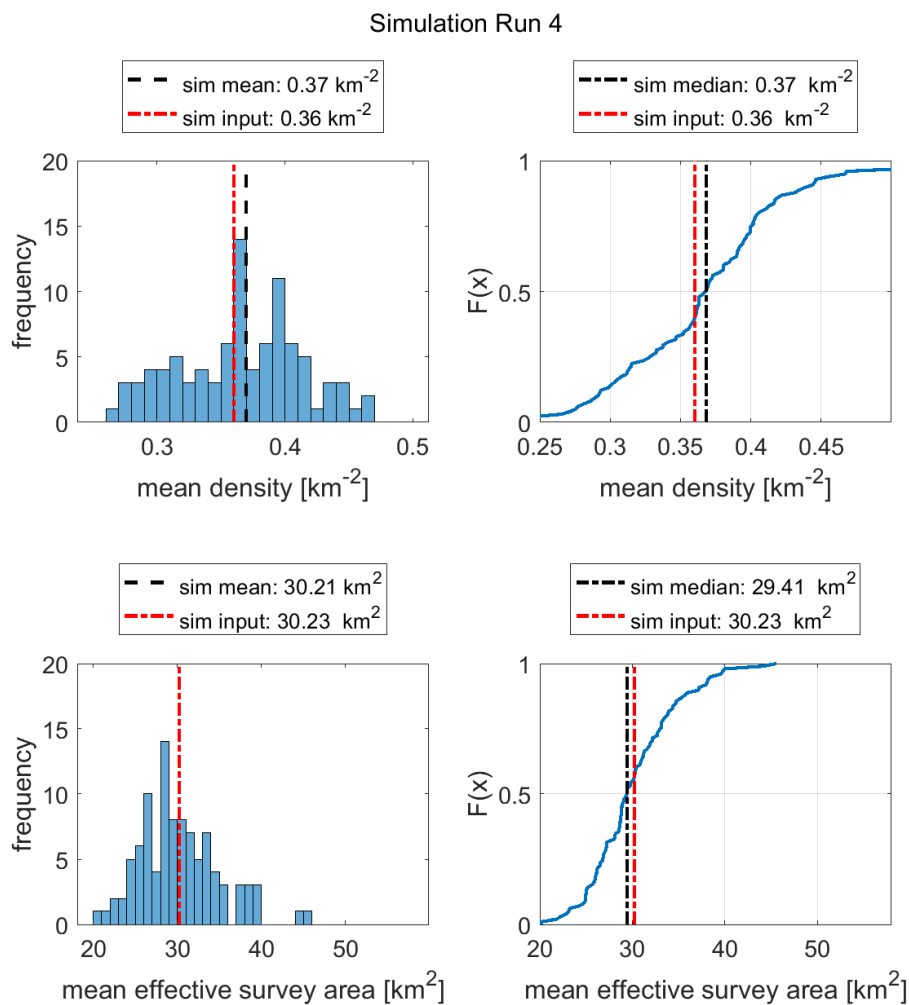


Figure 5.10. Histograms and empirical cumulative distribution functions of the stationary sensor spacing simulation results for density (top) and effective survey area (bottom) for 100 simulations. See Figure 5.7 caption for detailed plot descriptions.

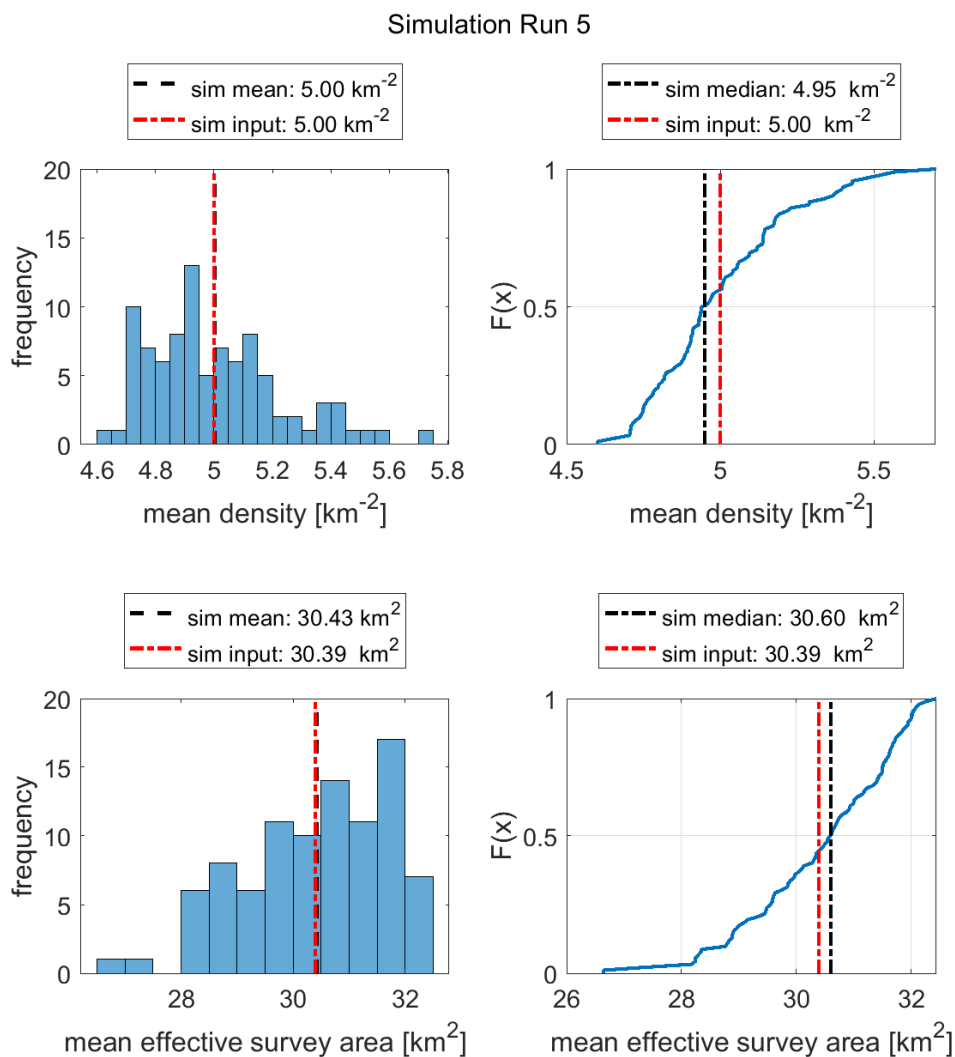


Figure 5.11. Histograms and empirical cumulative distribution functions of the increased sample size simulation results for density (top) and effective survey area (bottom) for 100 simulations. See Figure 5.7 caption for detailed plot descriptions.

CHAPTER 6: GENERAL CONCLUSIONS AND FUTURE DIRECTIONS

Contribution to the field

There is a constant effort to develop effective, efficient methods to survey wildlife populations. For aquatic species like marine mammals, this is no easy task. Passive acoustic monitoring is a key tool for marine mammal science and an exciting area of growth is the development and use of autonomous mobile platforms for acoustic monitoring, particularly underwater gliders. These platforms have allowed us to survey in regions and during seasons where little research had been conducted previously. Glider use is becoming more widespread, and meetings of the Acoustical Society of America now often have dedicated sessions for such technologies. Over the course of my PhD program, many lab groups have shown the efficacy of using underwater gliders for marine mammal research, and they are a promising frontier for passive acoustic monitoring (*e.g.*, Baumgartner *et al.*, 2013; Burnham *et al.*, 2019; Matsumoto *et al.*, 2015; Nieukirk *et al.*, 2016; Silva *et al.*, 2019).

However, when I began this dissertation there were no studies comparing these new technologies to traditional vessel-based and bottom-moored acoustic methodologies. Further, applications of density estimation techniques to glider-collected data were just beginning to be explored. Gkikopoulou (2018) has since assessed the effect of recorder depth on the detection function of Blainville's beaked whales and proposed a density estimation equation for Blainville's beaked whales recorded by a glider, through a simulation approach. An empirical detection function has been estimated from glider-recorded data for Blainville's beaked whales (Harris *et al.*, 2017; Thomas *et al.*, 2019) and for North Atlantic right whales (Johnson *et al.*, 2018, 2019) using trial-based approaches with whales localized using auxiliary hydrophone arrays. Küsel *et al.* (2017) demonstrated that a glider instrumented with two hydrophones can provide range estimates to detected sperm whales. Additionally, Harris *et al.* (in revision) provides an assessment of a slow-moving glider's ability to satisfy the distance sampling assumptions. This dissertation builds on these previous efforts and provides two key advances in our understanding of mobile autonomous platforms for marine mammal passive acoustic monitoring: direct comparisons to stationary recorders, which can be used to inform best practices for

choosing a recording platform for a particular survey, and two examples of detection function estimation and density estimation for mobile recorders.

First, this work addresses how slow-moving autonomous systems compare to stationary recorders (Chapters 2 and 4). I report the first quantitative comparisons of a glider and float to two types of stationary deep-water recorders, for four marine mammal species. These comparisons can be used to make recommendations for the ideal platform to be used in any particular survey. Choosing a recorder type typically requires a tradeoff between the quantity and quality of data collected and the instrument cost. Gliders can cover more area but are more expensive than stationary autonomous recorders and cannot be deployed for as long. For low-frequency vocalizing species including most species of baleen whales, the spatial advantages of mobile instruments may not be a significant advantage. In Chapter 2, I demonstrate that, for a glider that moves through the water, even at relatively slow speeds, flow noise may be introduced that masks these low-frequency call types and may be a disadvantage, or at least an important consideration, for data interpretation. For those low-frequency, omni-directional calls that can propagate tens of kilometers, a stationary recorder provides generally good spatial coverage at a low cost and is likely the preferred survey platform. For higher-frequency species, particularly beaked whales, gliders may provide a distinct advantage through their spatial movement, as demonstrated in Chapter 4. Beaked whales can be detected over only a few kilometers; their highly directional and high-frequency echolocation clicks attenuate much more rapidly underwater than the baleen whale calls. Therefore, if information about where animals occur is the question of interest, having a sensor that can cover a large area is quite important and likely worth the additional cost. Additionally, the cost of a glider is still considerably less than a vessel-based survey and can cover areas in seasons that may not be accessible by ship. For species like beaked whales, I envision ideal monitoring occurring through exploratory glider surveys to identify new and important habitat, combined with long-term stationary recorders in these hot-spots to monitor population trends over time.

Secondly, this dissertation tackled two new density estimation applications: from a single-hydrophone glider detecting fin whales (Chapter 3), and an array of surface drifters for Cuvier's beaked whales (Chapter 5). While it may seem like there is a variety of density

estimation methods for acoustic data and marine mammal research, these methods often must be tailored to a specific study species, region, and recording platform. Slow-moving platforms are no different, and in fact introduce a number of additional concerns and methods assumption violations. My PhD was part of a larger project, “AFFOGATO: A framework for cetacean density estimation using slow-moving autonomous ocean vehicles.” This project was one of the first to specifically explore the special considerations of novel mobile platforms and address a few of them, while developing a framework for what is necessary to push this research area forward. Chapter 3 of this dissertation provides an empirical estimate of detection probability for fin whales recorded by a glider and provides a framework for estimating fin whale density. The detection function estimated in this work could be applied to future glider surveys conducted in the same region (Southern California) and time (winter) to potentially estimate density over larger temporal and spatial scales. The work also demonstrated that simultaneous deployment of a glider within a stationary array could be used to set up a trial-based approach to estimate a detection function for baleen whales recorded on a glider. Chapter 5 provides a case study of the application of spatially explicit capture-recapture methods for a marine mammal using a moving acoustic array, which is a relatively novel approach to marine mammal density estimation. While the original goal of using such a method to estimate probability of Cuvier’s beaked whales from a glider was not possible, the method, and its subsequent comparison to other methods, demonstrates the feasibility of such an approach and is encouraging for future efforts.

Aside from the work presented in this dissertation, I had the opportunity to become a trained Seaglider pilot and pilot 13 gliders on 11 different occasions. These deployments were for my dissertation work in 2015 and 2016, and then as a Graduate Research Assistant on projects conducting monitoring work in the Gulf of Mexico and Southern California. While piloting, but also working on the analysis and interpretation of glider data, I was able to partially bridge the gap between equipment development and operation and biology, ecology, and management. I was able to learn from the issues I discovered from the early deployments that went into my dissertation (like flow noise occurring at a particular speed) and work to improve those issues during following deployments. I think there is often a

lack of understanding of the goals and priorities between engineers designing these systems and the biologist end users. My hope is that I can stay involved in both of these aspects in my future career and can work to keep these communication lines open and most helpful for all scientists involved.

Future directions

This dissertation is just one step towards understanding and applying density estimation methods to glider-collected data. I would like to focus future efforts in two primary areas: (1) estimating detection probability for Cuvier's beaked whales on a glider and (2) estimating animal density (likely fin whales) from an extended glider survey in Southern California.

I believe estimating detection probability for beaked whales on a glider is possible empirically and could be done either with existing data or with another field effort. The discussion of Chapter 5 covers in detail how the experiment conducted in summer 2016 could be improved for a more promising result. Alternatively, the winter 2015-2016 dataset used in Chapters 2 and 3 for fin whales also contains beaked whale clicks. I would like to explore an SECR application to those bottom-moored hydrophones, adding the glider as an additional sensor. The spacing of the hydrophones at SCORE does not allow for reliable tracking of beaked whales; the hydrophones are too widely spaced so the same click is not detected on 3 or more hydrophones very often. However, within a 1-minute snapshot, multiple hydrophones near one another did detect beaked whales and it is likely safe to assume that these were a single group of animals. After the promising results of SECR applied to the DASBR data in Chapter 5, I would be interested in applying that method to the SCORE dataset.

The fin whale density estimate and detection function estimated in this dissertation are from a short 90-hour dataset. I would like to apply the estimated detection function and snapshot-based approach to estimate fin whale density for a longer-duration glider deployment. A potential candidate deployment for such an effort is a recent deployment in Southern California in February and March 2020. The Seaglider used in that survey was

instrumented with a different acoustic recording system, so estimates may require recalibration, but that is an interesting direction worth pursuing.

DISSERTATION REFERENCES

- Amante, C., and Eakins, B. W. (2009). "ETOPO1 1 Arc-Minute Global Relief Model: Procedures, Data Sources and Analysis," NOAA Technical Memorandum NESDIS NGDC-24.
- Au, W. W. L. (1993). *The Sonar of Dolphins* (Springer, New York, NY).
- Barlow, J. (1995). "The abundance of cetaceans in California waters. Part I: Ship surveys in summer and fall 1991," *Fish. Bull.* **93**, 1–14.
- Barlow, J. (2016). "Cetacean abundance in the California Current estimated from ship-based line transect surveys in 1991-2014," NOAA Administrative Report LJ-16-01
- Barlow, J., Ferguson, M., Perrin, W., Gerrodette, T., Joyce, G., Macleod, C., Mullin, K., Palka, D., and Waring, G. (2006). "Abundance and densities of beaked and bottlenose whales (family Ziphiidae)," *J. Cetacean Res. Manag.* **7**, 263–270.
- Barlow, J., and Forney, K. A. (2007). "Abundance and population density of cetaceans in the California Current ecosystem," *Fish. Bull.* **105**, 509–526.
- Barlow, J., Fregosi, S., Thomas, L., Harris, D. V., and Griffiths, E. T. (in prep). "Acoustic detection range and population density of Cuvier's beaked whales estimated from near-surface hydrophones," Manuscript in preparation.
- Barlow, J., and Gisiner, R. (2006). "Mitigating, monitoring and assessing the effects of anthropogenic sound on beaked whales," *J. Cetacean Res. Manag.* **7**, 239–249.
- Barlow, J., and Griffiths, E. T. (2017). "Precision and bias in estimating detection distances for beaked whale echolocation clicks using a two-element vertical hydrophone array," *J. Acoust. Soc. Am.* **141**, 4388–4397.
- Barlow, J., Griffiths, E. T., Klinck, H., and Harris, D. V (2018). "Diving behavior of Cuvier's beaked whales inferred from three-dimensional acoustic localization and tracking using a nested array of drifting hydrophone recorders," *J. Acoust. Soc. Am.* **144**, 2030–2041.
- Barlow, J., Rankin, S., and Dawson, S. (2008). "A guide to constructing hydrophones and hydrophone arrays for monitoring marine mammal vocalizations," NOAA Technical Memorandum NOAA-TM-NMFS-SWFSC-417, available from NOAA Southwest Fisheries Science Center, La Jolla, CA.
- Barlow, J., Schorr, G. S., Falcone, E. A., and Moretti, D. J. (2020). "Variation in dive behavior of Cuvier's beaked whales with seafloor depth, time-of-day, and lunar illumination," *Mar. Ecol. Prog. Ser.* Article in press.
- Barlow, J., and Taylor, B. L. (2005). "Estimates of sperm whale abundance in the northeastern temperate Pacific from a combined acoustic and visual survey," *Mar. Mammal Sci.* **21**, 429–445.
- Barlow, J., Tyack, P. L., Johnson, M. P., Baird, R. W., Schorr, G. S., Andrews, R. D., and Aguilar de Soto, N. (2013). "Trackline and point detection probabilities for acoustic surveys of Cuvier's and Blainville's beaked whales," *J. Acoust. Soc. Am.* **134**, 2486–2496.
- Barnes, C. R., Best, M. M. R., Bornhold, B. D., Juniper, S. K., Pirenne, B., and Phibbs, P. (2007). "The NEPTUNE Project - a cabled ocean observatory in the NE Pacific: Overview, challenges and scientific objectives for the installation and operation of Stage I in Canadian waters," in *2007 Symposium on Underwater Technology and*

- Workshop on Scientific Use of Submarine Cables and Related Technologies*, IEEE, pp. 308–313.
- Baumann-Pickering, S., McDonald, M. A., Simonis, A. E., Solsona Berga, A., Merkens, K. P. B., Oleson, E. M., Roch, M. A., Wiggins, S. M., Rankin, S., Yack, T. M., and Hildebrand, J. A. (2013). “Species-specific beaked whale echolocation signals,” *J. Acoust. Soc. Am.* **134**, 2293–2301.
- Baumann-Pickering, S., Rice, A. C., Trickey, J. S., Hildebrand, J. A., Wiggins, S. M., and Širović, A. (2018). “Five years of whale presence in the SOCAL Range Complex 2013-2017,” *Marine Physical Laboratory Technical Memorandum 626* (La Jolla, CA: Scripps Institution of Oceanography University of California San Diego), p. 22, July 2018.
- Baumann-Pickering, S., Roch, M. A., Brownell Jr, R. L., Simonis, A. E., McDonald, M. A., Solsona Berga, A., Oleson, E. M., Wiggins, S. M., and Hildebrand, J. A. (2014). “Spatio-temporal patterns of beaked whale echolocation signals in the North Pacific.,” *PLoS One* **9**, e86072.
- Baumgartner, M. F., and Fratantoni, D. M. (2008). “Diel periodicity in both sei whale vocalization rates and the vertical migration of their copepod prey observed from ocean gliders,” *Limnol. Oceanogr.* **53**, 2197–2209.
- Baumgartner, M. F., Fratantoni, D. M., Hurst, T. P., Brown, M. W., Cole, T. V. N., Van Parijs, S. M., and Johnson, M. P. (2013). “Real-time reporting of baleen whale passive acoustic detections from ocean gliders,” *J. Acoust. Soc. Am.* **134**, 1814–1823.
- Baumgartner, M. F., Stafford, K. M., and Latha, G. (2018). “Near real-time underwater passive acoustic monitoring of natural and anthropogenic sounds,” in *Observing the Oceans in Real Time*, edited by R. Vankatesan, A. Tandon, E. D’Asaro, and M. A. Atmanand (Springer, Berlin), pp. 203–226.
- Baumgartner, M. F., Stafford, K. M., Winsor, P., Statscewich, H., and Fratantoni, D. M. (2014). “Glider-based passive acoustic monitoring in the arctic,” *Mar. Technology Soc. J.* **48**, 40–51.
- Bittencourt, L., Soares-Filho, W., de Lima, I. M. S., Pai, S., Lailson-Brito, J., Barreira, L. M., Azevedo, A. F., and Guerra, L. A. A. (2018). “Mapping cetacean sounds using a passive acoustic monitoring system towed by an autonomous Wave Glider in the Southwestern Atlantic Ocean,” *Deep. Res. Part I Oceanogr. Res. Pap.* **142**, 58–68.
- Borchers, D. (2012). “A non-technical overview of spatially explicit capture-recapture models,” *J. Ornithol.* **152**, 435–444.
- Borchers, D. L., and Efford, M. G. (2008). “Spatially explicit maximum likelihood methods for capture-recapture studies,” *Biometrics* **64**, 377–385.
- Borchers, D. L., and Marques, T. A. (2017). “From distance sampling to spatial capture–recapture,” *Adv. Stat. Anal.* **101**, 475–494.
- Branstetter, B. K., Moore, P. W., Finneran, J. J., Tormey, M. N., and Aihara, H. (2012). “Directional properties of bottlenose dolphin (*Tursiops truncatus*) clicks, burst-pulse, and whistle sounds,” *J. Acoust. Soc. Am.* **131**, 1613–1621.
- Bray, N. A., Keyes, A., and Morawitz, W. M. L. (2002). “The California Current system in the Southern California Bight and the Santa Barbara Channel,” *J. Geophys. Res. Ocean.* **104**, 7695–7714.
- Buckland, S. T. (2006). “Point-transect surveys for songbirds: Robust methodologies,”

- Auk **123**, 345.
- Buckland, S. T., Anderson, D. R., Burnham, K. P., Laake, J. L., Borchers, D. L., and Thomas, L. (2001). *Introduction to distance sampling* (Oxford University Press, Oxford).
- Buckland, S. T., Rexstad, E. A., Marques, T. A., and Oedekoven, C. S. (2015). *Distance Sampling: Methods and Applications* Methods in Statistical Ecology, (Springer International Publishing, Cham).
- Burgess, W. C., Tyack, P. L., Le Boeuf, B. J., and Costa, D. P. (1998). "A programmable acoustic recording tag and first results from free-ranging northern elephant seals," *Deep. Res. Part II Top. Stud. Oceanogr.* **45**, 1327–1351.
- Burnham, R. E., Duffus, D. A., and Mouy, X. (2019). "The presence of large whale species in Clayoquot Sound and its offshore waters," *Cont. Shelf Res.* **177**, 15–23.
- Campbell, G. S., Thomas, L., Whitaker, K., Douglas, A. B., Calambokidis, J., and Hildebrand, J. A. (2015). "Inter-annual and seasonal trends in cetacean distribution, density and abundance off southern California," *Deep. Res. Part II Top. Stud. Oceanogr.* **112**, 143–157.
- Cato, D. H. (1998). "Simple methods of estimating source levels and locations of marine animal sounds," *J. Acoust. Soc. Am.* **104**, 1667–1678.
- Cauchy, P., Heywood, K. J., Merchant, N. D., Queste, B. Y., and Testor, P. (2018). "Wind speed measured from underwater gliders using passive acoustics," *J. Atmos. Ocean. Technol.* **35**, 2305–2321.
- Cholewiak, D., DeAngelis, A. I., Palka, D., Corkeron, P. J., and Van Parijs, S. M. (2017). "Beaked whales demonstrate a marked acoustic response to the use of shipboard echosounders," *R. Soc. Open Sci.* **4**, 170940.
- Croll, D. A., Clark, C. W., Acevedo, A., Tershy, B., Flores, S., Gedamke, J., Urban, J., and Suki, B. (2002). "Only male fin whales sing loud songs.," *Nature* **417**, 809.
- D'Amico, A., Gisiner, R. C., Ketten, D. R., Hammock, J. A., Johnson, C., Tyack, P. L., and Mead, J. (2009). "Beaked whale strandings and naval exercises," *Aquat. Mamm.* **35**, 452–472.
- Davis, G. E., Baumgartner, M. F., Bonnell, J. M., Bell, J., Berchok, C., Bort Thornton, J., Brault, S., Buchanan, G., Charif, R. A., Cholewiak, D., Clark, C. W., Corkeron, P., Delarue, J., Dudzinski, K., Hatch, L., Hildebrand, J., Hodge, L., Klinck, H., Kraus, S., Martin, B., Mellinger, D. K., Moors-Murphy, H., Nieukirk, S., Nowacek, D. P., Parks, S., Read, A. J., Rice, A. N., Risch, D., Širović, A., Soldevilla, M., Stafford, K., Stanistreet, J. E., Summers, E., Todd, S., Warde, A., and Van Parijs, S. M. (2017). "Long-term passive acoustic recordings track the changing distribution of North Atlantic right whales (*Eubalaena glacialis*) from 2004 to 2014," *Sci. Rep.* **7**, 13460.
- Davis, R., Baumgartner, M., Comeau, A., Cunningham, D., Davies, K., Furlong, A., Johnson, H., L'Orsa, S., Ross, T., Taggart, C., and Whoriskey, F. (2016). "Tracking whales on the Scotian Shelf using passive acoustic monitoring on ocean gliders," in *Oceans 2016 MTS/IEEE*, Monterey, CA.
- Davis, R. E., Sherman, J. T., and Dufour, J. (2001). "Profiling ALACEs and other advances in autonomous subsurface floats," *J. Atmos. Ocean. Technol.* **18**, 982–993.
- Dawson, D. K., and Efford, M. G. (2009). "Bird population density estimated from acoustic signals," *J. Appl. Ecol.* **46**, 1201–1209.

- Dawson, S., Barlow, J., and Ljungblad, D. K. (1998). "Sounds recorded from Baird's beaked whale, *Berardius bairdii*," Mar. Mammal Sci. **14**, 335–344.
- Dawson, S., Wade, P., Sloaten, E., and Barlow, J. (2008). "Design and field methods for sighting surveys of cetaceans in coastal and riverine habitats," Mamm. Rev. **38**, 19–49.
- DeRuiter, S. L., Southall, B. L., Calambokidis, J., Zimmer, W. M. X., Sadykova, D., Falcone, E. A., Friedlaender, A. S., Joseph, J. E., Moretti, D., Schorr, G. S., Thomas, L., Tyack, P. L., and Zimmer, M. X. (2013). "First direct measurements of behavioural responses by Cuvier's beaked whales to mid-frequency active sonar," Biol. Lett. **9**, 20130223.
- Dong, C., Idica, E. Y., and McWilliams, J. C. (2009). "Circulation and multiple-scale variability in the Southern California Bight," Prog. Oceanogr. **82**, 168–190.
- Dugan, P. J., Klinck, H., Roch, M. A., and Helble, T. A. (2016). "RAVEN-X: A High Performance Data Mining Toolbox for Bioacoustic Data Analysis," ONR Report No. N00014-16-1-3156, <https://arxiv.org/ftp/arxiv/papers/1610/1610.03772.pdf> (Last viewed 01/26/2020).
- Dugan, P., Zollweg, J., Roch, M., Helble, T., Pitzrick, M., Clark, C., and Klinck, H. (2018). "The Raven-X Software Package. A scalable high-performance computing framework in Matlab for the analysis of large bioacoustic sound archives," Zenodo, Dataset <http://dx.doi.org/10.5281/zenodo.1221420>
- Efford, M. G. (2019). "secr: Spatially explicit capture-recapture models," R package version 3.2.1. <https://CRAN.R-project.org/package=secr>.
- Efford, M. G., Borchers, D. L., and Byrom, A. E. (2009a). "Density estimation by spatially explicit capture-recapture: Likelihood-based methods," in Modeling demographic processes in marked populations, edited by D. L. Thomson, E. G. Cooch, and M. J. Conroy (Springer, Boston, MA), pp. 255–269.
- Efford, M. G., and Dawson, D. K. (2009). "Effect of distance-related heterogeneity on population size estimates from point counts," Auk **126**, 100–111.
- Efford, M. G., Dawson, D. K., and Borchers, D. L. (2009b). "Population density estimation from locations of individuals on a passive detector array," Ecology **90**, 2676–2682.
- Efron, B. (1982). "The jackknife, the bootstrap and other resampling plans," CBMS Regional Conference Series in Applied Mathematics 38, Society for Industrial and Applied Mathematics, Philadelphia.
- Eriksen, C. C., Osse, T. J., Light, R. D., Wen, T., Lehman, T. W., Sabin, P. L., Ballard, J. W., and Chiodi, A. M. (2001). "Seaglider: A long-range autonomous underwater vehicle for oceanographic research," IEEE J. Ocean. Eng. **26**, 424–436.
- Frantzis, A. (1998). "Does acoustic testing strand whales?," Nature **392**, 29.
- Frasier, K. E., Wiggins, S. M., Harris, D. V., Marques, T. A., Thomas, L., and Hildebrand, J. A. (2016). "Delphinid echolocation click detection probability on near-seafloor sensors," J. Acoust. Soc. Am. **140**, 1918–1930.
- Fregosi, S., Harris, D. V., Matsumoto, H., Mellinger, D. K., Negretti, C., Moretti, D. J., Martin, S. W., Matsuyama, B., Dugan, P. J., and Klinck, H. (2020). "Comparison of fin whale 20 Hz call detections by deep-water mobile autonomous and stationary recorders," J. Acoust. Soc. Am. **147**, 961–977.
- Gassmann, M., Wiggins, S. M., and Hildebrand, J. A. (2015). "Three-dimensional tracking

- of Cuvier's beaked whales' echolocation sounds using nested hydrophone arrays," *J. Acoust. Soc. Am.* **138**, 2483–2494.
- Gerrodette, T., Taylor, B. L., Swift, R., Rankin, S., Jaramillo-Legorreta, A. M., and Rojas-Bracho, L. (2011). "A combined visual and acoustic estimate of 2008 abundance, and change in abundance since 1997, for the vaquita, *Phocoena sinus*," *Mar. Mammal Sci.* **27**, 79–100.
- Gillespie, D., Mellinger, D. K., Gordon, J., McLaren, D., Redmond, P., McHugh, R., Trinder, P., Deng, X., and Thode, A. (2009). "PAMGUARD: Semiautomated, open source software for real-time acoustic detection and localization of cetaceans.," *J. Acoust. Soc. Am.* **125**, 2547–2547.
- Gkikopoulou, K. C. (2018). "Getting below the surface: Density estimation methods for deep diving animals using slow autonomous underwater vehicles," Ph.D. thesis, University of St Andrews, St Andrews, Scotland.
- Glennie, R., Buckland, S. T., and Thomas, L. (2015). "The effect of animal movement on line transect estimates of abundance," *PLoS One* **10**, e0121333.
- Goldbogen, J. A., Calambokidis, J., Shadwick, R. E., Oleson, E. M., McDonald, M. A., and Hildebrand, J. A. (2006). "Kinematics of foraging dives and lunge-feeding in fin whales," *J. Exp. Biol.* **209**, 1231–1244.
- Goldbogen, J. A., Stimpert, A. K., DeRuiter, S. L., Calambokidis, J., Friedlaender, A. S., Schorr, G. S., Moretti, D. J., Tyack, P. L., and Southall, B. L. (2014). "Using accelerometers to determine the calling behavior of tagged baleen whales.," *J. Exp. Biol.* **217**, 2449–2455.
- Griffiths, E. T., and Barlow, J. (2015). "Equipment performance report for the Drifting Acoustic Spar Buoy Recorder (DASBR)," NOAA Technical Memorandum NOAA-TM-NMFS-SWFSC-543, available from NOAA Southwest Fisheries Science Center, La Jolla, CA.
- Griffiths, E. T., and Barlow, J. (2016). "Cetacean acoustic detections from free-floating vertical hydrophone arrays in the southern California Current," *J. Acoust. Soc. Am.* **140**, EL399–EL404.
- Griffiths, E. T., Keating, J. L., Barlow, J., and Moore, J. E. (2019). "Description of a new beaked whale echolocation pulse type in the California Current," *Mar. Mammal Sci.*, **35**, 1058-1069.
- Guazzo, R. A., Helble, T. A., Weller, D. W., Wiggins, M., and Hildebrand, J. A. (2017). "Migratory behavior of eastern North Pacific gray whales tracked using a hydrophone array," *PLoS One* **12**, e0185585.
- Guerra, M., Dawson, S. M., Brough, T. E., and Rayment, W. J. (2014). "Effects of boats on the surface and acoustic behaviour of an endangered population of bottlenose dolphins," *Endanger. Species Res.* **24**, 221–236.
- Hammond, P. S. (2010). "Estimating the abundance of marine mammals," in *Marine mammal ecology and conservation: A handbook of techniques*, edited by I. L. Boyd, W. D. Bowen, and S. J. Iverson (Oxford University Press, Oxford), pp. 42–67.
- Harris, D. V, Fregosi, S., Klinck, H., Mellinger, D. K., Barlow, J., and Thomas, L. (2017). "Evaluating autonomous underwater vehicles as platforms for animal population density estimation," *J. Acoust. Soc. Am.* **141**, 3606.
- Harris, D. V, Fregosi, S., Klinck, H., Mellinger, D. K., and Thomas, L. (in revision).

- “Assessing the effect of ocean glider movement on distance sampling assumptions,” Manuscript accepted at Remote Sens. Ecol. Conserv.
- Harris, D. V., Matias, L., Thomas, L., Harwood, J., and Geissler, W. H. (2013). “Applying distance sampling to fin whale calls recorded by single seismic instruments in the northeast Atlantic,” *J. Acoust. Soc. Am.* **134**, 3522–3535.
- Harris, D. V., Miksis-Olds, J. L., Vernon, J. A., and Thomas, L. (2018). “Fin whale density and distribution estimation using acoustic bearings derived from sparse arrays,” *J. Acoust. Soc. Am.* **143**, 2980–2993.
- Hatch, L. T., Clark, C. W., Van Parijs, S. M., Frankel, A. S., and Ponirakis, D. W. (2012). “Quantifying loss of acoustic communication space for right whales in and around a U.S. National Marine Sanctuary,” *Conserv. Biol.* **26**, 983–994.
- Hayes, R. J., and Buckland, S. T. (1983). “Radial-distance models for the line-transect method,” *Biometrics* **39**, 29–42.
- Helble, T. A., D’Spain, G. L., Campbell, G. S., and Hildebrand, J. A. (2013a). “Calibrating passive acoustic monitoring: correcting humpback whale call detections for site-specific and time-dependent environmental characteristics,” *J. Acoust. Soc. Am.* **134**, EL400–406.
- Helble, T. A., D’Spain, G. L., Hildebrand, J. A., Campbell, G. S., Campbell, R. L., and Heaney, K. D. (2013b). “Site specific probability of passive acoustic detection of humpback whale calls from single fixed hydrophones,” *J. Acoust. Soc. Am.* **134**, 2556–2570.
- Helble, T. A., Guazzo, R. A., Martin, C. R., Durbach, I. N., Alongi, G. C., Martin, S. W., Boyle, J. K., and Henderson, E. E. (2020). “Lombard effect: Minke whale boing call source levels vary with natural variations in ocean noise,” *J. Acoust. Soc. Am.* **147**, 698–712.
- Helble, T. A., Henderson, E. E., Ierley, G. R., and Martin, S. W. (2016). “Swim track kinematics and calling behavior attributed to Bryde’s whales on the Navy’s Pacific Missile Range Facility,” *J. Acoust. Soc. Am.* **140**, 4170–4177.
- Helble, T. A., Ierley, G. R., D’Spain, G. L., and Martin, S. W. (2015). “Automated acoustic localization and call association for vocalizing humpback whales on the Navy’s Pacific Missile Range Facility,” *J. Acoust. Soc. Am.* **137**, 11–21.
- Henderson, E. E., Martin, S. W., Manzano-Roth, R., and Matsuyama, B. M. (2016). “Occurrence and habitat use of foraging Blainville’s beaked whales (*Mesoplodon densirostris*) on a U.S. Navy Range in Hawaii,” *Aquat. Mamm.* **42**, 549–562.
- Hickey, B. M. (2003). “Local and remote forcing of currents and temperature in the central Southern California Bight,” *J. Geophys. Res.* **108**, 1–26.
- Hildebrand, J. A. (2009). “Anthropogenic and natural sources of ambient noise in the ocean,” *Mar. Ecol. Prog. Ser.* **395**, 5–20.
- Hildebrand, J. A., Baumann-Pickering, S., Frasier, K. E., Trickey, J. S., Merckens, K. P., Wiggins, S. M., McDonald, M. A., Garrison, L. P., Harris, D. V., Marques, T. A., and Thomas, L. (2015). “Passive acoustic monitoring of beaked whale densities in the Gulf of Mexico,” *Sci. Rep.* **5**, 16343.
- Hildebrand, J. A., Baumann-Pickering, S., Giddings, A., Brewer, A., Jacobs, E. R., Trickey, J. S., Wiggins, S. M., and McDonald, M. A. (2016). “Progress report on the application of passive acoustic monitoring to density estimation of Cuvier’s beaked

- whales,” Marine Physical Laboratory Technical Memorandum 606 (La Jolla, CA: Scripps Institution of Oceanography University of California San Diego), p. 15, March 2016.
- Holt, M. M., Noren, D. P., Veirs, V., Emmons, C. K., and Veirs, S. (2009). “Speaking up: Killer whales (*Orcinus orca*) increase their call amplitude in response to vessel noise,” *J. Acoust. Soc. Am.* **125**, EL27–EL32.
- Ierley, G., and Helble, T. A. (2016). “Fin whale call sequence analysis from tracked fin whales on the Southern California Offshore Range,” *J. Acoust. Soc. Am.* **140**, 3295.
- Ioup, G. E., Ioup, J. W., Sidorovskaia, N. A., Tiemann, C. O., Kuczaj, S. A., Ackleh, A. S., Newcomb, J. J., Ma, B., Paulos, R., Ekimov, A., Jr, G. H. R., Stephens, J. M., and Tashmukhambetov, A. M. (2016). “Environmental Acoustic Recording System (EARS) in the Gulf of Mexico,” in *Listening in the Ocean*, edited by W. W. L. Au and M. O. Lammers (Springer, New York), pp. 117–162.
- Janik, V. M. (2000). “Source levels and the estimated active space of bottlenose dolphin (*Tursiops truncatus*) whistles in the Moray Firth, Scotland,” *J. Comp. Physiol. - A Sensory, Neural, Behav. Physiol.* **186**, 673–680.
- Janik, V. M., and Sayigh, L. S. (2013). “Communication in bottlenose dolphins: 50 years of signature whistle research,” *J. Comp. Physiol. A* **199**, 479–489.
- Jarvis, S. M., Morrissey, R. P., Moretti, D. J., DiMarzio, N. A., and Shaffer, J. A. (2014). “Marine Mammal Monitoring on Navy Ranges (M3R): A toolset for automated detection, localization, and monitoring of marine mammals in open ocean environments,” *Mar. Technol. Soc. J.* **48**, 5–20.
- Johnson, H. D., Baumgartner, M., Lin, Y.-T., Newhall, A., and Taggart, C. (2018). “Probability of detecting right whales in near real-time using autonomous platforms,” Detection, Classification, Localization and Density Estimation of Marine Mammals Workshop, Paris, France, July 2018.
- Johnson, H. D., Baumgartner, M., Lin, Y.-T., Newhall, A., and Taggart, C. (2019). “Probability of passive acoustic detection of right whales from autonomous platforms equipped with a near real-time monitoring system,” World Marine Mammal Conference, Barcelona, Spain, December 2019.
- Johnson, M., Madsen, P. T., Zimmer, W. M. X., Aguilar de Soto, N., and Tyack, P. L. (2004). “Beaked whales echolocate on prey,” *Proc. R. Soc. B Biol. Sci.* **271**, S383–S386.
- Johnson, M., Madsen, P. T., Zimmer, W. M. X., Aguilar de Soto, N., and Tyack, P. L. (2006). “Foraging Blainville’s beaked whales (*Mesoplodon densirostris*) produce distinct click types matched to different phases of echolocation,” *J. Exp. Biol.* **209**, 5038–5050.
- Johnson, M. P., and Tyack, P. L. (2003). “A digital acoustic recording tag for measuring the response of wild marine mammals to sound,” *IEEE J. Ocean. Eng.* **28**, 3–12.
- Keating, J. L., and Barlow, J. (2013). “Summary of PAMGUARD beaked whale click detectors and classifiers used during the 2012 Southern California Behavioral Response Study,” NOAA Technical Memorandum NOAA-TM-NMFS-SWFSC-517, available from NOAA Southwest Fisheries Science Center, La Jolla, CA.
- Keating, J. L., Barlow, J., Griffiths, E. T., and Moore, J. E. (2018). “Passive Acoustics Survey of Cetacean Abundance Levels (PASCAL-2016) Final Report,” Honolulu

- (HI): US Department of the Interior, Bureau of Ocean Energy Management, OCS Study BOEM 25, p. 22.
- Keating, J. L., Barlow, J., and Rankin, S. (2016). “Shifts in frequency-modulated pulses recorded during an encounter with Blainville’s beaked whales (*Mesoplodon densirostris*),” *J. Acoust. Soc. Am.* **140**, EL166–EL171.
- Klinck, H., Fregosi, S., Matsumoto, H., Turpin, A., Mellinger, D. K., Erofeev, A., Barth, J. A., Shearman, R. K., Jafarmadar, K., and Stelzer, R. (2016a). “Mobile autonomous platforms for passive-acoustic monitoring of high-frequency cetaceans,” in *Robotic Sailing 2015*, edited by A. Friebe and F. Haug (Springer International Publishing, Cham), pp. 29–37.
- Klinck, H., Kindermann, L., and Boebel, O. (2016b). “PALAOA: The Perennial Acoustic Observatory in the Antarctic Ocean— Real- Time Eavesdropping on the Antarctic Underwater Soundscape,” in *Listening in the Ocean*, edited by W. W. L. Au and M. O. Lammers (Springer, New York), pp. 207–219.
- Klinck, H., Matsumoto, H., Fregosi, S., and Mellinger, D. K. (2014). “High-frequency observations from mobile autonomous platforms,” *J. Acoust. Soc. Am.* **136**, 2119.
- Klinck, H., Mellinger, D. K., Klinck, K., Bogue, N. M., Luby, J. C., Jump, W. A., Shilling, G. B., Litchendorf, T., Wood, A. S., Schorr, G. S., and Baird, R. W. (2012). “Near-real-time acoustic monitoring of beaked whales and other cetaceans using a Seaglider™,” *PLoS One* **7**, e36128.
- Klinck, H., Nieukirk, S. L., Fregosi, S., Klinck, K., Mellinger, D. K., Lastuka, S., Shilling, G. B., *et al.* (2015a). “Cetacean Studies in the Mariana Islands Range Complex in March–April 2015: Passive acoustic monitoring of marine mammals using gliders,” Final Report, prepared for Commander, U.S., Pacific Fleet, Environmental Readiness Division, Pearl Harbor, HI, submitted to Naval Facilities Engineering Command (NAVFAC) Pacific, Pearl Harbor, Hawaii, under Contract No. N62470-10-D-3011, Task Order KB25, issued to HDR, Inc., Honolulu, Hawaii. August 2015.
- Klinck, H., Nieukirk, S. L., Fregosi, S., Klinck, K., Mellinger, D. K., Lastuka, S., Shilling, G. B., and Luby, J. C. (2015b). “Cetacean Studies in the Hawaii Range Complex in December 2014–January 2015: Passive acoustic monitoring of marine mammals using gliders,” Final Report, prepared for Commander, U.S., Pacific Fleet, Environmental Readiness Division, Pearl Harbor, HI, submitted to Naval Facilities Engineering Command (NAVFAC) Pacific, Pearl Harbor, Hawaii, under Contract No. N62470-10-D-3011, Task Order KB25, issued to HDR, Inc., Honolulu, Hawaii. October 2015.
- Kuperman, W. A., and Roux, P. (2007). “Underwater Acoustics,” in *Springer Handbook of Acoustics* (Springer, New York), pp. 149–204.
- Küsel, E. T., Mellinger, D. K., Thomas, L., Marques, T. A., Moretti, D., and Ward, J. (2011). “Cetacean population density estimation from single fixed sensors using passive acoustics,” *J. Acoust. Soc. Am.* **129**, 3610–3622.
- Küsel, E. T., Munoz, T., Siderius, M., Mellinger, D. K., and Heimlich, S. (2017). “Marine mammal tracks from two-hydrophone acoustic recordings made with a glider,” *Ocean Sci.* **13**, 273–288.
- Kyhn, L. A., Tougaard, J., Thomas, L., Duve, L. R., Stenback, J., Amundin, M., Desportes, G., and Teilmann, J. (2012). “From echolocation clicks to animal density—Acoustic

- sampling of harbor porpoises with static dataloggers,” *J. Acoust. Soc. Am.* **131**, 550.
- Laake, J. L., and Borchers, D. L. (2004). “Methods for incomplete detection at distance zero,” in *Advanced distance sampling*, edited by S. T. Buckland, D. R. Anderson, K. P. Burnham, J. L. Laake, D. L. Borchers, and L. Thomas (Oxford University Press, Oxford), pp. 108–180.
- Lammers, M. O., and Au, W. W. L. (2003). “Directionality in the whistles of Hawaiian spinner dolphins (*Stenella longirostris*): A signal feature to cue direction of movement?,” *Mar. Mammal Sci.* **19**, 249–264.
- Lammers, M. O., Brainard, R. E., Au, W. W. L., Mooney, T. A., and Wong, K. B. (2008). “An ecological acoustic recorder (EAR) for long-term monitoring of biological and anthropogenic sounds on coral reefs and other marine habitats,” *J. Acoust. Soc. Am.* **123**, 1720–1728.
- Leroy, E. C., Thomisch, K., Royer, J.-Y., Boebel, O., and Van Opzeeland, I. (2018). “On the reliability of acoustic annotations and automatic detections of Antarctic blue whale calls under different acoustic conditions,” *J. Acoust. Soc. Am.* **144**, 740–754.
- Lesage, V., Barrette, C., Kingsley, M. C. S., and Sjare, B. (1999). “The effect of vessel noise on the vocal behavior of belugas in the St. Lawrence River Estuary, Canada,” *Mar. Mammal Sci.* **15**, 65–84.
- Lewis, T., Boisseau, O., Danbolt, M., Gillespie, D., Lacey, C., Leaper, R., Matthews, J., McLanaghan, R., and Moscrop, A. (2018). “Abundance estimates for sperm whales in the Mediterranean Sea from acoustic line-transect surveys,” *J. Cetacean Res. Manag.* **18**, 103–117.
- Lewis, T., Gillespie, D., Lacey, C., Matthews, J., Danbolt, M., Leaper, R., McLanaghan, R., and Moscrop, A. (2007). “Sperm whale abundance estimates from acoustic surveys of the Ionian Sea and Straits of Sicily in 2003,” *J. Mar. Biol. Assoc. United Kingdom* **87**, 353–357.
- Lillis, A., Caruso, F., Mooney, T. A., Llopiz, J., Bohnenstiehl, D., and Eggleston, D. B. (2018). “Drifting hydrophones as an ecologically meaningful approach to underwater soundscape measurement in coastal benthic habitats,” *J. Ecoacoustics* **2**, STBDH1.
- MacLeod, C. D., Perrin, W. F., Pitman, R. L., Barlow, J., Ballance, L., D’Amico, A., Gerrodette, T., Joyce, G., Mullin, K. D., Palka, D. L., and Waring, G. T. (2006). “Known and inferred distributions of beaked whale species (Cetacea: Ziphiidae),” *J. Cetacean Res. Manag.* **7**, 271–286.
- MacLeod, C. D., and Zuur, A. F. (2005). “Habitat utilization by Blainville’s beaked whales off Great Abaco, northern Bahamas, in relation to seabed topography,” *Mar. Biol.* **147**, 1–11.
- Madsen, P. T., Johnson, M., Aguilar de Soto, N., Zimmer, W. M. X., and Tyack, P. (2005). “Biosonar performance of foraging beaked whales (*Mesoplodon densirostris*),” *J. Exp. Biol.* **208**, 181–194.
- Marques, T. A., Munger, L., Thomas, L., Wiggins, S., and Hildebrand, J. A. (2011). “Estimating north pacific right whale *Eubalaena japonica* density using passive acoustic cue counting,” *Endanger. Species Res.* **13**, 163–172.
- Marques, T. A., Thomas, L., Martin, S. W., Mellinger, D. K., Jarvis, S., Morrissey, R. P., Ciminello, C.-A., and DiMarzio, N. (2012). “Spatially explicit capture-recapture methods to estimate minke whale density from data collected at bottom-mounted

- hydrophones,” *J. Ornithol.* **152**, 445–455.
- Marques, T. A., Thomas, L., Martin, S. W., Mellinger, D. K., Ward, J. A., Moretti, D. J., Harris, D. V., and Tyack, P. L. (2013). “Estimating animal population density using passive acoustics,” *Biol. Rev.* **88**, 287–309.
- Marques, T. A., Thomas, L., Ward, J., DiMarzio, N., and Tyack, P. L. (2009). “Estimating cetacean population density using fixed passive acoustic sensors: An example with Blainville’s beaked whales,” *J. Acoust. Soc. Am.* **125**, 1982–1994.
- Martin, S. W., and Matsuyama, B. (2015). “Suspected Bryde’s whales acoustically detected, localized and tracked using recorded data from the Pacific Missile Range Facility, Hawaii,” report available at http://www.navymarinespeciesmonitoring.us/files/7114/3826/9215/Martin_and_Matsuyama_2015_Suspected_Brydes_detected_at_PMRF_20JUL2015.pdf.
- Martin, S. W., Marques, T. A., Thomas, L., Morrissey, R. P., Jarvis, S., Dimarzio, N., Moretti, D., and Mellinger, D. K. (2013). “Estimating minke whale (*Balaenoptera acutorostrata*) boing sound density using passive acoustic sensors,” *Mar. Mammal Sci.* **29**, 142–158.
- Martin, S. W., Martin, C. R., Matsuyama, B. M., and Henderson, E. E. (2015). “Minke whales (*Balaenoptera acutorostrata*) respond to navy training,” *J. Acoust. Soc. Am.* **137**, 2533–2541.
- Matsumoto, H., Dziak, R. P., Mellinger, D. K., Fowler, M., Haxel, J., Lau, A., Meinig, C., Bumgardner, J., and Hannah, W. (2006). “Autonomous hydrophones at NOAA/OSU and a new seafloor sentry system for real-time detection of acoustic events,” in *Oceans 2006*, MTS/IEEE.
- Matsumoto, H., Haxel, J., Turpin, A., Fregosi, S., Klinck, H., Klinck, K., Baumann-Pickering, S., Erofeev, A., Barth, J. A., Dziak, R. P., and Jones, C. (2015). “Simultaneous operation of mobile acoustic recording systems off the Washington Coast for cetacean studies: System noise level evaluations,” in *Oceans 2006*, MTS/IEEE.
- Matsumoto, H., Jones, C., Klinck, H., Mellinger, D. K., Dziak, R. P., and Meinig, C. (2013). “Tracking beaked whales with a passive acoustic profiler float,” *J. Acoust. Soc. Am.* **133**, 731–740.
- McDonald, M. A., and Fox, C. G. (1999). “Passive acoustic methods applied to fin whale population density estimation,” *J. Acoust. Soc. Am.* **105**, 2643–2651.
- Mellinger, D., and Barlow, J. (2003). “Future directions for acoustic marine mammal surveys: Stock assessment and habitat use,” report of a workshop held in La Jolla, CA, 20-22 November, 2002, <https://www.pmel.noaa.gov/pubs/PDF/mell2557/mell2557.pdf>
- Mellinger, D. K., and Bradbury, J. W. (2007). “Acoustic measurement of marine mammal sounds in noisy environments,” in *Proceedings of the Second International Conference on Underwater Acoustic Measurements: Technologies and Results*, Heraklion, Greece, 25-29 June, 2007, <ftp://ftp.pmel.noaa.gov/newport/mellinger/papers/Mellinger+Bradbury07-BioacousticMeasurementInNoise-UAM,Crete.pdf>.
- Mellinger, D. K., and Clark, C. W. (2000). “Recognizing transient low-frequency whale sounds by spectrogram correlation,” *J. Acoust. Soc. Am.* **107**, 3518–3529.
- Mellinger, D. K., and Klinck, H. (2012). “Passive autonomous acoustic monitoring of

- marine mammals with Seagliders,” Final Report, ONR Grant N00014-10-1-0387.
- Mellinger, D.K., Martin, S. W., Morrissey, R. P., Thomas, L., and Yosco, J. J. (2011). “A method for detecting whistles, moans, and other frequency contour sounds,” *J. Acoust. Soc. Am.* **129**, 4055-4061.
- Mellinger, D. K., Nieukirk, S. L., Heimlich, S. L., Fregosi, S., Küsel, E. T., Siderius, M., and Sidorovskaia, N. (2017). “Passive acoustic monitoring in the Northern Gulf of Mexico using ocean gliders,” *J. Acoust. Soc. Am.* **142**, 2533.
- Mellinger, D. K., Roch, M. A., Nosal, E.-M., and Klinck, H. (2016). “Signal Processing,” in *Listening in the Ocean*, edited by W. W. L. Au and M. O. Lammers (Springer, New York, NY), pp. 359–409.
- Mellinger, D. K., Stafford, K., Moore, S., Dziak, R. P., and Matsumoto, H. (2007). “An overview of fixed passive acoustic observation methods for cetaceans,” *Oceanography* **20**, 36–45.
- Merchant, N. D., Barton, T. R., Thompson, P. M., Pirotta, E., Dakin, D. T., and Dorocicz, J. (2013). “Spectral probability density as a tool for ambient noise analysis,” *J. Acoust. Soc. Am.* **133**, EL262–EL267.
- Miksis-Olds, J. L., Harris, D. V., and Mouw, C. (2019). “Interpreting fin whale (*Balaenoptera physalus*) call behavior in the context of environmental conditions,” *Aquat. Mamm.* **45**, 691–705.
- Miller, P. J. O., Kvadsheim, P. H., Lam, F. P. a., Tyack, P. L., Cure, C., DeRuiter, S. L., Kleivane, L., Sivle, L.D., van IJsselmuide, S. P., Visser, F., Wensveen, P. J., von Benda-Beckmann, A. M., Martín López, L. M., Narazaki, T., and Hooker, S. K. (2015). “First indications that northern bottlenose whales are sensitive to behavioural disturbance from anthropogenic noise,” *R. Soc. Open Sci.* **2**, 140484.
- Miller, P. J., and Tyack, P. L. (1998). “A small towed beamforming array to identify vocalizing resident killer whales (*Orcinus orca*) concurrent with focal behavioral observations,” *Deep Sea Res. Part II Top. Stud. Oceanogr.* **45**, 1389–1405.
- Moore, S. E., Howe, B. M., Stafford, K. M., and Boyd, M. L. (2007). “Including whale call detection in standard ocean measurements: Application of acoustic Seagliders,” *Mar. Technol. Soc. J.* **41**, 53–57.
- Moore, S. E., Stafford, K. M., Dahlheim, M. E., Fox, C. G., Braham, H. W., Polovina, J. J., and Bain, D. E. (1998). “Seasonal variation in reception of fin whale calls at five geographic areas in the north Pacific,” *Mar. Mammal Sci.* **14**, 617–627.
- Moretti, D., Marques, T. A., Thomas, L., DiMarzio, N., Dilley, A., Morrissey, R., McCarthy, E., Ward, J., and Jarvis, S. (2010). “A dive counting density estimation method for Blainville’s beaked whale (*Mesoplodon densirostris*) using a bottom-mounted hydrophone field as applied to a mid-frequency Active (MFA) sonar operation,” *Appl. Acoust.* **71**, 1036–1042.
- Moretti, D., Morrissey, R., Jarvis, S., and Shaffer, J. (2016). “Findings from U.S. Navy hydrophone ranges,” in *Listening in the Ocean*, edited by W. W. L. Au and M. O. Lammers (Springer, New York, NY), pp. 239–256.
- Nieukirk, S. L., Fregosi, S., Mellinger, D. K., and Klinck, H. (2016). “A complex baleen whale call recorded in the Mariana Trench Marine National Monument,” *J. Acoust. Soc. Am.* **140**, EL274-EL279.
- Norris, T. F., Dunleavy, K. J., Yack, T. M., and Ferguson, E. L. (2017). “Estimation of

- minke whale abundance from an acoustic line transect survey of the Mariana Islands,” *Mar. Mammal Sci.* **33**, 574–592.
- Norris, T. F., Oswald, J. N., Yack, T. M., Ferguson, E. L., Hom-Weaver, C., Dunleavy, K., Coates, S., and Dominello, T. (2012a). “An analysis of acoustic data from the Mariana Island Sea Turtle and Cetacean Survey (MISTCS),” prepared for Commander, Pacific Fleet, Pearl Harbor, HI, submitted to Naval Facilities Engineering Command Pacific (NAVFAC), EV2 Environmental Planning, Pearl Harbor, HI, under contract No. N62470-10D-3011 CTO KB08, Task Order #002 issued to HDR, Inc., submitted by Bio-Waves Inc., Encinitas, CA.
- Norris, T., Martin, S. W., Thomas, L., Yack, T., Oswald, J. N., Nosal, E.-M., and Janik, V. (2012b). “Acoustic ecology and behavior of minke whales in the Hawaiian and Marianas Islands: Localization, abundance estimation, and characterization of minke whale ‘boings,’” in *The effects of noise on aquatic life*, edited by A. N. Popper and A. Hawkins (Springer, New York), pp. 149–153.
- Oswald, J. N., Au, W. W. L., and Duennebie, F. (2011). “Minke whale (*Balaenoptera acutorostrata*) boings detected at the Station ALOHA Cabled Observatory,” *J. Acoust. Soc. Am.* **129**, 3353–3360.
- Oswald, J. N., Ou, H., Au, W. W. L., Howe, B. M., and Duennebie, F. (2016). “Listening for whales at the station ALOHA cabled observatory,” in *Listening in the Ocean*, edited by W. W. L. Au and M. O. Lammers (Springer, New York), pp. 221–237.
- Quick, N. J., and Janik, V. M. (2012). “Bottlenose dolphins exchange signature whistles when meeting at sea,” *Proc. R. Soc. B Biol. Sci.* **279**, 2539–2545.
- R Core Team (2019). “R: A language and environment for statistical computing,” <https://www.r-project.org/>
- Rankin, S., and Barlow, J. (2005). “Source of the North Pacific ‘boing’ sound attributed to minke whales,” *J. Acoust. Soc. Am.* **118**, 3346–3351.
- Rankin, S., Barlow, J., and Oswald, J. N. (2008). “An Assessment of the accuracy and precision of localization of a stationary sound source using a two-element towed hydrophone array,” NOAA Technical Memorandum NOAA-TM-NMFS-SWFSC-416 (Southwest Fisheries Science Center, La Jolla, CA).
- Rankin, S., Oswald, J. N., Barlow, J., and Lammers, M. O. (2007). “Patterned burst-pulse vocalizations of the northern right whale dolphin, *Lissodelphis borealis*,” *J. Acoust. Soc. Am.* **121**, 1213–1218.
- Read, A. (2010). “Conservation biology,” in *Marine mammal ecology and conservation: A handbook of techniques*, edited by I. L. Boyd, W. D. Bowen, and S. J. Iverson (Oxford University Press, Oxford), pp. 340–359.
- Rice, A. C., Baumann-Pickering, S., Širović, A., Hildebrand, J. A., Rafter, M., Thayre, B. J., Trickey, J. S., and Wiggins, S. M. (2018). “Passive acoustic monitoring for marine mammals in the SOCAL Range Complex April 2016-June 2017,” Marine Physical Laboratory Technical Memorandum 618 (La Jolla, CA: Scripps Institution of Oceanography University of California San Diego), p. 30, February 2018.
- Rice, A. C., Baumann-Pickering, S., Širović, A., Hildebrand, J. A., Rafter, M., Thayre, B. J., Trickey, J. S., Wiggins, S. M., Reagan, E., Trickey, J. S., and Wiggins, S. M. (2019). “Passive acoustic monitoring for marine mammals in the SOCAL Range Complex March 2017-July 2018,” Marine Physical Laboratory Technical

- Memorandum 618 (La Jolla, CA: Scripps Institution of Oceanography University of California San Diego), p. 51, January 2019.
- Risch, D., Clark, C. W., Dugan, P. J., Popescu, M., Siebert, U., and Van Parijs, S. M. (2013). “Minke whale acoustic behavior and multi-year seasonal and diel vocalization patterns in Massachusetts Bay, USA,” *Mar. Ecol. Prog. Ser.* **489**, 279–295.
- Roch, M. A., Batchelor, H., Baumann-Pickering, S., Berchok, C. L., Cholewiak, D., Fujioka, E., Garland, E. C., Herbert, S., Hildebrand, J. A., Oleson, E. M., Van Parijs, S., Risch, D., Širović, A., and Soldevilla, M. S. (2016). “Management of acoustic metadata for bioacoustics,” *Ecol. Inform.* **31**, 122–136.
- Roemmich, D., Johnson, G., Riser, S., Davis, R., Gilson, J., Owens, W. B., Garzoli, S., Schmid, C., and Ignaszewski, M. (2009). “The Argo Program: Observing the global oceans with profiling floats,” *Oceanography* **22**, 34–43.
- Royle, J. A., Chandler, R. B., Sollmann, R., and Gardner, B. (2013). *Spatial capture-recapture* (Elsevier, Boston).
- Rudnick, D. L. (2016). “Ocean research enabled by underwater gliders,” *Ann. Rev. Mar. Sci.* **8**, 519–541.
- Rudnick, D. L., Davis, R. E., Eriksen, C. C., Fratantoni, D. M., and Perry, M. J. (2004). “Underwater gliders for ocean research,” *Mar. Technol. Soc. J.* **38**, 48–59.
- dos Santos, F. A., São Thiago, P. M., de Oliveira, A. L. S., Barmak, R., Lima, J. A. M., de Almeida, F. G., and Paula, T. P. (2016). “Investigating flow noise on underwater gliders acoustic data,” *J. Acoust. Soc. Am.* **140**, 3409.
- Sato, K., Watanuki, Y., Takahashi, A., Miller, P. J. O., Tanaka, H., Kawabe, R., Ponganis, P. J., Handrich, Y., Akamatsu, T., Watanabe, Y., Mitani, Y., Costa, D. P., Bost, C. A., Aoki, K., Amano, M., Trathan, P., Shapiro, A., and Naito, Y. (2007). “Stroke frequency, but not swimming speed, is related to body size in free-ranging seabirds, pinnipeds and cetaceans,” *Proc. R. Soc. B Biol. Sci.* **274**, 471–477.
- School of Oceanography and Applied Physics Laboratory (2011). “Seaglider Pilot’s Guide,” University of Washington, http://gliderfs.coas.oregonstate.edu/sliderweb/Seaglider_Pilot's_Guide.pdf
- Schorr, G. S., Falcone, E. A., Moretti, D. J., and Andrews, R. D. (2014). “First long-term behavioral records from Cuvier’s beaked whales (*Ziphius cavirostris*) reveal record-breaking dives,” *PLoS One* **9**, e92633.
- Seber, G. A. F. (1982). *The estimation of animal abundance and related parameters*, Vol. 8 (Blackburn Press, Caldwell, New Jersey).
- Silva, T., Mooney, T., Sayigh, L., and Baumgartner, M. (2019). “Temporal and spatial distributions of delphinid species in Massachusetts Bay (USA) using passive acoustics from ocean gliders,” *Mar. Ecol. Prog. Ser.* **631**, 1–17.
- Simonis, A. E., Brownell, R. L., Thayre, B. J., Trickey, J. S., Oleson, E. M., Huntington, R., and Baumann-Pickering, S. (2020). “Co-occurrence of beaked whale strandings and naval sonar in the Mariana Islands, Western Pacific,” *Proc. R. Soc. B Biol. Sci.* **287**, 20200070.
- Širović, A. (2016). “Variability in the performance of the spectrogram correlation detector for North-east Pacific blue whale calls,” *Bioacoustics* **25**, 145–160.
- Širović, A., Hildebrand, J. A., and Wiggins, S. M. (2007). “Blue and fin whale call source levels and propagation range in the Southern Ocean,” *Acoust. Soc. Am.* **122**, 1208–

- 1215.
- Širovic, A., Rice, A., Chou, E., Hildebrand, J. A., Wiggins, S. M., Roch, M. A. (2015). “Seven years of blue and fin whale call abundance in the Southern California Bight,” *Endanger. Species Res.* **28**, 61–76.
- Širović, A., Williams, L. N., Kerosky, S. M., Wiggins, S. M., and Hildebrand, J. A. (2013). “Temporal separation of two fin whale call types across the eastern North Pacific,” *Mar. Biol.* **160**, 47–57.
- Soldevilla, M. S., Henderson, E. E., Campbell, G. S., Wiggins, S. M., Hildebrand, J. A., and Roch, M. A. (2008). “Classification of Risso’s and Pacific white-sided dolphins using spectral properties of echolocation clicks,” *J. Acoust. Soc. Am.* **124**, 609–624.
- Soule, D. C., and Wilcock, W. S. D. (2013). “Fin whale tracks recorded by a seismic network on the Juan de Fuca Ridge, Northeast Pacific Ocean,” *Acoust. Soc. Am.* **133**, 1751–1762.
- Sousa-Lima, R. S., Norris, T. F., Oswald, J. N., and Fernandes, D. P. (2013). “A review and inventory of fixed autonomous recorders for passive acoustic monitoring of marine mammals,” *Aquat. Mamm.* **39**, 23–53.
- Spaulding, E., Robbins, M., Calupca, T., Clark, C. W., Tremblay, C., Waack, A., Warde, A., Kemp, J., and Newhall, K. (2009). “An autonomous, near-real-time buoy system for automatic detection of North Atlantic right whale calls,” *Proc. Meet. Acoust.* **6**, 010001.
- Stafford, K. M., Mellinger, D. K., Moore, S. E., and Fox, C. G. (2007). “Seasonal variability and detection range modeling of baleen whale calls in the Gulf of Alaska, 1999–2002,” *J. Acoust. Soc. Am.* **122**, 3378–3390.
- Stevenson, B. C. (2016). “Methods in spatially explicit capture-recapture,” Ph.D. thesis, University of St Andrews, St Andrews, Scotland.
- Stevenson, B. C., Borchers, D. L., Altwegg, R., Swift, R. J., Gillespie, D. M., and Measey, G. J. (2015). “A general framework for animal density estimation from acoustic detections across a fixed microphone array,” *Methods Ecol. Evol.* **6**, 38–48.
- Stimpert, A. K., DeRuiter, S. L., Flacone, E. A., Joseph, J., Douglas, A. B., Moretti, D. J., Friedlaender, A. S., Calambokidis, J., Gailey, G., Tyack, P. L., and Goldbogen, J. A. (2015). “Sound production and associated behavior of tagged fin whales (*Balaenoptera physalus*) in the Southern California Bight,” *Anim. Biotelemetry* **3**, 23.
- Stimpert, A. K., Deruiter, S. L., Southall, B. L., Moretti, D. J., Falcone, E. A., Goldbogen, J. A., Friedlaender, A. S., Schorr, G. S., and Calambokidis, J. (2014). “Acoustic and foraging behavior of a tagged Baird’s beaked whale (*Berardius bairdii*) exposed to simulated sonar,” *Sci. Rep.* **4**, 7031.
- Thode, A. (2004). “Tracking sperm whale (*Physeter macrocephalus*) dive profiles using a towed passive acoustic array,” *J. Acoust. Soc. Am.* **116**, 245–253.
- Thode, A. M. (2000). “Source ranging with minimal environmental information using a virtual receiver and waveguide invariant theory,” *J. Acoust. Soc. Am.* **108**, 1582–1594.
- Thomas, L., Harris, D. V, Klinck, H., Mellinger, D. K., and Barlow, J. (2019). “A framework for cetacean density estimation using slow-moving autonomous ocean vehicles,” Final Report, ONR Grant N00014-15-1-2142.
- Thomas, L., and Marques, T. A. (2012). “Passive acoustic monitoring for estimating animal

- density,” *Acoust. Today* **8**, 35-44.
- Thompson, P. O., and Friedl, W. A. (1982). “A long term study of low frequency sounds from several species of whales off Oahu, Hawaii, USA,” *Cetology* **45**, 1-19.
- Tiemann, C. O., Thode, A. M., Straley, J., O’Connell, V., and Folkert, K. (2006). “Three-dimensional localization of sperm whales using a single hydrophone,” *J. Acoust. Soc. Am.* **120**, 2355–2365.
- Tyack, P. L., Johnson, M., Aguilar de Soto, N., Sturlese, A., and Madsen, P. T. (2006). “Extreme diving of beaked whales,” *J. Exp. Biol.* **209**, 4238–4253.
- Tyack, P. L., Zimmer, W. M. X., Moretti, D., Southall, B. L., Claridge, D. E., Durban, J. W., Clark, C. W., D’Amico, A., DiMarzio, N., Jarvis, S., McCarthy, E., Morrissey, R., Ward, J., and Boyd, I. L. (2011). “Beaked whales respond to simulated and actual navy sonar,” *PLoS One* **6**, e17009.
- Urian, K., Gorgone, A., Read, A., Balmer, B., Wells, R. S., Berggren, P., Durban, J., Eguchi, T., Rayment, W., and Hammond, P. S. (2015). “Recommendations for photo-identification methods used in capture-recapture models with cetaceans,” *Mar. Mammal Sci.* **31**, 298–321.
- Urick, R. (1983). *Principles of Underwater Sound*, 3rd ed. (Peninsula Publishing, Westport, CT).
- Van Parijs, S. M., Clark, C. W., Sousa-Lima, R. S., Parks, S. E., Rankin, S., Risch, D., and Van Opzeeland, I. C. (2009). “Management and research applications of real-time and archival passive acoustic sensors over varying temporal and spatial scales,” *Mar. Ecol. Prog. Ser.* **395**, 21–36.
- Van Uffelen, L. J., Howe, B. M., Nosal, E. M., Carter, G. S., Worcester, P. F., and Dzieciuch, M. A. (2016a). “Localization and subsurface position error estimation of gliders using broadband acoustic signals at long range,” *IEEE J. Ocean. Eng.* **41**, 501–508.
- Van Uffelen, L. J., Nosal, E.-M., Howe, B. M., Carter, G. S., Worcester, P. F., Dzieciuch, M. A., Heaney, K. D., Campbell, R. L., and Cross, P. S. (2013). “Estimating uncertainty in subsurface glider position using transmissions from fixed acoustic tomography sources,” *J. Acoust. Soc. Am.* **134**, 3260-3271.
- Van Uffelen, L. J., Roth, E. H., Howe, B. M., Oleson, E. M., and Barkley, Y. (2017). “A Seaglider-integrated digital monitor for bioacoustic sensing,” *IEEE J. Ocean. Eng.* **42**, 800-807.
- Verfuss, U. K., Aniceto, A. S., Harris, D. V., Gillespie, D., Fielding, S., Jiménez, G., Johnston, P., Sinclair, R. R., Sivertsen, A., Solbø, S. A., Storvold, R., Biuw, M., and Wyatt, R. (2019). “A review of unmanned vehicles for the detection and monitoring of marine fauna,” *Mar. Pollut. Bull.* **140**, 17–29.
- von Benda-Beckmann, A. M., Lam, F. P. A., Moretti, D. J., Fulkerson, K., Ainslie, M. A., van IJsselmuide, S. P., Theriault, J., and Beerens, S. P. (2010). “Detection of Blainville’s beaked whales with towed arrays,” *Appl. Acoust.* **71**, 1027–1035.
- von Benda-Beckmann, A. M., Wensveen, P. J., Samara, F. I. P., Beerens, S. P., and Miller, P. J. O. (2016). “Separating underwater ambient noise from flow noise recorded on stereo acoustic tags attached to marine mammals,” *J. Exp. Biol.* **219**, 2271–2275.
- Wade, P. R. (1998). “Human-caused mortality of cetaceans and pinnipeds,” *Mar. Mammal Sci.* **14**, 1–37.

- Ward, J. A., Jarvis, S., Moretti, D. J., Morrissey, R. P., Dimarzio, N., Johnson, M. P., Tyack, P. L., Thomas, L., and Marques, T. A. (2011). "Beaked whale (*Mesoplodon densirostris*) passive acoustic detection in increasing ambient noise," *J. Acoust. Soc. Am.* **129**, 662–669.
- Ward, J. A., Thomas, L., Jarvis, S., Dimarzio, N., Moretti, D., Marques, T. A., Dunn, C., Claridge, D., Hartvig, E., and Tyack, P. (2012). "Passive acoustic density estimation of sperm whales in the Tongue of the Ocean, Bahamas," *Mar. Mammal Sci.* **28**, 444–455.
- Waring, G. T., Hamazaki, T., Sheehan, D., Wood, G., and Baker, S. (2001). "Characterization of beaked whale (Ziphiidae) and sperm whale (*Physeter macrocephalus*) summer habitat in shelf-edge and deeper waters off the northeast U.S.," *Mar. Mammal Sci.* **17**, 703–717.
- Watkins, W. A. (1981). "Activities and underwater sounds of fin whales," *Sci. Rep. Whales Res. Institut.*, **33**, 83–117.
- Watkins, W. A., Daher, M. A., Reppucci, G. M., George, J. E., Martin, N. A., Dimarzio, N. A., and Gannon, D. P. (2000). "Seasonality and distribution of whale calls in the North Pacific," *Oceanography* **13**, 62–67.
- Watkins, W. A., Tyack, P., Moore, K. E., and Bird, J. E. (1987). "The 20-Hz signals of finback whales (*Balaenoptera physalus*)," *J. Acoust. Soc. Am.* **82**, 1901–1912.
- Weirathmueller, M. J., Wilcock, W. S. D., and Soule, D. C. (2013). "Source levels of fin whale 20 Hz pulses measured in the Northeast Pacific Ocean," *J. Acoust. Soc. Am.* **133**, 741–9.
- Wiggins, S. M., and Hildebrand, J. A. (2007). "High-frequency Acoustic Recording Package (HARP) for broad-band, long-term marine mammal monitoring," in *2007 Symposium on Scientific Use of Submarine Cables and Related Technologies*, IEEE, pp. 351–357.
- Wiggins, S. M., and Hildebrand, J. A. (2016). "Long-term monitoring of cetaceans using autonomous acoustic recording packages," in *Listening in the Ocean*, edited by W. W. L. Au and M. O. Lammers (Springer, New York), pp. 35–59.
- Wiggins, S. M., McDonald, M. A., and Hildebrand, J. A. (2012). "Beaked whale and dolphin tracking using a multichannel autonomous acoustic recorder," *J. Acoust. Soc. Am.* **131**, 156–163.
- Wiggins, S. M., McDonald, M. A., Munger, L. M., Moore, S. E., and Hildebrand, J. A. (2004). "Waveguide propagation allows range estimates for North Pacific right whales in the Bering Sea," *Can. Acoust.* **32**, 146–154.
- Wiggins, S. M., Thayre, B. J., Trickey, J. S., Rice, A. C., Pickering, S. B., Širović, A., Roch, M. A., and Hildebrand, J. A. (2018). "Summary of five years of ambient and anthropogenic sound in the SOCAL Range Complex 2012 - 2017," *Marine Physical Laboratory Technical Memorandum 625* (La Jolla, CA: Scripps Institution of Oceanography University of California San Diego), p. 38, July 2018.
- Wiggins, S., Manley, J., Brager, E., and Woolhiser, B. (2010). "Monitoring marine mammal acoustics using wave glider," in *Oceans 2010 MTS/IEEE*, Seattle, WA.
- Wood, S., and Scheipl, F. (2017). "gamm4: Generalized Additive Mixed Models using 'mgcv' and 'lme4'," R package version 0.2-6. <https://CRAN.R-project.org/package=gamm4>.

- Yack, T. M., Barlow, J., Calambokidis, J., Southall, B., and Coates, S. (2013). "Passive acoustic monitoring using a towed hydrophone array results in identification of a previously unknown beaked whale habitat.," *J. Acoust. Soc. Am.* **134**, 2589–95.
- Zimmer, W. M. X., Harwood, J., Tyack, P. L., Johnson, M. P., and Madsen, P. T. (2008). "Passive acoustic detection of deep-diving beaked whales," *J. Acoust. Soc. Am.* **124**, 2823–2832.
- Zimmer, W. M. X., Johnson, M. P., Madsen, P. T., and Tyack, P. L. (2005). "Echolocation clicks of free-ranging Cuvier's beaked whales (*Ziphius cavirostris*)," *J. Acoust. Soc. Am.* **117**, 3919.
- Zuur, A. F., Ieno, E. N., Walker, N. J., Saveliev, A. A., and Smith, G. M. (2009). *Mixed Effects Models and Extensions in Ecology with R* (Springer, New York).

APPENDIX A: CHAPTER 2 SUPPLEMENTARY MATERIALS

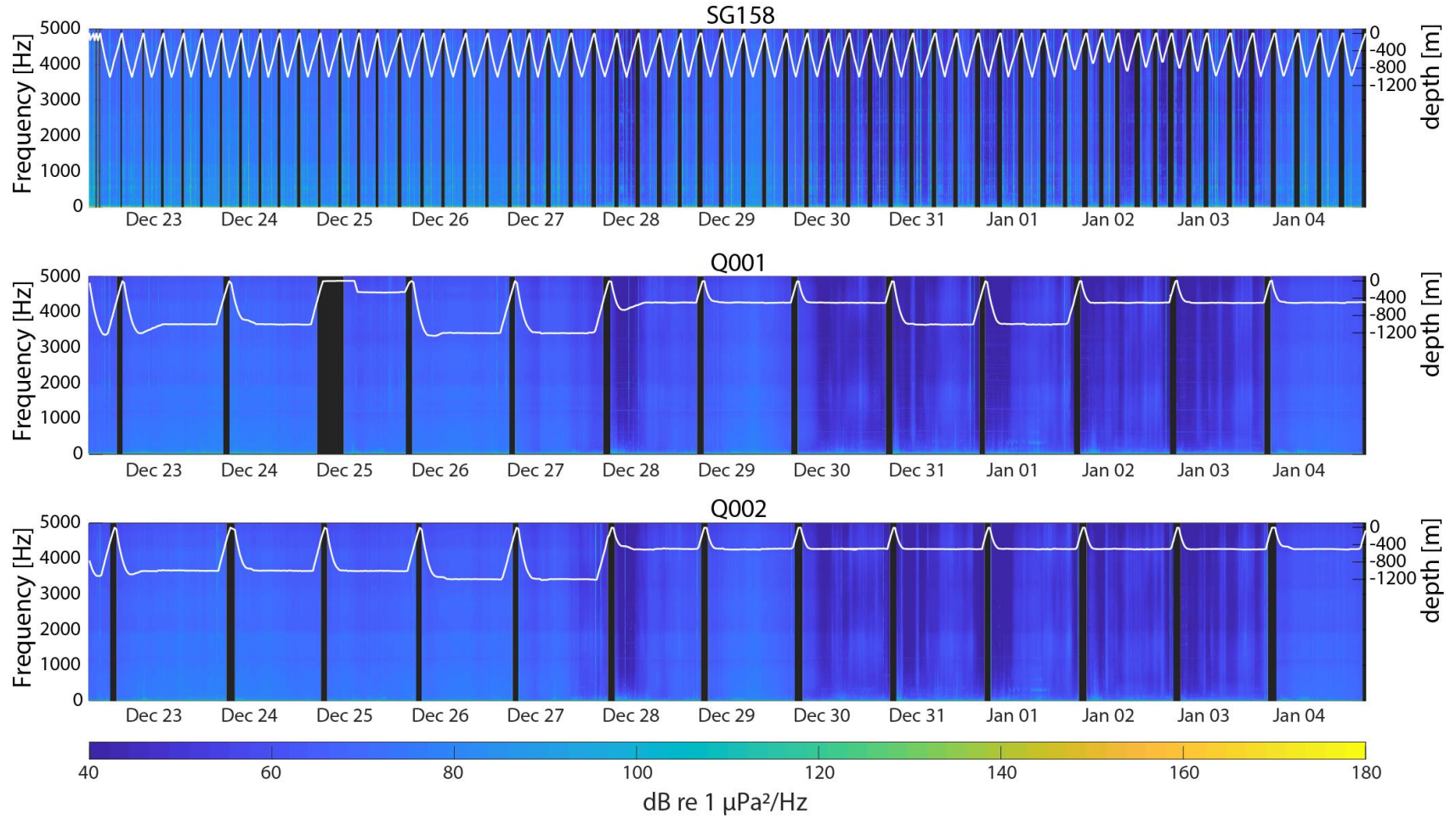


Figure A1. LTSA (80 sec, 10 Hz) of 10 kHz downsampled data for the deployment duration for SG158, Q001, and Q002 with each instruments dive profile overlaid (right y-axis). Black bars indicate time periods when the PAM system was off.

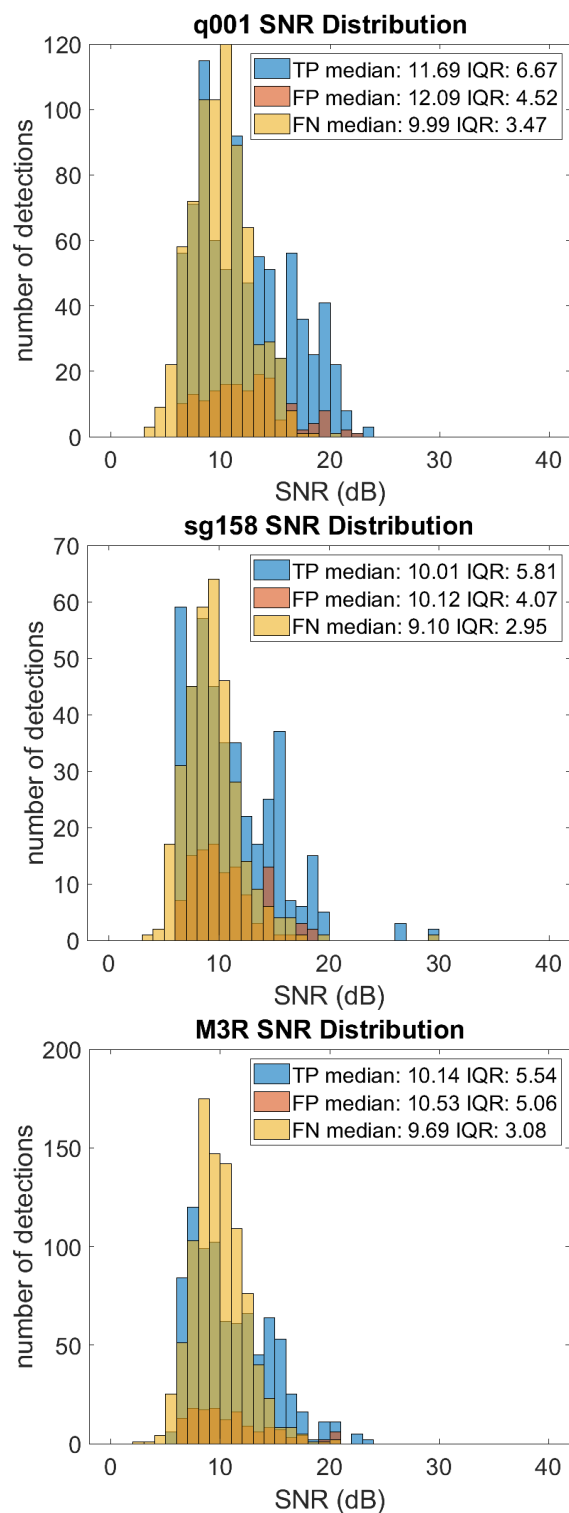


Figure A2. Distribution of signal-to-noise ratios (SNR) for true detections (TP: true positives), false alarms (FP: false positives), and missed calls (FN: false negatives). Median and interquartile range (IQR; 25-75%) are listed in the legend.

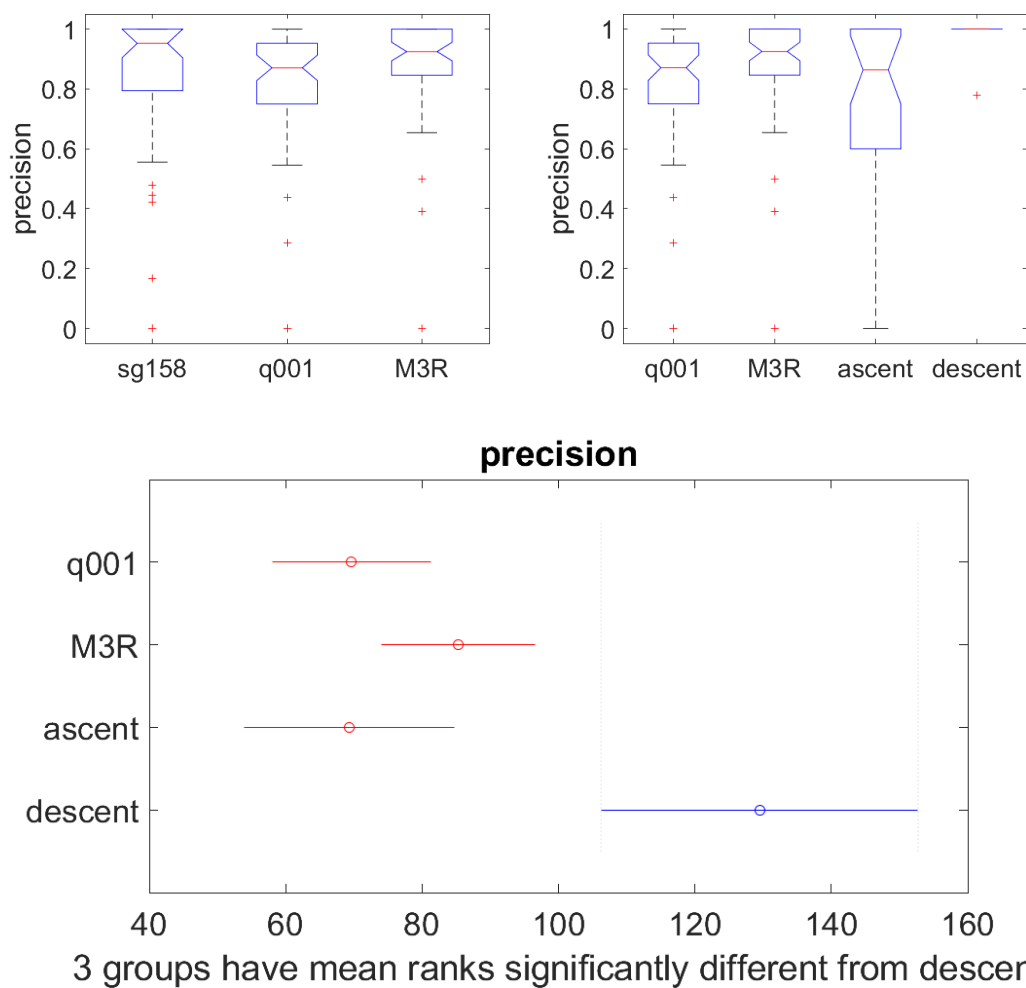


Figure A3. Top: Boxplots for Kruskal-Wallis test for differences in precision across the instrument types with all glider dive states together (left; sg158) and separated by ascent and descent (right) compared to the float (q001) and fixed-recorders (M3R). Bottom: Output of Dunn's multiple comparison test on precision with glider dive states analyzed separately, showing that descent is statistically different than Q001, M3R, and glider ascents.

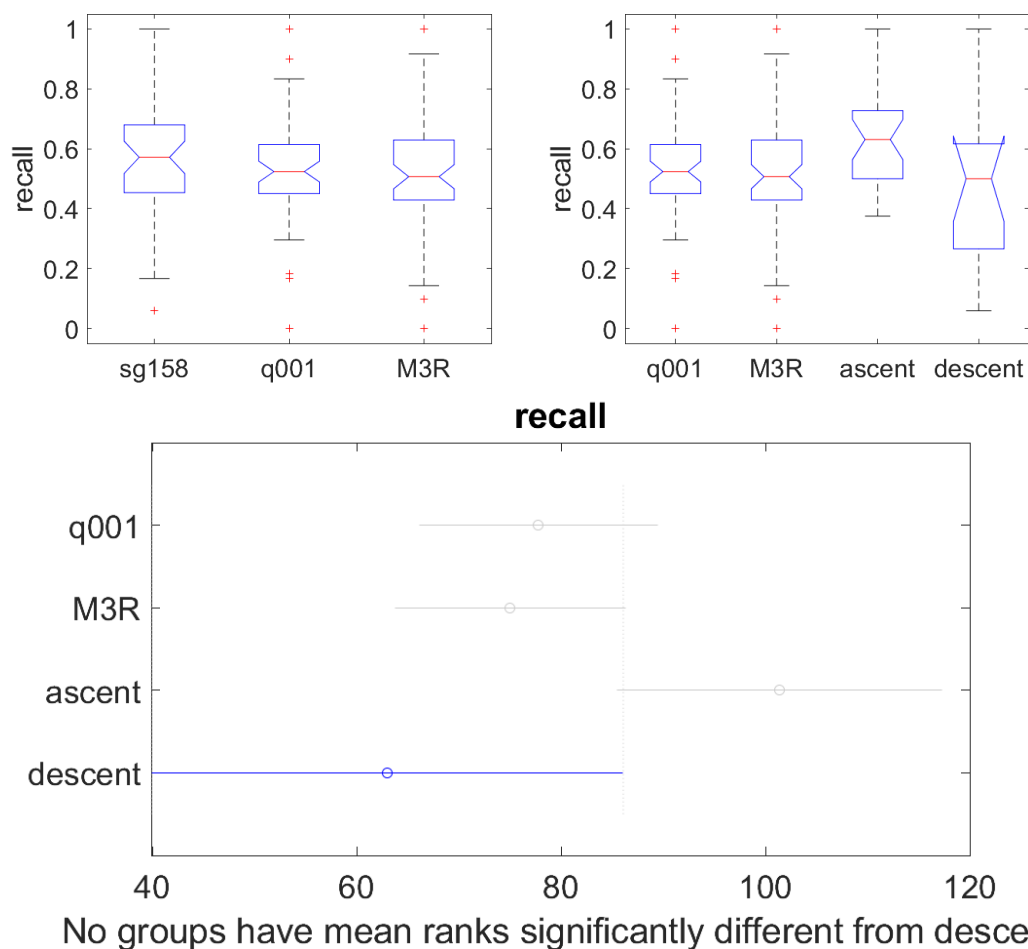


Figure A4. Top: Boxplots for Kruskal-Wallis test for differences in recall across instrument types, with all glider dive states together (left; sg158) and separated by ascent and descent (right), compared to the float (q001) and fixed-recorders (M3R). Bottom: Output of Dunn's multiple comparison test on recall with glider dive states analyzed separately, showing that recall did not differ by instrument or glider dive state.

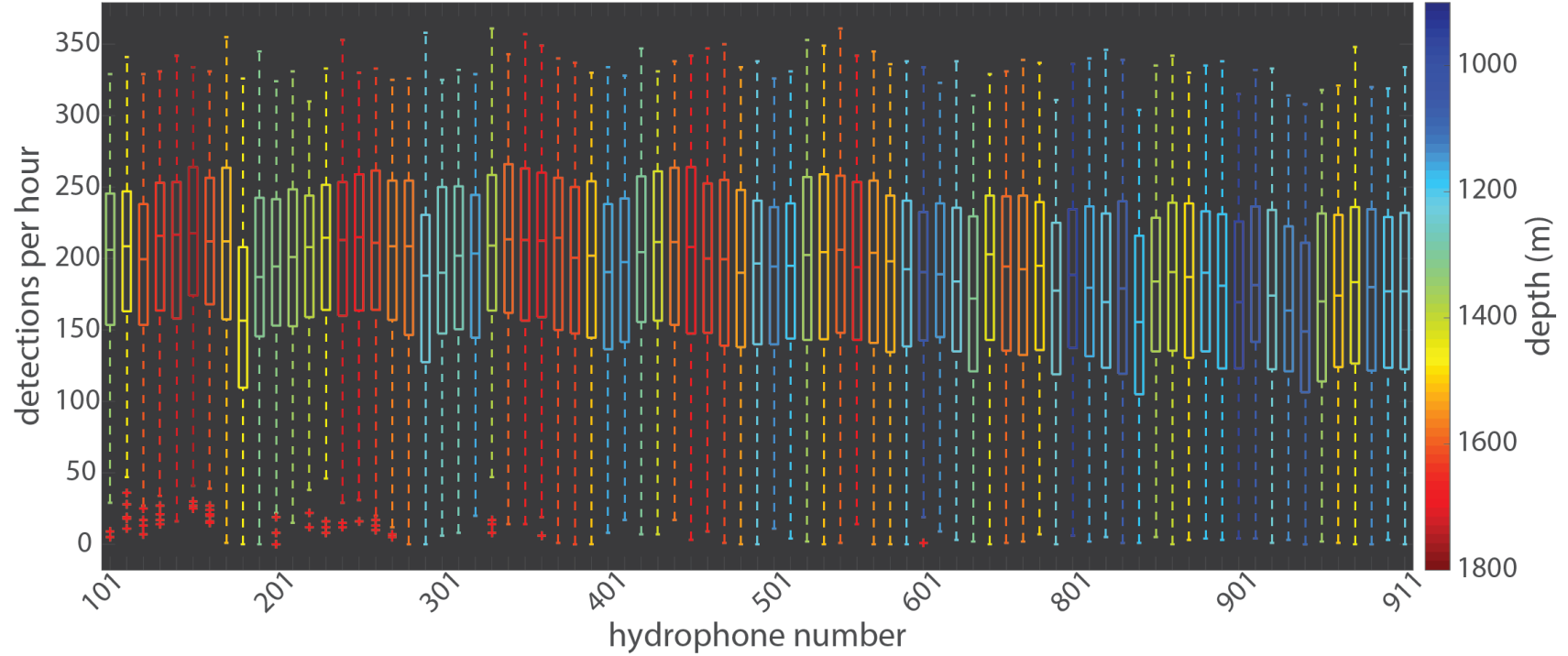


Figure A5. Boxplot of median detections per hour for each M3R hydrophone, colored by instrument depth. Hydrophone numbers are 101-110, 201-210, 301-310, 401-410, 501-509, 601-609, 801-810, and 901-911.

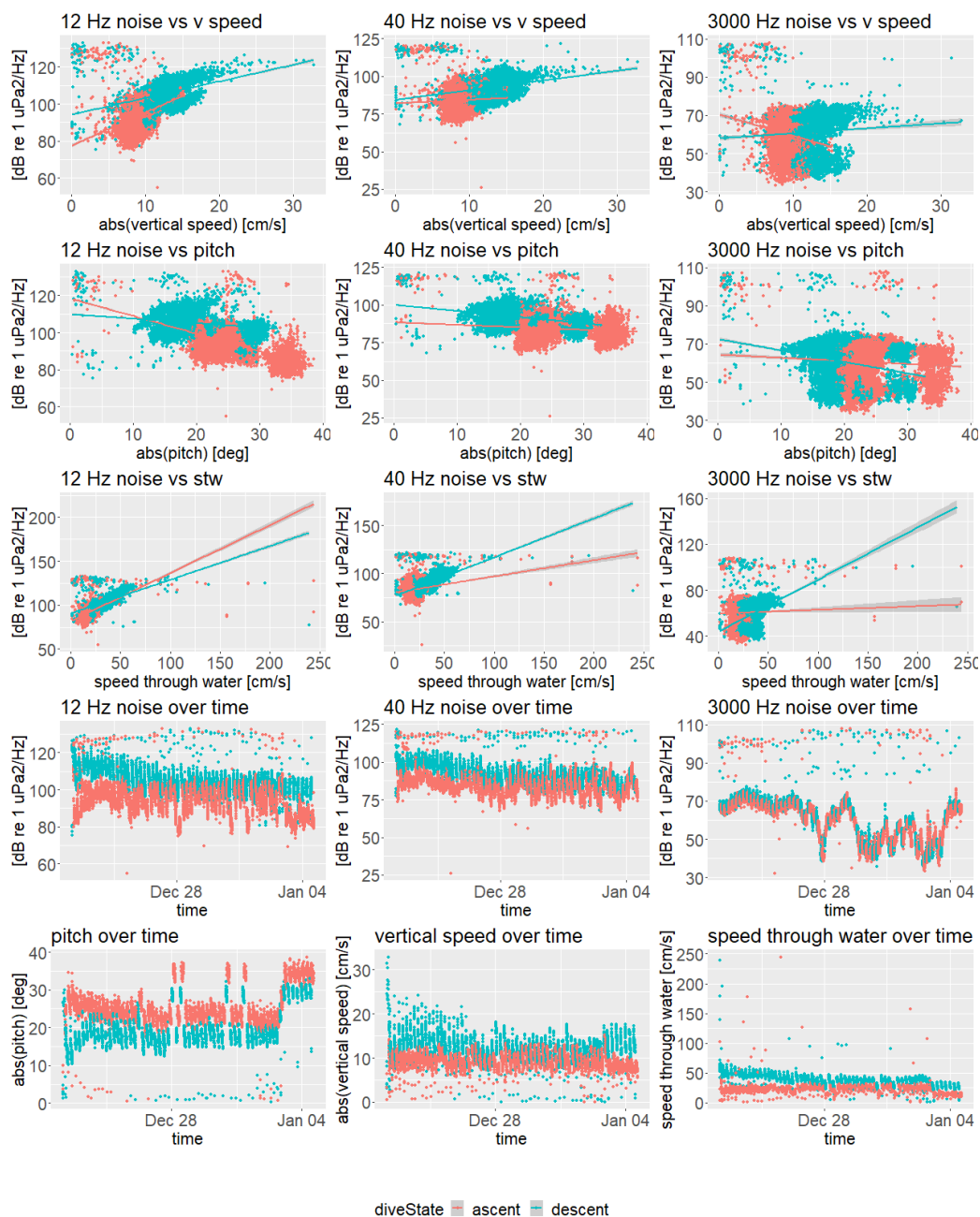


Figure A6. Exploratory plots of raw data (all minutes). Each spectrum density level (minimum level per minute) is plotted against the absolute value of vertical speed (“v speed”), absolute value of pitch, speed through water (“stw”), and over time in the first four plot rows. The bottom row includes plots of absolute value of pitch over time, absolute value of pitch, the absolute value of vertical speed, and speed through water over time. Data in each plot are colored by dive state with ascents in coral and descents in teal and the first three plot rows include a simple linear regression fit line, fit separately to ascent and descent data.

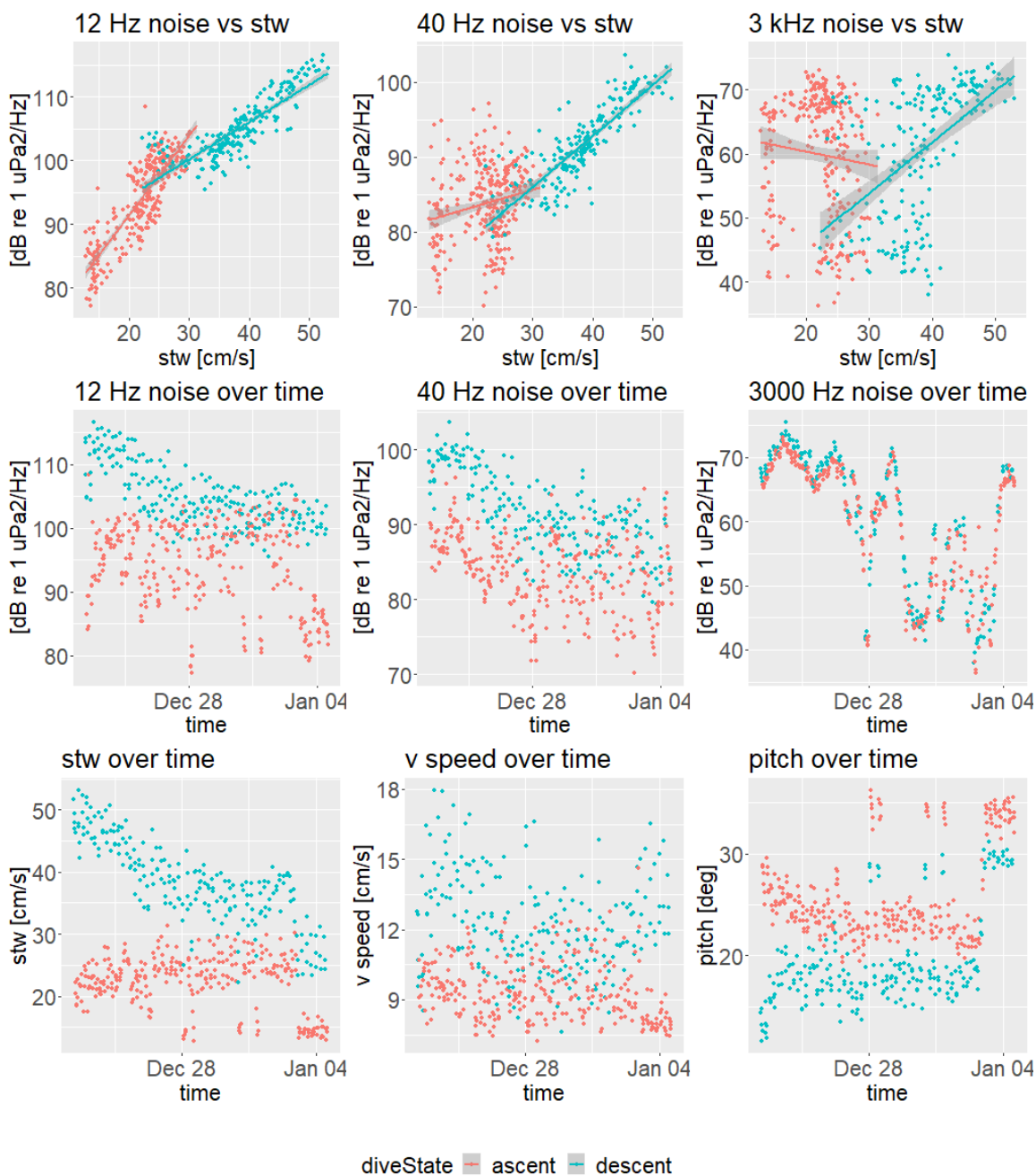


Figure A7. Exploratory plots of 30-minute binned median data. Median spectrum density level per 30-minute bin is plotted against median speed through water (“stw”; top row) and time (middle row). Median speed through water, vertical speed, and pitch are plotted against time in the bottom row. Data in each plot are colored by dive state with ascents in coral and descents in teal and the row’s plots include a simple linear regression fit line, fit separately to ascent and descent data.

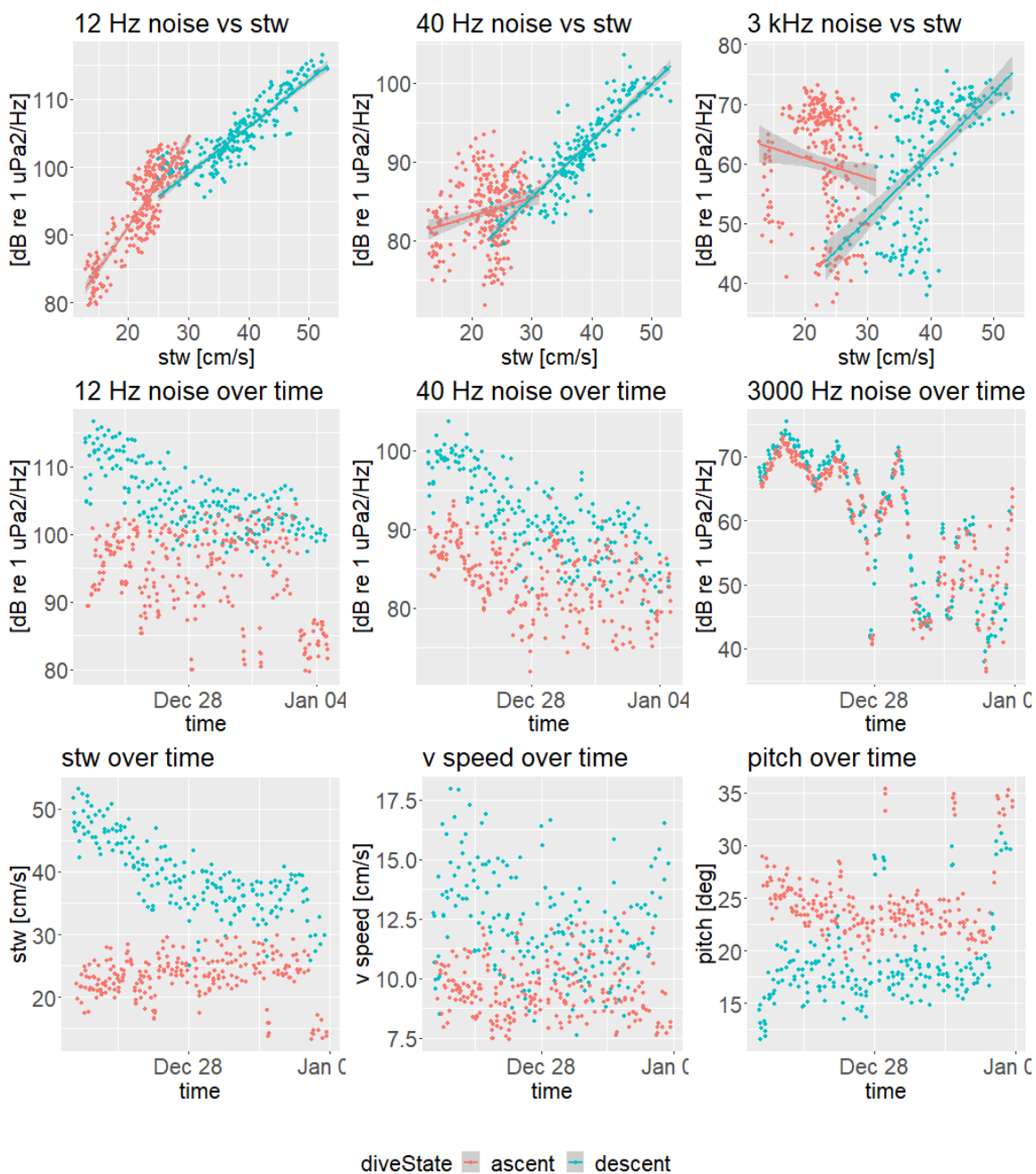


Figure A8. Exploratory plots of 30-minute binned median data, with outliers removed. Median spectrum density level per 30-minute bin is plotted against median speed through water (“stw”; top row) and time (middle row). Median speed through water, vertical speed, and pitch are plotted against time in the bottom row. Data in each plot are colored by dive state with ascents in coral and descents in teal and the row’s plots include a simple linear regression fit line, fit separately to ascent and descent data.

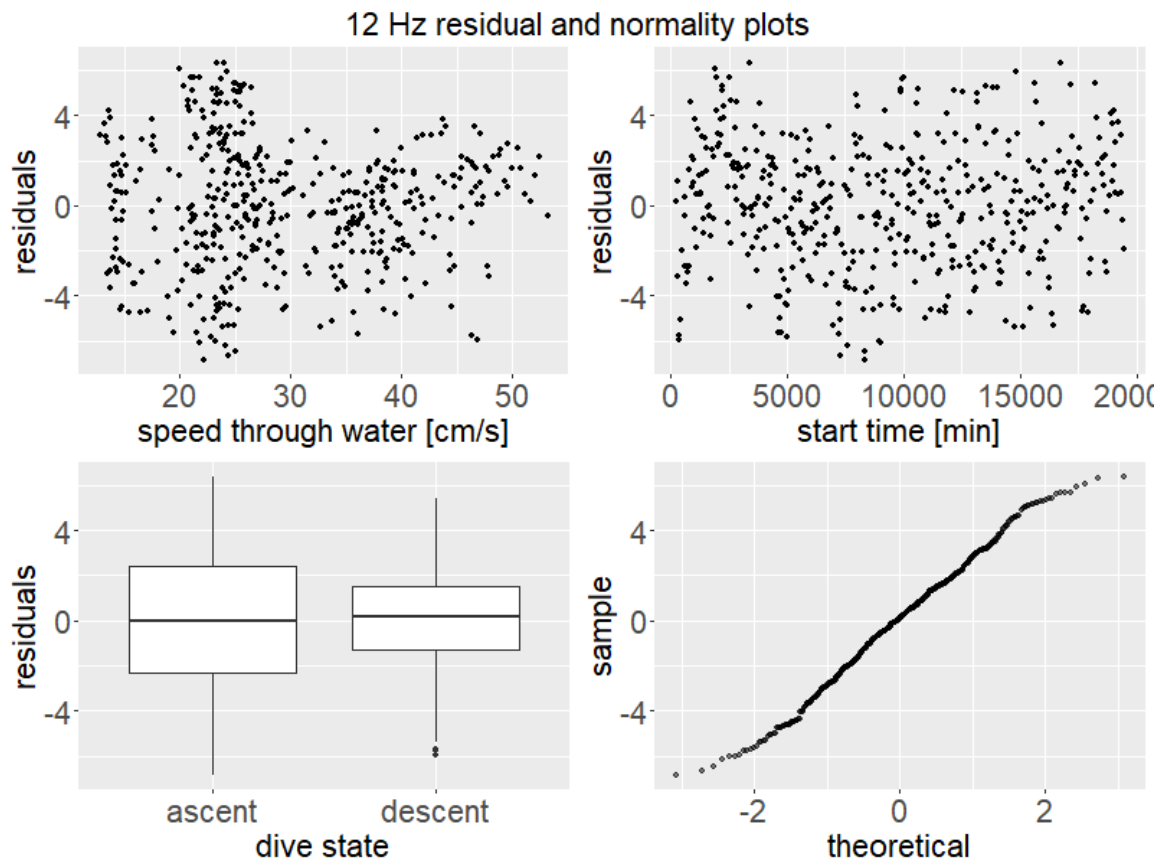


Figure A9. Residual and normality plots used for checking model assumptions for the median 12 Hz power spectrum density levels. These are residuals from a linear regression of the full model after removal of outliers. The top two panels are residuals plotted against speed through water and time (as minute from deployment start). They were used to examine the assumptions of constant error variance and independence. The bottom left panel is residuals by dive state, also used to examine constant error variance. The bottom right panel is a Q-Q normality plot used to assess the normality assumption.

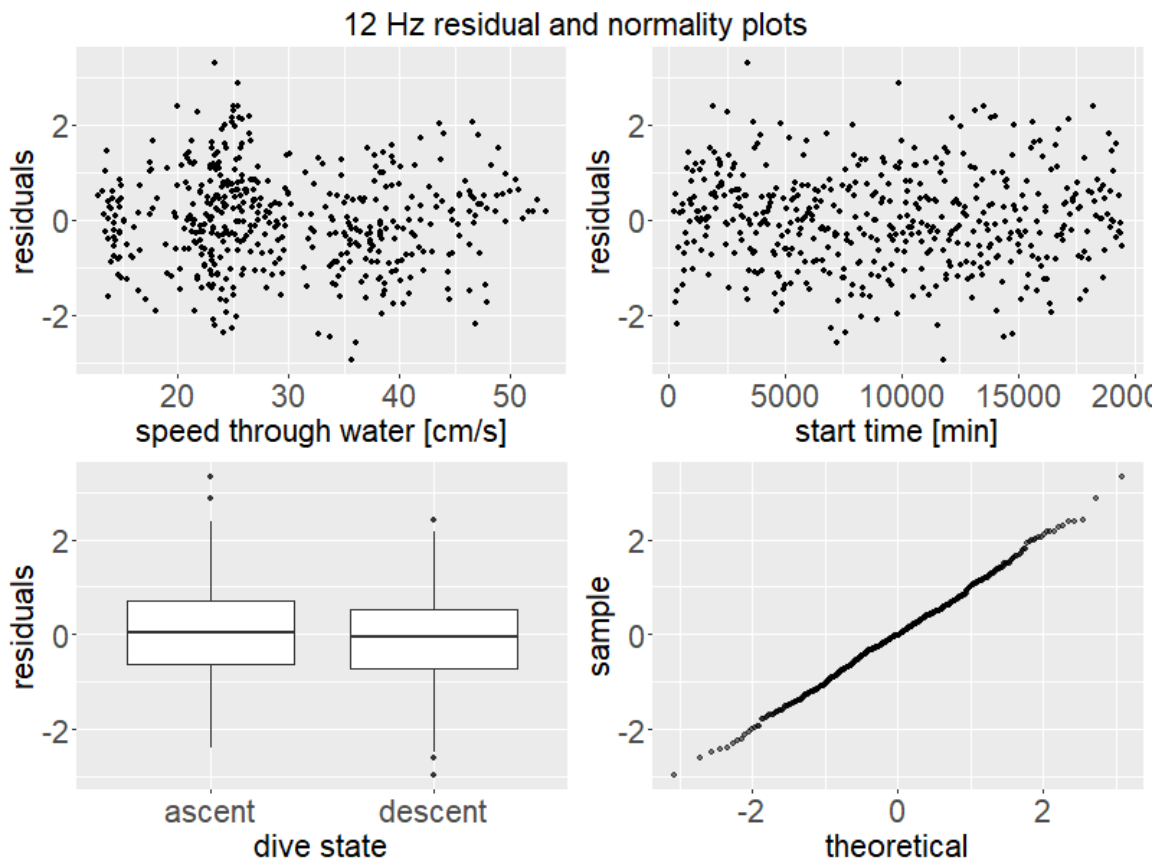


Figure A10. Normalized residual and normality plots for median 12 Hz power spectrum density levels after applying variance and correlation structures in a generalized least squares regression of the full model. The top two panels are normalized residuals plotted against speed through water and time (as minute from deployment start). They were used to examine the assumptions of constant error variance and independence. The bottom left panel is normalized residuals by dive state, also used to examine constant error variance. The bottom right panel is a Q-Q normality plot used to assess the normality assumption.

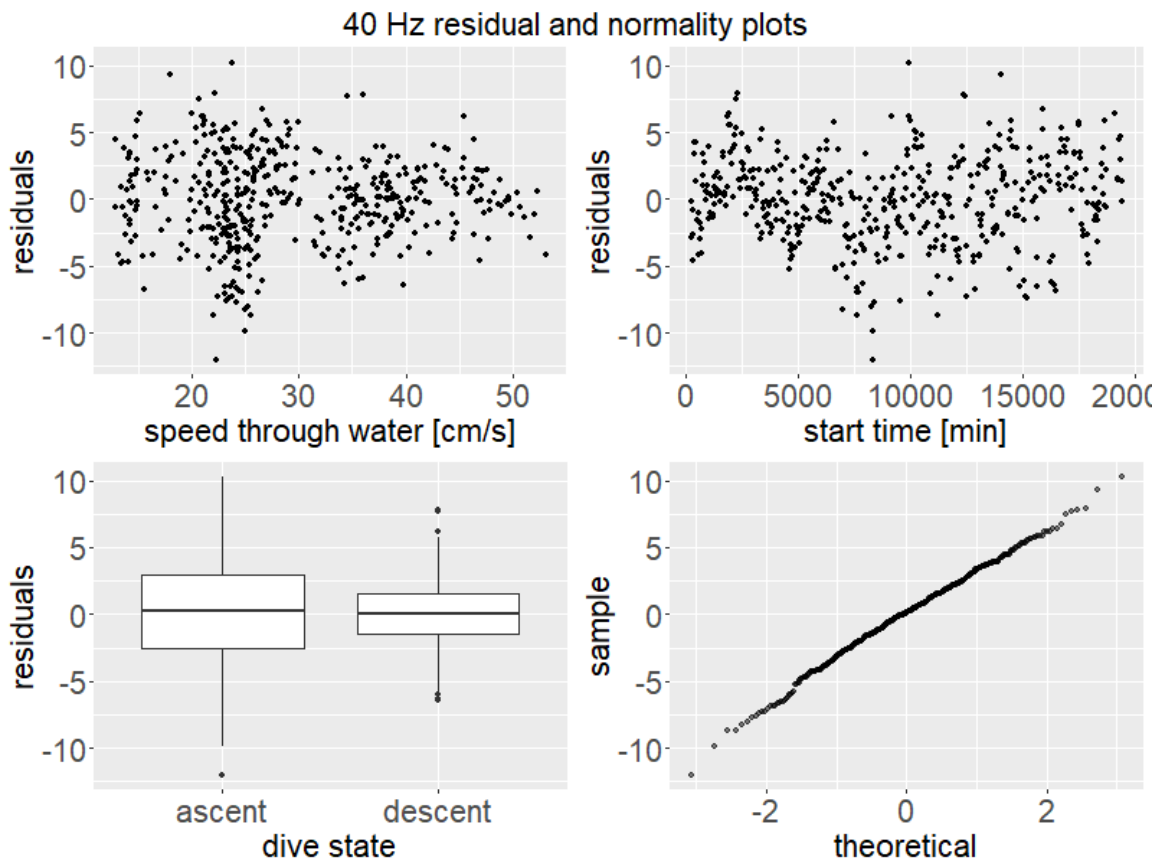


Figure A11. Residual and normality plots used for checking model assumptions for the median 40 Hz power spectrum density levels. These are residuals from a linear regression of the full model after removal of outliers. The top two panels are residuals plotted against speed through water and time (as minute from deployment start). They were used to examine the assumptions of constant error variance and independence. The bottom left panel is residuals by dive state, also used to examine constant error variance. The bottom right panel is a Q-Q normality plot used to assess the normality assumption.

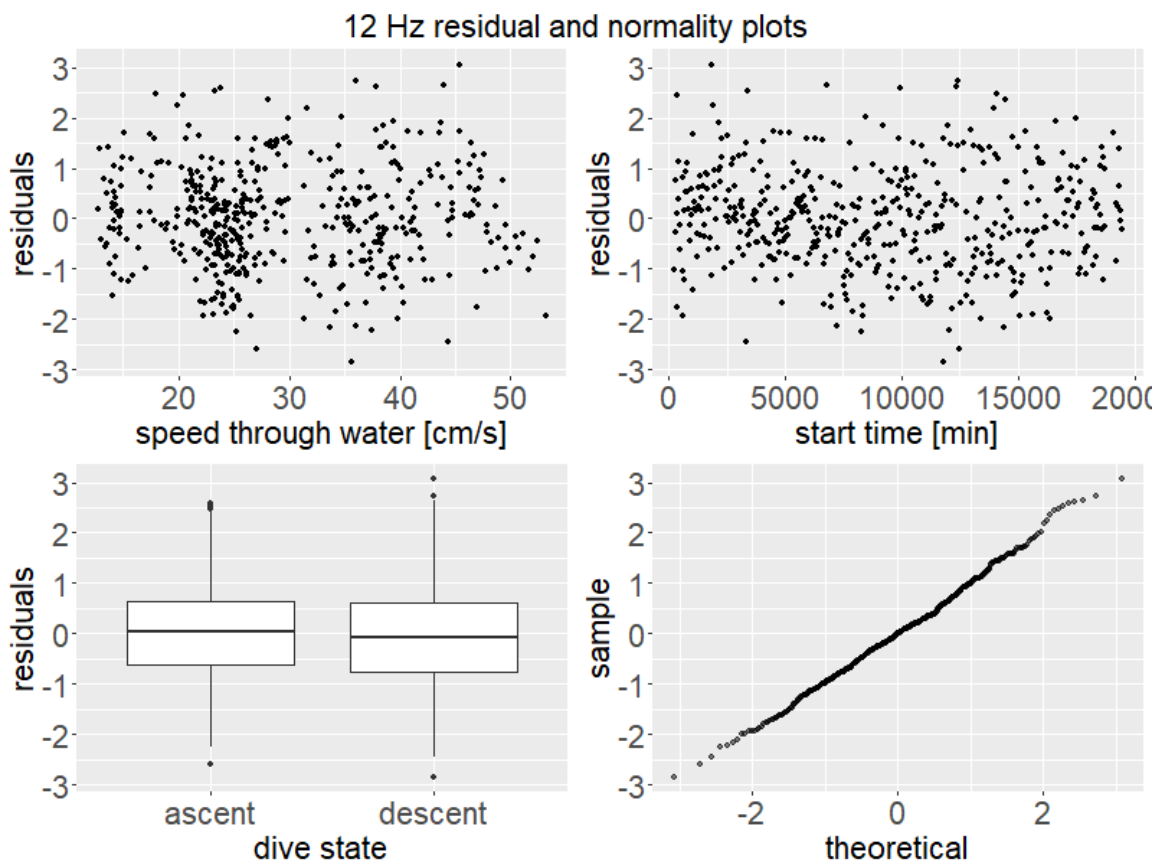


Figure A12. Normalized residual and normality plots for median 40 Hz power spectrum density levels after applying variance and correlation structures in a generalized least squares regression of the full model. The top two panels are normalized residuals plotted against speed through water and time (as minute from deployment start). They were used to examine the assumptions of constant error variance and independence. The bottom left panel is normalized residuals by dive state, also used to examine constant error variance. The bottom right panel is a Q-Q normality plot used to assess the normality assumption.

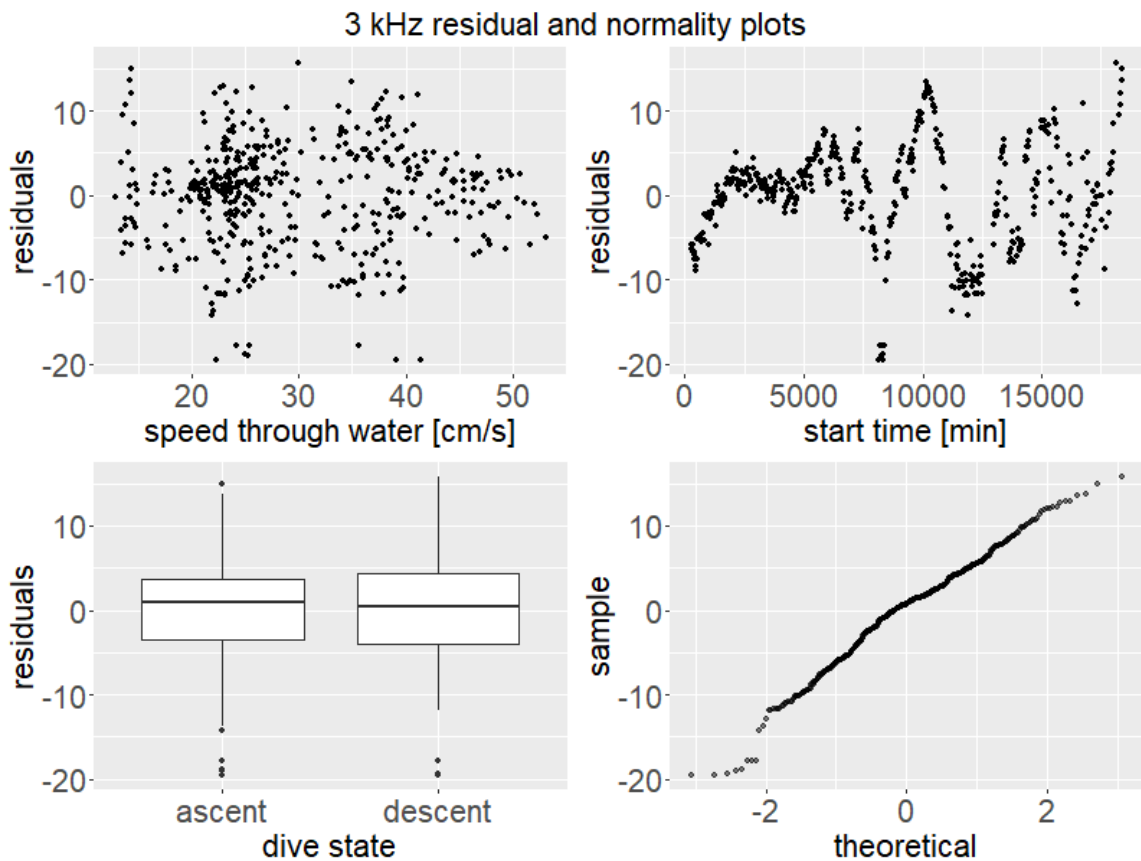


Figure A13. Residual and normality plots used for checking model assumptions for the median 3 kHz power spectrum density levels. These are residuals from a linear regression of the full model after removal of outliers. The top two panels are residuals plotted against speed through water and time (as minute from deployment start). They were used to examine the assumptions of constant error variance and independence. The bottom left panel is residuals by dive state, also used to examine constant error variance. The bottom right panel is a Q-Q normality plot used to assess the normality assumption.

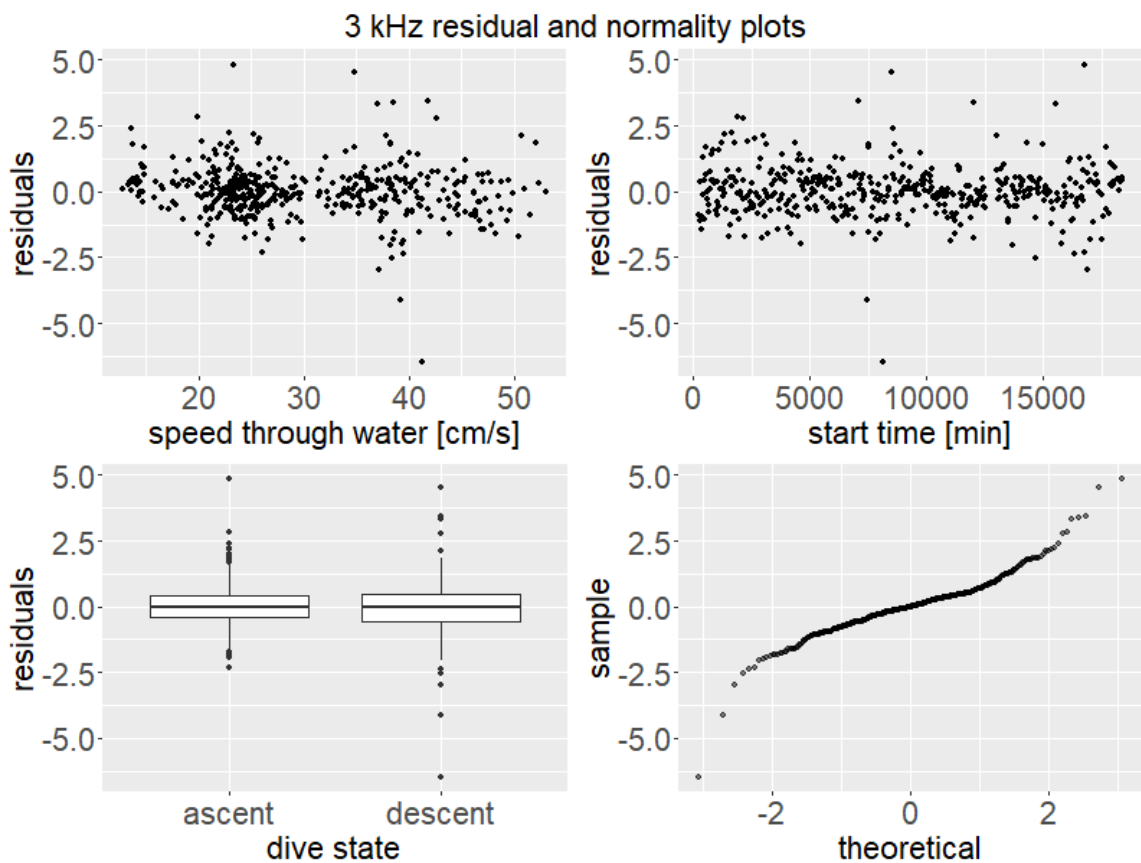


Figure A14. Normalized residual and normality plots for median 3 kHz power spectrum density levels after applying variance and correlation structures in a generalized least squares regression of the full model. The top two panels are normalized residuals plotted against speed through water and time (as minute from deployment start). They were used to examine the assumptions of constant error variance and independence. The bottom left panel is normalized residuals by dive state, also used to examine constant error variance. The bottom right panel is a Q-Q normality plot used to assess the normality assumption.

APPENDIX B: CHAPTER 3 SUPPLEMENTARY MATERIALS

Track 80 Window 5 done: cMax = 0.2133, offset seconds = -13.98

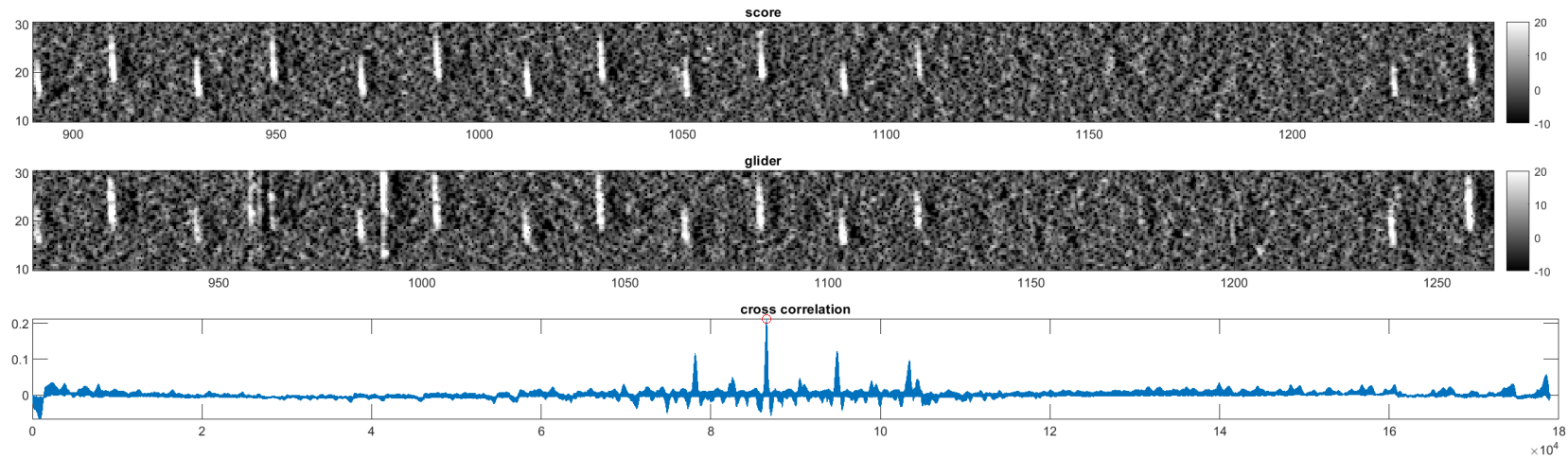


Figure B1. Example equalized spectrogram of a single snapshot on the focal SCORE hydrophone (top) and the glider (middle) showing a gap in calls used to confirm the tracked whale was recorded on the glider. The 2D cross-correlation score is shown in the bottom plot, with the peak location and value circled in red. The glider was 6.7 km from the tracked whale for this snapshot, and median 40 Hz spectrum level was 86.4 dB re $1 \mu\text{Pa}^2/\text{Hz}$.

Track 84 Window 15 done: cMax = 0.2641, offset seconds = -14.60

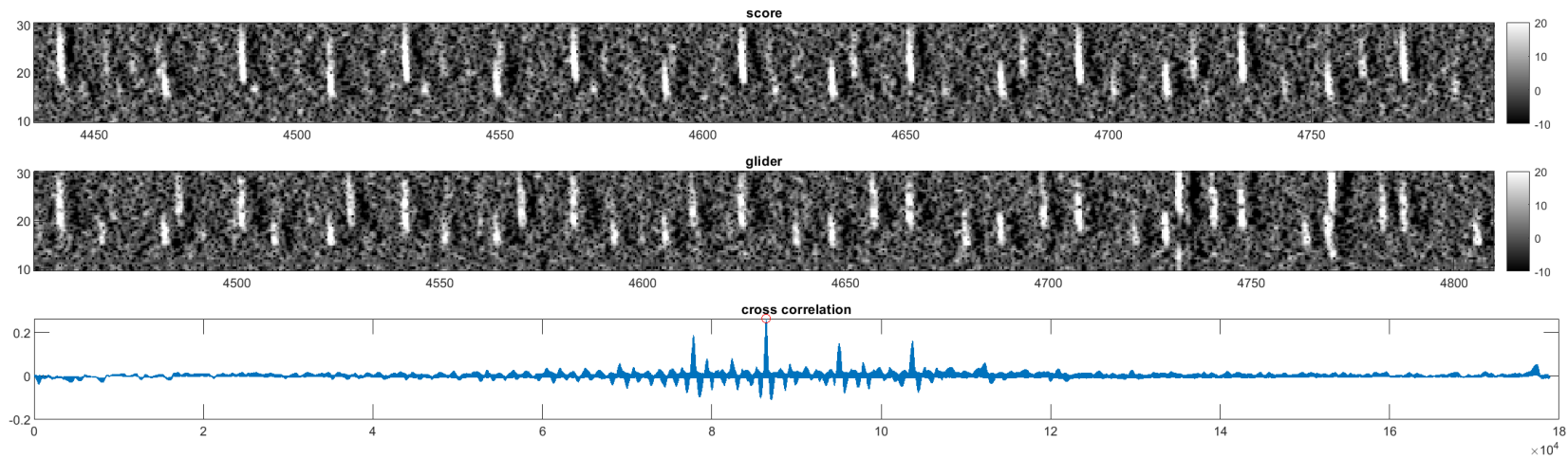


Figure B2. Example equalized spectrogram of a single snapshot on the focal SCORE hydrophone (top) and the glider (middle) showing multiple whales present on both recorders, but the pattern still allowed confirmation of the tracked whale being recorded by the glider. Note the unusually long inter-call interval in the top spectrogram between calls at approximately 4440 and 4465 s; the middle spectrogram shows an equal interval, aligned with the top spectrogram, with calls at approximately 4455 and 4580 s. Alignment of such anomalous intervals is an important part in accurately determining which call on one platform corresponds to which call on another. The 2D cross-correlation score is shown in the bottom plot, with the peak location and value circled in red. The glider was 9.7 km from the tracked whale for this snapshot, and median 40 Hz spectrum level was 85.7 dB re 1 $\mu\text{Pa}^2/\text{Hz}$.

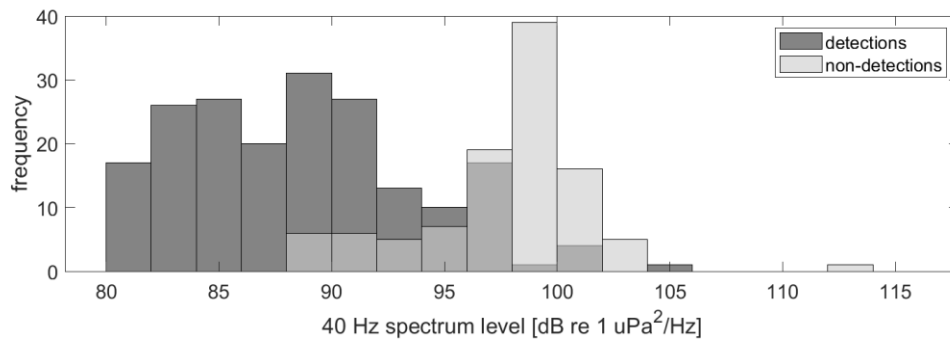


Figure B3. Distribution of scored snapshots ($n = 589$) by 40 Hz noise level on the glider. Non-detections typically had higher noise levels but did occur when noise levels were below 90 dB re 1 $\mu\text{Pa}^2/\text{Hz}$. Detections were more common at lower noise levels, but also occurred at high levels as high as 105 dB $\mu\text{Pa}^2/\text{Hz}$. The dataset used in the detection function modelling only included snapshots with noise levels between 90 and 100 dB re 1 $\mu\text{Pa}^2/\text{Hz}$.

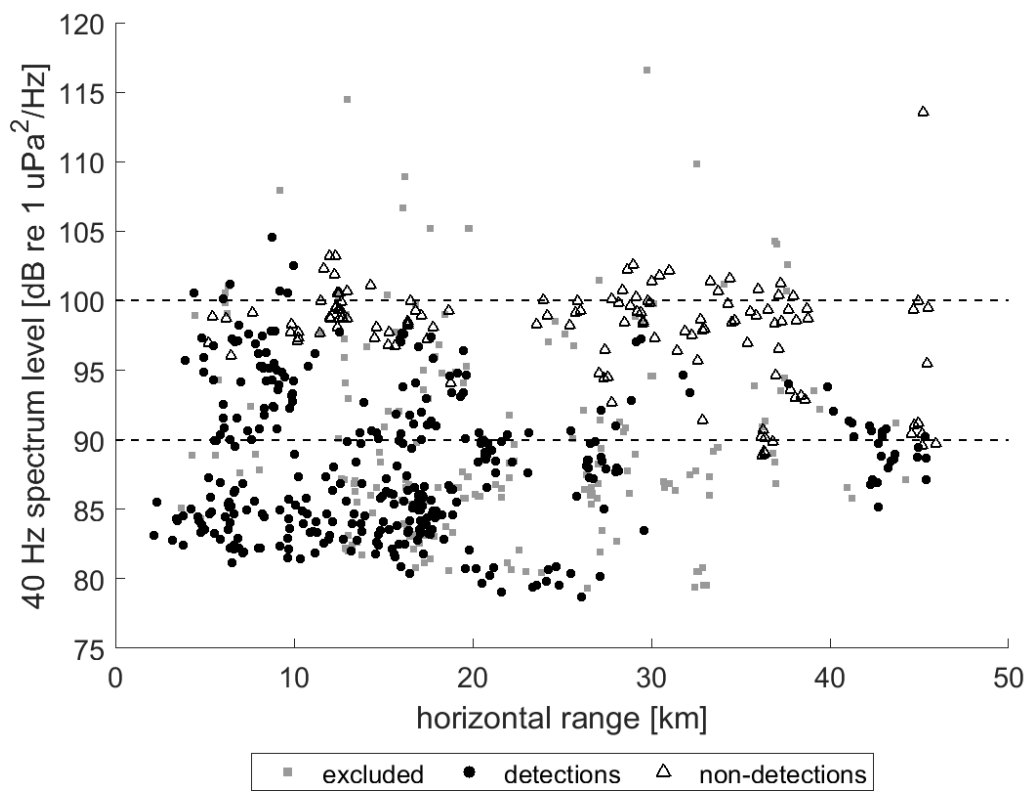


Figure B4. Snapshots that were detected (black circles) or not detected (outlined black triangles) by the glider as a function of distance from the track segment to the glider and the median 40 Hz spectrum level on the glider during that snapshot. Gray squares are snapshots that were excluded because there was not a clear detection or non-detection between the glider and SCORE focal phone. Black dashed lines indicate 90 and 100 dB re $1 \mu\text{Pa}^2/\text{Hz}$ and show the points (between dashed lines) that were used in the final detection probability estimation. Each datapoint is a single six-minute snapshot and this plot includes snapshots that overlapped in time and all snapshots regardless of 40 Hz noise level.

APPENDIX C: CHAPTER 4 SUPPLEMENTARY MATERIALS

Supplementary Figures and Tables

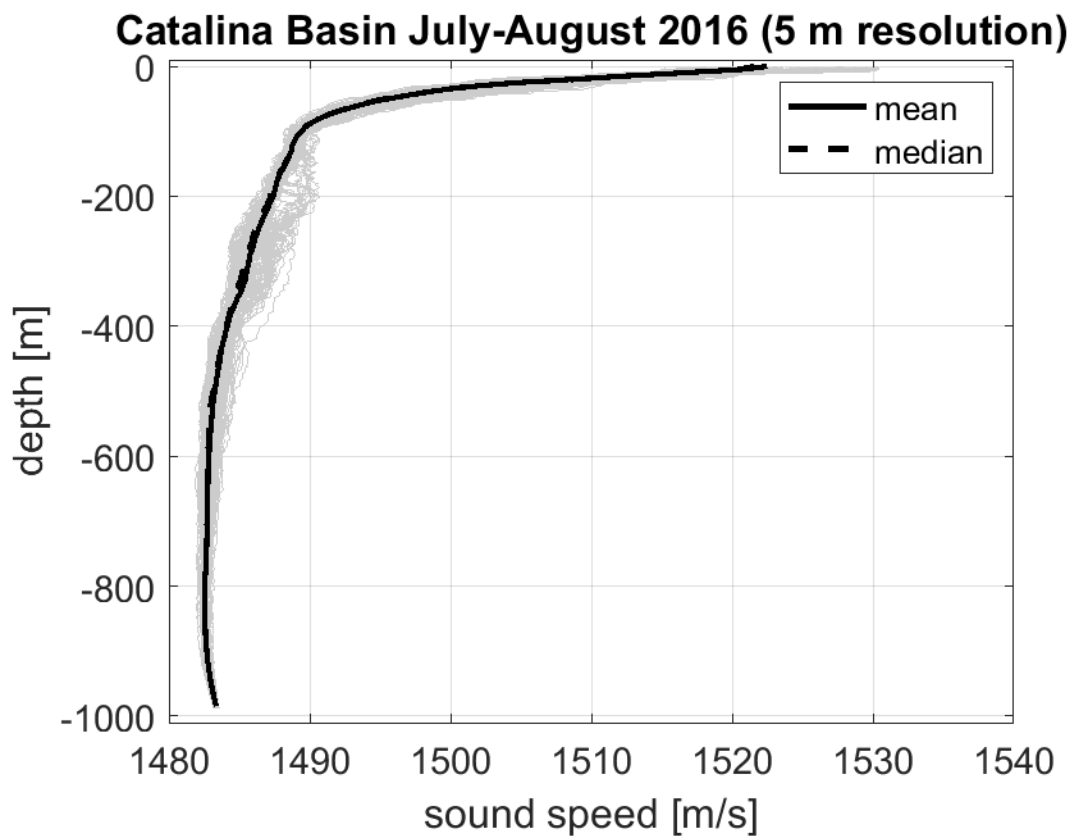


Figure C1. Sound speed profile collected by Seaglider SG607. Gray lines represent sound speeds calculated at all sampled depths (calculated on board Seaglider from CTD measurements of temperature and salinity). Black lines represent mean (solid line) and median (dashed line) sound speeds every 5 m.

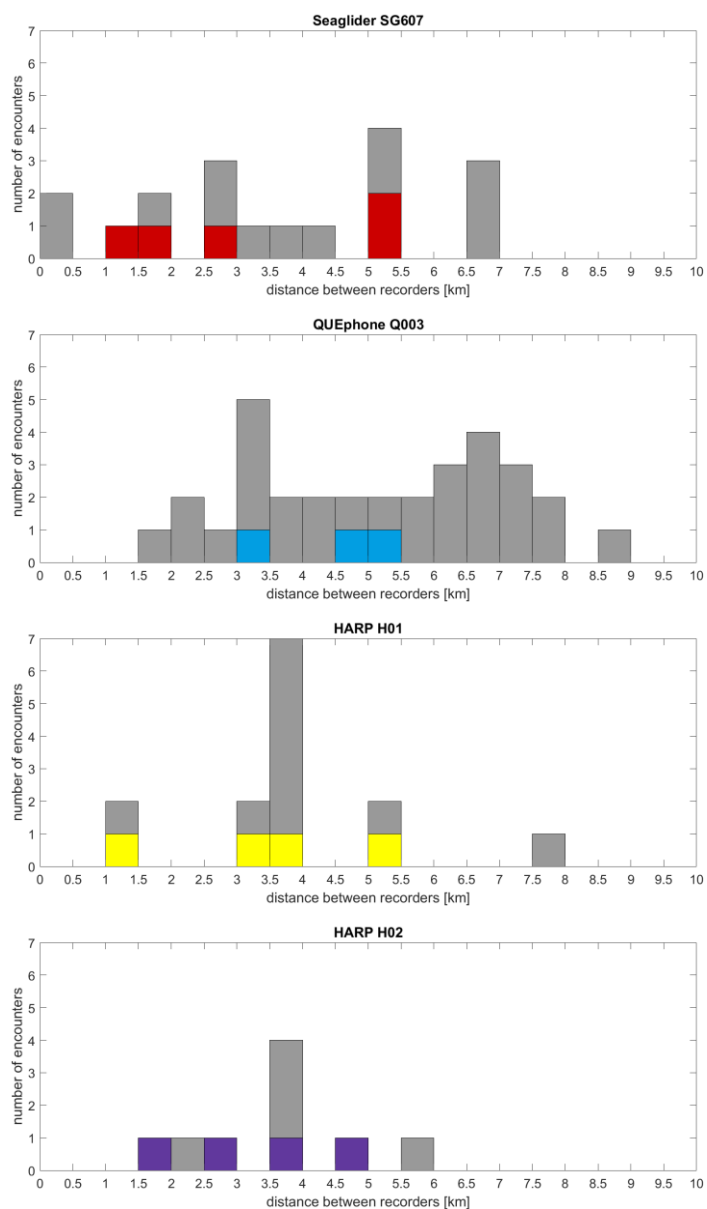


Figure C2. Distances between a single recording platform, shown in the title of each plot, and the three other deep-water recorders for all Cuvier's beaked whale encounters on the named recording platform. Pairwise distances for beaked whales encounters that were also detected on one of the other recorders are indicated with colored bars – Seaglider SG607 in red, QUEphone in blue, HARP H01 in yellow and HARP H02 in purple. Pairwise distances where beaked whales were not detected on both recorders are shown as stacked gray bars.

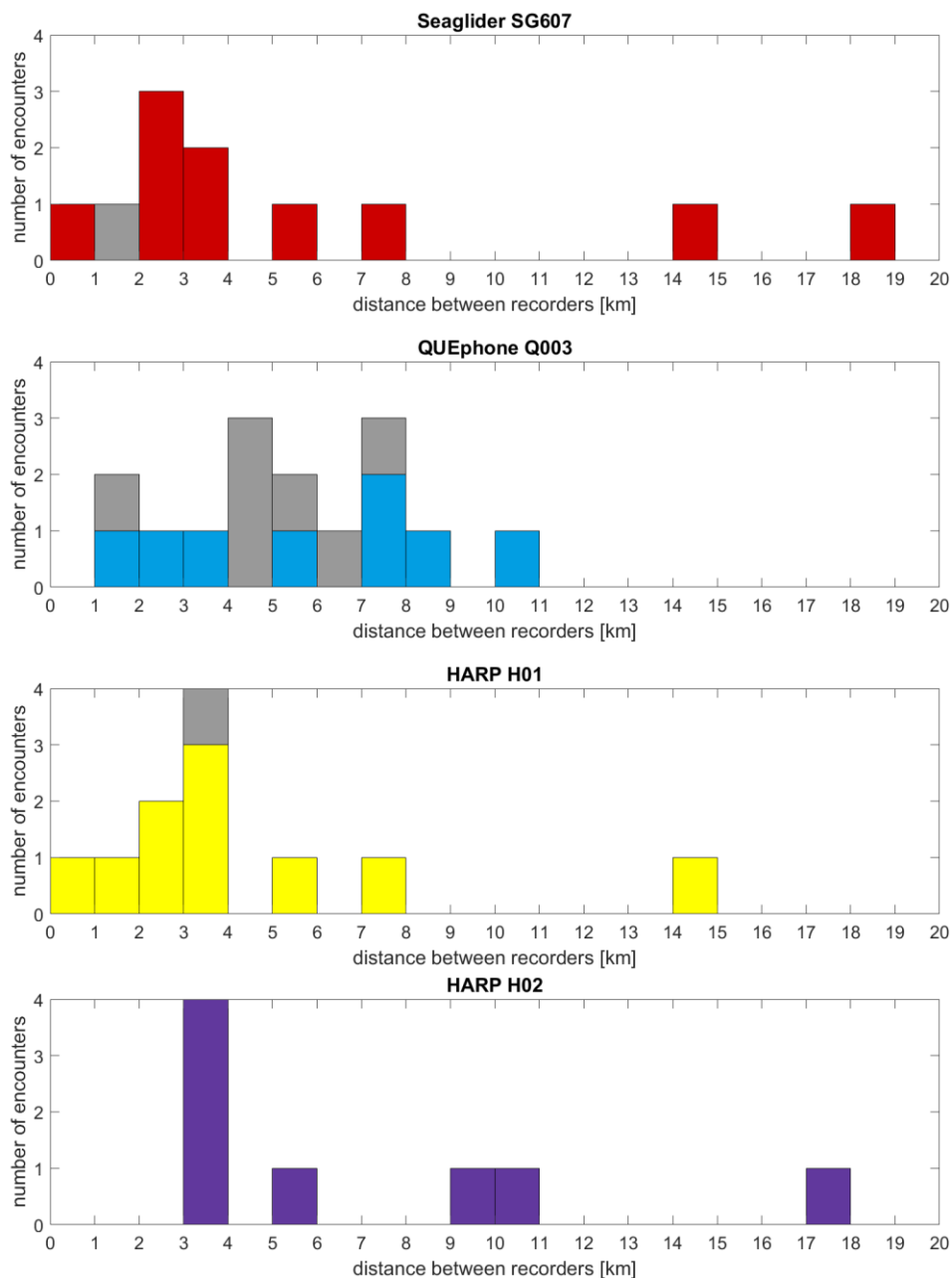


Figure C3. Distances between a single recording platform, indicated in the title of each plot, and the three other deep-water recorders for all minke whale boing encounters. Pairwise distances where boings were detected on both recorders are indicated with colored bars – Seaglider SG607 in red, QUEphone in blue, HARP H01 in yellow and HARP H02 in purple. Pairwise distances where boings were not detected on both recorders are shown as stacked gray bars.

Table C1. Localized Cuvier's beaked whales (from Barlow *et al.* 2018) with distances to deep-water recorders at that minute. Distances in bold indicate Cuvier's beaked whales were detected on that deep-water recorder at the same time. Times when the glider or QUEphone had the pam system off or were not deployed are indicated in italics. Note that for the first location for Dive BL-1 the glider was only 3.5 km away (horizontal distance) but was very near the surface.

Dive Label	Time [UTC]	Depth [m]	Distance recorder [km]			
			Glider	QUEphone	HARP 1	HARP 2
AI-1	7/22/2016 3:57	1191	<i>pam off</i>	6.30	4.27	7.70
AI-2	7/22/2016 4:24	952	5.61	5.69	4.14	7.31
AJ-5	7/22/2016 6:28	810	7.99	7.37	5.05	8.87
AP-1	7/24/2016 6:16	953	12.33	12.04	6.72	10.18
AP-1	7/24/2016 6:21	854	11.98	11.57	6.24	9.77
AP-1	7/24/2016 6:23	836	11.78	11.36	6.05	9.56
AR-1	7/24/2016 20:30	1193	6.49	5.36	7.87	4.98
AS-1	7/24/2016 23:43	734	6.91	3.48	5.39	2.78
AW-1	7/25/2016 7:54	959	5.79	2.22	3.43	6.59
AW-1	7/25/2016 7:55	925	5.89	2.31	3.51	6.68
AW-1	7/25/2016 8:10	840	6.07	2.45	3.03	6.71
AY-1	7/25/2016 10:57	1085	13.37	8.29	8.56	12.43
AY-1	7/25/2016 11:08	1067	13.29	8.01	8.37	12.25
AY-1	7/25/2016 11:14	1247	12.72	7.50	7.77	11.62
AY-1	7/25/2016 11:20	693	13.61	8.08	8.57	12.46
BH-1	7/26/2016 9:19	976	7.58	<i>not deployed</i>	6.65	10.42
BH-2	7/26/2016 9:39	954	7.09	<i>not deployed</i>	5.99	9.76
BL-1	7/27/2016 8:11	1169	3.55	5.88	4.26	7.17
BL-1	7/27/2016 8:19	1244	<i>pam off</i>	6.00	4.21	7.29
BM-2	7/27/2016 11:11	671	7.91	8.74	7.39	10.85
BM-3	7/27/2016 11:15	1136	6.43	7.27	5.86	9.36
BS-1	7/29/2016 12:44	1046	5.01	9.42	5.05	8.83
BS-1	7/29/2016 13:07	933	4.31	9.09	4.81	8.64

Minke whale boing detector – Ishmael preference file

```
# This is an Ishmael settings file.  It is okay to edit it with a text
# editor or word processor, provided you save it as TEXT ONLY.  It's
# generally safe to change the values here in ways that seem reasonable,
# though you could undoubtedly make Ishmael fail with some really poor
# choices of values.
#
# Also:
#   * Keep each line in its original section (Unit) or it will be ignored.
#   * A line beginning with '#', like this one, is a comment.
#   * Spaces and capitalization in parameter names ARE significant.
#   * If you delete a line containing a certain parameter, then loading
#     this settings file will not affect Ishmael's current value of that
#     parameter.  So you can create a settings file with only a handful of
#     lines for your favorite values, and when you load that file, it will
#     set those parameters and leave everything else alone.
#   * Ishmael's default settings file -- the one it loads at startup -- is
#     called IshDefault.ipf.
```

Unit: Spectrogram calculation, prefs version 1

```
frame size, samples = 2048
frame size, sec     = 0.20479999
zero pad            = 0
hop size            = 512
window type         = Hann
keep same duration  = true
quadratic scaling   = false
```

Unit: Equalization, prefs version 1

```
equalization enabled = true
equalization time    = 10
floor enabled        = true
floor is automatic   = false
gram floor value     = 0.208
ceiling enabled      = true
ceiling is automatic = false
gram ceiling value   = 0.65386504
```

Unit: Tonal detection 1, prefs version 1

```
enabled = true
lower frequency bound = 900
upper frequency bound = 1200
base percentage = 50
height above base = 0
peak neighborhood = 10
peak min difference = 10
line fit duration = 0.2
minimum duration = 1.5
minimum independent dur = 0.050000001
```

